2017

Development and Implementation of Methods to Study Crystallization in Cheese

Gil Fils Tansman
University of Vermont

DEVELOPMENT AND IMPLEMENTATION OF METHODS TO STUDY CRYSTALLIZATION IN CHEESE

A Dissertation Presented

by

Gil Tansman

to

The Faculty of the Graduate College

of

The University of Vermont

In Partial Fulfillment of the Requirements
for the Degree of Doctor of Philosophy
Specializing in Animal, Nutrition, and Food Sciences

May, 2017

Defense Date: March 21, 2017
Dissertation Examination Committee:

Paul S. Kindstedt, Ph.D., Advisor
John M. Hughes, Ph.D., Chairperson
Catherine, W. Donnelly, Ph.D.
Douglas J. Taatjes, Ph.D.
Cynthia J. Forehand, Ph.D., Dean of the Graduate College

ABSTRACT

Dissolved compounds and ions, including mineral elements and products of microbial metabolism, are present in many cheeses in relatively high concentrations. These dissolved substances may precipitate from the aqueous phase of cheese to form sparingly soluble crystals that can impart a crunchy, gritty, or sandy texture on the cheese. In the present work, optical and diffractometric methods were optimized for use with cheese samples to identify crystal phases in several cheese varieties. These techniques, which included powder X-ray diffractometry (**PXRD**), single crystal X-ray diffractometry (**SCXRD**), and petrographic microscopy (**PM**) have traditionally been used on geological specimens that are quite different from the cheese samples used in the present study. Nonetheless, these techniques were successfully used to gain valuable insight into crystal development in cheese.

Powder X-ray diffractometry was optimized to minimize the occurrence of artifacts that may occur due to the high water content and low crystallinity of some cheese samples. The use of enhanced sample preparation techniques facilitated the identification of organic and inorganic crystal phases such as tyrosine, leucine, brushite ($CaHPO_4 \cdot 2H_2O$), and calcite ($CaCO_3$) in hard and soft cheeses. SCXRD was used to determine the crystal structures of ikaite and struvite, which had been tentatively identified in washed-rind cheese using PXRD. PM was used to observe morphological and optical properties of crystals in white mold cheese and washed-rind cheese.

In two subsequent aging studies, PXRD was used to determine the approximate timing of crystal nucleation in the rinds of white mold cheese and washed-rind cheese. These observations were paired with inductively coupled plasma-atomic emission spectroscopy (ICP-AES) data to demonstrate that the onset of crystallization in the rinds coincided with a diffusion phenomenon in which mineral ions diffused from the center of the cheese and became concentrated in the rind. PM observations demonstrated that maximum crystal size in the rinds generally increased as aging progressed. These observations will be useful in future work that investigates the impact of crystallization on sensory properties of cheese.

CITATIONS

Material from this dissertation has been published in the following form:

Tansman, G., P. S. Kindstedt, and J. M. Hughes. (2015). Crystal fingerprinting: elucidating the crystals of Cheddar, Parmigiano-Reggiano, Gouda, and soft washed-rind cheeses using powder x-ray diffractometry. Dairy Science and Technology 95(5):651-664.

Material from this dissertation has been accepted for publication in The Canadian Mineralogist on August 22, 2016 in the following form:

Tansman, G., P. S. Kindstedt, and J. M. Hughes. (2015). Minerals in food: crystal structures of ikaite and struvite from bacterial smears on washed rind cheese. The Canadian Mineralogist.

Material from this dissertation has been accepted for publication in the Journal of Dairy Science on March 29, 2017 in the following form:

Tansman, G., P. S Kindstedt, and J. M. Hughes. Crystallization and demineralization phenomena in stabilized white mold cheese. Journal of Dairy Science.

ACKNOWLEDGEMENTS

I would like to dedicate this dissertation to my faculty mentors at the University of Vermont who guided me through this endeavor.

I am forever indebted to Dr. Paul Kindstedt, who introduced me to the world of scientific research as a Master's student and mentored me through my doctoral studies as well. I have strived to make Dr. Kindstedt's distinct style of scientific reasoning my own and after hundreds of hours of instruction, he has left an indelible and durable impression.

I must recognize Dr. John Hughes for his friendship and for his tutelage in the complex and delightful study of crystallography. Witnessing Dr. Hughes' incredible ability to integrate the study of Food Science into his extensive expertise has inspired me to seek insight and knowledge wherever available.

I offer my sincere gratitude to Dr. Catherine Donnelly and Dr. Douglas Taatjes for challenging the limits of my understanding in their disciplines.

To my parents, who treasure knowledge and are the foundation upon which my scientific undertakings and achievements are built.

And to my wife and life partner, Serach Eladia, whose energy and grace are inspiration for every idea and meditation.

TABLE OF CONTENTS

LIST OF TABLES

LIST OF FIGURES

CHAPTER 1: COMPREHENSIVE LITERATURE REVIEW

INTRODUCTION

The following review begins by exploring literature related to the ripening of soft surface ripened cheese, which sets the stage for an understanding of crystallization in soft surface ripened cheese aging. Particular emphasis is given to carbon dioxide in cheese aging to reflect the discovery of carbonate minerals, in addition to phosphate minerals, in cheese. Literature related to the thermodynamics and kinetics of carbonate and phosphate mineral precipitation is surveyed to articulate the complexity of mineral stability, even in relatively simple systems, such as cheese. A review of microbial biomineralization literature that details this process in diverse environments is presented to highlight the similarities between the microbial-induced mineralization that occurs on the surface of cheese and other environments. Finally, an overview of the methods of polarized light microscopy in crystal research is provided to highlight the usefulness of this technique and to explore the challenges and opportunities presented by this technology in cheese crystal research.

TEXTURE DEVELOPMENT DURING THE RIPENING OF TRADITIONAL WHITE MOLD CHEESE

FACTORS AFFECTING WHITE MOLD CHEESE SOFTENING

Camembert is a soft surface-ripened cheese variety that is characterized by a surface layer of *Penicillium camembertii* mold, a high moisture content, and a short ripening time (Fox *et al.* 2000). The texture of this cheese develops over a short ripening window from a chalky, acid consistency to a spreadable and sometimes flowing mass

(Gripon 1987). This substantial change is caused by numerous variables including the level of moisture, the mineral content, the degree of proteolysis, and the pH (Boutrou *et al.* 2002). These variables contribute to changes in the casein network's integrity and impact the degree of casein-water interactions. The final texture of Camembert cheese is determined by the extent to which these variables have impacted the casein network, with variations manifesting as different texture characteristics (Karahadian and Lindsay 1987).

Softening of Camembert cheese can be visually observed in cross-sections of the cheese mid-ripening (Gripon 1987). Before softening has affected the whole cheese, a radial cross-section can reveal a progressively softening outer layer with a chalky core, resembling the texture of the fresh cheese. Part of the change in texture is attributed to the proteolytic activity of surface microbes, especially *P. camembertii* (Gripon 1987). However, the direct impact of fungal proteolysis can only explain the phenomenon of paste softening up to a maximum depth of several millimeters from the surface, because the diffusion of fungal proteases is limited (Fox *et al.* 2000; Gripon 1987).

Effect of Moisture Content on Texture Development

Variations in the moisture content can have a profound effect on Camembert texture development. When the initial pH of the cheese is around 4.6 the texture is characterized by a brittle and acidic texture. During ripening, the texture changes to a soft gel, although cheeses with excessively high moisture will over-soften and flow when ripe (Gripon 1987). The tendency of excessively high-moisture Camembert to flow is greatest directly under the rind, where ripening-induced changes in pH and protein structure cause the largest changes in casein water sorption and softening (Gripon 1987).

Moisture content can be impacted post-production through moisture loss to the headspace, especially at low humidity (88%) (Leclercq-Perlat *et al.* 2015). Moisture loss through evaporation is a product of headspace relative humidity and temperature, with temperature increasing evaporation at a given relative humidity level (Leclercq-Perlat *et al.* 2015), while airflow speed can also affect water evaporation rates (Leclercq-Perlat *et al.* 2012). At any humidity level below 100%, some level of surface drying will occur (Leclercq-Perlat *et al.* 2013a), and moisture loss occurs linearly with time (Picque *et al.* 2010). However, humidity levels above 95% discourage the growth of *P. camembertii,* so some moisture loss is inevitable in Camembert production (Leclercq-Perlat *et al.* 2006). As moisture is lost from the cheese surface, additional moisture diffuses from the core to the surface to maintain equilibrium (Leclercq-Perlat *et al.* 2015). When sufficient moisture is lost through evaporation, cheese softening will not occur and the cheese may become hard (Leclercq-Perlat *et al.* 2015). Cheeses that lose more than 10 to 15% of the initial weight are typically unacceptable by the end of aging, and this level of excessive moisture loss occurs if Camembert is aged in a chamber with a relative humidity below 90% (Leclercq-Perlat *et al.* 2012).

The ideal moisture content of Camembert cheese is around 55% (Gripon 1987). In this range, the moisture content is high enough that enzymatic activity and diffusion of dissolved substrates is not inhibited (Gripon 1987), while also being sufficiently low to avoid excessive softening and liquefaction. The moisture level can be controlled by the level of acid produced by the starter culture (Gripon 1987). When excessive acidification occurs, moisture loss may be too great and the cheese can be dry, whereas when

insufficient acidification occurs, cheeses can be too moist, leading to excessive liquefaction.

Effect of Microbial Growth on pH

Acidification by the homofermentative mesophilic lactic acid starter culture results from the metabolic conversion of lactose to lactic acid. (Fox *et al.* 2000; Gripon 1987). Most of this acidification occurs during drainage (Gripon 1987), which results in a very demineralized curd (Boutrou *et al.* 2002; Lucey and Fox 1993). The extent of acidification by the starter culture can affect the level of cheese mineralization (Gripon 1987), which has an important effect of cheese buffering and the resistance to subsequent changes in pH (Lucey and Fox 1993). The pH at demolding is typically between 4.6-4.8 (Fox *et al.* 2000; Gripon 1987). The surface of Camembert becomes colonized by yeasts and mold, either through purposeful inoculation, or adventitious inoculation in traditional production (Fox *et al.* 2000). These species are able to colonize the rind due to their tolerance of high salt and low pH environments (Fox *et al.* 2000).

P. camembertii is an obligate aerobe and the main fungal species in Camembert. *G. candidum*, a yeast, may also be inoculated or may inoculate adventitiously. Heterofermentative adventitious yeasts are also present, and along with *P. camembertii*, they consume lactose while growing on the surface (Fox *et al.* 2000), resulting in a steady reduction in the amount of residual lactose (Gripon 1987). Although multiple species of yeasts and bacteria are typically present on the surface of Camembert (Lessard *et al.* 2012), *P. camembertii* and *G. candidum* dominate the rind ecosystem (Leclercq-Perlat *et al.* 2013b). Microbes at the surface metabolize lactose and cause rapid lactose exhaustion near the rind, whereas residual lactose at the core slowly diffuses toward the rind where it

too is metabolized by the surface microbes (Gripon 1987; Leclercq-Perlat *et al.* 2004a). Within several weeks, all residual lactose in the cheese is exhausted (Gripon 1987).

Lactic acid produced by the starter culture is also consumed by the microbes on the surface (Gripon 1987). *P. camembertii* prefers lactose as an energy source (Leclercq-Perlat *et al.* 2013b), and other surface microbes preferentially consume lactose before consuming lactate, whereas *G. candidum* does not consume lactose and only consumes lactate (Leclercq-Perlat *et al.* 2004a). Similar to lactose, lactate levels in the rind are consistently lower than in the core because the lactate bound for the rind slowly diffuses from the core to the rind (Fox *et al.* 2000). This slow diffusion creates a pH gradient between the rind and the core (Fox *et al.* 2000). Regardless of the specific combination of microbes competing for lactate on the surface, by the end of ripening the lactate concentration at the rind and core are negligible (Gripon 1987).

When lactose is exhausted at the surface, *P. camembertii* extensively metabolizes proteins, which produces enormous quantities of ammonia, although some ammonia production can be detected while some lactose is still available (Leclercq-Perlat *et al.* 2013b). The production of ammonia raises the pH at the rind (Karahadian and Lindsay 1987), which further contributes to the pH gradient created by the assimilation of lactate (Fox *et al.* 2000; Gripon 1987). Lactate consumption and ammonia production slowly neutralize the acidity that was originally produced by the lactic acid starter culture (Fox *et al.* 2000; Gripon 1987). The elevated pH near the rind can be visually assessed by the appearance of a soft layer under the rind (Gripon 1987), which slowly progresses toward the core as aging progresses.

FACTORS AFFECTING CASEIN HYDRATION

When the pH is near casein's isoelectric point at 4.6 in the fresh cheese, the net charge on the casein proteins is close to zero (Gripon 1987). As the pH becomes moderately acidic, neutral, or even slightly alkaline, the net charge becomes more negative (Fox *et al.* 2000; Schlesser *et al.* 1992). The elevated net charge on casein modifies the nature of casein-casein interactions and encourages casein-water interactions, which ultimately increase the water holding capacity of casein (Gripon 1987; Schlesser *et al.* 1992). The tendency of casein to hold more water at higher pH may explain why some investigators (Le Graet *et al.* 1983) have noted that the outer portion of traditional Camembert can hold more moisture than the core, despite the drying effect of surface evaporation (Gripon 1987). The firmness of Camembert is related to the quantity of intact casein and the level of hydration of the intact casein (Schlesser *et al.* 1992), which partially explains the softening of Camembert texture with increased pH.

Experiments by Noomen (1983) on rennet-free model cheese suggested that elevated pH in itself is not sufficient to cause softening in Camembert. In those experiments, rennet-free cheese exposed to ammoniated atmospheres to artificially raise the pH became hard and springy, whereas the proteolytic effect of residual rennet in control cheeses caused the cheese to soften upon exposure to ammonia. Proteolysis increases the water binding capacity of casein, and as Camembert ripening progresses, the hydrolysis of the casein network, as indicated by an elevated proportion of acid-soluble nitrogen to total nitrogen, makes available more water binding sites (Schlesser *et al.* 1992). Thus, upon exposure to elevated pH, the hydrolyzed casein network more readily absorbs water and softens.

PROTEOLYSIS AND TEXTURE DEVELOPMENT

The ability of residual rennet to promote paste softening is related to the proteolysis of α_{s1}-casein, the effect of which can be detected within hours of initial production (Gripon 1987). The optimum pH for residual rennet activity on casein is 5.0, which suggests that the activity of rennet diminishes as the pH increases beyond that optimum, especially at the surface (Gripon 1987). The activity of the milk proteinase plasmin is typically not as extensive as residual rennet during cheese ripening. Nonetheless, γ-caseins, which result from plasmin activity on β-casein, are observed in Camembert at the end of ripening (Gripon 1987). Given that the pH for optimum plasmin activity is approximately 8.0, one would expect plasmin to be active in Camembert, particularly in the rind, where the pH is neutral or slightly alkaline by the end of ripening (Fox *et al.* 2000; Gripon 1987).

β-casein hydrolysis is also fairly extensive in Camembert, although this is mostly attributed to the action of *Penicillium* proteinases at the surface (Gripon 1987). The breakdown product of rennet hydrolysis of β-casein, β-I, is not observed in Camembert cheese during ripening, indicating that rennet does not degrade β-casein in Camembert (Gripon 1987). In fact, investigation of the proteolytic activity of *P. camembertii* on curds revealed that, while plasmin and residual rennet undoubtedly contribute to casein proteolysis, the role of rennet is minor (Fox *et al.* 2000) and the major driver of proteolytic activity in Camembert is *P. camembertii* (Fox *et al.* 2000; Gripon 1987).

The level of proteolysis at the rind, starting around day 6 or 7 of ripening, is very high, whereas the proteolytic activity at the core remains minimal throughout aging (Gripon 1987). Presumably, the low level of rennet and plasmin activity is still sufficient

to create the necessary proteolysis for softening to occur at elevated pH, per the findings of Noomen (1983). The increase in proteolytic activity at the rind coincides with the growth of *P. camembertii* (Fox *et al.* 2000), whereas the low and unchanging level of proteolysis at the core supports previous observations that *P. camembertii* proteinases experience limited diffusion and is in agreement with the notion that proteolytic activity at the core is due to residual rennet and plasmin. Yeast may begin growing on the surface as early as day 2 (Rousseau 1984), although the elevated level of proteolysis does not occur until the initial growth of *P. Camembertii*.

In ripe cheese, soluble nitrogen as a percentage of total nitrogen is typically 35% and 25% in the rind and core, respectively (Gripon 1987). The soluble nitrogen fraction includes small peptides, amino acids, and ammonia. The ammonia is produced by deamination of amino acids, and results in a relatively high level of ammonia as a fraction of total nitrogen, which is typically in the range of 7-9% in ripe cheese (Gripon 1987). Given that the extensive *P. camembertii*-derived proteolysis is limited to a narrow band beneath the rind, the elevated level of soluble nitrogen in the core suggests that some of this soluble nitrogen diffuses to the core from the rind and is originally derived from the proteolytic activity of *P. camembertii* (Fox *et al.* 2000; Gripon 1987).

The active range of *P. camembertii*'s extracellular proteinases varies, with the acid proteinases stable under slightly acidic conditions and metalloproteinases stable at much higher pH (Gripon 1987). The cocktail of extracellular proteinases released by *P. camembertii* are active on α_{s1}-casein, β-casein, and κ-casein (Gripon 1987). Interestingly, the proteolytic activity of *P. camembertii* on aseptic model cheese resembles the proteolytic activity of commercial Camembert, which strongly suggests that the

proteolytic activities of *P. camembertii* are central to the overall proteolytic processes in Camembert cheese (Gripon 1987).

The soluble nitrogen fraction that results from *P. camembertii*'s proteolytic activity is further modified through the action of peptidases released by *P. camembertii*, *G. candidum*, the adventitious surface yeasts, and lactic acid bacteria (Gripon 1987). The greatest contribution to this activity is by the extracellular peptidases of *P. camembertii*, whereas the contribution of the yeasts and lactic acid bacteria is limited (Gripon 1987). The extracellular carboxypepidases and aminopeptidases released by *P. camembertii* are active over a wide pH range and have broad specificity (Gripon 1987), although *P. camembertii*'s proteolytic system tends to be more active overall when the pH is at least 6.0 (Leclercq-Perlat *et al.* 2015).

Production of Metabolic Gases

Peptidolytic activity results in the release of many amino acids that can be further metabolized to produce carbon dioxide and ammonia. Decarboxylation of amino acids results in the release of carbon dioxide (Picque *et al.* 2006), and the deamination of amino acids results in the production of ammonia (Gripon 1987). The ammonia can diffuse toward the core along the pH gradient and contributes to the deacidification process (Karahadian and Lindsay 1987). Interestingly, a metabolic synergy exists between *G. candidum* and *P. camembertii* in which *P. camembertii* liberates amino acids because of its peptidolytic activity, and *G. candidum* produces large amounts of ammonia by deaminating those liberated amino acids (Karahadian and Lindsay 1987).

Dynamic Between P. camembertii and G. candidum

Certain ripening conditions can affect the balance between *P. camembertii* and *G. candidum*. The level of salt can greatly impact the competition between *P. camembertii* and *G. candidum* (Gripon 1987). Low salt levels stimulate *P. camembertii* growth (Fox *et al.* 2000), although overall salt level does not have a very large direct impact on *P. camembertii* growth (Gripon 1987). Conversely, *G. candidum* is sensitive to salt levels as low as 1% (Fox *et al.* 2000). Although excessive salting can inhibit *G. candidum*, insufficient salting can favor *G. candidum* competition over *P. camembertii* and hinder the important metabolic functions of *P. camembertii* (Gripon 1987).

Different combinations of temperature and relative humidity can also affect the growth of the surface flora. For instance, at excessively high relative humidity (98%) and temperature (16°C), *P. camembertii* growth is diminished compared to that or *G. candidum*, whereas at cooler temperatures (8°C) the negative effect of high humidity on *P. camembertii* is less pronounced (Leclercq-Perlat *et al.* 2015). These departures from the ideal balance between *P. camembertii* and *G. candidum* can negatively impact the appearance of the surface flora and can also diminish the quality of the cheese paste by impacting the rate and extent of proteolysis and cheese softening (Leclercq-Perlat *et al.* 2015). At lower temperature, the rate of proteolysis is diminished because enzyme kinetics are slower and softening of the paste is thus decelerated (Leclercq-Perlat *et al.* 2015). The drying caused by low relative humidity (88%) can have a similar effect on enzyme function and can likewise also impede the softening process (Leclercq-Perlat *et al.* 2015).

Effects of Temperature on Metabolic Activities

Consumption of lactose is greatly affected by temperature but it is not greatly affected by humidity because the surface microbes that consume lactose tend to be more sensitive to temperature, and with decreased temperature their lactose consumption decreases as well (Leclercq-Perlat *et al.* 2012). The response of lactate consumption to temperature and humidity is somewhat more complicated because it is dependent on temperature as well as the interaction between temperature and relative humidity (Leclercq-Perlat *et al.* 2012). This may be due to the excessive amount of drying that can occur at low relative humidity later in the aging process once lactose has been exhausted but while lactate is still being consumed.

At high temperatures, the effect of excessive proteolysis directly under the rind can resemble the effect of excessive moisture content and cause the cheese directly under the rind to liquefy and flow (Leclercq-Perlat *et al.* 2015; Leclercq-Perlat *et al.* 2012). High temperatures also affect the time that it takes for the cheese under the rind to show the first indication of softening (Leclercq-Perlat *et al.* 2012). This may be because temperature increases biological activity on the rind as well as the rate of substrate diffusion from the rind to the core (Leclercq-Perlat *et al.* 2012). This would have the effect of hastening proteolysis as well as carbon substrate diffusion and consumption, and would speed up cheese texture development (Leclercq-Perlat *et al.* 2012). It should be noted that an increased rate of texture development is not indefinitely beneficial because it can lead to under-rind liquefaction and excessive cheese softening, in addition to visual and organoleptic defects (Leclercq-Perlat *et al.* 2006; Leclercq-Perlat *et al.* 2012).

DIFFUSION OF CALCIUM AND PHOSPHATE

The pH gradient that results from lactate consumption and ammonia production causes calcium and phosphate to exceed their solubility at the rind and precipitate (Amrane and Prigent 2008; Brooker 1987). This results in a calcium phosphate gradient in the cheese that causes calcium and phosphate to diffuse toward the rind (Fox *et al.* 2000; Gripon 1987). During this diffusion, the levels of those ions in the core decrease (Le Graet and Brule 1988; Le Graet *et al.* 1983). This is technologically noteworthy because calcium crosslinks casein proteins and removal of calcium from the matrix results in decreased casein network structure, increased casein solubilization, and cheese softening (Karahadian and Lindsay 1987).

Investigators originally attributed the elevated concentration of calcium and phosphate in the rind to the growth of the surface flora and the sequestration of minerals in the biomass of *P. camembertii* (Metche and Fanni 1978). Although calcium diffusion does coincide with the mold growth, the diffusion of calcium can be attributed to the deacidifying activity of the mold, rather than to a direct effect. This has been confirmed by trials that have artificially recreated the diffusion of calcium and phosphate by placing fungicide-treated cheeses in ammoniated chambers to simulate the deacidification of the rind (Amrane and Prigent 2008; Gaucheron *et al.* 1999; Le Graet *et al.* 1983).

The precipitation of calcium phosphate in the rind results in a high amount of pH buffering around pH 6 due to the release of protons from phosphate as phosphate complexes with calcium (Lucey and Fox 1993). Despite the buffering capacity, the pH steadily increases due to the surface microbe's metabolism (Boutrou *et al.* 1999). Calcium and phosphate ions steadily diffuse from the core to the rind throughout aging

(Amrane and Prigent 2008; Le Graet *et al.* 1983), which results in a considerable concentration of calcium and phosphate in the rind. By the end of aging, up to 80% of the calcium and 55% of the phosphate are concentrated in the rind (Fox *et al.* 2000). Although Camembert contains a relatively small quantity of calcium and phosphate at the beginning of aging, this amount is sufficient to participate in the structure of the curd by bridging negative phosphate residues and carboxyl groups on casein molecules (Boutrou *et al.* 2002). Therefore, the removal of calcium and phosphate through this mechanism has a meaningful impact on cheese softening (Karahadian and Lindsay 1987).

Interrelatedness of Softening Processes

By the end of a typical Camembert cheese ripening, the pH at the rind is near 7.0, whereas pH level at the core is still slightly acidic (Fox *et al.* 2000; Gripon 1987; Le Graet and Brule 1988). Although proteolysis, which disrupts the protein matrix, is mostly limited to the surface of the cheese, a limited proteolytic activity by residual rennet and plasmin, as well as the removal of calcium through the diffusion mechanism, compromises the casein network's integrity (Fox *et al.* 2000). The combination of proteolysis and demineralization creates the conditions for extensive softening upon exposure to elevated pH as deacidification progresses (Fox *et al.* 2000; Karahadian and Lindsay 1987; Lucey and Fox 1993).

A stepwise regression analysis of the physicochemical parameters affecting Camembert cheese texture revealed that pH has the greatest impact on texture, followed by dry matter content, with proteolysis and demineralization playing relatively minor roles (Vassal *et al.* 1986). However, these effects are difficult to separate because the processes of proteolysis, calcium diffusion, and elevated pH are interconnected. An

understanding of each of these processes and their interactions is critical for deconstructing the complex biological and physico-chemical ripening. Furthermore, previous ripening models, such as the aseptic cheese used by Noomen (1983), may have introduced analytical errors that over-emphasized some effects while ignoring others.

Noomen (1983) produced aseptic white mold cheese according to a method that was originally developed by Visser (1976); however, the original method was intended to produce an aseptic cheese that emulated the composition of Gouda. Even though Noomen (1983) produced an aseptic cheese with a pH of 4.6 and a moisture content of 55%, which resembles Camembert, the original technique does not seem entirely compatible with the manufacture of a white mold-style cheese. The aseptic technique used ion exchange to remove calcium from the milk before clotting, followed by renneting, heat-inactivation of the rennet, and addition of a calcium salt before heating. This sequence allowed the first phase of enzymatic coagulation to take place before clotting. Visser (1976) needed to add an excess of calcium to the milk to induce clotting. The excess calcium was then removed through a curd washing step, which is characteristic of Gouda production but not used in white mold cheese production. Noomen (1983) did not report calcium concentrations and therefore one cannot conclude what effect the calcium concentration had on the ability of the model cheese to soften.

Effect of O_2 and CO_2 on White Mold Cheese Texture Development

Aerobic Respiration of White Mold Cheese Microbes

The aerobic metabolism of carbon and amino acid substrates in Camembert results in water and carbon dioxide production (Abraham *et al.* 2007; Fox *et al.* 2000; Leclercq-Perlat *et al.* 2013a). The consumption of oxygen and production of carbon dioxide by the aerobic cheese rind microbes can influence the concentrations of these gases in the headspace (Helias *et al.* 2007). In return, the growth and biological activities of the cheese surface microbes are influenced by the gaseous composition of the headspace (Helias *et al.* 2007; Leclercq-Perlat *et al.* 2013a; Leclercq-Perlat *et al.* 2006). The composition of the headspace is important both during chamber aging, wherein the cheese in exposed to a relatively large headspace, as well as during packaging, when the cheese is exposed to a limited headspace inside of the wrapper.

Oxygen consumption and carbon dioxide production can be used to estimate the extent of respiratory metabolism (Helias *et al.* 2007). During ripening, the consumption of oxygen and the production of carbon dioxide are closely correlated (Leclercq-Perlat *et al.* 2006; Picque *et al.* 2006). The partial pressures of oxygen and carbon dioxide can impact the respiration rate of *P. camembertii* (Picque *et al.* 2010). At a low concentration of carbon dioxide, in the range of 2% or 0.4 atm, the metabolism of *P. camembertii* is highly stimulated (Picque *et al.* 2010), and at 4% carbon dioxide the mold can thrive, as long as the oxygen level is at least 19% (Picque *et al.* 2010). At progressively higher carbon dioxide concentrations, *P. camembertii* begins to die (Picque *et al.* 2010). Even at relatively high oxygen concentrations of 12% or more, increased carbon dioxide levels

cause *P. camembertii* growth to slow, and at carbon dioxide concentrations above 10%, *P. camembertii* growth is inhibited (Picque *et al.* 2006). *G. candidum* is also stimulated by low carbon dioxide concentrations, and at higher concentrations *G. candidum* dominates as *P. camembertii* growth suffers (Leclercq-Perlat *et al.* 2006). At carbon dioxide concentrations above 6%, the growth of *G. candidum* is reduced as well (Leclercq-Perlat *et al.* 2006)

When the headspace inside a ripening chamber is not recycled with fresh air, the levels of oxygen and carbon dioxide depend on the gaseous exchange with the cheese (Helias *et al.* 2007). Under completely static conditions, the level of carbon dioxide in the headspace can become excessive and result in defective cheese (Helias *et al.* 2007). The oxygen in a static chamber is quickly exhausted and replaced with carbon dioxide (Picque *et al.* 2006). In this scenario, the respiration rate of the mold decreases once the partial pressure of oxygen drops below approximately 0.05 atm (Roger *et al.* 1998). *P. camembertii* respiration rate is high and fairly constant when oxygen content in the head space is above 0.05 atm (Roger *et al.* 1998). Below 0.05 atm the respiration rate decreases until no respiration is detectable at 0 atm of oxygen (Roger *et al.* 1998). Thus, at a given oxygen content, assuming the carbon dioxide content is low, the rate of *P. camembertii* metabolism can be estimated (Roger *et al.* 1998), which can be used to predict the rate of substrate consumption, deacidification, and cheese softening.

Effect of Headspace Carbon Dioxide on Ripening

In order to keep the level of carbon dioxide down, the headspace in a ripening chamber may be subjected to a variety of treatments including continuous renewal and periodic renewal (Picque *et al.* 2006). Under continuous renewal, the level of carbon

dioxide remains negligible and the level of oxygen remains around the ambient concentration of approximately 20% (Picque *et al.* 2006). Under continuous renewal, early ripening progresses more slowly than if some carbon dioxide were present (Picque *et al.* 2006), presumably because of the stimulatory effect that low levels of carbon dioxide have on *P. camembertii*. The stimulatory effect of carbon dioxide can accelerate the softening of the cheese, as measured by the depth of the soft portion at a given time during ripening (Picque *et al.* 2006).

Although 2% and 6% carbon dioxide both have a stimulatory effect on respiration, the respiration rate at 6% is somewhat lower than at 2%, but still higher than it would be in the absence of carbon dioxide (Picque *et al.* 2006). In contrast, under static headspace conditions, the process of softening begins normally but ceases around the 9th day of aging (Picque *et al.* 2006). After day 9, carbon dioxide production from the cheese stops, which coincides with a diminished concentration of oxygen in the headspace (Picque *et al.* 2006). Shortly after respiration by surface microbes is arrested, the lactate gradient that was established by initial surface growth equilibrates, and lactate diffusion stops (Leclercq-Perlat *et al.* 2006). Under other headspace conditions, as long as the oxygen level remains above a minimum concentration, the oxygen level should not limit the growth *P. camembertii* regardless of the carbon dioxide level, although the minimum concentration cited by different authors varies from 1 to 5% (Picque *et al.* 2006).

Rind Texture Defects Under Elevated Headspace Carbon Dioxide

The under-rind portion of cheese aged under static headspace tends to become runny (Leclercq-Perlat *et al.* 2006; Picque *et al.* 2006), which suggests increased proteolysis or moisture retention. The texture of cheese aged under oxygenated

conditions with high (6%) carbon dioxide also tends to have a runny texture, which indicates that the poor texture is probably related to the level of carbon dioxide and not the level of oxygen (Leclercq-Perlat *et al.* 2006; Picque *et al.* 2006). Some of the minor yeasts on the surface tend to die earlier when exposed to elevated carbon dioxide levels, and it is possible that the runny texture results from extensive proteolysis by endocellular proteases released when these cells lyse (Leclercq-Perlat *et al.* 2006).

When cheeses are aged under static headspace the rinds tend to become sticky (Picque *et al.* 2006). The moisture content of the rinds from cheeses aged under high carbon dioxide levels tends to be higher than normal, and these cheeses tend to not hold their form (Leclercq-Perlat *et al.* 2006; Picque *et al.* 2006), although a mechanistic explanation for this type of softening has not yet been developed. The poor quality of the under-rind may be related to the tendency of carbon dioxide to dissolve in the water phase of the cheese if it is present at high concentrations in the headspace (Picque *et al.* 2006). A high level of dissolved carbon dioxide apparently diminishes the quality of cheese texture in unripened cheese varieties as well (Picque *et al.* 2006), although here too, a mechanistic explanation is lacking.

Stimulation of Under-Rind Development by Headspace Carbon Dioxide

The development of the soft under-rind is fastest for cheeses aged under a low (2%) concentration of carbon dioxide, which confirms that *P. camembertii* is stimulated by carbon dioxide (Leclercq-Perlat *et al.* 2006; Picque *et al.* 2006). The depth of the under-rind correlates closely with the liberation of carbon dioxide (Picque *et al.* 2006). Whereas the carbon dioxide almost certainly comes from the oxidation of lactate and the decarboxylation of amino acids (Picque *et al.* 2006), determining the effect on each

metabolic process is more complicated because multiple rind species contribute to the oxidation of substrate. For instance, the adventitious yeasts that consume lactose during the first days of aging before *P. camembertii* implantation are apparently not affected by the composition of the headspace (Picque *et al.* 2006), so it is not surprising that atmospheric composition does not have a large effect on lactose oxidation in the rind (Leclercq-Perlat *et al.* 2006).

During the intermediate part of ripening, starting on day 6, cheese aged in the presence of a small amount of carbon dioxide ripens faster than cheese under continuous or periodic atmospheric renewal, as indicated by the production of carbon dioxide and the depth of the soft under-rind (Leclercq-Perlat *et al.* 2006). Strangely, cheese aged in the presence of carbon dioxide does not metabolize lactate any faster than cheese in continuous renewal, and actually stops aging prematurely after being wrapped and placed in cold storage due to diminished ammonia production during cold storage (Leclercq-Perlat *et al.* 2006). These phenomena suggest that carbon dioxide dissolved in the cheese may have an inhibitory effect on peptidase and deaminase activities (Leclercq-Perlat *et al.* 2006). The impact of dissolved carbon dioxide on cheese ripening processes is quite complex and interesting, although it does not appear that extensive research has been conducted in this area.

Impact of Packaging on Cheese Ripening During Cold Storage

The concept of modified atmosphere packaging has not been extensively researched in the context of Camembert cheese, although it holds interesting possibilities for extended shelf-life (Picque *et al.* 2010; Rodriguez-Aguilera *et al.* 2011; Roger *et al.* 1998). Once inside of a package, the levels of oxygen and carbon dioxide are critically

important because the surface is alive and must be maintained throughout the shelf-life (Rodriguez-Aguilera *et al.* 2011). One of the major practical differences between modifying a ripening chamber's atmosphere and modifying a packaging atmosphere is that the cheese in the packing has already ripened for nearly two weeks, and the established surface microbes are not extensively growing anymore (Picque *et al.* 2010). This is important because many of the cheese ripening processes, such as surface deacidification, occur at an earlier point and are thus not affected by the composition of the packaging headspace (Picque *et al.* 2010). In contrast, modification of the ripening chamber atmosphere can have a profound impact on the development of texture, as described above.

When placed in gas-impermeable packaging, the surface microbes quickly exhaust the available volume of oxygen, while producing carbon dioxide (Rodriguez-Aguilera *et al.* 2011). Under the anaerobic conditions that quickly develop, low levels of carbon dioxide continue to be produced and *P. camembertii* rapidly discolors and dies (Rodriguez-Aguilera *et al.* 2011). Under anaerobic conditions, the texture of the Camembert continues to soften and becomes sticky (Rodriguez-Aguilera *et al.* 2011). This is very similar to the ripening of Camembert under static chamber headspace, in which cheeses also develop a sticky rind. This further suggests that an excessively high carbon dioxide concentration can result in cheese stickiness. As in the case of chamber aging, this softening cannot be attributed to the activity of the surface mold, which does not function without at least a minimum quantity of oxygen. Rodriguez-Aguilera *et al.* (2011) suggested that softening could result from α_{s1}-casein hydrolysis by rennet, increased surface pH, and calcium diffusion, although these processes also result in

cheese softening under aerobic conditions (Karahadian and Lindsay 1987), and therefore do not constitute a reasonable mechanistic explanation.

Inside of the packing, the Camembert core continues to deacidify because of the slow but steady metabolism of the rind microbes. Camembert packaged under anaerobic conditions experiences a smaller level of core deacidification than cheese in packages that are permeable to oxygen (Rodriguez-Aguilera *et al.* 2011), which is in agreement with the importance of *P. camembertii* aerobic metabolism. The presence of 2-3% oxygen exchange in the packaging allows *P. camembertii* to survive, although the pH increase at the core is slowed considerably compared to control conditions where oxygen is not limited (Rodriguez-Aguilera *et al.* 2011). The availability of oxygen is the major factor determining respiration rate during packaged cold storage (Roger *et al.* 1998). Lower metabolic rates are linked to slower proteolysis and slower deacidification of the core (Picque *et al.* 2010). Thus, any intervention that impacts the metabolic rate will likewise affect the rate of lactate consumption, ammonia production, and core softening. In the context of a packaged product, limiting the availability of oxygen and increasing the level of carbon dioxide can provide an extended shelf-life and is therefore desirable (Leclercq-Perlat *et al.* 2006).

CARBONATE AND PHOSPHATE MINERAL PHASE FORMATION AND TRANSFORMATION

THERMODYNAMIC AND KINETIC STABILITY OF CRYSTAL PHASES

The science of mineral formation is governed by principles that determine the outcome of crystallization phenomena (Noffke 2009). It is generally accepted that a system must be supersaturated with respect to a crystal phase and crystal nuclei must exist in order for that crystal phase to grow (Garside 1987). Although these principles are relatively straight forward, it is nonetheless difficult to predict the result of a crystallization reaction due to a multitude of variables that can affect the outcome (Johnsson and Nancollas 1992). The most stable mineral in an aqueous system is determined by the thermodynamics of the system, which reflect the solubility of a mineral in an aqueous system. Using just thermodynamics, one would expect the least soluble mineral that could result from a combination of available reactants to be the only phase at the end of a reaction. A trove of crystallographic research is available that demonstrates that crystallization is not governed by the principles of thermodynamics alone. Kinetic phenomena, which are affected by many different variables, often determine whether metastable phases can persist in a system at the expense of the most stable and least soluble phase (Arifuzzaman and Rohani 204).

Metastability appears to play an important role in the formation of mineral phases in geological systems, as well as in cheese, where metastable phases have recently been identified (Tansman *et al.* 2015b; Tansman *et al.* In Press). The metastable calcium phosphate brushite ($CaHPO_4 \cdot 2H_2O$) and the metastable calcium carbonate ikaite ($CaCO_3 \cdot 6H_2O$) have been observed in several different cheese varieties. In addition,

struvite ($NH_4MgPO_4 \cdot 6H_2O$), which is stable in saturated solution but unstable when exposed to air, has also been observed. Calcite ($CaCO_3$), which is the stable calcium carbonate phase at STP, has been observed in cheese alongside its hydrated counterpart ikaite. Brushite, the least stable calcium phosphate crystal phase, has been observed in cheese, whereas hydroxylapatite (**HAP**) ($Ca_5(PO_4)_3(OH)$), the most stable calcium phosphate, has not been observed in cheese. The manifestation of metastable phases in cheese highlights the complex chemistry involved in crystallization phenomena. In geological settings, the mineralization dynamics are complicated even further by the availability of a multitude of elements and ions that do not exist in cheese in appreciable quantities, which could add additional variables to the crystallization chemistry in geological systems.

Effect of pH on Calcium Phosphate Stability

Brushite was the first mineral that I observed in cheese and it is often the first mineral phase to form in the rinds of surface ripened cheeses. Calcium phosphates belong to a group of minerals that contain calcium and phosphate in a variety of molar ratios. Some of these phases may also contain stoichiometric water or hydroxyl molecules in their crystal structures. From slightly acidic to alkaline pH, HAP is the most soluble of the calcium phosphates, but below a pH of approximately 4, brushite is more stable than HAP (Ferreira *et al.* 2003; Johnsson and Nancollas 1992). As a result of this stability, brushite is often found in low pH systems such as guano caves (Kuz'mina *et al.* 2013). The solubility of brushite increases drastically (although less so than other calcium phosphates) as the pH decreases (Abbona *et al.* 1993; Kuz'mina *et al.* 2013). This is

reflected in experiments that have shown that at lower pH, increased concentrations of reactants are necessary to induce brushite precipitation (Arifuzzaman and Rohani 204; Toshima *et al.* 2014). Thus, even within its stable zone, the conditions needed for brushite precipitation are specific and somewhat rare in nature.

The increased solubility of calcium phosphates with decreasing pH is due to the shift in phosphate equilibrium from predominantly deprotonated phosphate at high pH to predominantly dihydrophosphate at very low pH. Brushite is a product of calcium and hydrophosphate (Miller *et al.* 2012), and it is therefore not surprising that it is most stable in the pH region where hydrophosphate predominates (Lee and Kumta 2010). The activity product of brushite is a product of the concentrations of calcium and hydrophosphate (Pak *et al.* 1971), which implies that brushite supersaturation is dependent on total phosphate content as well as pH (Arifuzzaman and Rohani 204). The tendency of phosphate to form ion pairs with various free ion species in solution can also greatly impact the phosphate protonation equilibrium (Johnsson and Nancollas 1992). The saturation index is determined from the concentration of the reactants, and in the case of brushite, only the concentration of hydrophosphate would impact the supersaturation calculation (Abbona *et al.* 1993), whereas unprotonated and doubly-protonated phosphate would be considered common ions. This concept applies universally and explains why the solubility of phases that contain molecules that act as proton buffers, including several other phases that will be discussed here, fluctuate with pH.

PRECIPITATION OF METASTABLE CALCIUM PHOSPHATE

Many of the systems in which brushite is found, including cheese, are within the pH region in which brushite is metastable with respect to HAP. In the metastable region, when solutions are supersaturated with respect to brushite they are also supersaturated with respect to monetite ($CaHPO_4$), octacalcium phosphate (**OCP**) ($Ca_8H_2(PO_4)_6 \cdot 2H_2O$) and HAP (Arifuzzaman and Rohani 204), with HAP as the most stable phase. The tendency of metastable phases to precipitate is based on the Ostwald rule, which states that when sequential precipitation occurs, the most soluble phases precipitate first (Johnsson and Nancollas 1992). Per this logic, even if brushite, as the least soluble crystal phase, should precipitate, it would be transient, with HAP eventually precipitating and causing brushite to dissolve. In many systems, such as cheese, metastable phases, including brushite, can persist, whereas the stable phases do not appear. In these systems, the kinetics of phase formation favor the metastable phase(s) at the expense of the stable phase, although the specific metastable phases that persist in a system depend on many conditions (Johnsson and Nancollas 1992).

The Ostwald rule reflects the kinetics of nucleation in supersaturated solutions. The magnitude of the minimum supersaturation needed before nucleation will occur is called the critical supersaturation (Arifuzzaman and Rohani 204). Phases that are more stable tend to have higher critical supersaturations compared to phases that are less stable. Among the calcium phosphate phases, HAP has the highest critical supersaturation followed by OCP and brushite. The magnitude of critical supersaturation is a product of the interfacial free energy between the crystal and the solution. Increasingly soluble phases tend to have lower interfacial free energies. As a result of the different interfacial

free energies, under moderately acidic conditions, the kinetic coefficient of brushite is 10 orders of magnitude greater than OCP and 18 orders of magnitude greater than HAP (Arifuzzaman and Rohani 204), which explains why brushite can exist in kinetically metastabilized equilibrium with HAP (Ferreira *et al.* 2003).

At a moderately acidic pH, the rate of HAP nucleation is so low and the rate of brushite nucleation so high that existing HAP nuclei cannot grow (Ferreira *et al.* 2003). At higher pH, the supersaturation of HAP drives the reaction toward HAP nucleation and growth at the expense of brushite (Ferreira *et al.* 2003; Johnsson and Nancollas 1992). Thus, although HAP is the stable phase at pH over 4, it only tends to form at neutral and basic pH for kinetic reasons (Johnsson and Nancollas 1992).

OCP can be formed on seed crystals around neutral pH if the reaction conditions are such that a solution is supersaturated with respect to OCP and HAP but not brushite (Johnsson and Nancollas 1992). In this scenario, OCP may be the preferred phase because the formation rate of HAP is much lower than that of OCP, while brushite would not be able to grow without being supersaturated. This technique could also be used to precipitate HAP without any metastable phases (Johnsson and Nancollas 1992) Although the kinetic stability of calcium phosphate phases depends on the solution pH (Toshima *et al.* 2014), other kinetically important variables can affect each metastable phase's region of stability.

Brushite has been observed as a metastable phase in systems with a pH as high as 6.9 (Pak *et al.* 1971) and 7.2 (Holt *et al.* 1987), although other researchers have observed that monetite ($CaHPO_4$), the anhydrous polymorph of brushite tends to form when the initial solution pH is above 5.8 (Kuz'mina *et al.* 2013). The disparity between these

findings likely results from conditions other than pH that affect the precipitation kinetics. Temperature, level of supersaturation, and initial concentration of reagents can also influence metastability (Ferreira *et al.* 2003). Monetite, OCP, and amorphous calcium phosphate (**ACP**), which is a short-lived non-crystalline phase that is composed of aggregates of primary nuclei (Johnsson and Nancollas 1992), can each be precipitated by modulating the concentration of reactants and the temperature of the solution (Abbona *et al.* 1993).

Elevated temperatures can be used to obtain a different set of products than can be obtained from equivalent reactions at room temperature. For instance, monetite can be crystallized from 40°C solutions with high supersaturation and low pH (Abbona *et al.* 1993), whereas equivalent conditions at room temperature would yield ACP or brushite, depending on the level of supersaturation (Abbona *et al.* 1993). Higher temperature (40°C) seems to have a negative effect on the kinetics of brushite formation, favoring monetite and ACP (Abbona *et al.* 1993). In a series of experiments, Abbona *et al.* (1993) found that a small amount of brushite tended to form alongside monetite and ACP at a higher reaction temperature, although these crystals were characterized by a (001) twin. Well-formed single brushite crystals displaying stable faces could be formed as a unique phase under relatively low supersaturation at room temperature (Abbona *et al.* 1993), which seems to imply that conditions that promote slower kinetics favor brushite as opposed to other metastable phases.

Effect of Additives on Metastable Calcium Phosphate Phases

Brushite tends to dehydrolyze into monetite over time (Lee and Kumta 2010) and rapidly transforms into HAP when placed into neutral or alkaline solutions (Lee and

Kumta 2010; Miller *et al.* 2012; Pak *et al.* 1971). Phase transformation to the most thermodynamically stable phases is irreversible (Johnsson and Nancollas 1992), although the presence of additives in solution can greatly stabilize brushite. In the presence of magnesium ions, brushite crystallizes as Mg-substituted brushite (Lee and Kumta 2010). The amount of substitution is related to the concentration of Mg in solution, with higher levels of substitution conveying greater kinetic stability. The Mg atoms apparently prevent a phase change by tightly bonding to the lattice water and preventing dehydrolysis (Lee and Kumta 2010). Mg also promotes the precipitation of brushite at the expense of HAP by stabilizing acidic precursors (Johnsson and Nancollas 1992), which would have a positive effect on the kinetics of brushite formation.

Additive ions, including Mg^{2+} and Zn^{2+}, electrostatically bind to the surface of HAP and have an inhibitory effect on HAP growth, whereas their inhibitory effect on hydrated metastable calcium phosphate phases is limited (Johnsson and Nancollas 1992). Lattice water in OCP and brushite may be responsible for the diminished electrostatic interaction between additive ions and growing surfaces, and may also reflect their diminished tendency to incorporate ions into their lattices (Johnsson and Nancollas 1992). At any rate, the inhibitory effect of additive ions does not have a pronounced effect on brushite growth, whereas HAP growth can be inhibited (Johnsson and Nancollas 1992). Pyrophosphate and peptides may also inhibit HAP growth, and therefore may stabilize brushite (Pak *et al.* 1971). In contrast, the introduction of even small amounts of sulfate into solution will promote the formation of ardealite and gypsum instead of brushite (Kuz'mina *et al.* 2013), presumably due to the thermodynamic or kinetic favorability of those phases.

When carbonate ions are introduced into a solution containing growing HAP or brushite crystals, the effect depends on the concentration of carbonate. Although the introduction of carbonate quickly catalyzes the formation of carbonated-HAP, incorporation of carbonate into the HAP lattice, where it substitutes mainly for phosphate, inhibits HAP. This may be due to poor coordination between carbonate and adjacent molecules or due to adsorption at surface sites where carbonate competes for growth sites with phosphate (Johnsson and Nancollas 1992). In contrast, the presence of a relatively low carbonate concentration, relative to phosphate, causes the solubility of brushite to somewhat decrease, although the morphology of the resulting brushite crystals is distorted and plate-like (Kuz'mina *et al.* 2013), suggesting a surface effect.

Factors Effecting the Precipitation of Calcium Carbonate Phases

In the presence of a sufficient concentration of carbonate, calcium carbonates will form instead of calcium phosphates. The concentration of phosphate in solution is the determining factor in whether calcium phosphate or calcium carbonate will form (Dove and Hochella 1993; Giannimaras and Koutsoukos 1987). Much like the calcium phosphates, the calcium carbonates are a group of hydrated and anhydrous polymorphs, with calcite as the most stable phase and ikaite as the least stable crystal phase (Rodriguez-Ruiz *et al.* 2014). In contrast to the calcium phosphates, where most polymorphs are composed of unique combinations of calcium and phosphate, the three anhydrous calcium carbonate phases all have the formula $CaCO_3$; they are calcite, aragonite, and vaterite. The hydrated phases, ikaite and monohydrocalcite (**MHC**) ($CaCO_3 \cdot H_2O$), also contain the unit $CaCO_3$ although with different proportions of lattice

water. Of all the calcium carbonate phases, only calcite is stable at atmospheric pressures (Johnston *et al.* 1916), although thermodynamic data suggest that aragonite has a zone of stability somewhere around absolute zero (Brooks *et al.* 1950; Johnston *et al.* 1916).

The difference in solubility between calcite and aragonite is small under all conditions, although calcite is more stable than aragonite (Brooks *et al.* 1950; Giannimaras and Koutsoukos 1987; Johnston *et al.* 1916) Thus, despite the similar stability of calcite and aragonite, aragonite is considered a metastable phase. Under certain reaction conditions, such as near boiling temperature, in the presence of lead or strontium (Johnston *et al.* 1916), or in the presence of large quantities of Mg (Rivadeneyra *et al.* 2006), aragonite can form at the expense of calcite. Once formed, aragonite does not tend to convert to calcite, even in aqueous solutions, probably due to the low thermodynamic driving force, although the introduction of calcite seed grains can induce the formation of calcite at the expense of aragonite (Brooks *et al.* 1950). Aragonite has a stable zone, however, at elevated pressure above 3 kbar and temperatures above zero (Whiticar and Suess 1998).

Vaterite is considerably less stable than calcite and aragonite, but like aragonite it also tends to be quite stable when dry; however, it recrystallizes to calcite readily when exposed to moisture (Brooks *et al.* 1950). The transformation of vaterite to calcite can be slowed or prevented by introducing additives to a vaterite suspension that prevent the phase transformation (Liu *et al.* 2012). Effective additives include glutamic acid, aspartic acid, ovalbumin and casein, which adsorb to the crystal surface and presumably prevent vaterite from interacting with moisture, thereby preventing the solvent induced phase

transformation. Although vaterite has been synthesized under laboratory conditions, it is rarely found in nature (Sanchez-Moral *et al.* 2003).

An amorphous calcium carbonate (**ACC**) also exists (Brooks *et al.* 1950), with properties that are very similar to ACP, including high solubility and a tendency to quickly transform into one of the crystalline forms. This phase can be precipitated at high supersaturations (Rodriguez-Ruiz *et al.* 2014), which suggests that it forms under conditions of rapid nucleation, analogously to ACP.

MHC is more soluble than the anhydrous phases but less soluble than ikaite and ACC (Rodriguez-Ruiz *et al.* 2014). This phase can be produced from ACC, and transforms slowly to aragonite or calcite in solution (Rodriguez-Ruiz *et al.* 2014). It can also be formed from the early phases of ikaite recrystallization to more stable forms (Buchardt *et al.* 2001). In contrast to ikaite, which is very unstable, MHC can persist for a long time in dry conditions at room temperature (Brooks *et al.* 1950).

At elevated pressures of 3.2 to 3.9 kbar, ikaite can exist as a stable form (Whiticar and Suess 1998) and above 6 kbar it can form spontaneously (Bischoff *et al.* 1993a; Suess *et al.* 1982). Elevated pressures do not contribute to ikaite formation in surface environments because the pressures necessary for ikaite formation are not present even in the deepest ocean basins (Marland 1975). Like all calcium carbonates, ikaite forms at elevated pH and dissolves in the presence of acid (Rysgaard *et al.* 2012). At atmospheric pressure and non-freezing temperatures, ikaite spontaneously decomposes, first into smaller ikaite fragments (Rysgaard *et al.* 2012) and eventually into ACC (Mikkelsen *et al.* 1999), although MHC can also be generated from dehydrating ikaite (Rodriguez-Ruiz *et al.* 2014). Several yet-to-be determined factors influence which anhydrous phases

result from ikaite decomposition, but ikaite is believed to decompose to vaterite or calcite, or a mixture of both (Rysgaard *et al.* 2012), although others opine that vaterite is an intermediate phase between ikaite and calcite (Marland 1975). Decomposition proceeds almost uniformly through the entire ikaite crystal due to the rapid thermal diffusion (Larsen 1994), with the unit cell expanding anisotropically along the *a*- and *c*-axis until the structure is lost (Tateno and Kyono 2014). The rate of decomposition is affected by the temperature as well as the relative humidity, with high temperatures and low humidity promoting dehydration (Tateno and Kyono 2014).

CO_3^{2-} Concentration and Carbonate Supersaturation

Regardless of the calcium carbonate polymorph, the supersaturation of a solution with respect to a given phase is a function of the activity product of the calcium and carbonate ions in solution (Boch *et al.* 2015). This is analogous to the activity product that is calculated for calcium phosphates, in part, from the concentration of various forms of phosphate in solution, depending on the phase. In the case of carbonate, however, only the non-protonated carbonate molecule CO_3^{2-}, directly influences mineral formation (Hu *et al.* 2014). Bicarbonate (HCO_3^-), and carbonic acid (H_2CO_3), do not crystallize into any known calcium phases and are thus considered common ions in this system. Just like with the phosphates, carbonate saturation is dependent on the total concentration of carbonate as well as the pH, which determines which carbonate species will predominate.

The dynamics of carbonate ions in solution are somewhat more complex than those of phosphate ions because carbonate can exist in solution as dissolved $CO_{2(aq)}$ that can be released from solution as CO_2 gas. Carbonate concentrations, and therefore carbonate mineral dynamics, are dictated by CO_2 partial pressure (Omelon *et al.* 2001), as

opposed to simple concentration and activity, as in the case of dissolved phosphate. The solubility of CO_2 in solution is a function of temperature, with greater concentrations of CO_2 dissolving at lower temperatures (Boch *et al.* 2015). Release or capture of CO_3^{2-} from the atmosphere above a solution also impacts the pH of the solution. Degassing of CO_2 results in increased pH due to the release of OH^- from the bicarbonate ion as it converts to $CO_{2(aq)}$ and subsequently evaporates. In some abiotic surface calcium carbonate deposits, such as travertines, degassing causes a sufficient rise in pH to induce carbonate mineralization (Arp *et al.* 1999; Dupraz *et al.* 2009). Degassing can be pronounced in aqueous systems by high surface area, such as are present in natural shallow waters, where a large interface leads to more efficient degassing (Omelon *et al.* 2001). Regardless of the source of a pH increase, any increase in pH will cause the fraction of CO_3^{2-} to increase and can therefore increase the saturation or supersaturation of the system with respect to carbonate minerals (Hu *et al.* 2014). At higher pH, more Ca^{2+} ions are complexed with carbonate (Whiticar and Suess 1998) because more CO_3^{2-} is available in solution, which reflects the higher saturation.

Just like the calcium phosphates, in order for a metastable calcium carbonate phase to precipitate, a solution must be saturated with respect to all of the more stable phases (Johnston *et al.* 1916). Ikaite, the least stable crystalline calcium carbonate, occasionally forms in nature when an aqueous solution is supersaturated with respect to this phase and conditions are present or additives are introduced that prevent the formation of the more stable anhydrous phases. Although a precise understanding of the kinetics of ikaite precipitation is still lacking (Dieckmann *et al.* 2008), a bounty of literature has accumulated that describes these dynamics in both natural and laboratory

synthesized ikaite. Several variables could prevent the anhydrous phases from nucleating and growing, thus allowing ikaite to grow.

Kinetic Inhibition of Calcite by Dissolved Additives

Small quantities of phosphate, if present in solution, exert a kinetic control over the anhydrous forms of calcium carbonate (Bischoff *et al.* 1993b), although larger quantities of phosphate in the system could result in calcium phosphate crystallization (Dove and Hochella 1993; Giannimaras and Koutsoukos 1987). Several different forms of phosphate have an inhibitory effect on the anhydrous calcium carbonates including phosphate (House 1987), hydrophosphate (House and Donaldson 1986), dihydrophosphate (Giannimaras and Koutsoukos 1987), and various polyphosphates (Brooks *et al.* 1950; Clarkson *et al.* 1992; Rodriguez-Ruiz *et al.* 2014; Suess *et al.* 1982). With respect to the orthophosphates, the particular species that exerts the inhibitory effect would depend on the pH of the solution and the predominant form of orthophosphate at that pH (Giannimaras and Koutsoukos 1987).

At low concentrations, phosphates can adsorb to the surfaces of existing anhydrous calcium carbonate crystals by chemisorption in much the same way that carbonate, Mg^{2+}, and Zn^{2+} adsorb to the surfaces of HAP (Millero *et al.* 2001). Phosphate ions adsorb to the growing surfaces along steps and kink sites, which are the sites where surface nucleation and growth take place (House 1987). Due to fact that the kinetics of calcite (and probably the other anhydrous phases as well) are surface controlled, the addition of phosphate to such a solution reduces the rate constant for growth, and at high enough phosphate concentrations, can inhibit growth entirely (House and Donaldson 1986). Elevated concentrations of phosphate can cause HAP to precipitate on the surface

of calcite (House and Donaldson 1986); this demonstrates that carbonate inhibition of HAP and phosphate inhibition of calcium carbonate represent something akin to a continuum, with the proportion of carbonate to phosphate determining whether a carbonate phase or a phosphate phase will form.

Phosphate uptake on calcite surfaces is dependent on ionic strength. At elevated ionic strength phosphate uptake is diminished (Millero *et al.* 2001), which suggests that this interaction is electrostatic (Giannimaras and Koutsoukos 1987). At low pH, the surface of calcite is characterized by $CaHCO_3^+$, which conveys an overall positive charge to the surface. The predominant phosphate species at low pH, hydrophosphate and dihydrophosphate, will bind to the positively charged surface to neutralize the positive charge (Giannimaras and Koutsoukos 1987). At higher pH, the surface of calcite is dominated by HCO_3^- and CO_3^{2-}, and the predominant phosphate species at that pH, phosphate and hydrophosphate, interact less with the surface as a result of the overall negative charge (Giannimaras and Koutsoukos 1987).

Interactions between phosphate and calcite can have the effect of sequestering large amounts of phosphate from natural waters that contain anhydrous calcium carbonate in the sediment (Kanel and Morse 1978). This effect is even more pronounced in the presence of dissolved Mg^{2+} and Ca^{2+}, which provide a bridge between phosphate and carbonate molecules on the surface of calcite and aragonite by diminishing the repulsion of negatively charged groups (Millero *et al.* 2001). The effect of Ca^{2+} is more pronounced than Mg^{2+} due to its ability to form stronger complexes with phosphate. Organic carbon in solution also appears to compete with carbonate for surface sites (Boch *et al.* 2015), which allows it to inhibit calcite to some extent as well.

The addition of sulfate ions reduces the effect of adding Mg^{2+} and Ca^{2+} by forming soluble complexes with these ions, and the addition of bicarbonate also has an inhibitory effect by competing with phosphate for surface sites (Millero *et al.* 2001). In the presence of Mg^{2+}, calcite incorporates a small quantity of Mg into its lattice, (Kunitake *et al.* 2012), which slows the growth of calcite because Mg^{2+} ions at growing sites dehydrate more slowly than Ca^{2+} (Bischoff *et al.* 1993a). Sufficient Mg^{2+} concentrations can inhibit calcite precipitation entirely (Bischoff *et al.* 1993a) . Regardless, when these ions interact with crystal surfaces they affect the growth by blocking crystal growth sites (Boch *et al.* 2015), although the extent of inhibition differs for each ion and affects each carbonate phase differently (Brooks *et al.* 1950).

At lower phosphate concentrations, the inhibitory effect of phosphate on calcite is observed as a reduced rate of growth (Giannimaras and Koutsoukos 1987), instead of complete inhibition. To understand this process, it is helpful to understand how crystal growth occurs at the crystal surface. Calcium carbonate growth units nucleate on surface sites at steps and kinks where layered crystal growth occurs. Adsorption of phosphate to kink and step sites on the calcite surface temporarily arrests layered growth at those sites (Giannimaras and Koutsoukos 1987). Complete inhibition of calcite occurs when sufficient phosphate is present to prevent the two-dimensional progression of nucleation on surface steps (House 1987). The presence of lesser quantities of phosphate could distort the nucleation and growth of surface steps (Dove and Hochella 1993), which could result in changes to the crystal habit (Brooks *et al.* 1950). Phosphate that interacts with kink sites may become trapped in the site and eventually incorporated into the crystal if growth is not completely impeded (House 1987). In contrast, phosphate adsorbed at step

sites does not tend to become incorporated into the lattice (House 1987). In some cases, coprecipitation of phosphate with calcite may be so extensive that phosphate levels in solution can become almost completely diminished (House 1987).

Precipitation of Metastable Carbonates in the Presence of Additives

Complete inhibition of calcite could allow more soluble phases to reach supersaturation and precipitate (Brooks *et al.* 1950). Phosphate, sulfate, and Mg^{2+} apparently do not interact with the surface of ikaite (Bischoff *et al.* 1993a), and ikaite does not tend to incorporate Mg into its growing lattice (Larsen 1994), although there is some evidence that phosphate can inhibit MHC (Hu *et al.* 2014). It is noteworthy that many natural waters contain enough dissolved ions, including phosphate, to completely inhibit calcite growth (House 1987), although not all natural systems contain the necessary supersaturation to cause other phases to precipitate. High supersaturations encourage metastable phase nucleation (Rodriguez-Ruiz *et al.* 2014) by exceeding the higher saturation levels needed to precipitate less stable phases, although this depends on the level of inhibitor as well as temperature. Solution temperature affects the efficiency of phosphate inhibition, with more phosphate required to achieve the same inhibition as temperature is increased (Brooks *et al.* 1950). At low and moderate temperatures, the complete inhibition of anhydrous phases results in ikaite precipitation, whereas above approximately 25°C, some MHC can be formed.

Ikaite can persist in solution only if the nucleation of anhydrous phases is prevented (Brooks *et al.* 1950; Whiticar and Suess 1998). In the absence of inhibition, ikaite will dissolve as vaterite and calcite crystals nucleate and grow. Aragonite can occasionally be produced from decomposing ikaite in the absence of inhibitors in boiling

solution (Brooks *et al.* 1950), which reflects the ability of aragonite, as mentioned above, to precipitate at the expense of calcite in hot solutions. The amount of time that it takes for ikaite to transform to anhydrous phases is dependent on the concentration of inhibitors, such as phosphate, in solution (Bischoff *et al.* 1993a; Whiticar and Suess 1998). Extensive incorporation of phosphate into inhibited anhydrous crystals and nuclei can eventually remove enough phosphate from a system to eliminate the inhibitory effect (Bischoff *et al.* 1993a; Clarkson *et al.* 1992). Inhibition of crystal nuclei is analogous to the inhibition of crystal growth on preexisting crystals, except that the amount of phosphate removed from the system by poisoned nuclei is dependent on the nucleation rate. In contrast, phosphate removal on preexisting crystals depends on the crystal surface area. Nucleation rate is related to the level of supersaturation (Hu *et al.* 2014; Johnston *et al.* 1916), and the extent of phosphate removal by nucleating crystals is related to the rate of nucleation (Hu *et al.* 2014). It is therefore not surprising that more phosphate can be removed from solution at elevated pH, where supersaturation of carbonates is higher and the nucleation rate is faster (Hu *et al.* 2014).

Precipitation of Ikaite in the Absence of Additives

Even though ikaite is metastable at all temperatures at atmospheric pressure (Bischoff *et al.* 1993a), ikaite can nonetheless form in the absence of inhibitors at sub-zero temperatures (Boch *et al.* 2015; Whiticar and Suess 1998). Unlike the anhydrates, the solubility of ikaite decreases with decreasing temperature, whereas the anhydrates become increasingly soluble with decreasing temperature (Bischoff *et al.* 1993a). The temperature dependence of ikaite is typical of inorganic hydrates, which tend to become less soluble at low temperatures because their lattice water thermodynamically behaves

like ice (Bischoff *et al.* 1993a). Cold temperatures also impact the kinetics of carbonate nucleation; the rate limiting step in the formation of an anhydrous lattice is the complete dehydration of Ca, which is not required in order to form ikaite's hydrated lattice (Bischoff *et al.* 1993a). Therefore, at cold temperatures, the rate of ikaite nucleation and growth is accelerated by the formation of hydrated $CaCO_3^0$ ion pairs (Buchardt *et al.* 2001).

Ikaite can precipitate faster at cold temperatures because the rate of anhydrous crystallization is hindered by the slow dehydration of the hydrated complexes at the crystal growth surfaces (Boch *et al.* 2015; Omelon *et al.* 2001). Cold temperatures also favor ikaite precipitation by lowering the thermodynamic threshold for supersaturation through ikaite's decreased solubility (Boch *et al.* 2015), although ikaite is still more soluble than the anhydrous phases and is therefore still metastable. Even though cold temperatures allow ikaite to form and persist, ikaite may eventually transform into an anhydrous phase if it is not stabilized with an additive (Whiticar and Suess 1998). Subsequent exposure to higher temperatures would remove the kinetic inhibition of anhydrates and lead to ikaite dissolution (Bischoff *et al.* 1993a; Boch *et al.* 2015).

Precipitation of Struvite

In contrast to the thermodynamic and kinetic complexity of the calcium carbonates and calcium phosphates, struvite is a relative simple phase because it is thermodynamically stable at ambient conditions. Nonetheless, as a highly hydrated phase, it tends to dehydrate when exposed to dry air (Chauhan and Joshi 2013; Han *et al.* 2015), although it does not transform into another crystal phase. Like the other phases discussed here, struvite's supersaturation and precipitation rate are controlled by pH, with elevated

pH leading to greater precipitation (Nelson *et al.* 2003). The precipitation of struvite is controlled by the speciation of both phosphate and ammonia (Nelson *et al.* 2003). Therefore, struvite is highly influenced by pH, which controls the concentrations of phosphate and ammonium ions in solution. Changes in phosphate speciation with pH tend to have a greater influence on struvite precipitation than changes in ammonia speciation because small changes in pH have a greater impact on phosphate speciation within the moderately alkaline pH range (Nelson *et al.* 2003). At much higher pH, Mg^{2+} exists as $MgOH^{+}$ (Gull and Pasek 2013), and struvite solubility subsequently increases as the activity of Mg^{2+} decreases.

Struvite tends to be more kinetically favorable than HAP because, as previously mentioned, Mg^{2+} kinetically inhibits the formation of HAP (Nelson *et al.* 2003); however, the thermodynamic stability of each of these phases would almost certainly depend on the ratio of Mg^{2+} to Ca^{2+} (Gull and Pasek 2013), with a higher ratio of Mg favoring struvite stability and a lower ratio favoring HAP. Under some conditions, struvite can be metastable and convert to HAP, although the specific conditions for this are not clear (Gull and Pasek 2013).

When the concentrations of Mg^{2+}, ammonium, and phosphate are similar, changes in the solution supersaturation can affect struvite crystal habit. At very high supersaturations, rapid growth kinetics favor the formation of bidirectional and tridirectional twins, whereas slower growth kinetics promote tabular crystals (Abbona and Boistelle 1979). At high Mg and phosphate concentrations and in the absence of ammonium, magnesium phosphate (Gull and Pasek 2013), K-struvite ($KMgPO_4 \cdot 6H_2O$) (Liu *et al.* 2013), or HAP (Griffith 1978) can form at the expense of struvite, although

very little ammonium is necessary in solution to make struvite the most stable phase (Gull and Pasek 2013).

Inhibitor ions, such as citrate, pyrophosphate (Stickler 1996), potassium, chloride, calcium, carbonate, and zinc (Le Corre *et al.* 2005) can also affect the nucleation and growth of struvite, in the same way that various ions can affect the growth of calcium carbonate and calcium phosphates. These ions block active growth sites on the struvite crystal surface and can impact crystal size or habit (Le Corre *et al.* 2005). From this list, it is noteworthy that both calcium and carbonate can impede nucleation, with higher calcium and carbonate concentrations complexing to form calcium carbonate and calcium phosphates (Le Corre *et al.* 2005). In addition, the sequestration of phosphate ions within the crystal lattice of struvite can remove the inhibitory effect of phosphate in systems that contain sufficient calcium and carbonate to precipitate calcium carbonates (Gonzalez-Munoz *et al.* 2008). These phenomena demonstrate the overlapping thermodynamics and kinetics of calcium phosphates, calcium carbonates, and struvite due to the common ions that interact with each crystal phase.

Precipitation of Phosphate and Carbonate Phases in Biotic Environments

Conditions in cheese allow a combination of brushite, calcite, ikaite, and struvite to form. Per an extensive review of the mineralogical literature, it does not appear that this combination of minerals has been observed in any natural setting. However, examples of some of these phases crystallizing together exist. For instance, struvite has been reported to form with calcite from cellular fractions of *M. xanthus* (Muynck *et al.* 2010a), and struvite crystallizes with several calcium carbonate polymorphs, including calcite, in the presence of *Chromohalobacter marismortui*, a mineralogically important

bacterium from the Dead Sea (Rivadeneyra *et al.* 2006). Brushite and struvite have also been identified together in fresh sheep manure (Barak and Staffort 2006).

Struvite appears to form preferentially in biological systems (Abbona and Boistelle 1979; Gull and Pasek 2013). Some calcite forms from biological activity, such as the deposits in microbial mats (Dupraz and Visscher 2005), whereas calcite deposits, such as travertines, are abiotic (Arp *et al.* 1999). Brushite tends to be associated with biotic processes, such as decaying guano (Abbona *et al.* 1993) whereas most sources suggest that ikaite is an abiotic mineral that results from the cold and alkaline environments in which it is most often found (Arp *et al.* 1999).

Of the four minerals that have been found in cheese, ikaite is the only one that has not been directly linked to microbial metabolism in at least some environments. There is, however, some evidence that bacterial biofilms may be associated with ikaite deposits (Last *et al.* 2013) and may protect this labile mineral from dissolution in unfavorable conditions (Schmidt *et al.* 2006). All known natural deposits of ikaite are in anoxic environments (Bischoff *et al.* 1993b) and often near or in organic-rich sediment (Suess *et al.* 1982), where sulfate reduction (Whiticar and Suess 1998) and organic sediment recycling (Bischoff *et al.* 1993a; Boch *et al.* 2015) are common. Although this is not conclusive evidence of a biological connection, the discovery of ikaite in the bacterial community on washed-rind cheese (Tansman *et al.* In Press) suggests that a microbiological connection is feasible in geological settings as well.

Given the tendency of struvite, brushite, calcite, and ikaite to form in the microbial communities on the surface of cheese, the most analogous geological systems are microbial communities that precipitate minerals in a geological setting. Microbial

mineralization is as old as single-celled organisms (Phoenix and Konhauser 2008) and the activity of microbes in geological settings often impacts the types and habits of minerals that form in their environment. It is a well-established principle that nucleation can occur much more easily on foreign particles than in bulk solution (Garside 1987), and the matrix of extracellular polymeric substances (**EPS**) produced by bacteria can provide an excellent nucleation template (Dupraz *et al.* 2009). The properties of EPS from different microbial communities varies widely, and the chemical functional groups characteristic of EPS can affect the mineralogy and morphology of the phases that they precipitate (Dupraz *et al.* 2009).

Effect of Biological System Characteristics on Crystallization

Self re-arrangement of EPS functional groups can create unique nucleation environments and preferentially precipitate certain minerals (Braissant *et al.* 2007). The viscosity, which is determined by the chemistry of the EPS (Arp *et al.* 1999), can also impact the kinetics of crystallization (Braissant *et al.* 2007), with different phases (Rivadeneyra *et al.* 2006) and different crystal habits (Gonzalez-Munoz *et al.* 2008) favored at various levels of viscosity. Microbes can also exude organic molecules that can inhibit the growth of certain crystal faces, thereby varying the crystal habit (Dupraz *et al.* 2009; Han *et al.* 2015). Mineralogical processes that result from microbial metabolism in geological settings are often so complex that linking a mineral product to a metabolic process is very difficult (Riding 2000; Visscher and Stolz 2005).

Microbial mats are the sites of extensive and diverse microbial metabolism that can precipitate and dissolve gypsum, anhydride (Dupraz and Visscher 2005), carbonates, silicates, oxides (Dupraz *et al.* 2009; Rivadeneyra *et al.* 2006), and oxi-hydroxides

(Benzerara *et al.* 2011). Microbial guilds in mats can modulate the concentrations of ammonia, CO_2, and sulfate (Riding 2000), and generate alkalinity (Baumgartner *et al.* 2006). Within microbial mats, large fluctuation in pH (Braissant *et al.* 2007) and redox potential (Visscher and Stolz 2005) can exist at different depths in the mat. At each depth, the types of minerals that can be formed vary by the chemical conditions that are generated by the prevailing microbial metabolism. It should be noted that within a given environment, the activity of microbes can create micro-environments that may precipitate or inhibit particular minerals (Dupraz *et al.* 2009); micro-environments often favor the precipitation of metastable phases (Sanchez-Moral *et al.* 2003), which makes these environments particularly dynamic and difficult to predict.

In the top layers of microbial mats, photosynthesis increases alkalinity and favors carbonate precipitation through the removal of CO_2, (Dupraz *et al.* 2009). Production of CO_2, by aerobic respiration in the top layers has also been linked to calcium carbonate precipitation (Visscher and Stolz 2005). Metal hydroxides and phosphates are also formed in the oxic upper layers whereas metal sulfides are mainly formed in the anoxic layers below (Remoudaki *et al.* 2003). Sulfate reducing bacteria (**SRB**) dominate the anoxic layers of microbial mats where they produce sulfide (Visscher and Stolz 2005) and raise the pH (Benzerara *et al.* 2011; Remoudaki *et al.* 2003). These activities favor metal sulfide, such as black iron sulfides (Dupraz *et al.* 2009; Oren *et al.* 1995). In the presence of barium and abundant sulfate, anoxic conditions in much thinner biofilms can lead to barium sulfate (Sanchez-Moral *et al.* 2004). SRB can consume organic acids (acetate, butyrate, lactate), which increases the activity of calcium (Braissant *et al.* 2007)

and can increase pH (Dupraz and Visscher 2005); this can further induce mineral formation.

The conditions that exist in cheese are much more limited than those that may exist in myriad geological settings. The number of microbial species are comparatively few (Button and Dutton 2012; Irlinger *et al.* 2015), with photosynthetic communities notably absent. In addition, metals such as barium and iron are either absent or in concentrations too low to contribute meaningfully to crystallization processes. Nonetheless, the physical laws and biological processes that are at play in geological settings are relevant in the study and understanding of mineral kinetics and thermodynamics in cheese.

MICROBIAL ECOSYSTEMS AND THEIR EFFECT ON MINERALIZATION

MICROBIAL ECOSYSTEMS AND BIOMINERALIZATION

For much of the history of microbiological investigation, microbial cells have been treated as solitary functional units floating in nutrient rich media. The reality of microbial life in most natural systems is much more reminiscent of a rainforest ecology (Visscher and Stolz 2005), in both biological and functional complexity. Integrated microbial systems are given a variety of names depending on the context and macroscopic properties, including biofilm, microbial mat, sludge, and slime. These communities may be composed of a single species or multiple bacteria species along with fungi, algae, and protozoa (Singh *et al.* 2006). Prokaryotic and eukaryotic species within these assemblages are often in competition for the same resources, although a bounty of recent research has revealed that these communities are also characterized by interspecies cooperation that maximizes productivity and resource use. The work of Dr. Rachel Dutton and her colleagues has paved the way for a much deeper understanding of the complex interactions that occur in natural microbial systems by using cheese rinds as tractable model systems of limited complexity that can be recreated with relative ease in the laboratory. Insights gained from observing cheese rinds may then be applied to more complex systems that cannot be as easily replicated in vitro.

Microbial communities, including cheese rinds, are frequently associated with biomineralization phenomena that result from microbial activity. The biominerals that form in an ecosystem are a function of the available substrates as well as microbial metabolites that may become available over time. Metabolites may also alter the

chemical environment or lower the activation energy of crystal formation by providing nucleation sites. The study of biomineralization is intimately tied to microbial metabolism and thus, a thorough understanding of the various types of microbial interactions and their aggregate impact on the crystallization environment is critical. Biomineralization occurs in various contexts including geological sediment (such as microbial mats in salt marshes), waste effluent (including sewage treatment and urinary medical devices), and in the surface smear of cheese. The microbial communities in each context vary in complexity, although the underlying principles can be applied in each case to justify the formation of observed crystal phases.

Cheese rind microbial communities are relatively simple because of the limited number of species (Button and Dutton 2012; Irlinger *et al.* 2015). In contrast, microbial mats are very thick and therefore provide the opportunity for many metabolic niches to support a large diversity of microbes (Franks and Stolz 2009). In that sense, the biofilms that form in effluent systems are probably more similar to the surface of cheese than to geological microbial mats. Nonetheless, niche diversity exists in cheese as a result of the changing nature of the cheese substrate during aging as microbial metabolism progresses.

Colonization of Cheese Rinds

The cheese rind community is initially inoculated by yeast species such as *Debaryonyces hansenii*, *Geotrichum candidum* (Gori *et al.* 2007), *Kluveromyces lactis*, *Saccharomyces cerevisiae* (Kagkli *et al.* 2006), and *Kluveromyces marxianus* (Irlinger *et al.* 2015). These first colonizers reflect the conditions on the surface of the cheese; initially, the cheese surface is acidic as a result of lactic acid production by the starter cultures (Leclercq-Perlat *et al.* 2004a) and high salt content as a result of the application

of salt or immersion in brine on the day of manufacture (Irlinger *et al.* 2015). The yeasts, and *D. hansenii* in particular, are well adapted to the acidic and salty conditions that initially exist on the cheese surface (Masoud and Jakobsen 2005). Consumption of lactic acid by the yeasts neutralizes the acidity at the cheese surface, which conditions the surface environment for the growth of acid-sensitive bacteria in washed rind cheese (Gori *et al.* 2007) and white mold cheese (Leclercq-Perlat *et al.* 2006). Yeasts may also secrete vitamins that are necessary for coryneform bacterial growth (Masoud and Jakobsen 2005).

As the surface pH is neutralized, bacterial species (Gori *et al.* 2007; Masoud and Jakobsen 2005) and fungi (Amrane *et al.* 1999) begin to grow according to their acid sensitivity and nutrient needs. In white mold cheese, this succession yields a three-layered structure consisting of yeasts on the cheese surface, a thick layer of fungal *Penicillium* mycelium on the surface, and a layer of the filamentous *Geotrichum candidum* yeast in between (Rousseau 1984). Rousseau (1984) also observed that coryneform bacteria in white mold cheese tend to be in close association with fungal conidiophores. This stratification is striking considering the narrow (~1mm) depth of the surface microbial layer. In washed rind cheese, no such stratification of the smear layer has been reported, although this could be due to the scrubbing that is regularly applied to the surface of this cheese, which could have a homogenizing effect. Very steep oxygen gradients, from supersaturation to anoxia in a few millimeters or less, have been observed in microbial mats (Franks and Stolz 2009; Visscher and Stolz 2005), but measurements on this have apparently not been performed on cheese rind communities.

Microbial Diversity and Complexity of Geological Microbial Mats

In contrast to the relatively thin microbial communities that exist on the surfaces of white mold and washed rind cheese, the microbial mats that exist in geological systems can be very thick. Oren *et al.* (1995) found that the uppermost cyanobacterial layer in a microbial mat was several times thicker than the entire community found on cheese, and Morales *et al.* (2006) sampled a sphagnum bog and found stratified diversity at a depth of one meter. In that study, Morales *et al.* (2006) only took two measurements of bacterial diversity, which consisted of an oxic surface sampling and an anoxic sampling at one-meter, but they found discrete microbial communities that reflected the two distinct abiotic microhabitats.

The microbial diversity at the two depths in different parts of the bog studied by Morales *et al.* (2006) were also very similar, reflecting the strong influence of the abiotic environment. Other studies of microbial mats have revealed even more stratified microbial diversity reflecting the gradients of light and redox potential. According to these studies, microbial mats possess different guilds with the phototrophic and most aerobic metabolism occurring at the surface, and with methanogenesis, reflecting the lowest energy yielding metabolic guild, occupying the lowest depths of the redox gradient (Dupraz *et al.* 2009). Anaerobic metabolic processes, such as nitrate and sulfate reduction, occur at intermediate points in the redox gradient according to their energy yielding potential (Riding 2000).

A variety of other parameters can affect microbial diversity with mat depth including temperature, pressure, oxygen content, pH, and salinity (Franks and Stolz 2009). Combinations of these parameters determine the particular guilds of microbes that

exist in each niche. For example, different photosynthetic pigments allow microbes to take advantage of changes in light intensity with increasing depth, and anoxygenic phototrophs can thrive beneath the oxic zone while taking advantage of longer wavelengths of light, reflecting evolutionary adaptations to particular conditions (Franks and Stolz 2009). Similarly, the cyanobateria that Oren *et al.* (1995) found on the surface of a hypersaline microbial mat have been found associated with similar mats all over the world, suggesting that the abiotic conditions have a greater effect than the geography in which they are found.

Microbial Diversity and Complexity of Wastewater Biofilms

In urinary tract infections, biofilms of similar nosocomial species have been cited in many different research contexts (Chauhan and Joshi 2013; Clapham *et al.* 1990; Griffith 1978; Percival *et al.* 2011; Stickler 1996). This could reflect the adaptation of these microbes for the human urinary tract or perhaps reflect an adaptation for urine as a nutrient substrate. It is not surprising that microbes isolated from infections of the urinary tract often display urease activity (Chauhan and Joshi 2013; Clapham *et al.* 1990; Griffith 1978; Stickler 1996). An understanding of microbial communities in waste effluent systems downstream is in its infancy (Jensen *et al.* 2016), but a unified model for biofilms in wastewater systems will probably be somewhat more elusive given the massive diversity of raw materials flowing into these systems, which determine the chemical oxygen demand and microbial processes that can dominate (Wang *et al.* 2013).

Regardless of the complexity of wastewater systems, investigation of well-defined systems such as the urinary catheters, granule batch reactors, and sewage piping could begin to explain how bacterial communities establish and thrive under conditions that

may change quite drastically over time. In this sense, the analogy to the changing conditions on the surface of cheese is quite striking, if not somewhat off-putting. Several points in the wastewater system can also be influenced by human intervention. For instance, the oxygenic conditions applied to batch reactors in wastewater treatment, whether aerobic or anaerobic, can favor certain biological processes which can aid the removal of compounds such as nitrite (Wang *et al.* 2013). In this context, the metabolism, efficiency, and community integrity of the microbes appear to be of interest to researchers, although the particular microbial species involved appear to be less important and are often omitted from the literature on this topic (Barak and Staffort 2006; Stratful *et al.* 2001; Wang *et al.* 2013). It is possible that particular microbes are adapted to downstream wastewater systems, although it is possible that the quantity of microbial species in systems as complex and varied as wastewater treatment would make such research less generalizable and therefore less interesting.

Microbial Diversity and Complexity of Cheese Rind Communities

Given the limited number of microbes on cheese, the individual microbial players can be easily researched to reveal adaptations to the environment. Indeed, cheese surface microbes show adaptations to the particular conditions that exist in cheese (Dugat-Bony *et al.* 2016; Irlinger *et al.* 2015) and in manufacturing facilities (Mounier *et al.* 2006), and a ubiquitous pool of cheese rind microbes appears to exist in broad geographical settings (Wolfe *et al.* 2014). For instance, the salt tolerance and ubiquity of *D. hansenii*, among other favorable traits, allow it to reside in such niches as the milk, brine, and washing solution, where it can inoculate the cheese surface without being applied intentionally by the cheesemaker (Lessard *et al.* 2012). Once on the cheese

surface, this yeast is well adapted to compete for resources, even against heavily inoculated microbes such as *P. camembertii* (Lessard *et al.* 2012), in part because of its ability to consume a variety of substrates that become available at different points during aging (Lessard *et al.* 2012). Another halotolerant species that resides in the brine, *Staphylococcus saprophyticus*, cannot immediately grow on the cheese due to its acid sensitivity (Mounier *et al.* 2006), which highlights the fact that a combination of adaptations determines whether and when species resident in the environment colonize the rind.

Some species are so adapted to both the cheese surface and the aging environment that they have begun to show signs of domestication (Wolfe *et al.* 2014). This makes sense given that the surface of a cheese is a highly anthropogenic environment in which cheesemakers use time-tested techniques to cultivate the desired microbial communities (Irlinger *et al.* 2015). Those microbial communities are highly influenced by the microorganisms that exist in the ripening environment and the production chain (Irlinger *et al.* 2015), although not all microbes that can survive in the manufacturing environment can be found on the cheese surface (Leclercq-Perlat *et al.* 2004a). The initial selection pressure for acid and salt tolerant yeasts on the surface of fresh cheese subsides as the conditions on the cheese change during early aging (Leclercq-Perlat *et al.* 2004a). These changes are driven by the changing availability of compounds that satisfy the needs of various groups of bacteria. These evolving conditions on the surface of cheese are very reminiscent of the changes in chemical conditions and microbial diversity that are observed in microbial mats with changes in depth.

EFFECT OF STRATIFICATION ON MICROBIAL DIVERSITY IN COMPLEX ECOSYSTEMS

Depth of a microbial mat is the greatest variable determining microbial diversity, although daily cycles that impact the photosynthetic output of phototrophs also have a temporal impact on microbial functions (Dupraz *et al.* 2009; Franks and Stolz 2009). The microbial mat is a light-driven ecosystem (Baumgartner *et al.* 2006; Visscher and Stolz 2005) that experiences rapid oxygen depletion when no light is available (Dupraz and Visscher 2005). A wide range of metabolic processes and extensive biogeochemical cycling are possible as a result of microbial mat stratification. These allow for thousands of different microbes to interact as a natural bioreactor within a single ecosystem (Franks and Stolz 2009; Visscher and Stolz 2005). The heterotrophs in microbial mats are classified by their preferred terminal electron acceptor, with strata below the surface using alternative terminal electron acceptors, depending on the redox conditions (Baumgartner *et al.* 2006).

Stratification is not unique to microbial mats and may be found in other systems where depth plays a role in microbial metabolism. In solar salterns that are used to harvest sea salt, depth of the salt bulk can lead to anoxia and can favor the growth of anaerobic microbes (Tsiamis *et al.* 2008). Furthermore, changes in light intensity with depth influence the survival of differently pigmented phototrophs that are adapted to a particular combination of light intensity and availability of reducible substrate. The dynamic between depth and microbial guild in salterns is very similar to the same phenomenon observed in microbial mats. However, the greatest changes in saltern community structure occur at different operational stages (Tsiamis *et al.* 2008). The diversity of microbes originally present in seawater is gradually replaced by a limited

community of native and introduced halotolerant archaea. The increased salinity at different stages reflects increasingly restrictive conditions and is strikingly similar to the restricted methanogenic environment at the deepest extremes of microbial mats (Dupraz *et al.* 2009). In contrast to the reported geographical uniformity of urinary and microbial mat species, the geography of salterns has a large impact on microbial diversity (Tsiamis *et al.* 2008).

The stratification of microbial mats (and perhaps of salterns as well) allows microbes to oxidize or reduce compounds in a stepwise fashion along the depth of the redox gradient (Visscher and Stolz 2005), although micro-niches exist at different depths that allow for some mixing of the redox guilds (Baumgartner *et al.* 2006; Dupraz and Visscher 2005). Members of some guilds can modulate their metabolism to reflect an available terminal electron acceptor, while other motile species can relocate to their preferred stratum, if conditions change (Baumgartner *et al.* 2006). When conditions change drastically, in an ecosystem disturbance for instance, microbial mat succession closely resembles terrestrial ecosystem colonization (Franks and Stolz 2009).

Microbial Succession on Cheese Rinds

Analogously, colonization of cheese surface microbes also proceeds in a succession of different metabolic preferences and environmental tolerances. The 'ecosystem disturbance' in cheesemaking would probably correspond to curd acidification and salting, which represent major environmental changes that can exert selective pressure on colonizing microbes (Irlinger *et al.* 2015). In contrast to the spatial separation between massive metabolic guilds in microbial mats, metabolic guilds on cheese are limited to a few genera each (Irlinger *et al.* 2015) and the separation between

metabolic groups on cheese is temporal, resembling the temporal changes in saltern microbial diversity. In contrast to salterns, however, the extent of microbial diversity on cheese rinds increases as aging progresses (Mounier *et al.* 2006), with the bacterial community at the end of aging displaying much more diversity than the fungi that initially colonize the surface (Dugat-Bony *et al.* 2016). This may reflect an environment that becomes less selective over time, whereas the saltern conditions become more restrictive over time.

As the first microbes to colonize the cheese surface, yeasts have access to the most abundant lactose. This reflects the colonizing yeasts' preference for lactose during their growth stage (Kagkli *et al.* 2006; Riahi *et al.* 2007b). When lactose has been depleted, some yeasts such as *D. hansenii* can consume lactate instead, although this is done for maintenance instead of growth (Riahi *et al.* 2007b). Other yeasts, such as *K. lactis* (Leclercq-Perlat *et al.* 2004a; Picque *et al.* 2006) and *K. marxianus* preferentially consume lactose, but these yeasts disappear from the ecosystem around the time that lactose is exhausted (Irlinger *et al.* 2015), presumably because their growth requirements make them poor competitors under the conditions that exist at later points during aging. *G. candidum* consumes lactose and does not consume lactate, although this yeast is characterized by strong peptidolytic activities (Leclercq-Perlat *et al.* 2004a; Picque *et al.* 2006), which allow it to persists in the ecosystem after lactose is exhausted.

Many microbes enter the rind ecosystem at later points because of the environmental changes that result from the colonizing microbes' collective metabolism (Leclercq-Perlat *et al.* 2004a). The exponential phases of major rind microbes tend to occur in sequence and often reflect the availability of preferred substrates (Leclercq-

Perlat *et al.* 2004a). Once the yeasts create the conditions necessary for the growth of adventitious bacteria, a succession of bacteria grow on the surface, reflecting the increasing abundance of biodiversity that becomes apparent as aging progresses (Mounier *et al.* 2006). Interestingly, bacterial ripening adjuncts that are inoculated onto the cheese surface are often not recovered during ripening, suggesting that they are not adapted to the specific conditions that exist on the rind, even at the latter points of aging (Feurer *et al.* 2004; Mounier *et al.* 2006).

Well adapted adventitious microbes such as *D. hansenii* and *G. candidum* experience rapid growth that corresponds to either the lags phase or decline of other microbes (Lessard *et al.* 2012) that would otherwise have competed for resources if their growth cycles had overlapped. This point is emphasized by the dominance of well integrated species such as *P. camembertii*, *G. candidum*, and *D. hansenii* (Leclercq-Perlat *et al.* 2013b) and the rapid disappearance of the poor competitor *K. lactis* when its growth overlaps with the growth of a more competitive species such as *D. hansenii* (Lessard *et al.* 2012). This may partially explain why some species such as *D. hansenii* can exist in the rind ecosystem throughout aging and why other species disappear over time.

Cooperative interactions between some species allow their complementary metabolisms to take advantage of the available nutrient sources. One excellent example of complementary metabolism is the exploitation of cheese proteins by *G. candidum* and *P. camembertii* (Boutrou *et al.* 2006). Proteolytic activity by *G. candidum* is limited compared to *P. camembertii*, and although *P. camembertii* can hydrolyze large peptides into amino acids with exopeptidases, it cannot consume small and medium peptides as quickly as *G. candidum*. Thus, when grown in mixed culture on cheese, these microbes

hydrolyze a variety of peptides faster than when each species is grown in monoculture. This synergistic effect can lead to more rapid amino acid deamination and faster deacidification of the cheese surface due to ammonia production. The cooperative interaction of these microbes on the surface of cheese and the increased metabolic efficiency that it yields is reminiscent of the stratification and step-wise oxidation and reduction of substrate in microbial mats.

Metabolite Accumulation and Nutrient Depletion in Cheese

One major difference between microbial mats and cheese rinds is the apparent absence of primary producers on the surface of cheese. The absence of phototrophs likely reflects the limited light in aging caves, although phototrophs have been observed as members of biofilms in Roman catacombs, where they derive energy from the lighting fixtures used to light the passages (Sanchez-Moral *et al.* 2004). Nonetheless, rind metabolism proceeds in a unidirectional manner, in contrast to microbial mats, many of which are stable biological ecosystems (Dupraz and Visscher 2005). In microbial mats, aerobic respiration is tightly coupled to photosynthesis (Visscher and Stolz 2005) to yield an extremely stable system.

The tendency of cheese rinds to form crystals reflects the linear nature to the heterotrophic respiration. Starting with the yeasts, surface microbes metabolize lactate and produce alkaline metabolites (Mounier *et al.* 2006), which raises the pH. The size of the cheese may affect the ability of the system to buffer against the metabolites produced by the rind, with large cheeses buffering more effectively than small cheeses (Wolfe *et al.* 2014). Regardless, the processes of heterotrophic consumption of carbon and nitrogen substrates proceed linearly and eventually raises the pH.

Upon depletion of lactose, some species on the surface of cheese, such as *P. candidum*, exhibit stress responses and survival strategies such as sporulation and partial mycelial death (Leclercq-Perlat *et al.* 2013b). The response of other species, such as *K. lactis*, is a loss of competitive advantage and population decline (Leclercq-Perlat *et al.* 2004a). The stress response by *P. candidum*, which is characterized by a robust peptidolytic activity (Leclercq-Perlat *et al.* 2004a), also corresponds to a shift in metabolism away from lactose. The mold can use lactate, peptides, and amino acids, which result in diminished acid levels and high ammonia concentrations (Leclercq-Perlat *et al.* 2013b), both of which raise the cheese pH. This activity eventually leads to the depletion of carbon substrates (Leclercq-Perlat *et al.* 2000a) and the accumulation of ammonia (Couriol *et al.* 2001). Ammonia could accumulate and raise the pH to a point where it inhibits the growth of surface microbes (Amrane *et al.* 1999). In combination with carbon depletion, this process would certainly doom the cheese rind community. This is a striking distinction from the ecological stability of many microbial mats.

Accumulation of Metabolic Gases in cheese and Other Microbial Systems

Consumption of lactose, lactate (Couriol *et al.* 2001; Picque *et al.* 2006), and amino acids (Picque *et al.* 2006) results in CO_2 production by the surface microbes**.** In addition, the deamination of amino acids results in the release of ammonia, which also raises the pH (Leclercq-Perlat *et al.* 2000b). The amount of CO_2 and ammonia released from ripening cheese depends on the atmospheric conditions in the ripening room, such as temperature and humidity, which are under the control of the cheesemaker and can be used to control the course of ripening (Picque *et al.* 2006). Temperature in particular can

be modulated to control the kinetics of particular microbes (Leclercq-Perlat *et al.* 2013b), but none of these variables can prevent the production of these gasses altogether.

In contrast, the tightly modulated phototrophic-heterotrophic ecosystem in a microbial mat ensures that these gasses do not accumulate in excess, making these relatively closed systems quite stable. Nonetheless, crystal precipitates are observed in many microbial mats, suggesting that accumulation of crystallization reactants can occur. However, the microbial mats that have a balance between photosynthesis and respiration will also display net dissolution of minerals, depending on the balance between photosynthesis and respiration, which varies by the time of the day (Dupraz and Visscher 2005). Some mats that experience catastrophic disturbances such as burial in sediment will experience extensive carbonate precipitation, with a new community growing above the old in a laminated structure (Visscher and Stolz 2005).

In cheese rinds, the accumulation of CO_2 is a function of CO_2 production in the cheese as well as the exchange of this soluble gas between the headspace and the cheese, which depends on the abundance of CO_2 in the headspace (Picque *et al.* 2006). The accumulation of ammonia would be expected to depend on the same variables. Although studies investigating the partitioning of ammonia in the headspace and cheese in surface ripened cheese production have not been conducted, Cortez *et al.* (2008) showed that ammonia readily dissolves from the headspace into mozzarella cheese, thereby raising the pH. One would expect a similar dynamic between the headspace and surface ripened cheeses, although the concentration of ammonia in the headspace would likely be much lower than the concentration used in the aforementioned study.

Effect of pH Changes on Crystallization in Microbial Systems

Processes in any system, including the various microbial systems mentioned in this work, can result in crystallization if the chemical prerequisites for crystallization are satisfied. In cheese, the accumulation of CO_2 and ammonia are necessary for the precipitation of ikaite and struvite, which contain CO_2 and ammonia, respectively (Tansman *et al.* In Press). In order to precipitate carbonates, including ikaite, a shift in alkalinity is required (Visscher and Stolz 2005). In many microbial mats, even a small shift in alkalinity is often sufficient to exceed the pH-dependent solubility threshold of carbonates and induce precipitation. Carbonate precipitation results in the release of hydrogen ions, thereby reducing the pH and solubilizing the newly precipitated carbonate mineral. In some microbial mat systems that contain very high concentrations of calcium, the pH is sufficiently buffered to allow an increase in heterotrophically generated CO_2 to induce precipitation of carbonate minerals without resulting in a drop in pH (Visscher and Stolz 2005).

Although cheese rinds are heterotrophic systems, CO_2 production and carbonate mineral precipitation does not result in a large enough drop in pH because the consumption of organic acids and production of ammonia continuously push the system toward increasing alkalinity. Interestingly, one would expect the precipitation of ikaite on the surface of cheese to release hydrogen ions and to provide some buffering effect, although this, of course, has never been mentioned in the food science literature. Research on this topic would be interesting considering the effect of carbonate precipitation on pH in microbial mat systems.

In microbial mats, CO_2 degassing causes a net increase in pH and has been implicated for carbonate precipitation in many geological sediments in the absence of direct microbial activity (Arp *et al.* 1999). This process has also been deemed important in microbial mats, along with the degradation of organic acids (Dupraz and Visscher 2005). As mentioned above, organic acid consumption by the surface microbes in cheese is an important driver of alkalinity. Likewise, CO_2 degassing has been reported in the cheese literature as an important contributor to cheese weight loss during aging (Picque *et al.* 2006), although the net effect on pH has apparently not been investigated.

Abundance of Reactants and Nucleation Sites as Predictors of Mineral Formation

Given the metabolic similarities between microbial mats and cheese rinds, and the abundance of calcium in both cheese and geological systems, it is not surprising that carbonates can form in both systems. Conversely, struvite, which can form in cheese, has only been observed in geological systems such as guano caves, in which an abundance of ammonia is present (Gull and Pasek 2013). It is possible that microbial mats that are rich in magnesium and phosphate, the other two components of struvite, are deficient in ammonia to the extent that struvite will not form. Although this hypothesis does not appear to have been tested, the rarity of struvite in geological settings (Gull and Pasek 2013) suggests that the formation conditions do not tend to exist outside of a few specialized environments.

In waste effluent systems, however, struvite frequently forms at various points along the stream, both in the vicinity of microbial biofilms as well as downstream. Biofilms in infected catheters (Stickler 1996) as well as biofilms within the urinary tract during infection (Clapham *et al.* 1990), tend to precipitate struvite. This suggests, and

research has confirmed, that these systems contain the correct proportions of reactants, as well as a prerequisite increase in pH, to precipitate this mineral. Struvite has also been observed in waste systems including swine lagoons (Nelson *et al.* 2003) and batch reactors (Wang *et al.* 2013) that are rich in ammonia-producing bacteria in addition to a large quantity of magnesium, phosphate, and alkalinity. Thus, it appears that struvite is quite commonplace in systems that have the conditions necessary for struvite formation.

Another characteristic that the aforementioned struvite-forming environments have in common is an abundance of organic material that can form nucleation sites for the crystals. The availability of nucleation sites lowers the free energy change that is necessary for crystallization to occur (Garside 1987), which lowers the supersaturation needed for crystallization to occur (Clapham *et al.* 1990) and increases the tendency of crystals to appear. Struvite that occurs in a biofilm is invariably associated with microbial materials known as extracellular polymeric substances (**EPS**), which contain many anionic functional groups that are capable of binding magnesium (Clapham *et al.* 1990; Stickler 1996). In many such systems, the crystals grow within the microbial material in which they precipitate (Clapham *et al.* 1990). Studies have demonstrated the ability of purified EPS from some bacteria to precipitate struvite in an abiotic laboratory setting (Stickler 1996), which represents one way of identifying the microbes that are responsible for nucleating the crystal, although it does not indicate the species that is responsible to producing the ammonia or raising the pH. Some type of EPS is also present in the smears on the surface of washed rind cheese (Larpin *et al.* 2006), and almost certainly plays a role in crystallization of ikaite and struvite, although it appears that even a preliminary analysis of the polymers has yet to be conducted.

In wastewater treatment facilities, evidence suggests that the struvite deposits that form on the surfaces of pipes result from abiotic factors such as increased water turbulence (Stratful *et al.* 2001). The working hypothesis states that water turbulence causes a decrease in pressure and a release of dissolved CO_2, and results in an elevated pH. This mechanism is somewhat reminiscent of the abiotic geological carbonate deposits described above that result from CO_2 degassing. The chemistry of the wastewater flowing through the piping, such as the initially high pH and abundant ammonia, is certainly controlled by biological processes upstream (Stratful *et al.* 2001), although interaction with microbial communities does not appear to be the direct cause of precipitation in this case. However, these abiotic struvite precipitates apparently nucleate on unspecified 'foreign solids' (Stratful *et al.* 2001), which could potentially be composed of microbial flocs or EPS.

Struvite precipitation requires a high ratio of magnesium to calcium (Gull and Pasek 2013), and under slightly elevated calcium conditions, precipitation of other crystal phases such as the calcium phosphate mineral brushite can occur in waste systems (Pak *et al.* 1971). Likewise, slightly elevated sulfate concentrations can yield the calcium sulfate mineral gypsum instead of brushite (Kuz'mina *et al.* 2013), suggesting that a thorough understanding of the environmental chemistry is necessary to achieve an accurate prediction of microbially-precipitated minerals in a given system (Dupraz and Visscher 2005). Even moderate differences in temperature with all other biotic and abiotic conditions kept constant could result in the formation of different crystal phases (Amrane and Prigent 2008). In addition, species and group metabolism could impact crystallization

environment and would therefore need to be thoroughly understood in order to predict the outcome of a biomineralization event (Dupraz and Visscher 2005).

Impact of Microbial Metabolism on Mineral Phase Nucleation

Little is known about the variables that contribute to the bio-crystal polymorph selection, which may be species-specific and may involve specific biomolecules or the microbial cell wall (Dhami *et al.* 2013). Biomolecules can influence the resulting crystal characteristics and mineralization rate (Wang and Muller 2009). Although a knowledge of the redox potential could provide insight into the broad types of crystals that are likely, namely hydroxides, carbonates, and phosphates in oxic zones and metal sulfides in anoxic zones (Remoudaki *et al.* 2003), the particular phases cannot be narrowed down as easily. Salt concentrations and ionic composition are just two of the myriad factors that may influence the mineralization (Rivadeneyra *et al.* 2006). In addition, and perhaps most enigmatically, the preexistence of minerals in a system can influence the precipitation of successive minerals through surface sorption phenomena (van Hullebusch *et al.* 2004)

Although predicting the resulting biomineral in a given environment seems prohibitively complex, identifying the species responsible for a mineralization event is possible. To achieve this, the identity and quantity of members of various species would need to be elucidated. This could be done by a variety of methods that each have benefits. One could make use of a PCR-based method (Larpin *et al.* 2006; Leclercq-Perlat *et al.* 2013b; Lessard *et al.* 2012) to amplify DNA in a sample. One of the disadvantages to using PCR-based amplification is the possibility that DNA from dead cells could be replicated (Tsiamis *et al.* 2008), thereby introducing an artifact and making it more

difficult to identify microbial succession in an ecosystem. To ensure that this is not the case, users of PCR-based methods can use a secondary technique to validate the method for a particular ecosystem. The members of a large microbial ecology can be identified using powerful techniques such as large scale sequencing, metatranscriptomic studies, and metagenomic analysis with 16SrRNA (Franks and Stolz 2009). Furthermore, molecular techniques could also help to elucidate the biomolecules that are present in the nucleation environment in order to understand the matrix-metal interactions that favor certain crystal phases over others (Gonzalez-Munoz *et al.* 2008).

Techniques for Studying Microbe-Mineral Interactions

Cheese agar mediums have been used to quantify cheese microbes (Lessard *et al.* 2012), but these techniques are limited by the culturability of the microbes (Wolfe and Dutton 2012) and may be biased by the composition of the culture media (Dupraz *et al.* 2009). Even when microbes can be cultured, minor populations could be overshadowed and difficult to enumerate using culture-dependent methods (Lessard *et al.* 2012). In heterotrophic systems, CO_2 production could be monitored with an IR detector to gain insight into the respiration rate and growth dynamics (Couriol *et al.* 2001; Picque *et al.* 2006), although this cannot provide detailed information in a mixed culture and is confounded by the precipitation of carbonate minerals and the dissolution of CO_2 in the growth media. Given the correlation between oxygen and CO_2 in microbial respiration (Picque *et al.* 2006), concurrent measurement of oxygen could, however, be used to determine the quantity of CO_2 that is deposited in the medium or in crystals, which could provide information on metabolism as well as crystallization. Although this technique has

been used, it has not been explicitly used to provide insight into crystallization phenomena.

The most developed techniques for this purpose involve microscopy, wherein the proximity of precipitates to microbial cells or their exudates provides insights about the microbes involved in the biomineralization. Microscopy can provide insights into the spatial arrangements and in situ interactions that exist between microbes in a community (Surman *et al.* 1996), which is especially important given the microspacial heterogeneity that may exist within a community (Decho 2010). Microanalysis, which can be used with certain kinds of microscopy, could provide elemental analysis of the particles identified by microscopy (Han *et al.* 2015; Watson and Demer 1996), which greatly enhances the information that can be gleaned from this technique. The microenvironments that exist at the cell wall as a result of cellular metabolism could create supersaturation conditions (Benzerara *et al.* 2011) that could become apparent by observing the proximity of micro-crystals to the cell wall (Rizzo *et al.* 1963). Imaging techniques may be misleading, however, if a community includes microbes that have evolved mechanisms to induce crystallization away from the cells, on EPS for instance (Benzerara *et al.* 2011). The identification of microbes responsible for exuding such EPS, or for exuding molecules that impact crystal morphology by poisoning certain growing faces, would be difficult and would likely not be possible with microscopy. In order to understand such complex systems, one would have to study the mineral and the microbial community as a single interacting unit (Benzerara *et al.* 2011).

Regardless of the technique, the ultimate challenge is to determine if minerals in a biological matrix are biologically induced, in which the microbial metabolism causes the

necessary shift in equilibrium, or biologically influenced, in which biomolecules produced by the microbes influence the chemical identity, morphology, and other characteristics of a crystal (Benzerara *et al.* 2011). In many cases, the goal of linking a particular product to a microbiological origin or process remains elusive (Riding 2000). The enhanced techniques of tomorrow will hopefully shed light on these systems by allowing users to efficiently identify the minerals, microbes, and processes involved in biomineralization phenomena.

THEORETICAL BASIS FOR POLARIZED LIGHT MICROSCOPY

PRINCIPLES OF THE POLARIZED LIGHT MICROSCOPE

The polarized light microscope is a modified light microscope that possesses several additional filters and a specialized rotating stage and is used for the observation of minerals and other isotropic anisotropic material. Polarized light microscopy (**PLM**) allows the user to take advantage of two optical phenomena that facilitate characterization and identification of specimens; the first is the plane-polarization of light and the second is the refraction of light in isotropic and anisotropic material. There are two types of polarized light microscopes, transmitted light and incident light, which correspond to the two types of light microscopes that are typically modified for PLM. Transmitted polarized light microscopes can be used to image translucent materials, whereas the incident polarized light microscope is used to image opaque materials that are not compatible with transmitted PLM. All of the specimens that were investigated in my research were compatible with transmitted PLM, therefore the following discussion will focus on the transmitted light microscope and will not discuss the finer points of PLM on opaque surfaces.

When light is emitted from a source, such as the sun or the tungsten filament on a light microscope, the ray vibrates in many random directions perpendicular to the ray's propagation direction. This type of ray is referred to as non-polarized light. When such a ray is passed through a polarizer, the light that emerges from the other side is polarized such that it only vibrates in a single plane perpendicular to the ray's propagation direction. On the polarized light microscope, a polarizer is installed between the light

source and the specimen so that the specimen is illuminated by plane-polarized light that is vibrating in the polarized direction, which depends on the microscope's manufacturer. A second polarizing filter that is oriented perpendicular to the polarizer, called an analyzer, sits between the objective and the ocular and can usually be removed so that the user can switch between viewing the field in plane-polarized light and crossed-polarized light. Under the latter setting, the vibration plane that emerges from the polarizer is blocked by the perpendicular analyzer. The result is a completely black field in which none of the light passes the analyzer.

Refractive Indices in Isotropic and Anisotropic Material

Crossed-polars are useful for observing anisotropic materials. Per Snell's law, when light passes into a material with a higher refractive index, the speed of light slows and the light is bent toward the normal of the interface; likewise, when light passes into a material with a lower refractive index, the speed of the light increases and the light is bent away from the normal of the interface. Whereas isotropic materials have one refractive index, anisotropic materials have two or three refractive indices. Thus, when light passes through an isotropic material, its refraction does not depend on the orientation of the specimen. In contrast, anisotropic materials characteristically refract light to a different extent depending on the orientation of the specimen. This phenomenon can be visualized with an indicatrix, which is a three-dimensional representation of a material's refractive indices. In an indicatrix, the three axes of an ovoid represent the three refractive indices, with larger refractive indices being drawn longer.

The refractive indices in an isotropic material are equivalent, so the indicatrix of an isotropic material is a perfect sphere. In contrast, the indicatrices of anisotropic

materials are more irregular and come in two varieties. In uniaxial materials one of the refractive indices is different from the other two, whereas in biaxial materials all of the refractive indices are different. In an anisotropic indicatrix, there are either one or two optical axes, which are axes whose perpendicular cross-sections within the indicatrix would yield a circle. As their names suggest, uniaxial materials possess one such axis and biaxial material possess two. To this effect, the refraction of an anisotropy measured under polarized light will differ depending on the orientation of the anisotropy's axes relative to the light beam (Smithson 1948).

Observation of Polarized Light Traversing Anisotropic and Isotropic Materials

When plane-polarized light passes through an isotropy, the light is refracted per Snell's law as a function of the one refractive index characteristic of that material. Although the plane-polarized light is refracted by the isotropy, the polarization of the light does not change and the light emerges from the isotropy with the same plane of vibration. When viewed under crossed-polars, the light emerging from isotropic materials is absorbed by the analyzer and the field appears completely black. Conversely, when plane-polarized light passes through an anisotropy, the light is split into two separate rays, called the ordinary and the extraordinary, whose vibrations are mutually perpendicular and whose vibrational planes depend on the orientation of the optical axis/axes of the material. Under crossed-polars, the two rays emerging from anisotropic material recombine into a polarized ray that is the product of the interference of the ordinary and extraordinary ray. This ray is not absorbed by the analyzer, assuming that the optical axis/axes are oriented such that the vibrational direction of the emerging ray does not overlap with the analyzer. Thus, under crossed-polars, anisotropic material will

appear illuminated against a black background, which not only provides excellent image contrast (Ivorra *et al.* 1999), but can also be used to definitively identify material as anisotropic. Furthermore, separation of the ordinary and extraordinary rays, and their subsequent recombination, produces optical properties that can be used to characterize and identify the particular anisotropic material in the specimen.

Due to their different paths through the anisotropy, the ordinary and the extraordinary rays are slowed to different extents before they emerge and recombine in a process called retardation. The difference in retardation between the two rays is called birefringence and it is caused by the phase differences between the two rays as they recombine into a ray with new wavelengths, and therefore new colors. Materials displaying high birefringence display a variety of rainbows, whose colors correspond to the interference of the two waves. These patterns, in combination with additional filters above the analyzer, can be used to identify well characterized materials. Also, because retardation and birefringence vary with the thickness of the anisotropic material, the apparent extent of birefringence can be used as an indicator of the thickness of the material.

INTERFERENCE FIGURES

Birefringence can also be harnessed to generate interference figures, which can help to identify an anisotropic material and can also indicate the orientation of the anisotropy. Interference figures are generated with the help of several implements that are unique to the polarized light microscope. The typical light source in a polarized light microscope is orthoscopic, meaning that the rays entering the specimen are roughly parallel. The conoscope is a series of additional lenses that project a cone-shaped light

source through the specimen so that an interference figure, which is the result of non-parallel rays traveling in many directions through the anisotropy, is projected on the objective lens. Another lens that resides above the analyzer, called a Bertrand lens, is used to focus on the projection so that it is observable through the ocular.

The interference figure is similar to the interference colors that form on the anisotropy as a result of birefringence, but the interference figure provides additional valuable information. If a uniaxial anisotropy is aligned on the microscope stage such that the optical axis is parallel or nearly parallel to the light ray, the interference figure will show characteristic features. The interference figure displays a circular pattern called a isochrome with isogyres, or black crosses, that result from the vibration of the polarizer and analyzer, and which are characteristic of a projection down the optical axis of a uniaxial anisotropy. If the anisotropy is biaxial, a projection down the axis that bisects the two optical axes, called a bisectrix, yields an interference figure that displays two isogyres some distance apart. An interference figure in which the two isogyres are a similar distance from the center is characteristic of a projection down the biaxial anisotropy's acute bisectrix. With this projection, the distance between the thinnest part of each isogyre corresponds to $2V$, which is the angle between the two optical axes, and which is a characteristic feature of a given biaxial anisotropy.

Extinction Angles

Characteristic extinction angles can be determined for anisotropies displaying directional elongation, or other directional features such as mineral cleavage. The extinction angle is a useful piece of information for identifying an anisotropy, but care must be taken as extinction angle varies with the orientation of the anisotropy. Extinction

angles are most often determined for anisotropies whose optical axis/axes are parallel to the light beam. This orientation may be implied by the tendency of the anisotropy to rest in a particular orientation, for instance on the cleavage face in the case of some minerals. Otherwise, a random anisotropy could yield a random extinction angle measurement, which would be useless for phase identification. In mineralogy, extinction angles can be described as parallel or inclined relative to a feature such as a cleavage plane or a growing axis. Minerals with inclined extinction can be further characterized by a specific offset angle relative to the feature, however, the orientation of the mineral must be known in order for the measured angle to be used for conclusive identification.

Identifying Crystal Phases by their Optical Properties

The addition of different types of compensators or accessory plates above and at a diagonal to the analyzer allows for the sign of elongation to be measured. This technique, in combination with some of the other optical techniques described above, can be used for identifying anisotropies based on the anisotropy's sign of birefringence (McCarty and Hollander 1961). In fact, this technique is considered the gold standard in medicine for identifying calcium pyrophosphate dehydrate and monosodium urate crystals in the inflamed joints of patients suffering from gout (Ivorra *et al.* 1999). The compensators, which may be constructed of a variety of materials with differing optical properties, characteristically interact with the interference colors displayed by an anisotropy. Compensators can be used when viewing interference colors in an interference figure or when viewing interference colors on an anisotropy under crossed polarized orthoscopic light. Characteristic changes in interference colors using different compensators can also contribute to conclusive identification of an anisotropy (McCarty

and Hollander 1961). Well characterized anisotropies, such as crystals with elongated growth axes, are described according to the elongation of their refractive indices. In uniaxial anisotropies, when the refractive index of the optical axis is greater than that of the other axes, the anisotropy is called ‘uniaxial positive;’ when the reverse is true, the anisotropy is called ‘uniaxial negative.’ The same nomenclature applies to biaxial anisotropies, but the mathematics of determining the sign of a biaxial anisotropy are considerably more complex. This elongation sign can be measured in uniaxial anisotropies by aligning the growth axes parallel or perpendicular to the compensator and observing whether higher or lower order interference colors become apparent. Many accessory plates are available, and their applications vary depending on the plate and the specimen.

The polarized light microscope is arguably one of the most powerful simple instruments available. A respected mineralogist once commented to me that if one were to be marooned on a desert island with only one scientific instrument, the instrument of choice would undoubtedly be the polarized light microscope, in lieu of more sophisticated but less versatile alternatives. Despite its apparently simple design, the application of plane-polarized light in combination with various auxiliary lenses and accessory plates allows the PLM user to gain great insight into a variety of anisotropic materials.

QUANTITATIVE METHODS OF OPTICS IN CRYSTAL RESEARCH

QUANTIFICATION OF CRYSTALS IN FOODS USING OPTICS

In the investigation of crystals in food, the most important parameters with respect to mouthfeel are size, abundance, and shape (Afoakwa *et al.* 2007; Hough *et al.* 1990; Imai *et al.* 1995). Although much of the past microscopy work on crystals in food has been non-quantitative, several studies have used image analysis techniques to determine quantitative metrics. Several of the analytical methods that have been used in food research are based on methods that were originally used to investigate geological mineral thin sections and grain mounts with petrographic polarized light microscopy. Food has some unique characteristics when compared to geological samples that must be considered when attempting to collect quantitative data on crystalline particles. For instance, the amorphous biological matrix is very different from the largely crystalline mass found in geological specimens, and the relatively soluble crystals that tend to form in food are more susceptible to artifacts from sample preparation than crystals in geological samples, which tend to be much less soluble. Nonetheless, the petrographic techniques have found useful applications in food science on several occasions.

When collecting quantitative data on crystals in cheese, it is critical for one to be able to identify the crystals in the specimen, especially if multiple crystal phases are suspected. Several cheese studies that have used PLM, including my work, have relied on birefringence of anisotropic crystals under cross-polars as the primary method for detecting the presence of crystals (Brooker 1987; Brooker *et al.* 1975; Tansman *et al.* In Press). This technique, although straightforward, cannot be used to image isotropic

crystals, which, if present, would be optically extinct under crossed polars. Although nearly all crystal phases, apart from sodium chloride, that have been cited in the cheese literature are anisotropic, the inability to image isotropic crystals represents a major limitation to quantifying crystals in cheese with confidence. Previous researchers apparently accepted this shortcoming as a limitation of the technique. Nonetheless, Miloslav Kalab, arguably the most prolific dairy foods microscopist, cautioned that multiple techniques should be employed whenever a food is imaged for the first time (Kalab 1995). In my work, powder X-ray diffractometry was employed to determine if isotropic phases were present within the detection threshold of the diffractometer, and similarly, Ware (2003) used X-ray fluorescence to validate point-counting against major element abundances. Validation of PLM imaging with a parallel technique is critical because the presence of an optically extinct isotropic phase could result in a gross under-estimation of the number or volume of crystals in a specimen.

Previous cheese researchers have used staining techniques, such as the von Kossa stain, to label particles of interest and to differentiate them from other crystal phases in the cheese (Brooker *et al.* 1975; Morris *et al.* 1988). It should be noted that the authors of those studies overstated the specificity of the staining technique, with one study stating the technique could identify phosphates and carbonates, and the other study stated that the stain could identify calcium phosphate. In reality, the stain can be used to identify a broad range of carbonate, phosphate, oxalate, sulfate, urate, chloride, and sulfocyanide salts (Thompson and Hunt 1966). Although oxalates, urates, and sulfocyanides are probably not present in cheese, I recently observed the presence of several carbonate and phosphate phases that would have been misidentified as a result of the assumptions made

about the specificity of the von Kossa technique (Tansman *et al.* In Press), which highlights the need to consider the specificity of an imaging technique.

On the few occasions that quantitative data were extracted from PLM observations of cheese, the authors borrowed a quantitative 'point-counting' technique from the mineralogical literature (Brooker 1987; Morris *et al.* 1988). Although the cited technique in the text entitled "On the Geometrical Methods of Quantitative Mineralogic Analysis of Rocks" was not available, the title and the sample preparation methods used by the aforementioned authors suggest that this technique is similar to the point counting technique described by Hunter (1967), with some important distinctions. Hunter (1967) used point-counting to calculate weight percentages of specific minerals in a samples, whereas Brooker (1987) and Morris *et al.* (1988) used point counting to determine the volume fractions of crystals in cheese. These techniques differ only in the mathematical treatment of the point-counting results, with the volume fraction calculation relying on an estimation of the volume of each crystal, whereas the weight percentage calculation also included a density correction for each type of crystal.

Quantification of the Number Frequency

Point-counting involves applying a grid of equally spaced lines on a sample (Neilson and Brockman 1977), either physically or digitally. Particles underlying equidistant points on the grid are counted. Using this method, particles can be counted uniformly and efficiently. However, application of the grid and selection of the starting point must be done at random in order to avoid biasing the measurement. The combination of the uniformity of the point-counting grid and random grid placement typify the principles of systematic uniform random sampling (**SURS**), which is intended

to provide unbiased yet efficient sampling (Altunkaynak *et al.* 2012). Point counting is similar to the Line Method, wherein lines are drawn across a field and all particles that fall on that line are counted. Similar to point-counting, the placement of the lines must be random in order to reflect the potential heterogeneity of particles within a field (Galehouse 1969). The metric that one obtains from point-counting or the Line Method is known as the 'number frequency' (Galehouse 1969). The number frequency reflects the number of particles present in the sample as well as the area represented by a type of particle because particles with a larger area are more likely to fall on the line or grid-points, and are therefore proportionally more likely to be counted (Galehouse 1969). The size of the point-grid should be slightly larger than the largest particles in the population so that no particle is counted more than once and the grid size must remain constant throughout the experiment (Neilson and Brockman 1977).

Quantification of the Number Percentage

Several other techniques are used to count particles in a field, although the resulting metric is not a number frequency and must therefore be treated differently. These techniques include the Fleet Method and the Ribbon and Area Methods (Galehouse 1969). Using the Fleet Method, one would count all of the points within a field. The Ribbon and Area Methods are variations of the Fleet Method, in which points within a representative portion of the field are counted. In the Ribbon Method, two parallel lines are drawn, either physically or digitally, and only points that fall entirely between the lines are counted. Similarly, in the Area Method, a rectangle or square is applied to the field and only points within the selected area are counted. The Fleet, Ribbon, and Area Methods are similar in the sense that all points within the relevant counting region are

equally weighted, without consideration for the size or dimensions of the particle (Galehouse 1969). The resulting metric is called a 'number percentage' and it is a one-dimensional quantification of the particles without consideration for the area attributable to each particle. Although these methods provide a mathematically unbiased estimate of the number of particles in a field, a number percentage cannot be used to calculate volume or weight fractions without using image analysis to calculate the area attributable to each type of particle (Galehouse 1969). In addition, these techniques are susceptible to edge effects that could result from particles falling partially outside of the counting region. Such edge effects are minimized by disqualifying any particles that are not entirely within the counting region.

Despite the limitations of the number percentage, a version of the Fleet Method was used to investigate lactose crystals in a South American dairy food known as Dulce de Leche (Hough *et al.* 1990). In this study, a small quantity of Dulce de Leche was weighed onto a glass slide and gently pressed into a nearly circular dispersion using a cover slip. The area of the circle under the cover slip was calculated and 10 randomly chosen fields were observed using PLM. The crystals in each field were counted in a manner resembling the Fleet Method. The number of crystals on a weight basis in the bulk material was calculated by multiplying the number crystals in each field by the ratio of the area of the sample on the slide to the area of the microscopic field and dividing by the weight of the sample on the slide. These values, calculated for each of the 10 randomly chosen fields, were averaged to obtain an estimate of the number of crystals on a weight basis in the bulk material. The authors conceded that experimental error was introduced because the number of crystal in each field varied depending on the location

within the sample on the slide. This concession highlights the importance of randomly selecting fields within a specimen so that the non-uniformity of particles within the specimen does not influence the user's selection of fields. To this end, SURS can be used here as well for selecting the number and location of fields within a specimen (Altunkaynak *et al.* 2012).

Effective Sampling of Matrices Containing Crystals

SURS sampling is often used in the selection of cryomicrotome sections (Gardi *et al.* 2008), with the frequency of sections determined beforehand while the first section sampled is decided randomly. Although consecutive sectional profiles may be useful for obtaining stereological data in sliceable biological samples, their use in samples containing brittle crystals would be limited because the crystals would either shatter or pop out of the section, unless the crystals were small or the microtome section sufficiently thick. Therefore, investigation of matrices with large crystals would likely be limited to a technique analogous to the method of Hough *et al.* (1990) in their study of Dulce de Leche or the method of Johansson *et al.* (2008) in their study of mineral grains mounted on glass slides. In any case, stereological serial section is probably not feasible to anyone working with large brittle crystals and therefore one would be limited to measuring particles in two dimensions. Some additional insight into the thickness of mineral grains in a grain mount could be provided by using an optical dissector, wherein different "sections" of a specimen are observed by light microscopy by varying the plane of focus (Altunkaynak *et al.* 2012); however, it is unclear if this technique would be sufficient to determine the thickness of grains and arrive at a correction factor for volume. In one study, where some of the observed crystals were assumed to be equant,

the volume correction factor used was the cube of the crystal diameter (Hunter 1967). In that study, when somewhat irregular crystals were encountered, the cube of the shortest visible diameter was used in the calculation of volume, with the assumption that the grains would tend to lie on their flat surfaces. Hunter (1967) assumed that using the cube of the small diameter for grains that were not equant would not introduce a large error for most minerals, although for excessively platy crystals, this assumption would probably not be valid.

Whether SURS is used on a series of thin sections, a single thin section, or a grain mount, the selection of a sufficient number of fields to represent the specimen is required in order to minimize the experimental error. The coefficient of error, which can be estimated by dividing the standard deviation by the sample average (Altunkaynak *et al.* 2012), is an effective measurement of the error associated with the sampling frequency. A high coefficient of error indicates that the frequency of sampling is insufficient compared to the variability of the specimen. The number of samplings must be increased until the coefficient of error is acceptably low. An acceptable coefficient of error is typically 0.05 or less (Altunkaynak *et al.* 2012). If multiple subpopulations, such as multiple types of crystals, are being measured, a similar calculation can be performed to estimate the variability with respect to each subpopulation. In this case, the population standard deviation is divided by the mean of each subpopulation. This calculation is called the 'coefficient of variation' and is treated similarly to the coefficient of error. A consideration of both of these calculations could help the user minimize systematic deviations that could result from the heterogeneous nature of the population as a whole, or heterogeneity between subpopulations. It is advisable that preliminary studies be

conducted to determine if the amount of error in a given sampling scheme is acceptable (Altunkaynak *et al.* 2012).

A sufficient quantity of particles overall must also be counted in order to decrease the confidence interval and increase the reliability of the estimate (Johansson *et al.* 2008). To this end, authors have used various strategies to ensure that the particles of interest are counted in sufficient numbers. For instance, Ware (2003) substituted SEM for PLM in order to effectively point-count small silt particles with image analysis. At the other extreme, Johansson *et al.* (2008) used an innovative photographic set up involving a camera on a track to capture images of entire slides, thereby maximizing the number of crystals available for image analysis. Hunter (1967) stated that similar accuracy could be obtained with point-counting, the Line Method, and the Ribbon Method if crystals were similarly sized and packed closely on the microscope slide. Regardless of the strategy, it is apparent that a sufficiently large population of particles must be measured in order to achieve reliable results with image analysis.

Accurate Identification of Crystals as a Prerequisite for Quantitative Methods

Regardless of the imaging analysis technique in use, accurate identification of crystals in the sample is fundamental to acquiring accurate measurements. This is especially true in the case where multiple phases are present and where different correction factors for volume or weight are used. Effective identification can either be achieved through the use of stains such as the von Kossa, or by differentiating crystals based on their optical properties (Johansson *et al.* 2008), which would avoid the ambiguity of non-specific staining (Gardi *et al.* 2008). In order to use optical mineralogy in image analysis one would need to be familiar with the optical properties of the crystals

at various orientations, and this would necessitate preliminary work if such crystallographic characterizations were not available.

Despite the nuanced complexity of the various imaging techniques, it is apparent that PLM in combination with image analysis is a superior method for quantification of crystalline particles. Even though relatively little quantitative research has been done in Food Science using PLM, the availability of imaging techniques that have been developed and perfected in other disciplines makes these powerful techniques readily accessible to the Food Scientist. Further quantitative PLM work using the unique crystal-bearing specimens found in some foods will undoubtedly provide new insights into the application of PLM that will hopefully contribute to the discipline.

CHAPTER 2: CRYSTAL FINGERPRINTING: ELUCIDATING THE CRYSTALS OF CHEDDAR, PARMIGIANO-REGGIANO, GOUDA, AND SOFT WASHED-RIND CHEESES USING POWDER X-RAY DIFFRACTOMETRY

G.F. Tansman[1], P.S. Kindstedt[1] and J.M. Hughes[2]

[1]Department of Nutrition and Food Sciences and [2]Department of Geology

University of Vermont, Burlington, USA

Short title: X-ray Diffraction of Cheese Crystals

Corresponding author: P.S. Kindstedt: paul.kindstedt@uvm.edu; tel. 01 802 656 2935; fax. 01 802 656 0001

ABSTRACT

Crystals in cheese may be considered defects or positive features, depending on the variety and mode of production (industrial, artisanal). Powder X-ray diffractometry (PXRD) offers a simple means to identify and resolve complex combinations of crystals that contribute to cheese characteristics. For example, in studies of Parmigiano-Reggiano and long-aged Gouda, PXRD has confirmed that hard (crunchy) crystals that form abundantly within these cheeses consist of tyrosine. Furthermore, PXRD has tentatively identified the presence of an unusual form of crystalline leucine in large (up to 6 mm diameter) spherical entities, or "pearls", that occur abundantly in two-year old Parmigiano Reggiano and long aged Gouda cheeses, and on the surface of rindless hard Italian-type cheese. Ongoing investigations into the nature of these "pearls" are providing

new insight into the roles that crystals play in the visual appearance and texture of long-aged cheeses. Crystals also sometimes develop profusely in the eyes of long-aged Gouda, which have been shown by PXRD to consist of tyrosine and the afore-mentioned presumptive form of crystalline leucine. Finally, crystals have been shown by PXRD to form in the smears of soft washed-rind cheeses. These crystals may be associated in some cheeses with gritty mouth feel, and with zonal body softening that occurs during ripening. Heightened interest in artisanal cheeses highlights the need to better understand crystals and their contributions to cheese characteristics

Key words: X-ray Diffraction, crystals, cheese, tyrosine, leucine

INTRODUCTION

Crystals that form in cheese have been the subject of scientific inquiry for over a century, and X-ray diffraction (**XRD**) has been marshaled as a direct analytical approach to identify cheese crystals for almost as long, the earliest studies dating back to the 1930's (Tuckey et al., 1938[a,b]). Most XRD investigations of cheese crystals have been restricted to Cheddar cheese and have focused primarily on calcium lactate pentahydrate (**CLP**) crystals (Agarwal et al., 2006; Chou et al., 2003; Conchie et al., 1960; Dybing et al., 1988; Harper et al., 1953; Tuckey et al., 1938[a]; Washam et al., 1985). A few studies of Cheddar also identified the occurrence of crystals consisting of tyrosine (Conchie et al., 1960; Harper et al., 1953; Shock et al., 1948), cysteine (Harper et al., 1953; Shock et al., 1948), and calcium phosphate (Conchie and Sutherland, 1965). In the United States, visible crystals are often viewed by the Cheddar industry as defects and sources of

confusion for consumers (Johnson, 2014). Therefore, there has been considerable interest to understand the factors that promote crystal formation and develop measures to prevent their occurrence. In contrast, in some traditional cheeses such as Parmigiano-Reggiano and hand-crafted artisanal cheeses, crystals are viewed as important contributors to cheese character and quality (Noël et al., 1996; Zannoni et al., 1994). Growing consumer appreciation of traditional and artisanal cheeses is also fueling interest in understanding the nature and origins of crystals and their contributions to cheese quality and character.

Studies of crystals in cheeses other than Cheddar, such as tyrosine crystals in Roquefort (Dox, 1911), CLP, calcium phosphate and tyrosine crystals in Grana cheeses (Bottazzi et al., 1982; Bottazzi et al., 1994), calcium phosphate crystals in soft white mold surface-ripened (bloomy rind) cheeses (Boutrou et al., 1999; Brooker, 1987; Gaucheron et al., 1999; Karahadian and Lindsay, 1987), and CLP and calcium phosphate crystals in Serra cheese (Parker et al., 1998), have generally employed indirect methods such as chemical analyses or microscopy coupled with differential staining and X-ray microanalysis to identify presumed crystalline species. Although indirect approaches may provide useful presumptive identification of crystalline species, only XRD can furnish direct and definitive results because the XRD pattern of a specific crystal is determined by its three-dimensional atomic arrangement, which is unique to that crystal and thus analogous to a fingerprint. Consequently, the XRD pattern of an unknown species can be compared to those of known crystals; a perfect match with one of the known patterns provides definitive identification. Today, a growing database of over 250,000 known XRD patterns is accessible through the International Centre for Diffraction Data (**ICDD)**.

Powder X-ray diffractometry (**PXRD**), which utilizes crystalline specimens that ideally have been pulverized to a fine powder, is a versatile and user-friendly application of XRD. Major enhancements in the computing power of PXRD instrumentation, and advances in the software algorithms for data analysis, have opened up new opportunities for the study of cheese crystals. For example, the authors recently demonstrated that the two different enantiomeric forms of CLP that were presumed to occur in Cheddar cheese (i.e., the L(+) and D(-)/L(+) forms) can be identified and differentiated using PXRD, based on subtle differences in the XRD patterns of the two enantiomeric configurations (Tansman et al., 2014). The application of PXRD to study crystals in Cheddar and other cheese varieties could offer new insights into the factors that govern crystallization phenomena in cheese and the roles that crystals play in determining cheese character and quality. Therefore, the objective of the present research was to demonstrate the application of PXRD to study crystals from a range of different cheese types, specifically Cheddar, Parmigiano-Reggiano, Gouda and soft washed-rind (smear ripened) cheeses.

MATERIALS AND METHODS

CHEESE SAMPLES AND CRYSTAL COLLECTION

All cheese samples were commercially produced and purchased from local retail outlets, and crystals were harvested for analysis as described below, except for Cheddar cheese and a hard Italian-style cheese. In the case of Cheddar, the manufacturer harvested large (up to *ca.* 5 mm) internal crystals from the body of a Cheddar cheese sample (aged

2 y before sale) and delivered the crystals to the University of Vermont for identification after the manufacturer received a consumer complaint about unknown objects in their cheese. Crystals from a hard Italian-style cheese (obtained courtesy of Mark Johnson, Center for Dairy Research, University of Wisconsin) were scraped from the cheese surface using a spatula. Small (*ca.* 1-2 mm) dense crystals embedded in the body of Parmigiano-Reggiano cheese samples (aged 2 y) and Gouda cheese samples (aged 2 y) were physically excised from the surrounding cheese matrix using a dissecting needle and tweezers. The isolated crystals were brushed free of adhering cheese matrix. Parmigiano-Reggiano samples also contained white spherical entities that ranged from barely visible to around 6 mm in diameter, which will be referred to as "pearls" in this publication. Pearls were separated from the surrounding cheese matrix by slicing the sample with a wire cutter into 1 cm sections and gently applying pressure to the cheese surrounding the pearl using thumb and index finger. Gentle pressure caused the surrounding matrix to fracture and separate from the pearls, enabling the pearls to be isolated and brushed free of adhering cheese matrix. Similar pearls, though smaller in size distribution, also were harvested from the Gouda samples. Gouda samples also displayed extensive crystal formation along the surfaces of internal eyes. Crystals were scraped free from the surfaces of eyes using a spatula. The six soft washed-rind (smear ripened) cheeses that were examined in this study were produced by different companies, four located in the United States and two in Italy.

ANALYTICAL METHODS

Pearls collected from Parmigiano-Reggiano samples were evaluated for size distribution by placing them on a vibrating stack of 4 sieves of successively smaller mesh

size (5.6, 4.00, 3.35 and 2.00 mm) and counting the number of pearls retained by each sieve. The pearls were then pooled to form a composite sample, grated to fine particles in a blender and analyzed in duplicate for total solids content by drying in a forced-draft oven at 100°C for 24 h, fat content by a modified Babcock method (Atherton and Newlander, 1977), and for soluble leucine (i.e., free amino acid) content by a modified gas chromatography-mass spectrometry method as follows. Thirteen milligrams of pearls were homogenized in 100 ml of deionized water adjusted to a pH of 1 with HCl. The suspension was vortexed for 10 min and centrifuged at 5000 RPM for an additional 5 min to remove particulate material from the solution. A 1 ml aliquot of the mixture was removed for analysis and to this was added 0.1 ml of 8.37 mM 555 d_3 leucine (Isotec 486825 Lot TPI633-SP). The sample was mixed with 1 ml of 50% acetic acid and passed through cation exchange resin (Biorad AG50W-x8 cation exchange resin 100-200 mesh). The resin was then rinsed three times with 2 ml of deionized water. Amino acids were eluted off the resin by the addition of 2 ml of 4N ammonium hydroxide. The eluate was collected and evaporated under nitrogen gas. To the dry vial was added 200 µl of a 50:50 mixture of N-methyl-N-(t-Butyldimethylsilyl) trifluoro-acetamide+1%t-butyldimethylchlorosilane (MtBSTFA+1%t-BDMCS):acetonitrile. The solution was heated for 30 min in a heating block at 80°C and then transferred to an autosampler vial. A 1 µl aliquot was injected into a ZB1 gas chromatographer (**GC)** column (30 m in length; 0.25 mm inner diameter with 0.25 µm film). The GC was run isothermally at 165°C with a column flow rate of 1mL helium per minute. The mass spectrometer (**MS**) was run in selected ion monitoring mode and monitored for a mass to charge of 200 m/z for leucine and 203 m/z for labeled leucine.

Pooled samples of the cheese matrix surrounding the pearls were similarly grated and analyzed for total solids and fat contents. Gouda samples that displayed extensive crystal formation along the surfaces of internal eyes were examined by stereoscopic microscopy before the crystals were harvested for analysis. Smear material was scraped from the surface of soft washed-rind (smear ripened) cheeses employing a spatula, using care not to remove the underlying cheese matrix along with the smear. Smear material was analyzed for selected mineral content by inductively coupled atomic emission spectrometry as follows. A scraping of surface smear from one Vermont washed-rind cheese was dried and defatted in acetone and analyzed for Ca, Mg, K, and P by ICP-OES (Optima 3000DV, Perkin Elmer Corp, Norwalk, CT, USA). Calibration standards were prepared according to instrument manufacturer's suggested guidelines, to cover the range of concentrations in the sample set. Two-point calibrations (plus a Calibration Blank) were used for ICP analysis. Continuing Calibration Verification samples, prepared from an independent source, were used to check the calibration periodically.

In preparation for PXRD, dense internal crystals obtained from Cheddar, Parmigiano-Reggiano and Gouda cheeses, as well as crystals scraped from the surface of the hard Italian-style cheese and from the eyes of Gouda, were dried and defatted in acetone, finely ground using a mortar and pestle and transferred to a glass diffraction slide with a well. The powder in the slide well was leveled with the surface of the diffraction slide using a microscope slide. Diffraction patterns were generated from cheese crystals using a MiniFlex II powder X-Ray diffractometer (Rigaku, The Woodlands, TX). Diffractograms were generated at a speed of 2°2θ/minute between 5

and 50°2θ. Diffraction patterns were compared to existing entries archived in the ICDD database to determine matches using a proprietary calculation called a 'figure of merit.' The figure of merit was calculated automatically using PDXL, the diffractometer software package (Rigaku, The Woodlands, TX). An acceptance threshold of 1.0 was set for the figure of merit. Diffraction patterns were also generated from finely grated samples of pearls, and samples of the surrounding cheese matrix, from Parmigiano-Reggiano and Gouda cheeses as described. Samples of smears scraped from the surfaces of soft washed-rind (smear ripened) cheeses were loaded directly onto the slide well and immediately analyzed without any additional sample preparation.

RESULTS AND DISCUSSION

CHEDDAR

Cheddar cheese crystals in this study were large internal crystals (Figure 1), not surface crystals, which were of particular interest because their presence triggered a consumer complaint to the cheese manufacturer about possible foreign objects in the cheese. The X-ray diffraction pattern, shown in Figure 2, identified the crystals as CLP in the D(-)/L(+) enantiomeric configuration based on different XRD patterns of the two enantiomeric forms reported previously (Tansman et al., 2014). CLP crystals at the surface of Cheddar cheese have been studied extensively. However, little work has been conducted on internal crystals, and only one previous report identified large internal CLP crystals as occurring in the D(-)/L(+) form (Tansman et al. 2014). In the present study, the large internal D(-)/L(+) CLP crystals suggest a microbial origin involving nonstarter

lactic acid bacteria (**NSLAB**) because conventional starter cultures for Cheddar cheese are comprised of strains of *Lactococcus lactis* ssp. *lactis* and *cremoris*, which ferment lactose to L(+) lactate exclusively and which lack the capacity to convert L(+) lactic acid to the D(-) form. In contrast, various NSLAB, including several strains of *Pediococcus* pentosaceus (Thomas and Crow, 1983) and *Lactobacillus curvatus* (Somers et al., 2001), are able to racemize L(+) lactate to D(-) lactate and promote D(-)/L(+) CLP crystallization. Furthermore, racemizing NSLAB have been shown to produce biofilms on equipment surfaces, which can be a source of contamination leading to the formation of D(-)/L(+) CLP crystals in Cheddar (Somers et al., 2001). Thus, a possible strategy to reduce or prevent the occurrence of large internal D(-)/L(+) CLP crystals might involve identifying and eradicating the offending source of NSLAB contamination. Alternatively, D(-) lactate in Cheddar cheese could also be produced if *Lactobacillus helveticus*, which ferments lactose to D(-) lactate, were included in the starter culture, as is sometimes practiced in Cheddar manufacture to enhance flavor (Johnson, 2014). In this scenario, corrective action might involve removing *Lb. helveticus* from the starter. In either case, determining the enantiomeric form of CLP by PXRD can provide useful diagnostic information.

PARMIGIANO-REGGIANO

In traditional practice, Grana-type cheeses such as Parmigiano-Reggiano are pierced and pried open, which results in very rough and irregular internal cheese surfaces. In contrast, Parmigiano-Reggiano cheese for retail sale in the United States is sometimes cut into wedge-shaped slices with very smooth surfaces and then vacuum packaged in

clear film. Smooth surfaces accentuate visible heterogeneities within the cheese body, such as small white crystals (Figure 3, solid arrows) and spherical pearls that appear as pale white circles against the darker cheese matrix (Figure 3, dashed arrows). Thus, these heterogeneous elements strongly influence the visual appearance of cheese samples packaged in this manner for the American market. Small white entities in Parmigiano-Reggiano (Bottazzi et al., 1982) and Grana Padano (Bianchi et al., 1974) cheese were presumptively identified as tyrosine crystals based on analyses of amino acid content, but studies using XRD to confirm the crystalline identities of such elements are lacking. The diffraction pattern generated by PXRD (Figure 4) from the small white elements collected from Parmigiano-Reggiano (Figure 3, solid arrows) confirms that they were tyrosine crystals, and only tyrosine crystals.

The striking abundance of visible pearls in the Parmigiano-Reggiano samples, which the authors have also observed in similarly packaged samples of Grana Padano, prompted closer examination. Pearls having diameters ≥ 2 mm, collected from a single cheese sample weighing *ca.* 680 g, are shown in Figure 5. The pearls are grouped according to size based on retention by sieves of successive mesh sizes ranging from 5.60 to 2.00 mm. The pearls displayed remarkably consistent, nearly spherical geometries irrespective of size (Figure 5). Approximately 67 pearls per 100 g of cheese, which accounted for about 2% of the total weight of the cheese, were collected from the sample. The volume fraction of the cheese matrix occupied by pearls in this cheese appeared to be quite considerable. Given the abundance of the pearls, and their distinctly different body relative to that of the cheese matrix, which enabled the pearls to be easily harvested by hand, it seems likely that pearls influence the fracture properties of the cheese. The size

distribution of pearls harvested from five different commercial samples of Parmigiano-Reggiano, all weighing about 680 g, is presented in Table 1. All five samples contained a few pearls greater than 5.6 mm in diameter, many more between 4 and 5.6 mm, and the greatest number between 2 and 4 mm. Assuming that all pearls grow at the same rate, the smallest pearls harvested were presumably the most recent to form during aging. Continued aging of the cheese, therefore, would be expected to result in nonlinear increases in the volume fraction occupied by pearls as the large number of smaller pearls increase in diameter. Such a bloom in pearl volume is likely to exert an increasingly greater effect on cheese fracture properties as aging progresses.

The total solids and fat contents of composite samples of the pearls and surrounding cheese matrix are shown in Table 2. The total solids content was 8.72% higher in the pearls than in the cheese matrix, but the fat content was 4% lower, indicating that the higher solids content of the pearls was not caused simply by greater loss of moisture from the pearls relative to losses from the surrounding matrix during aging. Instead, the accumulation of solids other than fat contributed to higher total solids, and lower fat content, in the pearls relative to the matrix; presumably, this increase in solids was associated with the growth in scaffolding that enabled the pearls to expand spherically, and which contributed to the firmer texture of the pearls relative to the surrounding matrix. The high fat content of the pearls (28%) indicates that pearls' scaffolding engulfed and occluded fat globules as the pearls increased in diameter.

The chemical makeup of the pearl scaffolding and its structural organization are unknown but may be related to crystallization phenomena. For example, Bianchi et al. (1974) observed large (up to 6 mm) entities in Grana Padano cheese, apparently similar

to the pearls observed in the present study, which they referred to as "spots". Spots collected from cheeses aged for 18 and 25 mo contained around 9.9 and 7.7% leucine, respectively (Bianchi et al., 1974). Such extraordinarily high leucine levels suggest a possible structural role of crystalline leucine in the Grana Padano spots. However, the composite sample of pearls from Parmigiano-Reggiano in the present study contained only 1.0% leucine present as free amino acids. Currently the authors have no explanation for this discrepancy, but it is worth noting that analysis of the Parmigiano-Reggiano pearls by PXRD gave a diffraction pattern, shown in Figure 6, that corresponded to a partial diffraction pattern for crystalline leucine, which is characterized by a very strong peak at 6.00 degrees 2-theta. In contrast, a composite sample of the cheese matrix surrounding the pearls did not diffract X-rays (data not shown). Sou et al. (2012) recently observed a similar partial diffraction pattern for leucine, which they postulated corresponds to an alternative crystalline form of leucine. Further studies will be needed to determine whether this presumptive alternative leucine crystal contributes to the structural scaffolding of pearls in Parmigiano-Reggiano and Grana Padano cheeses. However, it is interesting to note that crystals collected from the surface of the hard Italian style cheese, shown in Figure 7, also yielded the same partial diffraction pattern for leucine (data not shown), indicating that the same presumptive crystals can occur in both pearls located internally in cheese and at the surface of cheese when the right conditions are present.

GOUDA

Like Parmigiano-Reggiano, the two-year aged Gouda samples in this study displayed visible heterogeneities within the cheese body, including small white crystals (Figure 8A, solid arrows) and spherical pearls that appear as pale white circles against the darker cheese matrix (Figure 8A, dashed arrows). Profuse crystal blooms also were observed in the eyes of the cheese (Figure 8B, solid arrow). Analysis by PXRD confirmed that the small white crystals embedded in the cheese body consisted of tyrosine (data not shown), and that the pearls contained the presumptive alternative form of crystalline leucine characterized by an intense XRD peak at 6.00 degrees 2-theta (data not shown), similar to the pattern obtained with Parmigiano-Reggiano pearls (Figure 6). This is perhaps surprising because the starter cultures used for Gouda traditionally do not include the thermophilic strains used in Grana type cheeses, although the inclusion of thermophilic adjuncts in Gouda manufacture is becoming more common (Düsterhöft, 2011). Again, further studies will be needed to determine whether the presumed crystalline leucine contributes to the structural scaffolding of pearls.

When the crystals that lined the eyes of Gouda were observed using phase contrast microscopy, the visual appearance suggested the presence of two different crystal morphologies, one characterized by an open structure (Figure 9, solid arrows) and the other by a compact structure (Figure 9, dashed arrows). The diffraction pattern of the crystals generated by PXRD confirmed the presence of 2 different crystalline species: tyrosine crystals plus leucine in the presumed alternative configuration, as indicated by the intense peak at 6.00 deg 2-theta (Figure 10). Thus, the same presumptive crystals can

occur in both pearls located internally in cheese and on a cheese surface, in this case the surface of eyes.

Soft Washed Rind (Smear-Ripened) Varieties

The mineral content of a surface smear collected from one of the soft washed rind (smear ripened) cheeses is shown in Table 3. Calcium and P were present in the smear at concentrations around ten times higher than that of other minerals measured, which suggests that calcium and phosphate ions migrated from the cheese body to the surface in a manner similar to what is believed to occur in bloomy rind cheeses; i.e., as a result high surface pH that develops during ripening, which triggers surface crystallization of calcium phosphate (Boutrou et al., 1999; Brooker, 1987; Gaucheron et al., 1999; Karahadrian and Lindsay, 1987). Therefore, the authors expected to find one or more forms of crystalline calcium phosphate in the smears of the six soft washed rind cheeses that were analyzed by PXRD. However, smears from all six cheeses each produced a unique XRD pattern that could not be matched to any pattern in the ICDD database.

Diffraction of X-rays indicates the presence of crystals in a sample, thus the XRD patterns confirmed that crystalline species were present in the smears of all six cheeses but none could be identified. A possible explanation for the unknown XRD patterns became evident during the course of the analyses when the authors noted the samples dried out extensively during the diffraction procedure, perhaps dehydrating the extant phases. This strongly suggested that the PXRD results contained artifacts of the experimental conditions. Consequently, the preparation of smear samples for PXRD was

modified to include the addition of a thin layer mineral oil over the sample well to prevent sample desiccation. This modification produced reproducible data, thereby preempting artifacts obtained previously. When the modified sample preparation procedure was applied to smear material from two of the washed rind cheeses analyzed previously, the XRD pattern for ikaite, which consists of calcium carbonate in an unusual hexahydrate form, was identified in the smears (Figure 11). Additional analyses of other washed rind cheeses are underway and will be presented in a subsequent report.

The formation of surface crystals, whether of calcium phosphate or other species, is of great interest because of the possible implications for zonal softening, which has been studied extensively in bloomy rind cheeses but not well characterized in soft washed rind cheeses. Surface crystal formation also has implications for the development of sandiness or grittiness, which the authors have heard anecdotally from cheesemakers and cheesemongers may be considered desirable or undesirable depending on the market.

CONCLUSION

Powder X-ray diffractometry is a versatile and powerful analytical approach to identify and differentiate crystalline species in cheese. Crystals influence the quality and character of many cheeses, ranging from extra hard, long-aged types, such as grana cheeses, to soft, rapidly ripened cheeses such as surface ripened washed-rind and bloomy-rind types. This study confirmed the presence of tyrosine crystals and a crystalline species presumptively identified as leucine in both Parmigiano-Reggiano and Gouda cheeses, as well as large interior crystals of D(-)/L(+) calcium lactate pentahydrate

in Cheddar cheese and ikaite crystals at the surface of a soft washed rind cheese. Advancements in PXRD technology have facilitated new avenues of research relating to structure-function implications of crystallization phenomena, such as the role of leucine crystals in the formation and growth of pearls in Parmigiano-Reggiano and Gouda cheeses, and the role of surface crystals in the zonal softening of soft surface ripened cheeses.

ACKNOWLEDGEMENTS

This study was funded by United States Department of Agriculture Hatch Project VT-H01905. Purchase of the X-ray diffractometer was funded by National Science Foundation Grant EAR-0922961.

CONFLICTS OF INTEREST

Author Tansman, author Kindstedt and author Hughes declare that they have no conflict of interest.

STATEMENT OF HUMAN AND ANIMAL RIGHTS

This article does not contain any studies with human or animal subjects performed by any of the authors.

REFERENCES

Agarwal, S., K. Sharma, B.G. Swanson, G. Ü. Yüksel and S. Clark. 2006. Nonstarter lactic acid bacteria biofilms and calcium lactate crystals in Cheddar cheese. J. Dairy Sci. 89:1452-1466.

Bianchi, A., G. Beretta, G. Caserio and G. Giolitti. 1974. Amino Acid Composition of Granules and Spots in Grana Padano Cheeses. J. Dairy Sci. 57:1504-1508.

Bottazzi, V., B. Battistotto and F. Bianchi. 1982. The microscopic crystalline inclusions in Grana cheese and their X-ray microanalysis. Milchwissenschaft Milk Sci. Internat. 37(10):577-580.

Bottazzi, V., F. Lucchini, A. Rebecchi and G.L. Scolari. 1994. I cristalli del formaggio grana (Crystals present in Grana cheese). Scienza e Tecnica Lattiero-Casearia 45(1):7-14.

Boutrou, R., F. Gaucheron, M. Piot, F. Michel, J-L. Maubois and J. Léonil. 1999. Changes in the composition of juice expressed from Camembert cheese during ripening. Lait 79:503-513.

Brooker, B.E. 1987. The crystallization of calcium phosphate at the surface of mould-ripened cheeses. Food Microstruc. 6:25-33.

Chou, Y-E, C.G. Edwards, L.O. Luedecke, M.P. Bates and S. Clark. 2003. Nonstarter lactic acid bacteria and aging temperature affect calcium lactate crystallization in Cheddar cheese. J. Dairy Sci. 86:2516-2524.

Conchie, J. and B.J. Sutherland. 1965. The nature of steaminess in Cheddar cheese. J. Dairy Res. 32:35-44.

Conchie, A.J. Lawrence, J. Czulak and W.F. Cole. 1960. Aust. J. Dairy Technol. 15:120.

Dox, A.W. 1911. The occurrence of tyrosine crystals in Roquefort cheese. J. Amer. Chem. Soc., 33:423-425.

Düsterhöft, E.M., W. Engels, and G. van den Berg. 2011. Dutch-Type Cheeses. *In* Encyclopedia of Dairy Sciences 2nd ed., Academic Press/Elsevier, London.

Dybing, S.T., J.A. Wiegand, S.A. Brudvig, E.A. Huang and R.C. Chandan. 1988. Effect on processing variables on the formation of calcium lactate crystals on Cheddar cheese. J. Dairy Sci. 71:1701-1710.

Gaucheron, F., Y. Le Graët, F. Michel, V. Briard and M. Piot. 1999. Evolution of various salt concentrations in the moisture and in the outer layer and centre of a model cheese during its brining and storage in an ammoniacal atmosphere. Lait 79:553-566.

Harper, W. J., A. M. Swanson, and H. H. Sommer. 1953. Observations on the Chemical Composition of White Particles in Several Lots of Cheddar Cheese. J. Dairy Sci. 36:368-372.

Johnson, M. 2104. Crystallization in cheese. Dairy Pipeline, Wisconsin Center for Dairy Research, 26(3): 1-5.

Karahadrian, C. and R.C. Lindsay. 1987. Integrated roles of lactate, ammonia, and calcium in texture development of mod surface-ripened cheese. J. Dairy Sci. 70:909-918.

Noël, Y., M. Zannoni and E.A. Hunter. 1996. Texture of Parmigiano Reggiano cheese: Statistical relationship between rheological and sensory variates. Lait 76:243-254.

Parker, M.L., P.A. Gunning, A.C. Macedo, F.X. Malcata and T.F. Brocklehurst. 1998. The microstructure and distribution of micro-organisms within mature Serra cheese. J. Appl. Microbiol. 84:523-530.

Shock, A.A., W.J. Harper, A.M. Swanson and H.H. Sommer. 1948. What's in those "white specks" on Cheddar. Wisconsin Agric. Experiment Station Bull. 474, p.31-32

Somers, E.B., M.E. Johnson and A.C.L. Wong. 2001. Biofilm formation and contamination of cheese by nonstarter lactic acid bacteria in the dairy environment. J. Dairy Sci. 84:1926-1936.

Sou, T. L.M. Kaminskas, T.-H. Nguyen, R. Calberg, M.P. McIntosh and D.A.V. Morton. 2013. The effect of amino acid excipients on morphology and solid-state properties of multi-component spray dried formulations for pulmonary delivery of biomacromolecules. European J. of Pharmaceutics and Biopharmaceutics 83:234-243.

Tansman, G., P. S. Kindstedt, and J. M. Hughes. 2014. Powder X-ray diffraction can differentiate between enantiomeric variants of calcium lactate pentahydrate crystal in cheese. J. Dairy Sci. 97:7354-7362.

Thomas, T.D. and V.L. Crow. 1983. Mechanism of D(-) –lactic acid formation in Cheddar cheese. N. Z. J. Dairy Sci. Technol. 18:131-141.

Tuckey, S. L., H. A. Ruehe, and G. L. Clark. 1938 a. X-Ray Diffraction Analysis of White Specks in Cheddar Cheese. J. Dairy Sci. 21:161.

Tuckey, S. L. and H. A. Ruehe. 1938b. An X-ray Diffraction Analysis of Cheddar Cheese. J. Dairy Sci. 21:777-789.

Washam, C.J., T.J. Kerr, V.J. Hurst and W.E. Rigsby. 1985. A scanning electron microscopy study of crystalline structures in commercial cheese. *In* Developments in industrial microbiology, vol. 26, pp. 749-761.

Zannoni, M., L. Bertozzi and E.A. Hunter. 1994. Comparison of Parmigiano-Reggiano and American Parmesan Cheeses by Sensory Analysis of Texture. Scienza E Technica Lattiero-Casearia 45(6):505-518.

Table 1. Average number of "pearls" collected from 5 different commercial samples of Parmigiano-Reggiano cheese. Each cheese sample weighed approximately 680 g. Means and standard deviations correspond to the numbers of pearls retained on stacked sieves of decreasing mesh size from 5.60 to 2.00 mm.

Sieve Mesh Size	Mean[1]	Standard Deviation[1]
5.60	7	8
4.00	127	46
2.00	321	84

[1]n=5

Table 2. Compositional analyses of a composite sample of "pearls", and the cheese matrix surrounding the pearls, collected from 5 different commercial samples of Parmigiano-Reggiano cheese.

	Pearls	Cheese Matrix
Total Solids (%)	**79.09**	**70.37**
Fat (%)	**28**	**32**
FDM (%)	**35.4**	**45.5**
Free leucine (%)	**1.0**	**-**

Table 3. Concentrations (g/Kg) of selected minerals in dried and defatted smear material collected from the surface of a soft washed rind (smear-ripened) cheese.

Mineral	Concentration (g/Kg)
Ca	78.66
P	33.26
K	4.34
Mg	2.10
Na	9.67

Figure 1. Large interior crystals collected from the body of a commercial Cheddar cheese that was aged for 2 y before distribution for retail sale. The scale is in mm.

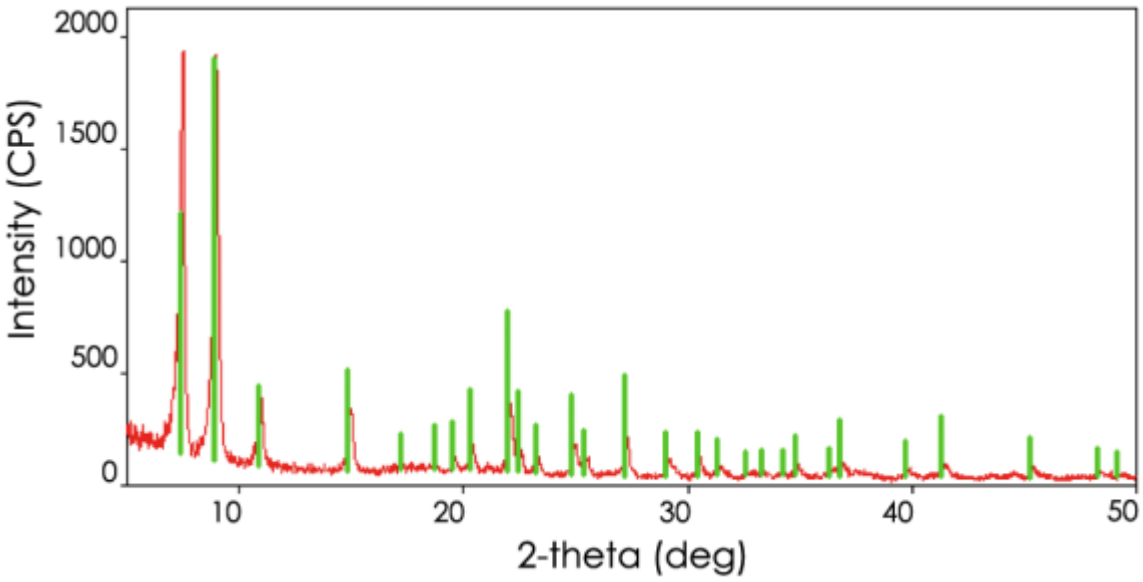

Figure 2. X-ray diffraction pattern (in red) from large interior crystals collected from the body of a commercial Cheddar cheese that was aged for 2 y before distribution for retail sale (See Figure 1). The green bars represent the reference card (ICDD card number: 00-029-1596) labeled “calcium lactate pentahydrate”.

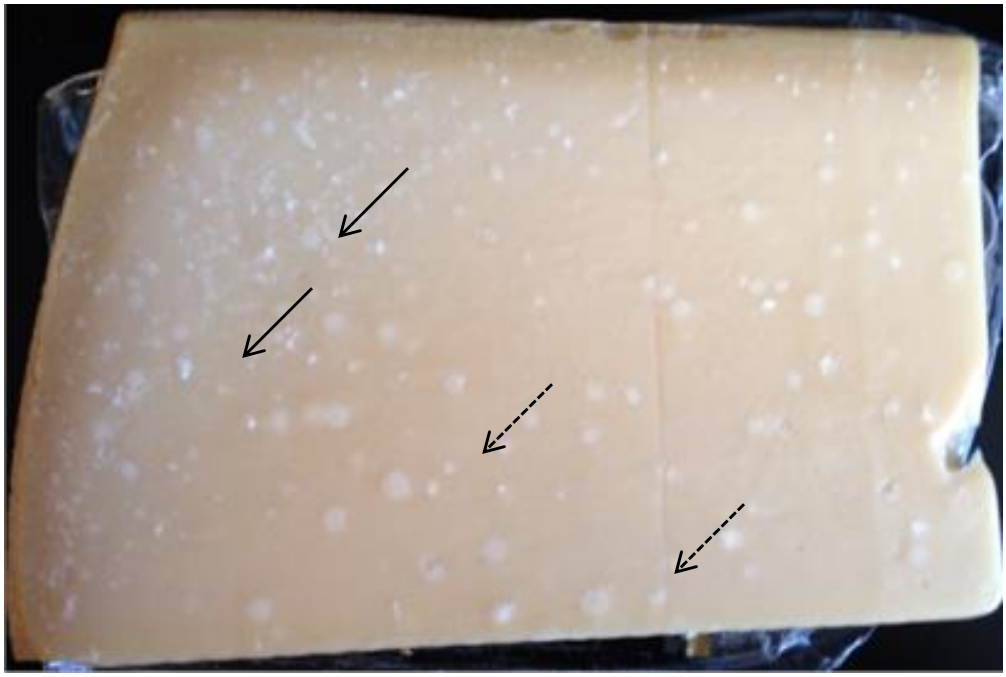

Figure 3. Visual appearance of a wedge sample of commercially produced Parmigiano-Reggiano cheese that was aged for 2 y before retail distribution. Small white crystals (solid arrows) and pale white spherical "pearls" (dashed arrows) are noted.

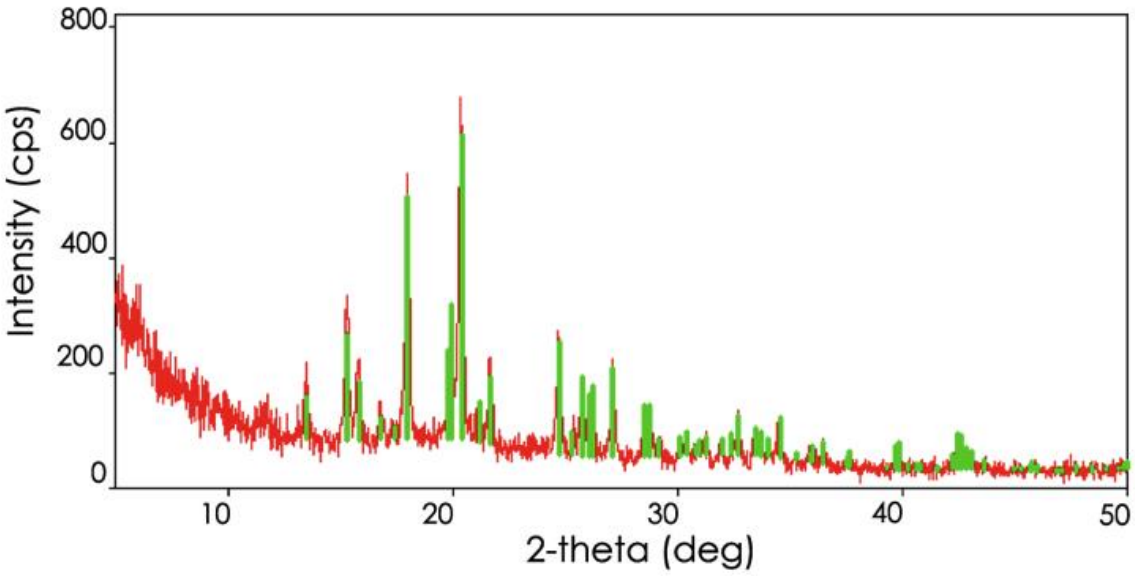

Figure 4. X-ray diffraction pattern (in red) from small white interior crystals collected from the body of a commercial Parmigiano-Reggiano cheese that was aged for 2 y before distribution for retail sale (See Figure 3). The green bars represent the reference card (ICDD card number: 00-039-1840) labeled “tyrosine”.

Figure 5. "Pearls" having diameters ≥ 2 mm, which were collected from a single sample of Parmigiano-Reggiano cheese weighing ca. 680 g. The pearls are grouped according to retention on sieves of successive mesh size. The ruler is 300 mm long.

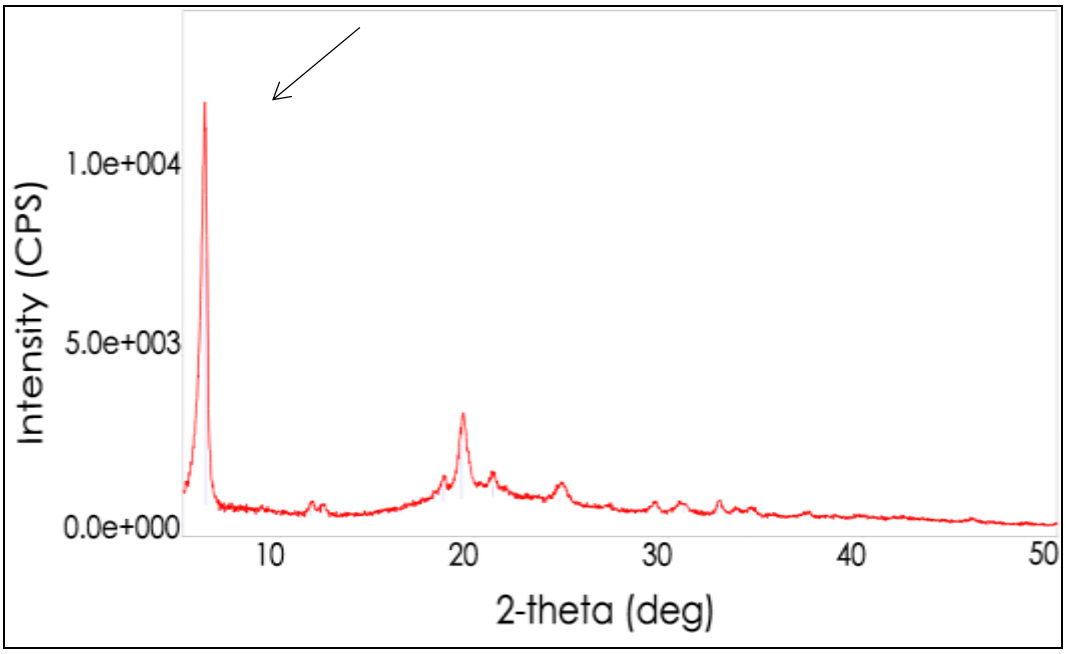

Figure 6. X-ray diffraction pattern from a composite sample of interior "pearls" collected from five commercial Parmigiano-Reggiano cheese samples that were aged for 2 y before distribution for retail sale. The pattern displays a prominent peak at 6.00 degrees 2-theta (see arrow).

Figure 7. Surface of a hard Italian-style cheese from the United States displaying extensive crystal coverage.

A

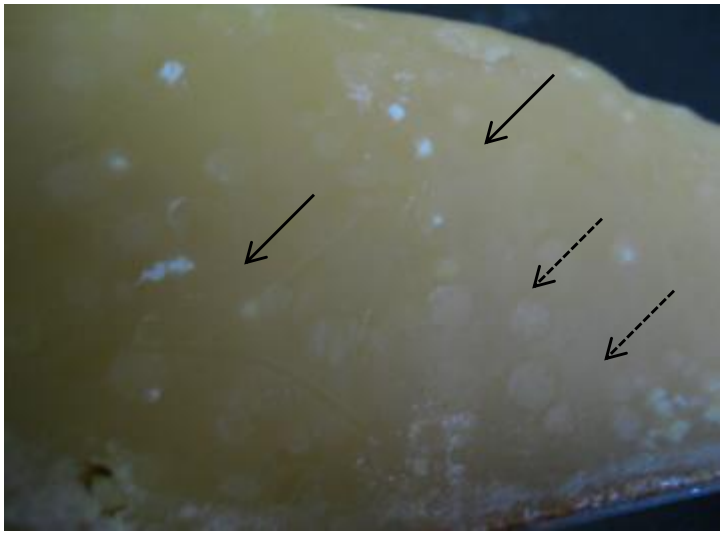

B

Figure 8. Visual appearance of a commercially produced Gouda cheese that was aged for 2 y before retail distribution. Small white crystals (solid arrows, Fig. 8A) and pale white spherical "pearls" (dashed arrows, Fig. 8A) are noted. Also, eyes within the cheese were lined with crystals (solid arrow, Fig. 8B).

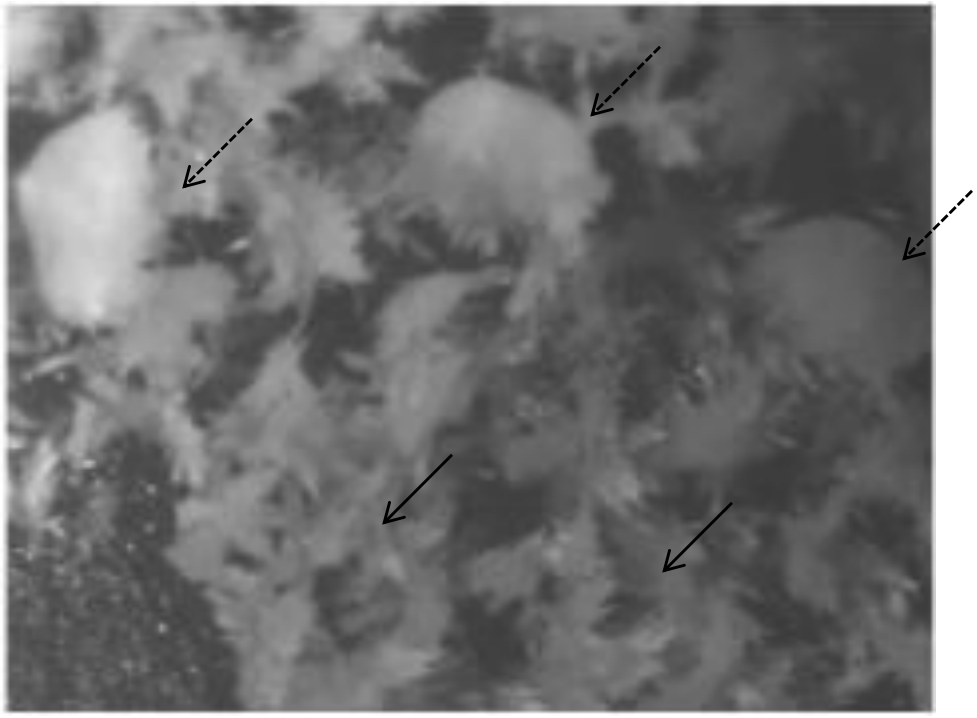

Figure 9. Phase contrast photomicrograph (11.25 X magnification) of crystals lining the surface of an eye in a commercially produced Gouda cheese that was aged for 2 y before retail distribution (See Figure 8B). Two different crystal morphologies, one characterized by an open structure (solid arrows) and the other by a compact structure (dashed arrows), appear to be present.

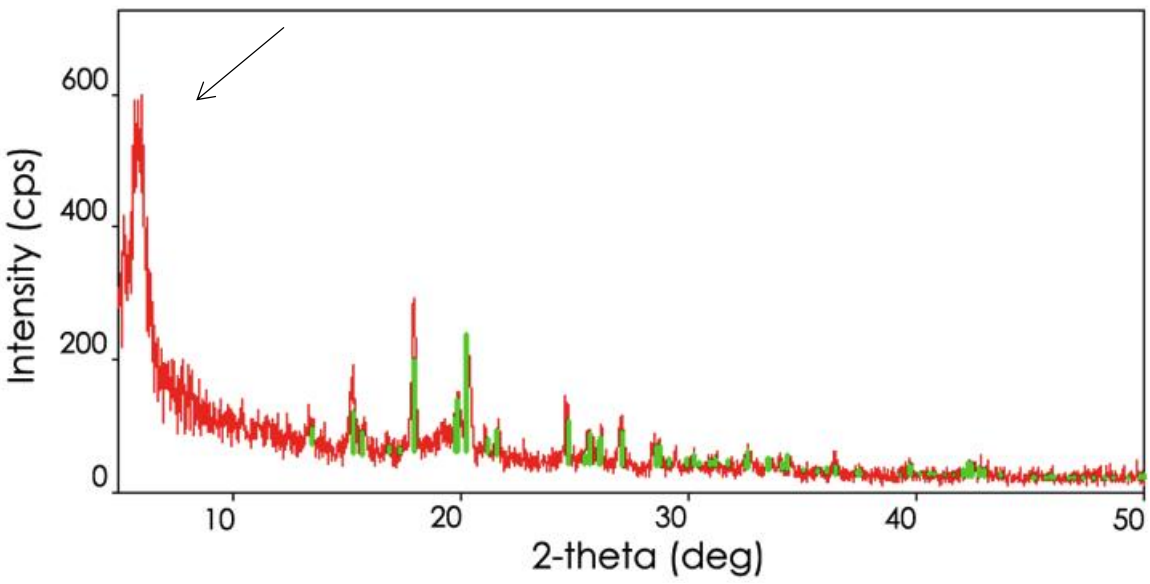

Figure 10. X-ray diffraction pattern (in red) from crystals collected from the surfaces of eyes in a commercial Gouda cheese sample that was aged for 2 y before distribution for retail sale (See Figure 8B). The green bars represent the reference card (ICDD card number: 00-039-1840) labeled “tyrosine”. Also evident is a prominent peak at 6.00 degrees 2-theta (see arrow).

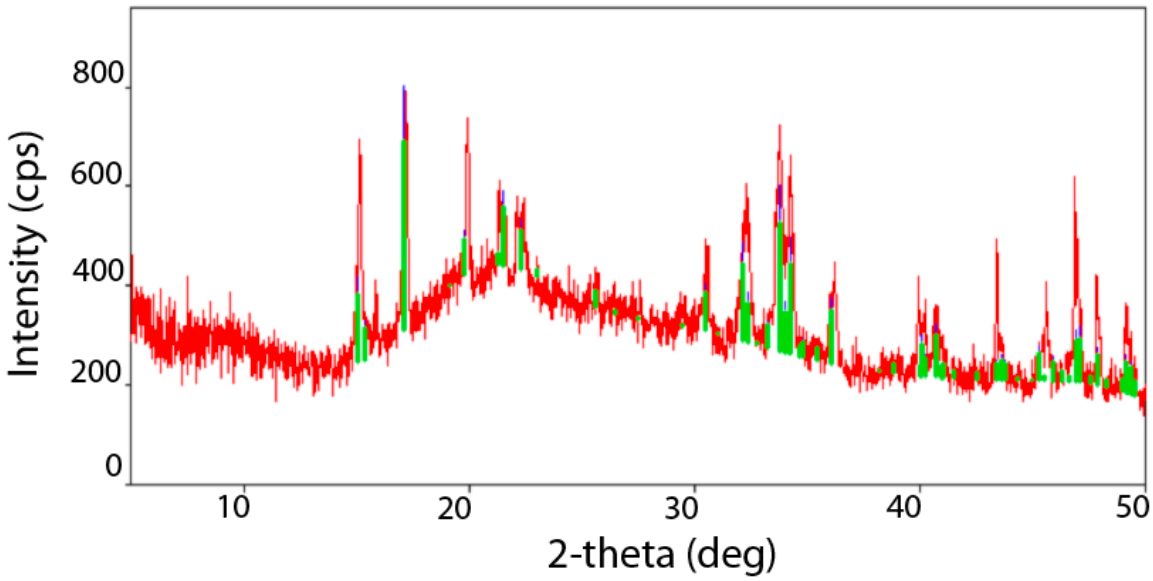

Figure 11. X-ray diffraction pattern (in red) from smear material collected from surface of a commercial soft washed rind cheese. The green bars represent the reference card (ICDD card number: 00-074-7174) labeled “ikaite”.

CHAPTER 3: MINERALS IN FOOD: CRYSTAL STRUCTURES OF IKAITE AND STRUVITE FROM BACTERIAL SMEARS ON WASHED-RIND CHEESE

GIL F. TANSMAN[§], PAUL S. KINDSTEDT

Department of Nutrition and Food Sciences, University of Vermont, Burlington, VT 05405, U.S.A.

JOHN M. HUGHES

Department of Geology, University of Vermont, Burlington, VT 05405, U.S.A.

ABSTRACT

Food contains inorganic elements and compounds that are important for human nutrition and human health. Although these substances have been investigated and characterized in many foods for their nutritive value, little is known about the crystal phases that form in foods. In this study, we investigated crystals that form in the bacterial smears on the surface of washed-rind cheese. Washed-rind cheeses have been consumed for centuries, but the crystals that often contribute detectable grittiness to the surface of these cheeses have never been identified. The crystals were characterized with petrographic microscopy and identified with single crystal X-ray diffractometry as ikaite ($CaCO_3 \cdot 6H_2O$), a rare metastable phase that has only been observed in freezing marine and lacustrine environments, and struvite ($NH_4MgPO_4 \cdot 6H_2O$), a mineral that is often associated with bacterial activity. These crystals are important to cheesemakers because they affect cheese texture and sensory characteristics. The potential importance of the

[§] *Email address:* gtansman@uvm.edu

bacterial smear in the nucleation of these phases is discussed, and the possibility of using cheese as a model system to investigate geological biomineralization phenomena is explored.

Keywords: crystals in cheese, ikaite, struvite, crystal structures

INTRODUCTION

Dietary minerals must be consumed regularly to maintain normal bodily function and to avoid diseases associated with deficiency (Soetan *et al.* 2010). Many of the inorganic ions that are necessary for human health are found in significant quantities in cheese. Cheese is an ancient food that consists of a porous protein matrix containing fat droplets and an aqueous phase, and retains many of the elements that are naturally found in milk, such as calcium, magnesium, potassium, phosphate, iron, copper, and zinc. These ions may be found in the aqueous phase or in association with the protein matrix in dynamic equilibrium with the aqueous phase. Some ions are presents in such high quantities that during the course of aging they supersaturate the aqueous phase (Gaucheron *et al.* 1999; Morris *et al.* 1988); however, most of the minerals that are supersaturated in the aqueous phase have never been observed in crystalline form in cheese. In fact, the only mineral phase to have been conclusively identified in cheese before the present studies is brushite ($CaHPO_4 \cdot 2H_2O$; (Conochie and Sutherland 1965).

Supersaturation of ions and crystal formation are believed to have important roles in the manufacturing of important white mold cheese varieties (such as Camembert), according to a working model (Gaucheron *et al.* 1999). Calcium is particularly important in cheese manufacturing because protein-calcium interactions

impact cheese texture (Lawrence *et al.* 1987; Lucey and Fox 1993). In the working model, calcium phosphate crystal growth provides a sink for calcium and reduces the amount of calcium that is available to interact with proteins. In combination with other processes such as proteolysis, alkalization, and protein hydration these cheeses characteristically soften as aging progresses (Karahadian and Lindsay 1987). Although the alleged crystals cited in the working model were observed by electron microscopy (Brooker 1987), no crystallographic technique has been successfully employed and the composition of the phase has remained elusive. Preliminary powder X-ray diffraction (PXRD) data from our group suggests that the calcium phosphate phase in a Vermont white mold cheese is brushite (unpublished data), although other phases may be involved.

Other cheese varieties may also rely on mineral growth to sequester calcium and encourage cheese softening. Washed-rind cheeses are characterized by a sticky biofilm on their surface, and cheese makers refer to the surface biofilm as a 'bacterial smear,' which is how it will be signified in this present study. Although considerably less work has been conducted to determine the mechanism of cheese softening in washed-rind cheese compared to white mold cheese, the ripening mechanisms behave similarly, with cheese softening beginning at the rind and progressing toward the center during aging. Sensory evaluations of washed-rind cheeses often reveal the presence of grittiness in the bacterial smear, which PXRD and petrographic microscopy indicate is caused by an accumulation of crystalline material (Tansman *et al.* 2015a; Tansman *et al.* 2015b). This contrasts with the crystals in white mold cheeses that are either too small or too few to be perceived as grittiness, although grittiness in white mold cheeses is occasionally reported (Karahadian and Lindsay 1987). Cheesemakers are very sensitive to the development of

grittiness, and thus the growth of minerals, in washed-rind cheeses. Although a moderate amount of grittiness contributes to the complexity of the cheese, and may even be considered desirable in certain markets, an abundance of grittiness tends to lower the desirability and salability of the cheeses. Although the cause of grittiness has never been elucidated, anecdotal evidence suggests that certain traditional manufacturing practices have been used to limit the manifestation of grittiness (personal communication with a Vermont cheesemaker).

Single crystals of sufficient size and quality for single-crystal X-ray diffraction (SCXRD) had not been observed in cheese until recently, when our group collected data on a calcite crystal from the surface of fully-ripened white mold cheese (Tansman *et al.* 2015a). This was an important observation because it revealed that carbon dioxide, which has an important impact on cheese microbiology (Leclercq-Perlat *et al.* 2006), accumulates in the cheese in sufficient quantities to exceed the solubility product of calcite. Even more interesting is the tentative identification by petrographic microscopy of single crystals in washed-rind bacterial smears. According to PXRD, the crystals have been identified as struvite ($NH_4MgPO_4 \cdot 6H_2O$) and ikaite ($CaCO_3 \cdot 6H_2O$), which have not been previously observed in cheese (Tansman *et al.* 2015b). Ikaite and struvite are interesting because they are precipitates of carbon dioxide and ammonia, respectively, both of which are important dissolved gases in cheese. Ammonia (Karahadian and Lindsay 1987) and carbon dioxide (Picque *et al.* 2006) are produced by microbial metabolism and have been shown to regulate the activity of certain microorganisms on surface ripened cheeses (Corsetti *et al.* 2001; Leclercq-Perlat *et al.* 2006).

Struvite has been observed in some canned seafood products (Purcell and Hickey 1922) and ikaite has been associated with frozen shrimp (Mikkelsen *et al.* 1999), but their association with food has been limited to these observations. Ikaite is a cold-water mineral that has been found in underwater tufa towers (Buchardt *et al.* 2001), and as precipitates in Arctic (Dieckmann *et al.* 2010) and Antarctic (Dieckmann *et al.* 2008) ice cores. Both struvite (Stickler 1996) and ikaite (Schmidt *et al.* 2006) are associated with bacterial biofilms, although the two phases have apparently never been observed together in the same environment. Given the vastly different formation chemistry and temperature environments in which these phases have been found, the most evident similarity is their propensity to form in association with bacterial growth.

Washed-rind bacterial smears present an interesting nucleation environment and provide a useful model system to study other biofilm and microbial mat crystallization phenomena. In geological studies crystal phases in microbial mats are used to recreate climate history (Higley 2015), to elucidate the ancient microbial processes that caused lithification and preservation of microbial mats in the formation of stromatolites (Dupraz and Visscher 2005; Riding 2000), and in the study of other microbial-influenced geological sediments (Muynck *et al.* 2010; Noffke 2009). Cheese smears bear many similarities to microbial structures that are important in geological systems, and the presence of carbonate minerals in both systems makes the comparison particularly relevant. Thus, crystallization in cheese smears could provide insight into ancient crystallization phenomena that are difficult to routinely sample and whose biotic processes have long-ago ceased.

Minerals in food have important economic consequences for manufacturers and play an important role in nutrition and well-being, and thus the use of X-ray diffraction techniques in food research is a novel technique that warrants optimization. Cheese is among the most well studied foods due to the complex chemical and microbiological processes that are involved in its manufacture and the cheese environment provides a wide variety of conditions in which mineral phases could potentially form. Thus, cheese may provide an ideal model system in which to study mineral-biotic interactions.
The intention of this paper is to identify the minerals that exist in microbial mats in select cheeses and, because of the high-quality of these crystals, to provide superior crystal structure refinements of these minerals from this unexpected food environment.

EXPERIMENTAL

CHEESE SOURCING

Both bacterial smears were collected from cheeses obtained at a local retail outlet where they were kept in an open refrigerated display case. The precise age of the cheeses was not known although both cheeses were fully ripe at the time of purchase and analysis. Based on the packaging dates on the retail packages, it appears that *smear A* was collected approximately 10 weeks after manufacture and *smear B* collected approximately 6 weeks after manufacture. Both cheeses were produced in the same creamery and aged at the same facility. Details of the cheese manufacture and ripening were obtained from subsequent interviews with the producer and are presented below.

Some details of the manufacturing and aging process were omitted due to their proprietary nature.

CHEESE MANUFACTURE

Cheese A (corresponding to *smear A*) is produced from raw cow's milk during the winter months. The curds are dipped at a pH of 6.55, after which the curds drain overnight in a refrigerated chamber. *Cheese A* is demolded at a pH of 5.45 and is dry salted to a target salt-in-moisture of 2.6%. The outer diameter is wrapped with a strip of spruce bark fastened with a rubber band. *Cheese A* is aged in a 13-14°C (94-95% humidity) room for the first week, after which it is transferred to the 10-11°C (96% humidity) aging vault. It is scrubbed with a medium-length-bristle brush three times in the first week and them twice per week until the fourth week. It is aged on wire racks for six weeks in total and then wrapped in semi-permeable paper and stored at 4.5°C until shipment. At the time of wrapping, each wheel weighs approximately 570 grams with a diameter of 14 cm and a height of 3 cm.

Cheese B (corresponding to *smear B*) is produced from pasteurized cow's milk year-round. The curds are dipped at a pH of 6.50 and drained overnight in a refrigerated chamber. *Cheese B* is demolded at a pH of 5.1 and is dry salted to a target salt-in-moisture of 2.6%. Each wheel weighs approximately 225 grams with a diameter of 10 cm and a height of 2.5 cm. Like *cheese A, cheese B* is aged in a 13-14°C (94-95% humidity) room for the first week, after which it is transferred to the 10-11°C (96% humidity) aging vault. It is hand-scrubbed three or four times during the first week and then every other

day for another week and a half. *Cheese B* is aged on wire racks for three weeks in total and them wrapped in semi-permeable paper and stored at 4.5°C until shipment.

Powder X-ray Diffraction

Diffractograms were generated from smear samples taken from the surface of the two cheeses. The samples were collected using a metal spatula to scrape the surface of each wheel until the lightly colored underlying cheese surface was visible, with care taken to exclude cheese material from the smear sample. Diffraction slides were prepared using an optimized method for cheese smears (Tansman *et al.* 2015c), slightly modified, wherein the smears were homogenized in a mortar and pestle with a few drops of mineral oil, loaded onto glass diffraction slides, and a drop of mineral oil was applied to each diffraction surface. Excess oil was removed with a Kim wipe with enough oil remaining to prevent water loss; smears rapidly dry and shrink upon exposure to the X-ray beam, which results in preferred orientation artifacts and complicates phase identification. Even with the extended sample preparation, some preferred orientation was still apparent, although not enough to prevent phase identification. Diffractograms were generated on a Miniflex II powder X-ray diffractometer (Rigaku, The Woodlands, TX) at a speed of 2° 2θ/min between 5 and 50° 2θ.

Single Crystal X-ray Diffraction

Single crystals were collected from the bacterial smears by gently spreading collected material on glass microscope slides using a metal spatula. The smears were

observed under polarized light microscopy and single crystals were selected based on size and optical properties. Crystals were extracted from the bacterial smears with a dissecting needle and mounted for diffraction experiments. Crystals were coated in glue to prevent dehydration under the X-ray beam, which had occurred in several test runs on suspected ikaite crystals and resulted in rapid loss of crystallinity and incomplete data collection.

X-ray diffraction data were collected with a Bruker Apex II CCD single-crystal diffractometer using graphite-monochromated Mo K_α radiation; details of data collection and structure refinement for ikaite and struvite are contained in Table 1. Tables 2 and 3 list the atomic coordinates and equivalent isotropic atomic displacement for ikaite and struvite, respectively. Tables 4 and 5 list the atomic distances and bond valences for ikaite and struvite, respectively. Bond valences were calculated using the constants from Brese and O'Keeffe (1991). Redundant data were collected for a sphere of reciprocal space (4,500 frames, 0.20º scan width; average redundancy = 3.4 for ikaite, 5.8 for struvite). The Bruker Apex2 package of programs was used throughout the solution and refinement. The atomic arrangement was refined in space group $C2/c$ for ikaite and $Pmn2_1$ for struvite, with final R_1 values of 0.0157 for ikaite and 0.0250 for struvite. These R values are the lowest reported for any natural or synthetic samples of these phases.

Ikaite crystals were collected from both smears but crystal structure was only determined for an ikaite crystal collected from *smear B*, whereas the identity of ikaite crystals from *smear A* were confirmed by determining the unit cell parameters.

OCCURRENCE

Single crystals were harvested from the surfaces of two varieties of washed-rind cheese aged by The Cellars at Jasper Hill (Greensboro, VT). According to PXRD analyses, ikaite was present in the bacterial smear of both varieties whereas struvite was present in only one variety's bacterial smear. The bacterial smear containing struvite and ikaite (smear A) was dark orange in color, whereas the cheese containing only ikaite (smear B) was much lighter and had a dusting of white mold in addition to the bacterial biomass. The difference in color may reflect the species composition of the bacterial smears, which becomes more red-colored with greater numbers of the pigment-producing bacterium *Brevibacterium linens* (Brennan *et al.* 2002).

RESULTS

Crystals of struvite and ikaite were observed under crossed polars using petrographic microscopy and distinguished by differences in morphology and optical properties. Ikaite displayed inclined extinction and showed low birefrigence, whereas struvite displayed parallel extinction and displayed high birefringence. Most ikaite crystals had an elongated and irregular morphology that in many instances could be described as spear-tip-shaped. Struvite crystals appeared to have a generally more regular, trapezoidal shape. In both bacterial smears, crystals varied in size from less than 100 μm on the long axis to over 500 μm. In *smear A* the size range of each crystal phase was similar, although there appeared to be considerably more ikaite crystals in the 500 μm range; the vast majority of struvite crystals were less than 300 μm in length. Crystals in *smear B* were generally smaller than the crystals in smear A, and the discrepancy in

size between the ikaite in *smear A* and *smear B* can likely be explained by the fact that the cheese from which *smear A* was collected was aged more than twice as long as the cheese from which *smear B* was collected. It is well established that crystal size is related to growing time and thus the ikaite crystals in *smear A* likely had more time to grow after their initial nucleation than the ikaite in *smear B*. The observed difference in size between struvite and ikaite crystals in *smear A* may reflect differences in the rate of growth or time of initial nucleation, although additional investigation is necessary to determine the cause of this difference.

DISCUSSION

DEHYDRATION OF IKAITE AND STRUVITE AND RELATIONSHIP TO CRYSTAL STRUCTURE

Ikaite is unstable at room temperature and rapidly dehydrates to calcite (Boch *et al.* 2015). Struvite also dehydrates when exposed to air (Chauhan and Joshi 2013); however, temperature does not appear to play a role in the dehydration of struvite as it does in the case of ikaite. The dehydration phenomena associated with both of these minerals may be related to their atomic structures, both of which are composed of isolated units that are loosely bonded by hydrogen bonds. The isolated units of ikaite are $CaCO_3(H_2O)_6$ (Figure 1) and the isolated units of struvite are NH_4, PO_3, and $Mg(H_2O)_6$ (Figure 3, partially observable). Extensive hydrogen bonding between isolated units results in a layered structure, which can be observed in both ikaite (Figure 2) and struvite (Figure 3) by projecting down [010]. The extent of hydrogen bonding and the high

proportion of stoichiometric water in the crystal structures may explain why these crystals are prone to dehydrate under ambient conditions.

In the present study, when bacterial smears were removed from the cheese surface and allowed to dry, ikaite and struvite crystals became opaque and lost their crystalline optical properties within minutes. Interestingly, when bacterial smear samples on glass slides were covered with immersion oil and glass cover slips the ikaite and struvite crystals remained stable for many weeks, even at room temperature. This appears to contradict the thermodynamic work of Marland (1975), who demonstrated that ikaite is unstable and readily converts to calcite at ambient temperature and pressure. As evidenced from the persistence of ikaite and struvite on bacterial smears of cheese at refrigeration temperatures and the preservation of ikaite and struvite in bacterial smear material at room temperature on glass slides, the bacterial smear matrix appears to have a protective effect on these typically unstable minerals.

THE BACTERIAL SMEAR AS A UNIQUE NUCLEATION ENVIRONMENT FOR IKAITE

The precipitation of ikaite in the bacterial smear of washed-rind cheese raises several questions about the nucleation environment. In aqueous solutions, ikaite is typically metastable and converts to calcite within just a few hours (Marland 1975). In the bacterial smears observed in the present study, ikaite was found in a significant quantity even after weeks of aging at 10^{o}C, suggesting that the smears, or perhaps dissolved compounds, inhibit the thermodynamically favorable conversion of ikaite to calcite. In addition, calcite is considerably less soluble than ikaite and precipitates more readily in aqueous solution at room temperature (Brooks *et al.* 1950), although the

inclusion of additives, such as phosphate (Clarkson *et al.* 1992) and magnesium (Boch *et al.* 2015) has been found to inhibit calcite precipitation and favor ikaite precipitation. Phosphate and magnesium are both present in the aqueous phase of cheese, and these ions may stabilize ikaite by poisoning calcite nuclei, which has been found to allow metastable ikaite to form (Boch *et al.* 2015). Additional magnesium may be added to the cheese from the brine, which is applied to the surface of the cheese over the course of aging. The magnesium content of salt, such as the salt used in brine, is highly variable depending on the source (Drake and Drake 2011), and this adds an additional variable that could prove to have an important impact on the formation of ikaite in cheese. As a consequence of these factors, the stability of ikaite in the bacterial smears appears to be more complex than the stability of struvite because struvite does not spontaneously convert to another phase in aqueous solution and by extension is governed by considerably simpler chemistry than that which governs ikaite.

In nature, ikaite has been found exclusively in cold marine environments including Arctic sea ice (Dieckmann *et al.* 2010; Rysgaard *et al.* 2012), Antarctic sea ice (Dieckmann *et al.* 2008), Antarctic marine sediment (Suess *et al.* 1982), mineral columns growing from the sea floor in a Greenland fjord (Buchardt *et al.* 2001; Schmidt *et al.* 2006), and in terrestrial systems during the winter months when the temperature drops below freezing (Bischoff *et al.* 1993b; Boch *et al.* 2015; Omelon *et al.* 2001; Whiticar and Suess 1998). In addition, several geological structures including glendonites (Boch *et al.* 2015; Buchardt *et al.* 2001; Suess *et al.* 1982; Swainson and Hammond 2003; Tateno and Kyono 2014; Whiticar and Suess 1998) and thinolites (Bischoff *et al.* 1993a; Bischoff *et al.* 1993b; Omelon *et al.* 2001; Tateno and Kyono 2014; Whiticar and Suess

1998) have been hypothesized to be calcite pseudomorphs after ikaite, which are presumed to have formed near freezing and later to have converted to calcite under higher temperatures. Using carefully controlled experimental conditions, ikaite has been precipitated in the laboratory at temperatures as high as 27°C (Brooks *et al.* 1950). Nonetheless authors often refer to ikaite as a 'cold-temperature' or 'cold-water' mineral (Last *et al.* 2013; Swainson and Hammond 2003; Whiticar and Suess 1998), and this may reflect the widespread assumption that pseudomorphs after ikaite must have initially formed under cold conditions. Although this assumption has been supported by the absence of ikaite in non-freezing natural environments, the discovery of ikaite at higher temperatures (10°C) in bacterial smears in the present study seriously brings into question the assumption that ikaite is exclusively a cold temperature mineral in nature.

THE BACTERIAL SMEAR AS A NUCLEATION TEMPLATE FOR IKAITE AND STRUVITE

The bacterial smear seems to provide a unique environment for crystal nucleation and growth that encourages the formation of large crystal grains of phases that are not present in similar cheeses that lack a bacterial smear (Tansman *et al.* 2015b). In addition, ikaite and struvite have not been observed in the portion of washed rind cheese directly underlying the bacterial smear (Tansman *et al.* 2015b), which suggests that the bacterial cells or extracellular material such as exopolysaccharides (EPS) in the bacterial smear could be important contributors to ikaite and struvite nucleation. Although EPS in bacterial smears have not be characterized, the main genera of bacteria in washed rind cheese smears have been identified as *Brevibacterium*, *Arthrobacter*, *Micrococcus*, and

Corynebacterium (Corsetti *et al.* 2001), and *Brevibacterium* (Asker and Shawky 2010), *Arthrobacter* (Senchenkova *et al.* 1995), *Micrococcus* (Kilic and Donmez 2008), and *Corynebacterium* (Shams and Jaynes 1983) have all been characterized as prolific EPS producers. Thus, one cannot rule out the potential importance of the bacteria or extracellular material in the nucleation and growth of ikaite and struvite in bacterial smears.

Important interactions between EPS and nucleating minerals have been documented in the context of microbiologically-precipitated carbonate minerals in the geologic literature (Arp *et al.* 1999; Baumgartner *et al.* 2006; Dupraz *et al.* 2009; Dupraz and Visscher 2005; Riding 2000) and microbiologically-precipitated struvite in the medical (McLean *et al.* 1989) and wastewater treatment (Lin *et al.* 2012) literature. According to one model, EPS contributes to carbonate precipitation by binding and concentrating metal ions, which precipitate in the presence of carbonate as the pH rises and shifts the carbonate equilibrium (Arp *et al.* 1999). According to another model, EPS contributes to struvite precipitation by weakly binding magnesium ions, which provides a nucleation environment when phosphate and ammonia are present (Lin *et al.* 2012). It is likely that elevated pH plays a role in the precipitation of both ikaite and struvite as the solubilities of ikaite (Hu *et al.* 2014) and struvite (Nelson *et al.* 2003) both decrease with increasing pH. Large pH increases have been observed at the surface of washed-rind cheeses during aging (Gobbetti *et al.* 1997) and a preliminary aging study using *cheese A* demonstrated that the pH of the surface smear increased from 5.5 at the beginning of aging to over 7.5 by the end of aging (unpublished data). In order to gain insight into the importance of extracellular material in the precipitation of ikaite and struvite at the

surface of washed rind cheese, the metal binding capacity of the smear material should be studied.

Possible interaction between constituent ions and phase inhibition

The nucleation and growth of ikaite and struvite in the same bacterial smear (*smear A* in the present study) is important because of the complex interaction of ions that comprise the two phases. As stated previously, phosphate and magnesium ions can inhibit calcite and thus allow ikaite to nucleate and grow. Magnesium and phosphate are both incorporated into growing struvite crystals and it would be interesting to determine if these ions could be sufficiently sequestered so as to remove the inhibitory effect on calcite, thereby facilitating the growth of calcite at the expense of ikaite. Conversely, struvite has limited stability in solutions containing a high proportion of calcium to magnesium (Gull and Pasek 2013). It is possible that the growth of ikaite and sequestration of excess calcium ions contributes to an environment that is stable with respect to struvite; this dynamic could shed light on the process of struvite precipitation, and the cheese environment could be an interesting model system in which to conduct this research while simulating the complex conditions present in the biogeochemical environment.

Bacterial smears on cheese as a model system

Bacterial smears have been previously used as a model system to study the complex progression of microbial ecology (Wolfe *et al.* 2014; Wolfe and Dutton 2015),

and the present study strongly suggests that cheese can likewise be used to study the complex relationship between crystallization and microbial activity. The unforeseen discovery of ikaite and struvite in bacterial smears emphasizes the need to study these minerals in the context of modifiable complex systems, as a complement to controlled laboratory experiments and empirical observations. Cheese can provide an array of interesting biological conditions that can be used as model systems to test hypotheses at the mineral-biological boundary. Fermentation in foods such as cheese involves easily reproducible and measureable microbial metabolism of substrate (Wolfe *et al.* 2014), and given the ease with which the substrate can be modified, many biological and chemical questions may be investigated in further detail. In cheese, the inorganic components, including the ions that form ikaite and struvite, have been extensively characterized due to their importance in human health and cheese manufacturing. Cheese, as a model system, also lends itself to modification through the addition of ions that are not naturally found in food. The addition of ions such as manganese, which precipitate in the presence of bacteria in geologic systems (Gonzalez-Munoz *et al.* 2008), would allow other mineral phases to be investigated. Ions could be added to cheese at various points during production of cheese in a laboratory setting, which would increase the versatility of cheese as a model system to investigate mineralogical questions. The potential insights that could be gained from investigating minerals in food should not be underestimated.

CONCLUSION

The identification of struvite and ikaite crystals in bacterial smears of washed-rind cheese is a major discovery for the cheese technology community. In an effort to control the abundance and size of these crystals, and thus the grittiness of washed-rind cheeses, a chemical understanding of these mineral phases facilitates an informed scientific approach. However, this discovery is also interesting to the mineralogy community for two reasons. The first is because of the apparent similarity between the bacterial smears on washed-rind cheese and geologically important bacterial phenomena, which also induce crystallization under certain conditions. Secondly, the fact that minerals are present in food, and that the crystal type and size can affect the quality of that food, opens a new area of research for mineralogists and food scientists.

The ease with which cheese and the precipitated minerals therein can be sampled and observed suggests that cheese could provide interesting model systems in which to study questions of biological mineralogy. The inherent complexity of cheese allows investigation to take place under complex biological conditions that could add sophistication to previous mineralogical investigations that were conducted under less ideal laboratory conditions. The study of minerals in cheese is a fertile area of research that could benefit the food science community while contributing insights to the study of mineralogy as well.

ACKNOWLEDGEMENTS

This study was funded by United States Department of Agriculture Hatch Project VT- H01905. The National Science Foundation is gratefully acknowledged through

support of grant EAR-0922961 for the purchase of the Powder X-ray diffractometer and through support of grant NSF-MRI 1039436 for the purchase of the Single Crystal X-ray diffractometer. The Cellars at Jasper Hill is also gratefully acknowledged for providing information about the manufacture of the cheeses used in the present study.

REFERENCES CITED

ARP, G., THIEL, V., REIMER, A., MICHAELIS, W., AND REITNER, J. (1999) Biofilm exopolymers control microbialite formation at thermal springs discharging in the alkaline Pyramid Lake, Nevada, USA. *Sedimentary Geology* **126**, 159-176.

ASKER, M.M.S., AND SHAWKY, B.T. (2010) Structural characterization and antioxidant activity of an extracellular polysaccharide isolated from *Brevibacterium otitidis* BTS 44. *Food Chemistry* **123**, 315-320.

BAUMGARTNER, L.K., REID, R.P., DUPRAZ, C., DECHO, A.W., BUCKLEY, D.H., SPEAR, J.R., PRZEKOP, K.M., AND VISSCHER, P.T. (2006) Sulfate reducing bacteria in microbial mats: changing paradigms, new discoveries. *Sedimentary Geology* **185**, 131-145.

BISCHOFF, J.L., FITZPATRICK, J.A., AND ROSENBAUER, R.J. (1993a) The solubility and stabilization of ikaite ($CaCO_3$ $6H_2O$) from 0° to 25°C: environmental and paleoclimatic implications for thinolite tufa. *The Journal of Geology* **101**, 21-33.

BISCHOFF, J.L., STINE, S., ROSENBAUER, R.J., FITZPATRICK, J.A., AND STAFFORT, T.W. (1993b) Ikaite precipitation by mixing of shoreline springs and lake water, Mono Lake, California, USA. *Geochemica et Cosmochimica Acta* **57**, 3855-3865.

BOCH, R., DIETZEL, M., REICHL, P., LEIS, A., BALDERMANN, A., MITTERMAYR, F., AND POLT, P. (2015) Rapid ikaite ($CaCO_3$ $6H_2O$) crystallization in a man-made river bed: hydrogeochemical monitoring of a rarely documented mineral formation. *Applied Geochemistry* **63**, 366-379.

BRENNAN, N.M., WARD, A.C., BERESFORD, T.P., FOX, P.F., GOODFELLOW, M., AND COGAN, T.M. (2002) Biodiversity of the bacterial flora on the surface of a smear cheese. *Applied and Environmental Microbiology* **68(2)**, 820-830.

BRESE, N.E., AND O'KEEFFE, M. (1991) Bond-valence parameters for solids. *Acta Cryst* **B47**, 192-197.

BROOKER, B.E. (1987) The crystallization of calcium phosphate at the surface of mould-ripened cheeses. *Food Microstructure* **6**, 25-33.

BROOKS, R., CLARK, L.M., AND THURSTON, E.F. (1950) Calcium carbonate and its hydrates. *Philosophical Transactions of the Royal Society of London* **243(861)**, 145-167.

BUCHARDT, B., ISRAELSON, C., SEAMAN, P., AND STOCKMANN, G. (2001) Ikaite tufa towers in Ikka Fjord, Southwest Greenland: their formation by mixing of seawater and alkaline spring water. *Journal of Sedimentary Research* **71(1)**, 176-189.

CHAUHAN, C.K., AND JOSHI, M.J. (2013) In vitro crystallization, characterization and growth-inhibition study of urinary type struvite crystals. *Journal of Crystal Growth* **362**, 330-337.

CLARKSON, J.R., PRICE, T.J., AND ADAMS, C.J. (1992) Role of metastable phases in the spontaneous precipitation of calcium carbonate. *J. Chem. Soc. Faraday Trans.* **88(2)**, 243-249.

CONOCHIE, J., AND SUTHERLAND, B.J. (1965) The nature and cause of seaminess of Cheddar cheese. *Journal of Dairy Research* **32**, 35-44.

CORSETTI, A., ROSSI, J., AND GOBBETTI, M. (2001) Interactions between yeasts and bacteria in the smear of surface-ripened cheeses. *International Journal of Food Microbiology* **69**, 1-10.

DIECKMANN, G.S., NEHRKE, G., PAPADIMITRIOU, S., GOTTLICHER, J., STEININGER, R., KENNEDY, H., WOLF-GLADROW, D., AND THOMAS, D.N. (2008) Calcium carbonate as ikaite crystals in Antarctic sea ice. *Geophysical Research Letters* **35(8)**.

DIECKMANN, G.S., NEHRKE, G., UHLIG, C., GOTTLICHER, J., GERLAND, S., GRANSKOG, M.A., AND THOMAS, D.N. (2010) Brief communication: ikaite ($CaCO_3$ $6H_2O$) discovered in arctic sea ice. *The Cryosphere* **4**, 227-230.

DRAKE, S.L., AND DRAKE, M.A. (2011) Comparison of salty taste and time intensity of sea and land salts from around the world. *Journal of Sensory Studies* **26**, 25-34.

DUPRAZ, C., REID, R.P., BRAISSANT, O., DECHO, A.W., NORMAN, R.S., AND VISSCHER, P.T. (2009) Processes of carbonate precipitation in modern microbial mats. *Earth-Science Reviews* **96**, 141-162.

DUPRAZ, C., AND VISSCHER, P.T. (2005) Microbial lithification in marine stromatolites and hypersaline mats. *Trends in Microbiology* **13(9)**, 429-438.

GAUCHERON, F., LE GRAET, Y., MICHEL, F., BRIARD, V., AND PIOT, M. (1999) Evolution of various salt concentrations in the moisture and in the outer layer and centre of a model cheese during its brining and storage in an ammoniacal atmosphere. *Le Lait* **79**, 553-566.

GOBBETTI, M., LOWNEY, S., SMACCHI, E., BATTISTOTTI, B., DAMIANI, P., AND FOX, P.F. (1997) Microbiology and biochemistry of Teleggio cheese during ripening. *International Dairy Journal* **7**, 509-517.

GONZALEZ-MUNOZ, M.T., LINARES, C., MARTINEZ-RUIZ, F., MORCILLO, F., MARTIN-RAMOS, D., AND ARIAS, J.M. (2008) Ca-Mg kutnahorite and struvite production by *Idiomarina* strains at modern seawater salinities. *Chemosphere* **72**, 465-472.

GULL, M., AND PASEK, M.A. (2013) Is struvite a prebiotic mineral? *Life* **3**, 321-330.

HIGLEY, M.C. (2015) A geochemical archive of climate variability in Kiritimati Island lake sediment. *Geological Society of America Abstracts with Programs* **47(7)**, 757.

HU, Y.B., WOLF-GLADROW, D.A., DIECKMANN, G.S., VOLKER, C., AND NEHRKE, G. (2014) A laboratory study of ikaite ($CaCO_3$ $6H_2O$) precipitation as a function of pH, salinity, temperature and phosphate concentration. *Marine Chemistry* **162**, 10-18.

KARAHADIAN, C., AND LINDSAY, R.C. (1987) Integrated rales of lactate, ammonia, and calcium in texture development of mold surface-ripened cheese. *Journal of Dairy Science* **70(5)**, 909-918.

KILIC, N.K., AND DONMEZ, G. (2008) Environmental conditions affecting exopolysaccharide production by *Pseudomonas aeruginosa*, *Micrococcus* sp., and *Ochrobactrum* sp. *Journal of Hazardous Materials* **154**, 1019-1024.

LAST, F.M., LAST, W.M., FAYEK, M., AND HALDEN, N.M. (2013) Occurrence and significance of a cold-water carbonate pseudomorph in microbialites from a saline lake. *J Paleolimnol* **50**, 505-517.

LAWRENCE, R.C., CREAMER, L.K., AND GILLES, J. (1987) Texture development during cheese ripening. *Journal of Dairy Science* **70**, 1748-1760.

LECLERCQ-PERLAT, M.N., PICQUE, D., RIAHI, H., AND CORRIEU, G. (2006) Microbiological and biochemical aspects of Camembert-type cheeses depend on atmospheric composition in the ripening chamber. *Journal of Dairy Science* **89(8)**, 3260-3273.

LIN, Y.M., BASSIN, J.P., AND VAN LOOSDREHT, M.C.M. (2012) The contribution of exopolysaccharides induced struvites accumulation to ammonium adsorption in aerobic granular sludge. *Water Research* **46**, 986-992.

LUCEY, J.A., AND FOX, P.F. (1993) Importance of calcium and phosphate in cheese manufacture: a review. *Journal of Dairy Science* **76**, 1714-1724.

MARLAND, G. (1975) The stability of $CaCO_3$ $6H_2O$ (ikaite). *Geochemica et Cosmochimica Acta* **39**, 83-91.

MCLEAN, R.J.C., NICKEL, J.C., BEVERIDGE, T.J., AND COSTERTON, J.W. (1989) Observations of the ultrastructure of infected kidney stones. *J. Med. Microbiol.* **29**, 1-7.

MIKKELSEN, A., ANDERSEN, A.B., ENGELSEN, S.B., HANSEN, H.C.B., LARSEN, O., AND SKIBSTED, L.H. (1999) Presence and dehydration of ikaite, calcium carbonate hexahydrate, in frozen shrimp shell. *J. Agric. Food Chem.* **47**, 911-917.

MORRIS, H.A., HOLD, C., BROOKER, J.B., AND MANSON, W. (1988) Inorganic constituents of cheese: analysis of juice from a one-month-old Cheddar cheese and the use of light and electron microscopy to characterize the crystalline phases. *Journal of Dairy Research* **55**, 255-268.

MUYNCK, W.D., VERBEKEN, K., BELIE, N.D., AND VERSTRAETE, W. (2010) Influence of urea and calcium dosage on teh effectiveness of bacterially induced carbonate precipitation on limestone. *Ecological Engineering* **36**, 99-111.

NELSON, N.O., MIKKELSEN, R.L., AND HESTERBERG, D.L. (2003) Struvite precipitation in anaerobic swine lagoon liquid: effect of pH and Mg:P ratio and determination of rate constant. *Bioresource Technology* **89**, 229-236.

NOFFKE, N. (2009) The criteria for biogeneicity of microbially induced sedimentary structures (MISS) in Archean and younger, sandy deposits. *Earth-Science Reviews* **96**, 173-180.

OMELON, C.R., POLLARD, W.H., AND MARION, G.M. (2001) Seasonal formation of ikaite ($CaCO_3$ $6H_2O$) in saline spring discharges at Expidition Fjord, Canadian High Arctic: assessing conditional constraints for natural crystal growth. *Geochemica et Cosmochimica Acta* **65(9)**, 1429-1437.

PICQUE, D., LECLERCQ-PERLAT, M.N., AND CORRIEU, G. (2006) Effect of atmospheric composition on respiratory behavior, weight loss, and appearance of Camembert-type cheeses during chamber ripening. *Journal of Dairy Science* **89**, 3250-3259.

PURCELL, C.S., AND HICKEY, C.H. (1922) Note on the occurrence of struvite in canned shrimps. *Analyst* **47(550)**, 16-18.

RIDING, R. (2000) Microbial carbonates: the geological record of calcified bacterial-algal mats and biofilms. *Sedimentology* **47(Suppl. 1)**, 179-214.

RYSGAARD, S., GLUD, R.N., LENNERT, K., COOPER, M., HALDEN, N., LEAKEY, R.J.G., HAWTHORNE, F.C., AND BARBER, D. (2012) Ikaite crystals in melting sea ice -

inplications for pCO_2 and pH levels in Arctic surface waters. *The Cryosphere* **6**, 901-908.

SCHMIDT, M., PRIEME, A., AND STOUGAARD, P. (2006) Bacterial diversity in permanently cold and alkaline ikaite columns from Greenland. *Extremophiles* **10**, 551-562.

SENCHENKOVA, S.N., KNIREL, Y.A., LIKHOSHERSTOV, L.M., SHASHKOV, A.S., SHIBAEV, V.N., STARUKHINA, L.A., AND DERYABIN, V.V. (1995) Structure of simusan, a new acidic exopolysaccharide from *Arthrobacter* sp. *Carbohydrate Research* **266**, 103-113.

SHAMS, M.A., AND JAYNES, H.O. (1983) Characterization of exopolysaccharide produced by Corynebacterium #98 in cheese whey substrate. *Journal of Food Science* **48**, 208-211.

SHELDRICK, G.M. (2008) A short history of SHELX. *Acta Crystallographica* **A64**, 112-122.

SOETAN, K.O., OLAIYA, C.O., AND OYEWOLE, O.E. (2010) The importance of mineral elements for humans, domestic animals and plants: a review. *African Journal of Food Sciences* **4(5)**, 200-222.

STICKLER, D.J. (1996) Bacterial biofilms and the encrustation of urethral catheters. *Biofouling* **9(4)**, 293-305.

SUESS, E., BALZER, W., HESSE, K.F., MULLER, P.J., UNGERER, C.A., AND WEFER, G. (1982) Calcium carbonate hexahydrate from organic-rich sediments of the Antarctic Shelf: precursers of glendonites. *Science* **216(4)**, 1128-1130.

SWAINSON, I.P., AND HAMMOND, R.P. (2003) Hydrogen bonding in ikaite, $CaCO_3$ $6H_2O$. *Mineralogical Magazine* **67(3)**, 555-562.

TANSMAN, G., KINDSTEDT, P.S., AND HUGHES, J.M. (2015a) Characterization of single crystals in the rinds of white mold and smear ripened cheeses with single crystal X-ray diffractometry. *Journal of Dairy Science* **98(Suppl. 2)**, 668-669.

TANSMAN, G., KINDSTEDT, P.S., AND HUGHES, J.M. (2015b) Identification of crystalline entities in the rinds of white mold ripened cheese and smear ripened cheese with powder X-ray diffractometry. *Journal of Dairy Science* **98(Suppl. 2)**, 668.

TANSMAN, G., KINDSTEDT, P.S., AND HUGHES, J.M. (2015c) Novel sample preparation for smear ripened cheese rinds evaluated by powder X-ray diffractometry. *Journal of Dairy Science* **98(E-Suppl. 2)**, 587-588.

TATENO, N., AND KYONO, A. (2014) Structural change induced by dehydration in ikaite ($CaCO_3$ $6H_2O$). *Journal of Mineralogical and Petrological Sciences* **109**, 157-168.

WHITICAR, M.J., AND SUESS, E. (1998) The cold carbonate connection between Mono Lake, California adn the Bransfield Strait, Antarctica. *Aquatic Geochemistry* **4**, 429-454.

WOLFE, B.E., BUTTON, J.E., SANTARELLI, M., AND DUTTON, R.J. (2014) Cheese rind communities provide tractable systems for in situ and in vitro studies of microbial diversity. *Cell* **158**, 422-433.

WOLFE, B.E., AND DUTTON, R.J. (2015) Fermented foods as experimentally tractable microbial ecosystems. *Cell* **161**, 49-55.

TABLE 1. DATA COLLECTION AND STRUCTURE REFINEMENT DETAILS FOR IKAITE AND STRUVITE

	Ikaite		Struvite	
Space group	*C*2/*c*		*Pmn*2$_1$	
Unit cell dimensions	*a* = 8.8407(16) Å		*a* = 6.9411(7) Å	
	b = 8.3333(15) Å	β = 110.683(3)°	*b* = 6.1323(6) Å	
	c = 11.072(2) Å		*c* = 11.2048 Å	
Volume	763.1(2) Å^3		476.93(8) Å^3	
Z	2		2	
Density (calculated)	1.812 Mg/cm^3		1.709 Mg/cm^3	
Theta range for data collection	3.47 to 30.00°		3.32 to 29.99°	
Index ranges	-12< h <=10		-9< *h* <=9	
	-11<= k <=11		-8<= k <=8	
	-11<= ℓ <=15		-15<= ℓ <=15	
Reflections collected	3798		8593	
Independent reflections	1108 [R(int) = 0.0122]		1491 [R(int) = 0.0429]	
Coverage of independent reflections	98.70%		100.00%	
Absorption correction	multi-scan		multi-scan	
Structure solution technique	direct methods		direct methods	
Structure solution program	SHELXS-97 (Sheldrick, 2008)		SHELXS-97 (Sheldrick, 2008)	
Refinement method	Full-matrix least-squares on F^2		Full-matrix least-squares on F^2	
Refinement program	SHELXL-97 (Sheldrick, 2008)		SHELXL-97 (Sheldrick, 2008)	
Function minimized	$\Sigma\, w(F_o^2 - F_c^2)^2$		$\Sigma\, w(F_o^2 - F_c^2)^2$	
Data / restraints / parameters	1108 / 0 / 78		1491 / 1 / 108	
Goodness-of-fit on F^2	1.182		1.02	
Final R indices	1074 data; I>2σ(I)	R1 = 0.0157, wR2 = 0.0423	1327 data; I>2σ(I)	R1 = 0.0250, wR2 = 0.0537
	all data	R1 = 0.0164, wR2 = 0.0426	all data	R1 = 0.0338, wR2 = 0.0569
Weighting scheme	$w=1/[\sigma^2(F_o^2)+(0.0198P)^2+0.2335P]$ where $P=(F_o^2+2F_c^2)/3$		$w=1/[\sigma^2(F_o^2)+(0.0320P)^2+0.0000P]$ where $P=(F_o^2+2F_c^2)/3$	
Largest diff. peaks	0.265 and -0.179 eÅ^{-3}		0.232 and -0.286 eÅ^{-3}	

TABLE 2. ATOMIC COORDINATES AND EQUIVALENT ISOTROPIC ATOMIC DISPLACEMENT PARAMETERS ($Å^2$) FOR IKAITE. U(*EQ*) IS DEFINED AS ONE THIRD OF THE TRACE OF THE ORTHOGONALIZED U_{IJ} TENSOR

Atom	*x/a*	*y/b*	*z/c*	*U(eq)*
Ca	1/2	0.64714(2)	1/4	0.01516(8)
C	1/2	0.30567(12)	1/4	0.01695(19)
O1	1/2	0.15237(10)	1/4	0.0293(2)
O2	0.52639(7)	0.38534(7)	0.15943(6)	0.02078(13)
OW1	0.61282(8)	0.72232(8)	0.09065(6)	0.02612(14)
OW2	0.78709(8)	0.55874(8)	0.38343(6)	0.02340(14)
OW3	0.67063(8)	0.88549(7)	0.35805(6)	0.02107(13)

TABLE 3. ATOMIC COORDINATES AND EQUIVALENT ISOTROPIC ATOMIC DISPLACEMENT PARAMETERS ($Å^2$) FOR STRUVITE. U(*EQ*) IS DEFINED AS ONE THIRD OF THE TRACE OF THE ORTHOGONALIZED U_{IJ} TENSOR

Atom	*x/a*	*y/b*	*z/c*	*U(eq)*
P	0	0.00637(8)	0.96006(5)	0.01576(12)
Mg	0	0.62367(11)	0.33200(7)	0.0174(2)
O1	0.81808(14)	0.88627(17)	0.00218(11)	0.0225(2)
O2	0	0.2375(2)	0.01382(15)	0.0234(3)
O3	0	0.0225(2)	0.82270(15)	0.0233(3)
O4	0.78190(18)	0.7381(2)	0.22219(11)	0.0278(3)
O5	0	0.3173(3)	0.24626(19)	0.0382(5)
O6	0.78865(18)	0.5147(2)	0.44528(14)	0.0331(3)
O7	0	0.9213(3)	0.4253(2)	0.0411(6)
N	0	0.6350(5)	0.6931(2)	0.0336(5)

TABLE 4: ATOMIC DISTANCES AND BOND VALENCES (*VU*) FOR IKAITE

Ca -	Distance	*vu*	C -	Distance	*vu*
OW1	2.3965(7)	0.31	O1	1.2775(13)	1.36
OW1’	2.3965(7)	0.31	O2	1.2908(8)	1.31
O2	2.4464(7)	0.27	O2’	1.2908(8)	1.31
O2’	2.4464(7)	0.27	Mean, Sum	1.286	3.98
OW3	2.5253(7)	0.22			
OW3’	2.5253(7)	0.22			
OW2	2.5531(7)	0.21			
OW2’	2.5531(7)	0.21			
Mean, Sum	2.480	2.02			

TABLE 5: ATOMIC DISTANCES AND BOND VALENCES (*VU*) FOR STRUVITE

Mg -	Distance	*vu*	P -	Distance	*vu*
O6	2.0519(14)	0.38	O3	1.5422(16)	1.18
O6’	2.0519(14)	0.38	O2	1.5403(15)	1.19
O4	2.0732(13)	0.36	O1	1.5361(11)	1.20
O4’	2.0731(13)	0.36	O1’	1.5361(10)	1.20
O7	2.103(2)	0.33	Mean, Sum	1.539	4.77
O5	2.110(2)	0.32			
Mean, Sum	2.077	2.13			

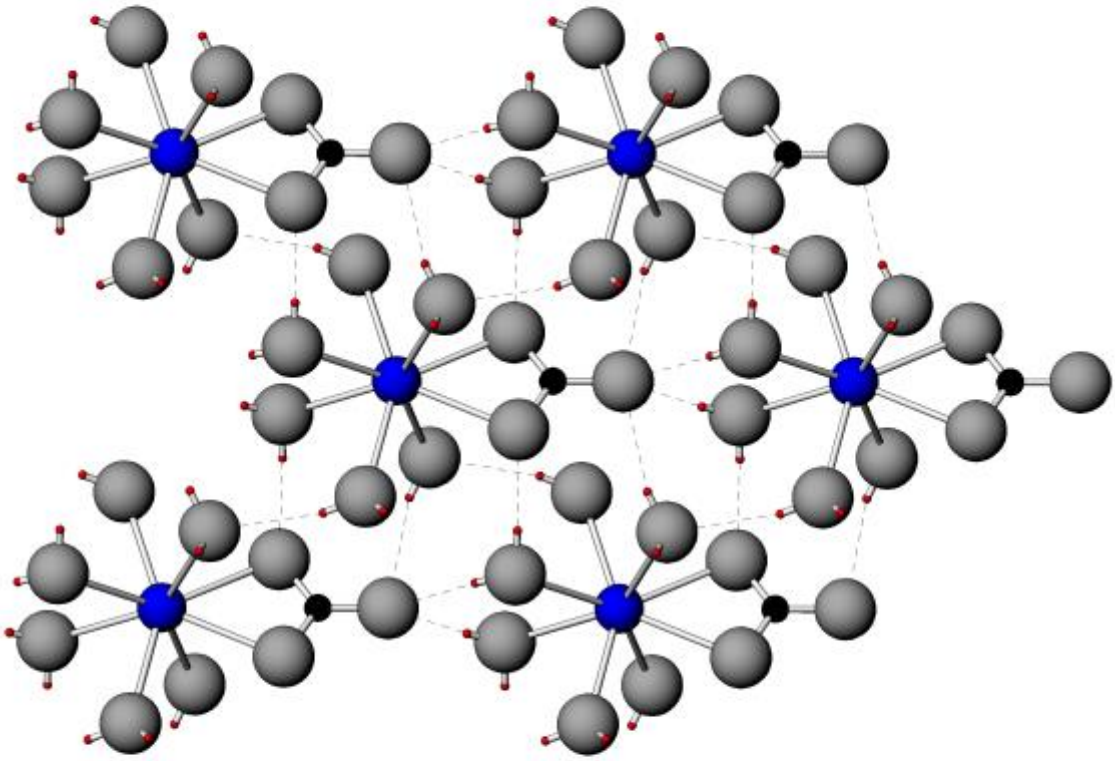

FIG. 1: Structure of ikaite projected down ~[101], *b*-axis horizontal, depicting the $CaCO_3 \cdot 6H_2O$ unit. Atom colors are as follows: calcium (blue), carbon (black), oxygen (grey), and hydrogen (red). Hydrogen bonds are oxygen-acceptor distances < 3.2Å.

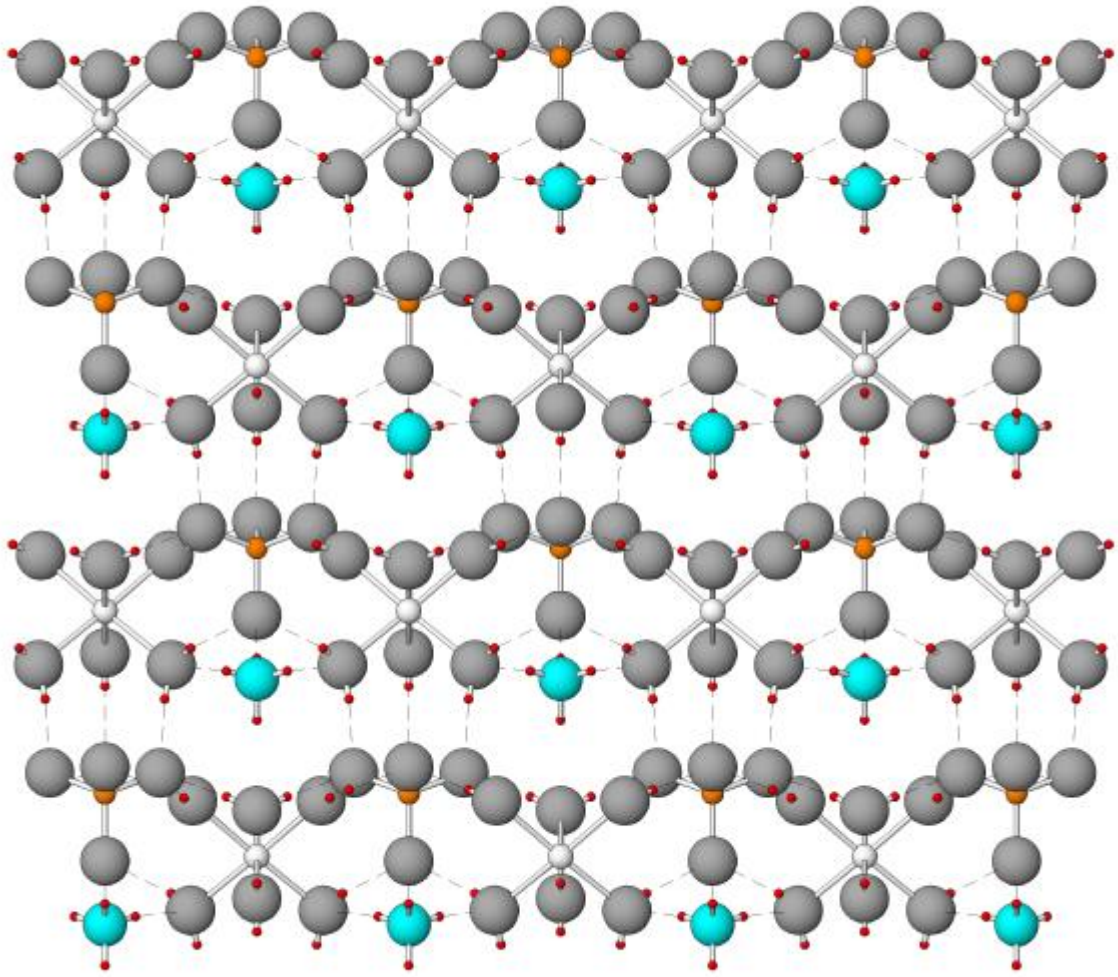

FIG 2: Structure of struvite projected down [010], *a*-axis horizontal, depicting hydrogen bonding between layers. Atom colors are as follows: magnesium (white), oxygen (grey), nitrogen (sky blue), phosphorus (orange), and hydrogen (red). Hydrogen bonds are oxygen-acceptor distances < 3.2Å.

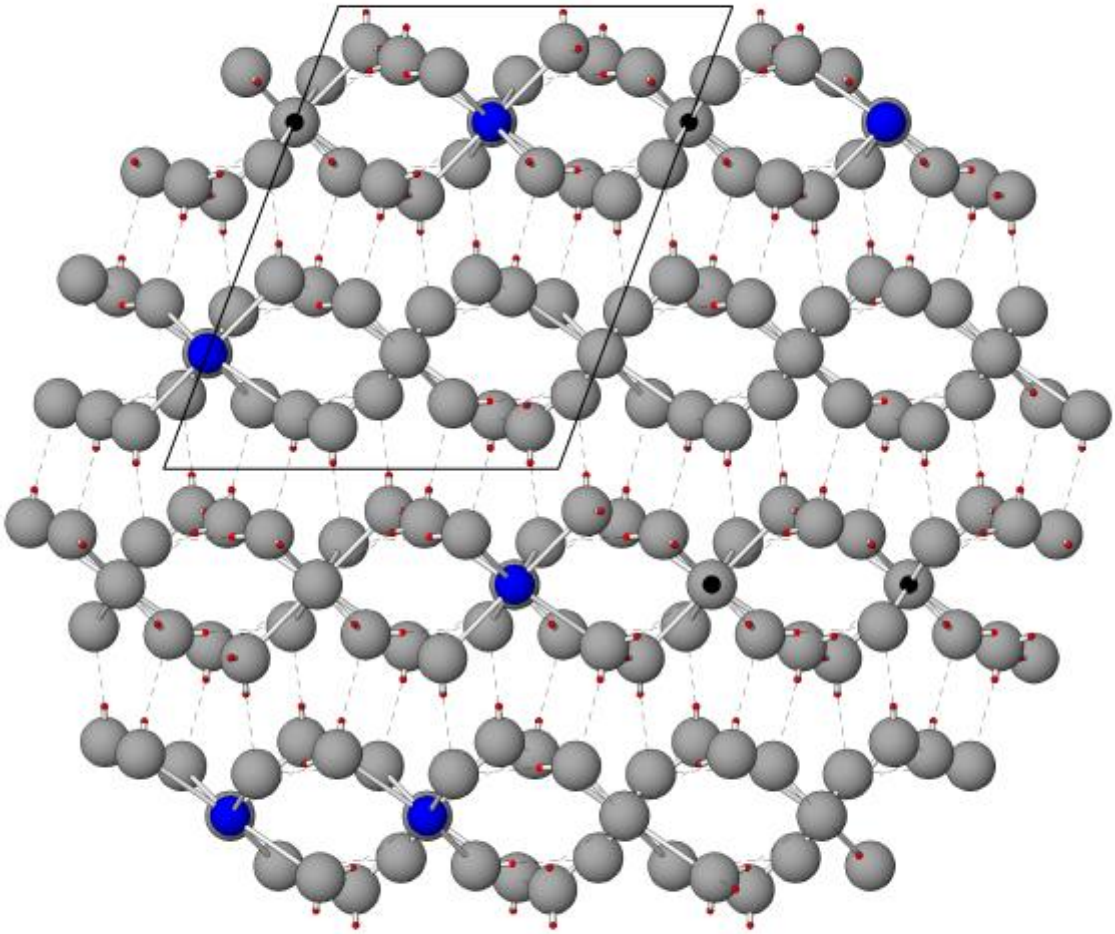

FIG. 3: Structure of ikaite projected down [010], *a*-axis horizontal, depicting hydrogen bonding between layers. Atom colors are as follows: calcium (blue), carbon (black), oxygen (grey), and hydrogen (red). Hydrogen bonds are oxygen-acceptor distances < 3.2Å.

CHAPTER 4: CRYSTALLIZATION AND DEMINERALIZATION PHENOMENA IN STABILIZED WHITE MOLD CHEESE

INTERPRETIVE SUMMARY

Although extensive work has investigated the impact of crystallization on traditional white mold cheeses, this research has not been applied to stabilized varieties. This report documents a crystallization phenomenon in the rind of stabilized white mold cheese and links this phenomenon to the accumulation of mineral elements in the rind and concurrent withdrawal of mineral elements from the center of the cheese. Given the importance of mineral elements in cheese structure development, this study provides insights about stabilized ripening processes and indicates an important homology between traditional and stabilized white mold cheeses.

CRYSTALS IN STABILZED WHITE MOLD CHEESE

Crystallization and demineralization phenomena in stabilized white mold cheese

Gil F. Tansman,* Paul S. Kindstedt,* and John M. Hughes†

*Department of Nutrition and Food Sciences and

†Department of Geology

University of Vermont,

Burlington, VT 05405, U.S.A.

Gil F. Tansman, Corresponding Author

234 Marsh Life Science, 109 Carrigan Dr.

e-mail: gtansman@uvm.edu

tel: 802-656-3374

fax: 802-656-0001

ABSTRACT

Stabilized white mold cheese is a commercially important variant of traditional white mold cheese (sometimes called bloomy rind cheese) that has an extended shelf life compared to the traditional permutation. The objectives of this observational study were to document mineral element movements and the development of a pH gradient in stabilized white mold cheese, and to use novel crystallographic techniques to identify crystals that form in the rind of this cheese. Cheeses from three separate batches were collected from a commercial supplier at Days 1, 4, 10, 14, and 18 days of aging and analyzed in a randomized block design. Samples from the center and rind of each cheese were analyzed for calcium, magnesium, phosphorus, sodium, and moisture content. The effect of location within the cheese wheel was significant for all effects, whereas the effect of aging time was significant for all effects except sodium content. The interaction between location within the cheese and aging time was significant for all effects. Using powder X-ray diffractometry, the crystals that formed in the rind during aging were identified as brushite ($CaHPO_4 \cdot 2H_2O$). The accumulation of mineral elements in the rind resulted in a substantial decrease in calcium, magnesium, and phosphorus in the center. After 18 days, calcium, magnesium, and phosphorus in the center had decreased by

26.4%, 14.8%, and 12.1%, respectively, compared to the first day of aging. The observations in the present study represent the first definitive identification of crystals in the rind of a white mold cheese. The use of novel crystallographic techniques in the present study lays the groundwork for the use of this technology in future investigations of mineral element diffusion phenomena in surface ripened cheese.

Key Words: crystal, brushite, stabilized, white mold cheese

INTRODUCTION

Texture development in traditional soft, surface ripened, white mold cheese is a complex process that involves biological and chemical factors. During aging, these cheeses develop radially, from the rind to the center, from an acidic chalky curd to a soft, viscous semisolid. An intricate framework that describes the mechanism of curd softening has developed over the past four decades. This framework involves several interconnected factors that affect casein solubilization and hydration. The three main processes that lead to cheese softening are elevated pH, demineralization of calcium, and proteolysis (Lucey and Fox 1993).

Some proteolytic activity can be attributed to proteases released by the surface mold; however, these proteases have limited mobility in the cheese and are only significant near the surface (Noomen 1983). Proteolytic activity in the body of surface ripened cheese has been attributed to plasmin and residual rennet (Karahadian and Lindsay 1987), which, on account of their distribution throughout the cheese, cannot explain the radial ripening pattern that is characteristic of this class of cheese.

A surface-to-center pH gradient that develops as a result of surface mold activity is closely linked to the radial development of texture in surface ripened cheese (Vassal *et al.* 1986). The surface mold consumes lactic acid as an energy and carbon source, and in doing so raises the pH of the curd; the mold also metabolizes the cheese proteins near the surface as a nitrogen source and releases ammonia, which also contributes to alkalinization (Amrane and Prigent 2008). In general, at a pH close to 4.6, the isoelectric point of casein, cheese texture is short and casein proteins are compact (Lawrence *et al.* 1987). Fresh traditional white mold cheese is acidic, crumbly, and lacks the viscous texture of fully ripened white mold cheese. As the pH rises, on account of the surface mold's activity, the texture softens and becomes semisolid (Noomen 1983). The change in texture, however, is confounded by the amount of calcium in the curd and a pH-dependent ion diffusion phenomenon (Le Graet and Brule 1988).

In traditional white mold cheese, minerals diffuse from the body of the cheese and collect in an unknown form under the rind (Brooker 1987; Le Graet *et al.* 1983). This diffusion mechanism is technologically important because as aging progresses, the amount of calcium phosphate in the center of the curd diminishes (Le Graet and Brule 1988). Calcium phosphate removal is important for the development of white mold cheese texture because at diminished calcium phosphate concentrations, the swelling of cheese proteins increases (Lucey and Fox 1993). Ion diffusion occurs because crystals precipitate in the rind at high pH, which causes a reduction in the local solubility of mineral elements. As a result, ions diffuse from the center of the cheese, where the solubility is higher, toward the rind where they are deposited into the crystals as the

crystals nucleate and grow (Gaucheron *et al.* 1999; Le Graet and Brule 1988; Le Graet *et al.* 1983).

Ratios of calcium-to-phosphorus in the cheese rind have repeatedly been used to investigate the mechanism of ion diffusion (Amrane and Prigent 2008; Boutrou *et al.* 1999; Brooker 1987; Gaucheron *et al.* 1999; Le Graet *et al.* 1983; Metche and Fanni 1978). These measurements have generated values ranging from 0.86 (Boutrou *et al.* 1999) to 2 (Gaucheron *et al.* 1999), which suggests that crystal phases with various stoichiometries may form in the rinds of different cheeses. Authors have attributed their calcium-to-phosphorus ratios to different crystal phases including dicalcic phosphate (Amrane and Prigent 2008), hydroxylapatite (Amrane and Prigent 2008), tricalcic phosphate (Boutrou *et al.* 1999; Gaucheron *et al.* 1999; Le Graet *et al.* 1983), and magnesium phosphate (Boutrou *et al.* 1999). It is possible that all of these phases form in different cheeses or at different stages of ripening as a result of varying levels of alkalinity, but it is impossible to make a definitive conclusion without having used a crystallographic technique. Several authors have acknowledged the speculative nature of using the calcium-to-phosphorus ratio, suggesting that conclusive identification of the crystal phases with other techniques, such as X-ray diffraction, would be beneficial (Amrane and Prigent 2008; Boutrou *et al.* 1999; Gaucheron *et al.* 1999).

In the present study, a stabilized-style variant of white mold cheeses was used as the experimental subject. This cheese is similar to traditional Camembert-style cheeses investigated by many of the aforementioned investigators but has some important differences. Stabilized white mold cheese has a higher initial pH (Lawrence *et al.* 1987), which results in a much higher level of mineral element retention in the fresh curd. Due

to the very different initial pH and mineral element content, we propose that a detailed characterization of this type of cheese would be an interesting addition to the literature. Preliminary observation in our laboratory noted that a limited but non-trivial pH gradient develops in this cheese, which raised the possibility that crystallization and demineralization could be factors in the ripening of stabilized white mold cheese.

The primary goal of the present study is to determine the extent of the pH gradient that develops in a stabilized white mold cheese and to determine if this gradient results in crystallization and demineralization phenomena, as it does in traditional white mold cheese. Novel techniques were employed to observe the onset of crystallization and to identify the crystal phases in the rind in order to illuminate the chemical conditions that facilitate crystallization and mineral diffusion.

MATERIALS AND METHODS

CHEESE MANUFACTURE

Cheeses were obtained from The Cellars at Jasper Hill (Greensboro, VT, herein referred to as *The Cellars*). The general recipe for this variety is as follows: Cheeses are manufactured from non-standardized pasteurized milk produced at Jasper Hill Farm using a stabilized procedure approximately similar to that described in Kosikowski and Mistry (1997). The milk is inoculated with cultures that are proprietary and therefore the specific cultures are not included in this description. The vat is drained at pH 6.1 and molded into wheels with a 7.5 cm diameter and 3 cm height. The wheels are demolded at a pH of 5.15 and dry salted to a target salt-in-moisture of 2.4% to 2.6%. Final cheese moisture on Day 0 is 50% to 52%. Wheels are kept on wire racks in a pre-aging room at 16°C for three

days and then transferred to an atmospherically-controlled aging vault with temperatures ranging from 11°C to 12°C and a relative humidity of 94% to 96%.

Cheese Sampling

Cheeses were sampled on Days 1, 4, 7, 10, 14, and 18. This sampling schedule was selected because it resembled the sampling schedule of Le Graet *et al.* (1983), although it was offset by one day because in the present study cheeses were not available for sampling on Day 0, which was the day of manufacture. The cheeses were wrapped in cheese paper and transported to the Department of Nutrition and Food Sciences at the University of Vermont in an insulated cooler with ice packs. Two wheels were collected from *The Cellars* on Days 1, 4, 7, and 10. Four wheels were collected on Day 14, which was the last day of cave-aging and the first day of packaging and cold storage. Two of the wheels collected on Day 14 were used for analysis on Day 14 and the additional two wheels were stored in an incubator at 4.5°C until Day 18, thereby simulating the cold storage conditions used in the manufacturing facility. The entire experiment was replicated three times using three different batches of cheese produced on different days one week apart.

Cheese Preparation for Mineral Analysis

An illustration of the sampling scheme is found in Figure 1 and is described as follows: The cheeses were precisely segmented with a wire cutter to remove a 2 cm-wide section along the diameter of the cheese. The center portion was laterally bisected to yield two pieces of cheese with dimensions measuring roughly 7.5 cm x 2 cm x 3 cm (L x

W x H). The remainder of the wheel was set aside for pH analysis, microscopic observation, and powder X-ray diffractometry (**PXRD**). A small wire cutter was used to remove approximately 3 mm from each end of one of the 7.5 cm x 2 cm x 3 cm cheese portions and the 3 mm thick samples were trimmed to 1 cm in height so as to leave only the middle portion of the sample. This sampling procedure yielded two samples with dimensions measuring 20 mm x 10 mm x 3 mm; one sample represented the approximate center of the wheel the other represented a composite sample of the fungal rind and underlying cheese from the outer rim of the wheel. Center and rind samples were placed in pre-weighed ceramic drying dishes and weighed. The dishes were then placed in a draft oven at 100°C for 12 hours, which was found to dry the samples to a constant weight.

The dried samples were removed from the oven, cooled for several minutes and reweighed to calculate the percent moisture. The dishes were then placed in a muffle furnace at 600°C for 12 hours to completely vaporize the organic material until all that remained was a small mass of acid-soluble inorganic material. Several milliliters of deionized water and 0.5 mL of reagent grade concentrated sulfuric acid (Fisher Scientific, Pittsburgh, PA) were added to the dishes. The dishes were heated on a laboratory stove to completely dissolve the material, and the solutions were quantitatively transferred to 50 mL volumetric flasks, cooled to room temperature, and brought up to volume.

MINERAL ANALYSIS

Aliquots of the dissolved ash were analyzed for calcium, magnesium, phosphorus, and sodium by ICP-OES (Optima 3000DV, Perkin Elmer Corp, Norwalk,

CT, USA). Calibration standards were prepared according to instrument manufacturer's suggested guidelines, to cover the range of concentrations in the sample set. Four-point calibrations (plus a Calibration Blank) were used for ICP analysis. Continuing calibration verification samples, prepared from an independent source, were used to check the calibration periodically. Concentrations of minerals were calculated on a cheese dry-weight basis.

pH Measurements

A segment of cheese, left over from the sectioning of the wheel, was used in the measurement of pH at the rind and at the approximate center. A spear-tip pH electrode (Thomas Scientific, Swedesboro, NJ) was used for these measurements. The probe was inserted as close to the surface of the rind as possible without breaking through the rind and a reading was taken at the approximate center of the wheel. Readings were allowed to stabilize for one minute before recording.

Microscopy and Powder X-Ray Diffraction

Samples were collected from the leftover cheese for microscopic observation and PXRD. Samples were removed from the approximate center and from the top 3 mm of the cheese with a metal spatula. The samples were smeared to nearly translucent thickness on a glass microscope slide using a metal spatula. Micrographs were captured using a Nikon E200POL petrographic microscope with a rotating stage (Nikon Corporation, Tokyo, Japan) and a SPOT Idea 1.3 Mp color camera (SPOT Imaging

Solutions, Sterling Heights, MI). When the polarizers were crossed, particles that were illuminated and displayed uniform extinction were identified as crystals.

For PXRD analysis, cheese samples from the approximate center and rind were loaded onto glass diffraction slides and data were collected on a MiniFlex II powder X-Ray diffractometer (Rigaku, The Woodlands, TX) according to the method that we previously employed to investigate calcium lactate on Cheddar (Tansman *et al.* 2014). The method in the present experiment was similar except that the samples were not dried and defatted with acetone. Diffractograms were generated at a speed of 2°2θ/minute between 5°2θ and 50°2θ.

Due to the large amorphous hump that resulted from the non-crystalline mass of the samples in the present study, the software had difficulty differentiating the background from diffraction peaks because it could not accurately identify the background pattern. However, we established that the pattern generated from Day 1 samples (before any crystals had formed) was apparent in diffractograms throughout the sampling timeframe and thus served as the universal background pattern. Peaks that emerged from the characteristic amorphous pattern in diffractograms collected after Day 1 were manually identified as diffraction peaks. This method was beyond the capabilities of the automated functions in the software and may reflect the fact that typical diffraction samples, such as geological specimens, rarely contain as high a mass fraction of non-crystalline material as the samples in the present study.

To initially find a matching reference diffraction pattern, a literature search was conducted to compile a list of crystal phases that have been mentioned in the cheese literature. These phases included crystals that had been directly observed in cheeses such

as Cheddar and Gouda, as well as phases that were mentioned in the literature as possible candidates for the identity of crystals in the rind of white mold cheese. Reference diffraction patterns from the International Center for Diffraction Data (**ICDD**) database that corresponded to the phases on the list were compared to diffraction patterns from Day 18 diffractograms and eliminated from the list if any of the main peaks in the reference pattern were missing from the experimental diffractograms. Once a good match was found, the reference pattern for the selected phase was compared to each experimental diffractogram to determine if the reference pattern accounted for all the diffraction peaks that appeared above the characteristic Day 1 background pattern, with the absence of additional peaks indicating that the reference pattern was the only pattern in the experimental diffractogram, within the sensitivity of the instrument.

Statistical Analysis

The experiment was conducted as a three-factor randomized block design with batches representing blocks and seven sampling points per batch. Data for pH, selected mineral elements on a dry weight basis, moisture content, and salt-in-moisture were analyzed in the statistical package JMP Pro 12.0.0 (SAS Institute Inc., Cary, NC).

Results

Summary statistics for pH, selected mineral elements on a dry weight basis, moisture content, and salt-in-moisture are presented in Table 1. The summary data in Table 1 demonstrate that all main and interaction effects measured for pH, calcium, phosphorus, magnesium, and moisture content were significant. ‘Batch’ and ‘Day of

Aging' effects were not significant for sodium and salt-in-moisture, although 'Sampling Location' and the interaction between 'Sampling Location' and 'Day of Aging' were. Notably, the interaction between 'Day of Aging' and 'Sampling Location' was highly significant for all variables.

Graphical representation of pH development during aging (Figure 2) demonstrates that as aging progressed, the pH of the rind and center, having been nearly identical at Day 1, diverged so that by Day 18 the pH of the rind was approximately 0.7 pH units higher than the center. Most of this change was due to increased rind pH, although there was also a non-trivial decrease in center pH. Rind pH did not rise until Day 10, and even decreased slightly, along with the center pH, until Day 7.

The elevated rind pH after Day 7 was accompanied by increased concentrations of calcium (Figure 3), phosphorus (Figure 4), and magnesium (Figure 5) in the rind. Increases in rind pH, rind calcium, rind phosphorus, and rind magnesium were closely correlated according to the correlation coefficients for those variables (Table 2), with the largest increases of all four variables occurring between Days 7 and 14. As calcium, phosphorus, and magnesium accumulated in the rind, the concentration of these elements in the center concurrently diminished.

The concentrations of sodium in the rind and center were also recorded over the aging timeframe (Figure 6), but appeared to be independent of changes in rind pH, in contrast to the other mineral elements. On a dry weight basis, the concentrations of sodium in the center and rind appeared to converge by the end of the experimental timeframe. The changes in sodium content in the center and rind represent the inward diffusion of salt, which is applied to the surface of new cheese wheels after demolding.

Salt-in-moisture (data not shown) appeared to develop very similarly to sodium on a dry weight basis, although the salt-in-moisture content of the center and rind did not fully converge by the end of the experiment. Nonetheless, the mean salt-in-moisture of the center by Day 18 was 2.49, which is within the target salt-in-moisture as reported by *The Cellars*.

Moisture contents of the center and rind diverged over the course of aging with the moisture content at the center remaining fairly stable and the moisture content of the rind diminishing by several percent by the end of the observation period (Figure 7). The decreased moisture content in the rind was likely a result of evaporative moisture loss, which appeared to be a localized effect that did not affect the moisture content in the center.

Diffractograms of rind samples from Days 1 (Figure 8A) and 4 (data not shown) did not show any evidence of crystal growth, but consistently displayed a characteristic amorphous spectrum that was interpreted as the baseline for the cheese matrix, as described in the Materials and Methods. Diffractograms from center samples throughout the experiment displayed the characteristic background spectrum, devoid of any evidence of crystal growth (data not shown). All diffractograms of rind samples starting on Day 10 showed evidence of crystal growth (Figure 8B) in the form of distinct peaks along the background spectrum; these diffractograms displayed the same set of peaks with roughly the same relative intensity between peaks. Some of the Day 7 rind diffractograms displayed peaks, although the peaks were exceedingly small and only peaks at approximately 12°2θ and 30°2θ, corresponding to the largest peaks in rind diffractograms from Day 10 and onward could be distinguished from the background (data not shown).

When rind diffractograms displaying peaks were compared with known diffraction patterns from the ICDD database, the peaks matched the reference pattern for brushite ($CaHPO_4 \bullet 2H_2O$, ICDD card # 01-075-4365), which is represented by the vertical bars in Figure 8B and C. Figures of merit (**FOM**), which are values produced by PDXL to determine the degree of fit of a reference card to a diffractogram, are presented with Day 10 and Day 18 diffractograms in Figure 8 to indicate the degree of fit. As demonstrated in our work with calcium lactate enantiomeric variants (Tansman *et al.* 2014), a FOM of 1 or less indicates a very good fit. In the present experiment, Day 10 rind diffractograms generally had FOM around 1 when fitted to ICDD card # 01-075-4365. By Day 18, rind diffractograms fitted to the same reference card had FOM well below 1 indicating that brushite was a very good fit.

Diffractograms of rind samples from Days 14 and 18 showed progressively larger brushite peaks (Figure 8C), which can be interpreted as an increase in the quantity of brushite in the samples. The increased intensity of diffraction peaks above the baseline probably contributed to the reduced FOM as aging progressed. None of the diffractograms displayed peaks other than those attributable to brushite or to the characteristic background spectrum, indicating that within the sensitivity of the instrument, no other crystal phases were present throughout the experiment.

Microscopy imaging revealed crystals of varying sizes with larger crystals tending to appear later in aging. Crystals around 5 μm in size were observed in all rind samples starting on Day 10 (Figure 9A), with slightly larger crystals observed in the rind by Day 14 (Figure 9B) and crystals up to 20 μm observed in the rind by Day 18 (Figure 9C).

DISCUSSION

EXTENT OF PH GRADIENT DEVELOPMENT

By the end of the 18-day observation period, a pH gradient of approximately 0.7 pH units had developed between the center and rind of the wheel. The gradient began to appear after Day 10 and was a result of a pH increase at the rind as well as a pH decrease at the center. The decreased pH at the center was likely caused by continued fermentation of residual lactose by the starter cultures, which can happen at the center while salt levels are low (Lawrence *et al.* 1987) and until the salt has diffused sufficiently from the surface to the center.

From Day 7 to Day 18 the pH at the rind steadily increased, with the greatest increase occurring between Day 7 and Day 14. The increase was likely caused by the fungal consumption of lactic acid and production of ammonia (Amrane and Prigent 2008), although neither of these parameters were measured in the present study. The decreased rate of alkalinization between Day 14 and Day 18 likely reflects the typical decrease in metabolic activity that accompanies a decrease in temperature, as the cheeses were placed in cold storage on Day 14.

Compared to the observations of previous investigators (Karahadian and Lindsay 1987; Le Graet and Brule 1988; Le Graet *et al.* 1983), who used traditional Camembert or Brie as their subjects, the pH gradient that developed in the present study was quite modest. The aforementioned authors observed pH gradients that ranged from approximately 4.6 at the center to approximately 7 at the rind over the same aging period as the present study. In contrast, the stabilized technology of the cheese used in the

present study appears to retard rind alkalinization. This could be related to the higher buffering capacity associated with greater calcium and phosphate retention in curd at elevated pH (Lucey and Fox 1993), or could be related to factors that limit lactic acid consumption or ammonia production. Further investigation, including measurement of lactic acid and ammonia concentrations in the rind of stabilized cheese during aging, would be needed to elucidate the factors that control rind pH in this variety and in other stabilized white mold cheeses.

Moisture Development During Aging

The observed retention of moisture at the cheese center in the present study contrasts with the work of Leclercq-Perlat *et al.* (2012) who observed that the center of traditional Camembert-type cheese lost moisture over approximately the same timeframe as the present study. Those findings confirmed the observations of Le Graet *et al.* (1983) who noted an increase in dry matter content at the center of traditional Camembert during aging. It should be noted that the stabilized-style cheese in the present study had a considerably lower initial moisture content than the traditional white mold cheeses used in the aforementioned studies. Differences in the humidity and airflow in the ripening chamber are known to affect the rate of moisture loss (Leclercq-Perlat *et al.* 2012), and it is likely that curd characteristics, as well as cheese dimensions, influence moisture retention as well. Further studies on stabilized white mold cheese would be needed to determine if this moisture pattern is characteristic of stabilized white mold cheese or is an artifact of the sampling methods.

SIGNIFICANCE OF BRUSHITE CRYSTALLIZATION

Brushite solubility is influenced by pH, and under acidic conditions it is quite soluble; however, as the pH tends towards neutrality the solubility of brushite decreases by several degrees of magnitude (Johnsson and Nancollas 1992). Under moderately acidic conditions, brushite is the least soluble calcium phosphate phase, but as the pH increases other calcium phosphate phases, such as hydroxylapatite, eventually become less soluble than brushite (Ferreira *et al.* 2003). Over the pH environment that may be found in both stabilized and traditional white mold cheeses (roughly 4.6 to 7), brushite is less thermodynamically stable than hydroxylapatite, tricalcium phosphate, and octacalcium phosphate, although kinetic factors may result in the preferential formation of brushite (Johnsson and Nancollas 1992). Thus, even though brushite is not the most thermodynamically stable calcium phosphate phase, the appearance of brushite in the present study at a pH between 5.3 and 5.6 is not precluded.

As stated previously, the pH of the rinds of traditional Camembert-style cheeses that were investigated by other workers climbed to around 7. At this pH the solubilities of other calcium phosphates are much lower than that of brushite (Johnsson and Nancollas 1992) and the possibility of other calcium phosphate phases crystalizing in the rind is likewise increased. Thus, the elevated ratios of calcium-to-phosphorus that were found by other investigators could reflect phase transitions that can occur at elevated pH. Using electron microscopy, Brooker (1987) described two distinct morphologies of crystals in the rind of Coulomnier cheese, and these could potentially represent two co-occurring calcium phosphate phases. Therefore, it may be fruitful to apply PXRD to the study of

traditional white mold cheeses to determine if phases other than brushite appear as a function of elevated rind pH.

In the present study, the molar increases in calcium and phosphorus in the rind, corrected for the initial quantities of those elements on Day 1, were not statistically different throughout aging ($P = 0.048$), which conforms to the one-to-one molar ratio of calcium-to-phosphorus in brushite. However, these data alone would not necessarily lead to the conclusion that the crystal phase in the present study was brushite. Several calcium phosphate phases contain stoichiometric equivalents of calcium and phosphorus, and thus any of these phases could account for the observed accumulation of calcium and phosphate in the rind. Similarly, based on their elemental analysis of a model cheese system containing crystals, Amrane and Prigent (2008) proposed that the crystals were dicalcic phosphate, which is a term that encompasses several crystal phases containing the unit $CaHPO_4$, including brushite. In this case, as well as in the present study, the particular crystal phase could not be precisely determined from elemental analyses alone.

In the present study, when the uncorrected molar quantities of calcium and phosphorus were compared, there was a statistically significant ($P < 0 .0001$) excess of calcium in the rind throughout aging. In the absence of a crystallographic technique, the uncorrected data could have led one to believe that a crystal phase or several different crystal phases containing a higher proportion of calcium-to-phosphorus were present. It should be noted that the data in the present study cannot explain the excess of calcium in the rind. Nonetheless, these data may be used to demonstrate the potential pitfalls of using elemental analysis to indirectly identify crystal phases in cheese rinds.

ACCUMULATION OF MINERAL ELEMENTS IN THE RIND

Starting on Day 10 there was a steady accumulation of calcium, phosphorus, and magnesium in the rind that tapered off between Day 14 and Day 18. This closely correlated with the degree of increase in rind pH during the same period of aging (Table 2), which suggests a link between the rate of pH elevation and the rate of brushite crystallization. The latter point seems to imply that brushite in the present study was only slightly supersaturated at the range of rind pH's because as the increase in rind pH slowed so did the rate of calcium, phosphorus, and magnesium accumulation in the rind.

Calcium and phosphorus accumulation could be easily attributed to brushite, which contains both elements in its chemical formula ($CaHPO_4 \cdot 2H_2O$). Even though the chemical formula does not include magnesium, elemental analysis indicated that magnesium accumulated in the rind as well. The mass of magnesium that deposited in the rind was very small compared to calcium and almost certainly deposited in calcium sites in the brushite lattice. Magnesium and calcium are both alkaline earth elements, and due to magnesium's smaller atomic radius, magnesium may substitute for calcium in the brushite crystal lattice (Lee and Kumta 2010). Further studies would be necessary to confirm this assumption because diffractograms of moderately substituted brushite cannot be distinguished from pure brushite, and therefore the diffractograms in the present study cannot be used to verify this premise.

CHEESE DEMINERALIZATION

The results of this study demonstrate that a mineral element diffusion phenomenon occurs in stabilized white mold cheese that had not been previously

observed. The processes of brushite crystallization and concurrent calcium, phosphate, and magnesium diffusion result in a significant reduction of calcium, phosphate, and magnesium in the center of the wheel by the end of the study timeframe. By the final day of observation, the center of the cheese contained on average 26.4% less calcium, 14.8% less phosphorus, and 12.1% less magnesium. On a molar basis, the calcium content at the center was reduced by approximately twice that of phosphorus. This may reflect the slower diffusion of phosphate in the cheese matrix due to its larger ionic radius. Further investigations that include measurements of phosphorus and calcium at intermediate points between the rind and the center would be needed to fully explain how the concentration of calcium at the center can decrease more extensively than the concentration of phosphorus. Nonetheless, these observations suggest that the diffusion of mineral elements may be a complex process that warrants additional study.

The diminished concentrations of these elements, and especially the reduction in calcium, is potentially important from a cheese technology standpoint, given the significance attributed to calcium in casein-casein interactions and casein hydration (Feeney *et al.* 2002). Although the concentration of calcium in the cheese center at the end of the present study was higher than the concentration previously reported for traditional Camembert over the same aging time (Le Graet *et al.* 1983), the demineralization observed in the present study is still noteworthy. Further research is necessary to determine if demineralization in stabilized white mold cheese has an impact on the texture of the ripened cheese.

CONCLUSION

The process of rind alkalinization and cheese demineralization that had been previously observed in traditional white mold cheese was observed in a limited form in a stabilized white mold cheese. A relatively small pH gradient developed between the rind and center of the cheese, which was accompanied by a significant diffusion of calcium, phosphorus, and magnesium from the center to the rind. Crystallographic techniques aided in determining that brushite crystals precipitated in the rind and were responsible for the accumulation of mineral elements in the rind. Further research is necessary to determine the role that demineralization plays in texture development of stabilized white mold cheese. Studies designed to investigate the effect of modulating the degree of demineralization, while holding the pH constant, could provide great insight into the role that calcium concentration plays in texture characteristics of stabilized white mold cheese and cheese universally.

ACKNOWLEDGEMENTS

This study was funded by United States Department of Agriculture Hatch Project VT- H02102. The National Science Foundation is gratefully acknowledged through support of grant EAR-0922961 for the purchase of the X- ray diffractometer. *The Cellars* is also gratefully acknowledged for supplying the cheeses used in this study.

REFERENCES

Amrane, A. and Y. Prigent. 2008. Diffusion of calcium and inorganic phosphate at the surface of a solid model medium in relation with growth of *Geotrichum candidum* and *Penecillium camembertii*. Journal of Food Biochemistry 32:813-825.

Boutrou, R., F. Gaucheron, M. Piot, F. Michel, J. Maubois, and J. Leonil. 1999. Changes in the composition of juice expressed from Camembert cheese during ripening. Le Lait 79:503-513.
Brooker, B. E. 1987. The crystallization of calcium phosphate at the surface of mould-ripened cheeses. Food Microstructure 6:25-33.
Feeney, E. P., T. P. Guinee, and P. F. Fox. 2002. Effect of pH and calcium concentration on proteolysis in Mozzarella cheese. Journal of Dairy Science 85:1646-1654.
Ferreira, A., C. Oliveira, and F. Rocha. 2003. The different phases in the precipitation of dicalcium phosphate dihydrate. Journal of Crystal Growth 252:599-611.
Gaucheron, F., Y. Le Graet, F. Michel, V. Briard, and M. Piot. 1999. Evolution of various salt concentrations in the moisture and in the outer layer and centre of a model cheese during its brining and storage in an ammoniacal atmosphere. Le Lait 79:553-566.
Johnsson, M. S. A. and G. H. Nancollas. 1992. The role of brushite and octacalcium phosphate in apatite formation. Critical Reviews in Oral Biology and Medicine 3:61-82.
Karahadian, C. and R. C. Lindsay. 1987. Integrated rales of lactate, ammonia, and calcium in texture development of mold surface-ripened cheese. Journal of Dairy Science 70(5):909-918.
Kosikowski, F. V. and V. V. Mistry. 1997. Cheese and Fermented Milk Foods. Vol. 1. F.V. Kosikowski, Great Falls, VA.
Lawrence, R. C., L. K. Creamer, and J. Gilles. 1987. Texture development during cheese ripening. Journal of Dairy Science 70:1748-1760.
Le Graet, Y. and G. Brule. 1988. Migration des macro et oligo-éléments dans un fromage à pâte molle de type Camembert. Le Lait 68(2):219-234.
Le Graet, Y., A. Lepienne, G. Brule, and P. Ducruet. 1983. Migration du calcium et des phosphates inorganiques dans les fromages à pâte molle de type Camembert au cours de l'affinage. Le Lait 63:317-332.
Leclercq-Perlat, M. N., M. Sicard, I. C. Trelea, D. Picque, and G. Corrieu. 2012. Temperature and relative humidity influence the microbial and physicochemical characteristics of Camembert-type cheese ripening. Journal of Dairy Science 95:4666-4682.
Lee, D. and P. N. Kumta. 2010. Chemical synthesis and stabilization of magnesium substituted brushite. Materials Science and Engineering C 30:934-943.
Lucey, J. A. and P. F. Fox. 1993. Importance of calcium and phosphate in cheese manufacture: a review. Journal of Dairy Science 76:1714-1724.
Metche, M. and J. Fanni. 1978. Rôle de la flore fongique dans l'accumulation du calcium et du phosphore à la surface des fromages du type camembert. Le Lait 58(557):336-354.
Noomen, A. 1983. The role of the surface flora in the softening of cheeses with a low initial pH. Neth. Milk Dairy Journal 37:229-232.
Tansman, G., P. S. Kindstedt, and J. M. Hughes. 2014. Powder x-ray diffraction can differentiate between enantiomeric variants of calcium lactate pentahydrate crystal in cheese. Journal of Dairy Science 97(12):7354-7362.
Vassal, L., V. Monnet, D. Le Bars, C. Roux, and J. C. Gripon. 1986. Relation entre le pH, la composition chimique et la texture des fromages de type Camembert. Le Lait 66(4):341-351.

Table 1. Mean squares, probabilities (in parentheses), and degrees of freedom for pH, selected mineral elements on a dry weight basis, moisture content, and salt-in-moisture during 18 days of aging (16°C from Day 1 to Day 4, 11-12°C from Day 4 to Day 14 and 5°C from Day 14 to Day 18). Statistical significance (with $P < 0.05$) is denoted by an asterisk

Factors	df	pH	Ca	P	Mg	Na	Moisture Content	Salt-in-Moisture
Batch (blocked)	2	0.0953 (<0.001*)	31.975 (<0.001*)	11.302 (<0.001*)	0.0382 (<0.001*)	0.413 (0.791)	0.001 (0.025*)	0.0377 (0.712)
Day of Aging (Day)	5	0.126 (<0.001*)	8.016 (<0.001*)	4.858 (<0.001*)	0.004 (<0.001*)	1.881 (0.385)	0.001 (0.021*)	0.161 (0.215)
Sampling Location (rind or center) (SL)	1	1.328 (<0.001*)	86.134 (<0.001*)	37.148 (<0.001*)	0.0514 (<0.001*)	648.723 (<0.001*)	0.001 (0.043*)	47.127 (<0.001*)
Day x SL	5	0.250 (<0.001*)	31.490 (<0.001*)	9.687 (<0.001*)	0.017 (<0.001*)	129.494 (<0.001*)	0.002 (0.001*)	6.310 (<0.001*)
Error	58	0.003	0.631	0.193	0.001	1.753	0.0003	0.110

*$P < 0.05$

Table 2. Matrix of correlation coefficients for rind pH and concentrations of selected mineral elements in the rind on a dry weight basis.

	pH	Ca	P	Mg
pH	1.0000	0.8581	0.8839	0.7914
Ca		1.0000	0.9360	0.8628
P			1.0000	0.9355
Mg				1.0000

Figure Captions

Figure 1. Illustration of the sampling scheme used for quantitative measurement of calcium, phosphorus, magnesium, and sodium content in rind and center locations

Figure 2. Average pH values of rind and center sampling locations during aging. Error bars represent standard error from all three batches and duplicate cheeses on each sampling day

Figure 3. Average calcium concentrations of rind and center sampling locations during aging on a dry weight basis (grams of calcium per kilogram of dry cheese). Error bars represent standard error from all three batches and duplicate cheeses on each sampling day

Figure 4. Average phosphorus concentrations of rind and center sampling locations during aging on a dry weight basis (grams of phosphorus per kilogram of dry cheese). Error bars represent standard error from all three batches and duplicate cheeses on each sampling day

Figure 5. Average magnesium concentrations of rind and center sampling locations during aging on a dry weight basis (grams of magnesium per kilogram of dry cheese). Error bars represent standard error from all three batches and duplicate cheeses on each sampling day

Figure 6. Average sodium concentrations of rind and center sampling locations during aging on a dry weight basis (grams of sodium per kilogram of dry cheese). Error bars represent standard error from all three batches and duplicate cheeses on each sampling day

Figure 7. Average percent moisture of rind and center sampling locations during aging. Error bars represent standard error from all three batches and duplicate cheeses on each sampling day

Figure 8. Examples of powder X-ray diffractograms of the rind on Day 1 (A), Day 10 (FOM: 1.104) (B), and Day 18 (FOM: 0.770) (C). Vertical bars represent the reference diffraction pattern for brushite ($CaHPO_4 \bullet 2H_2O$, ICDD card # 01-075-4365)

Figure 9. Examples of micrographs displaying crystals in Day 10 (A), Day 14 (B), and Day 18 (C) rind samples

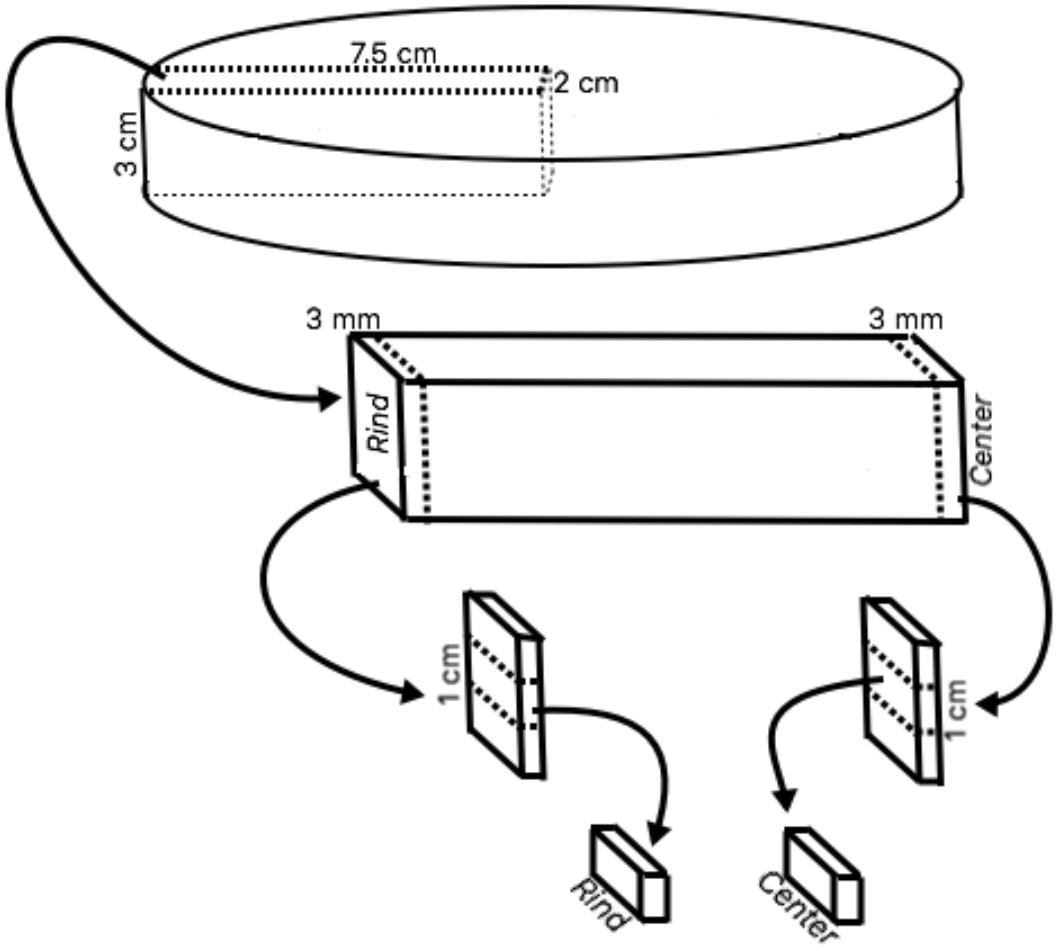

Tansman
Figure 1

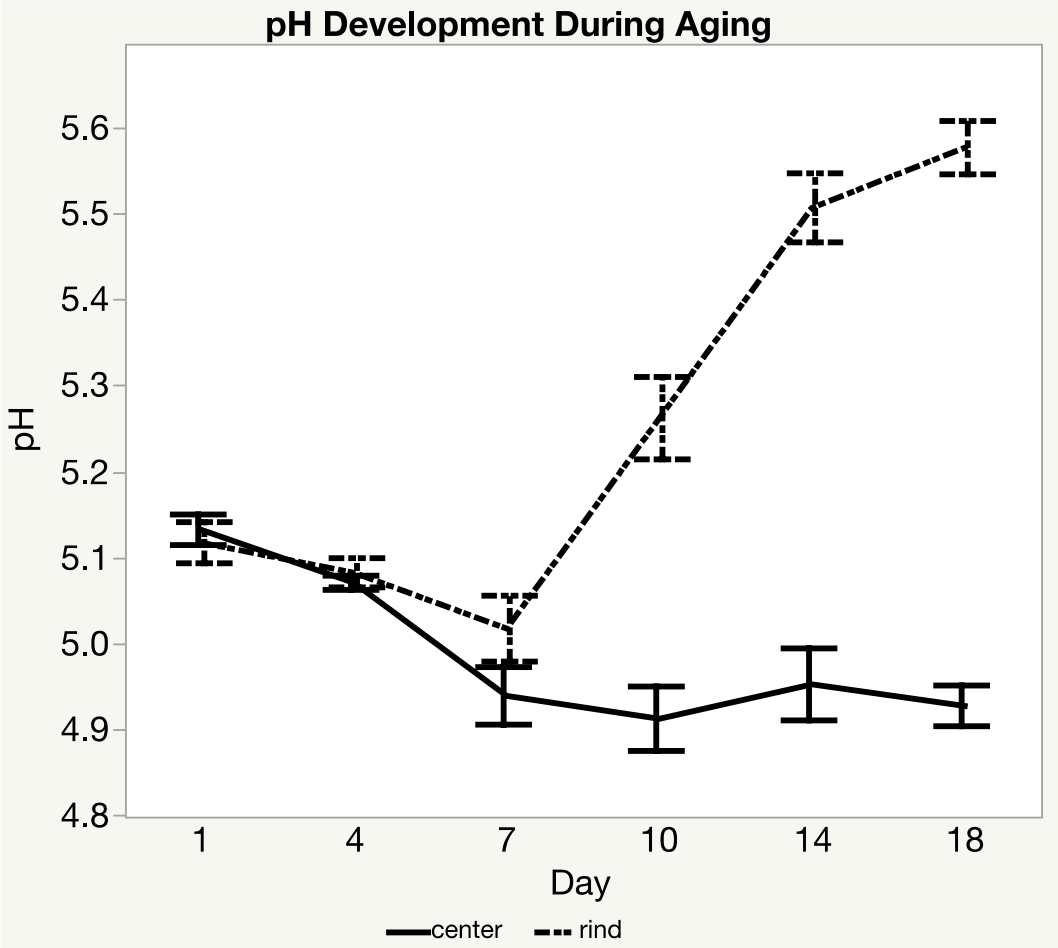

Tansman
Figure 2

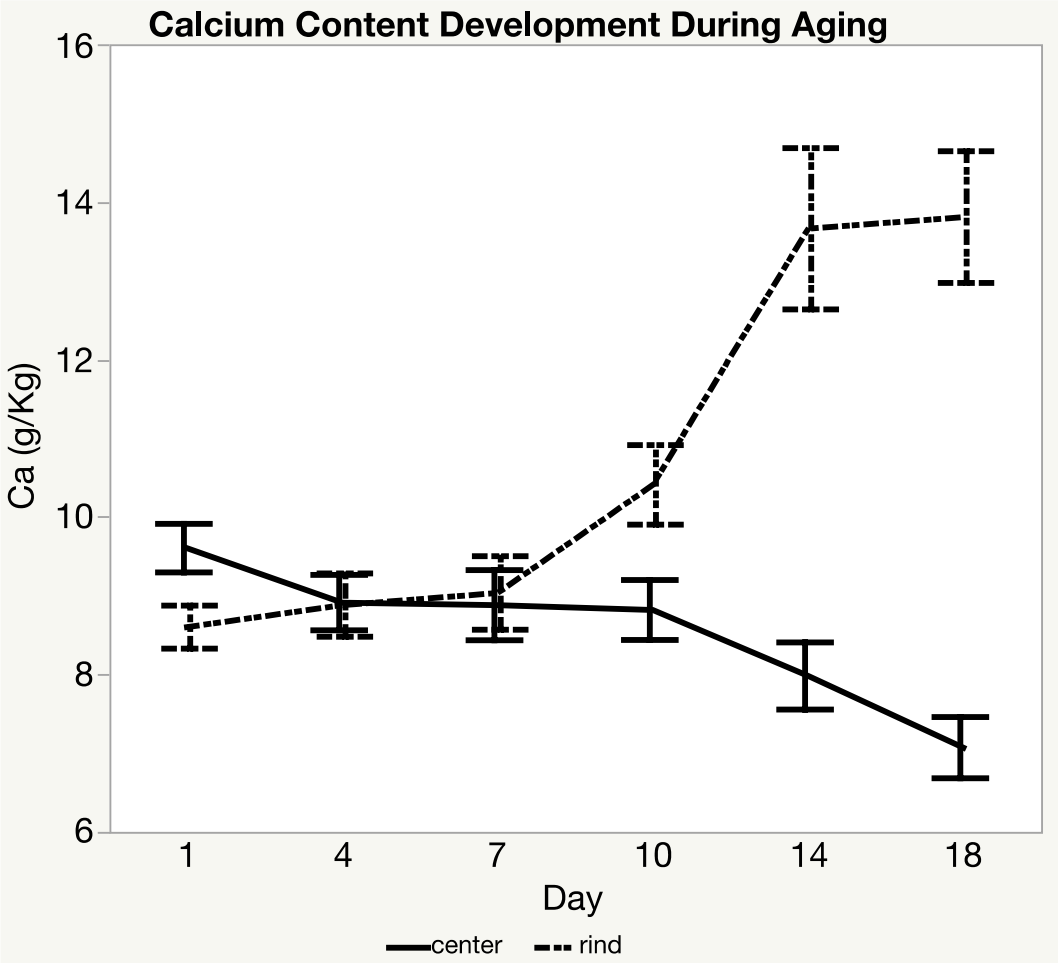

Tansman
Figure 3

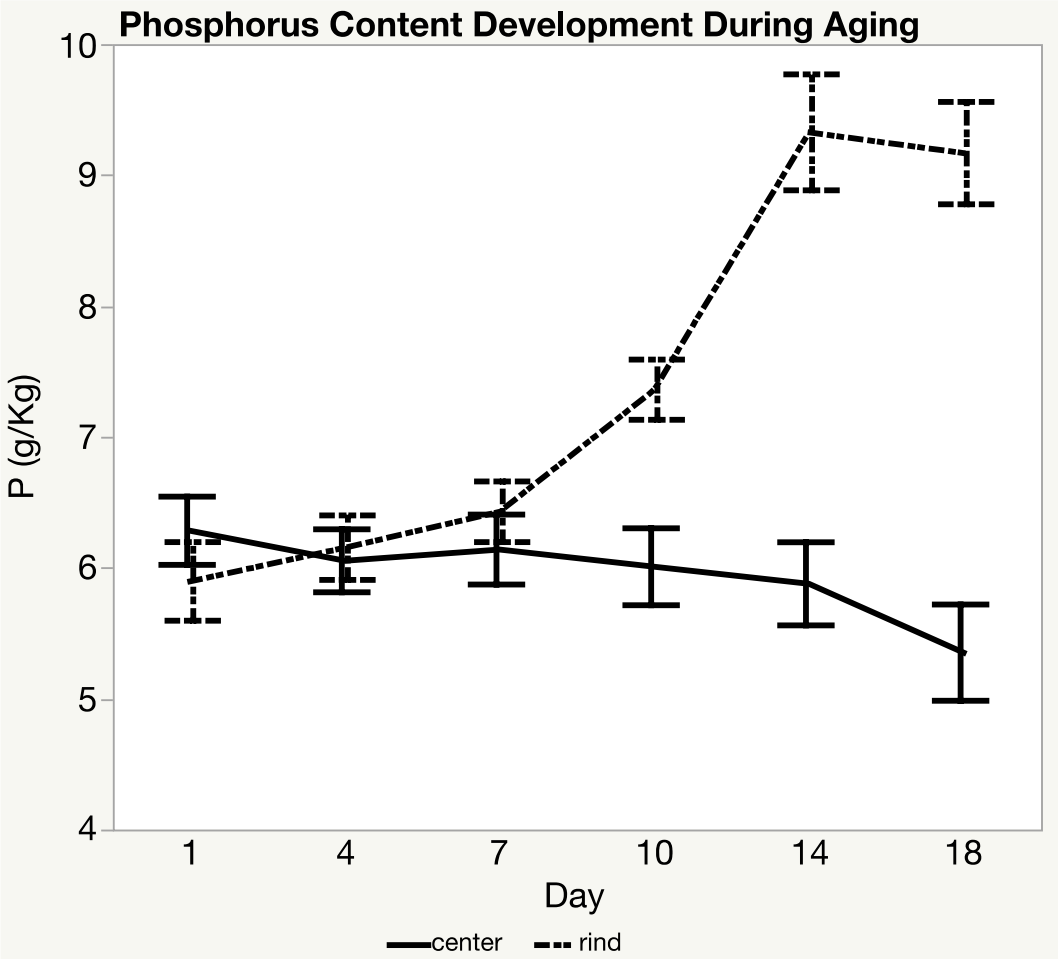

Tansman
Figure 4

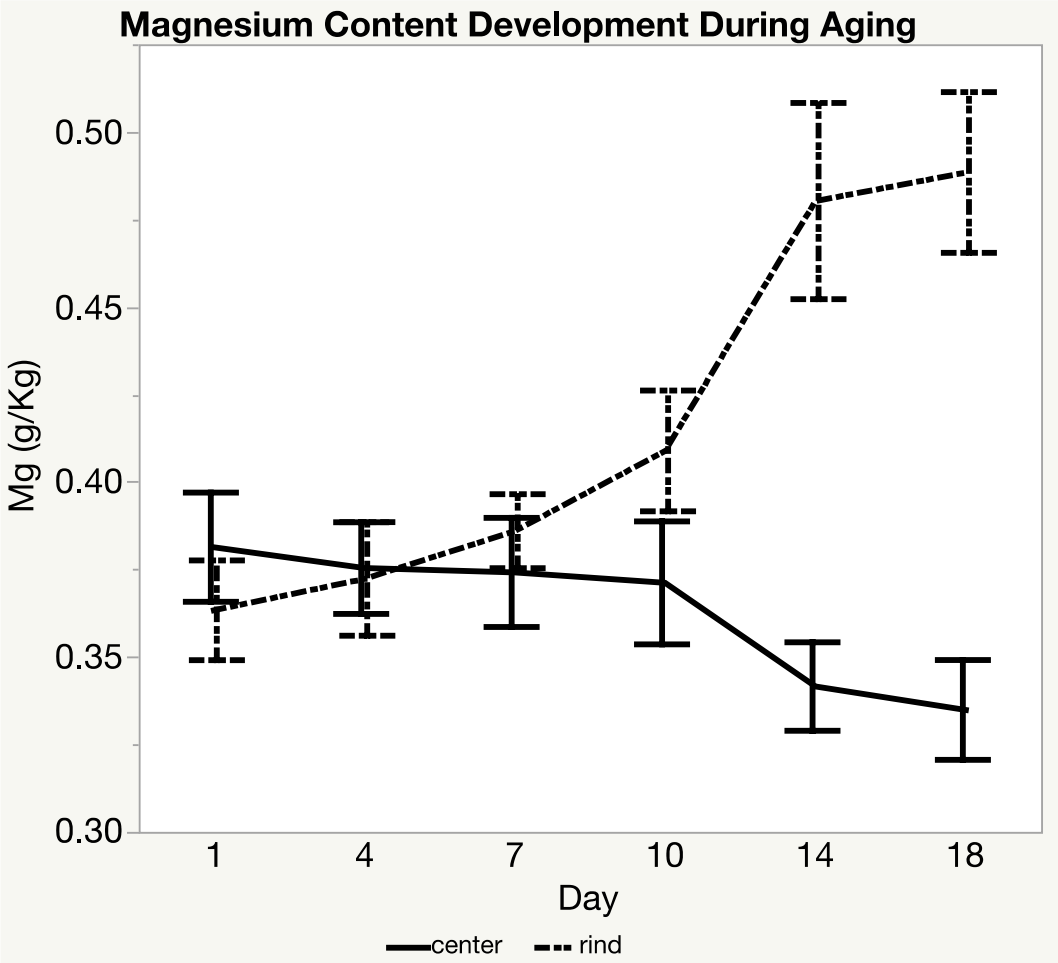

Tansman
Figure 5

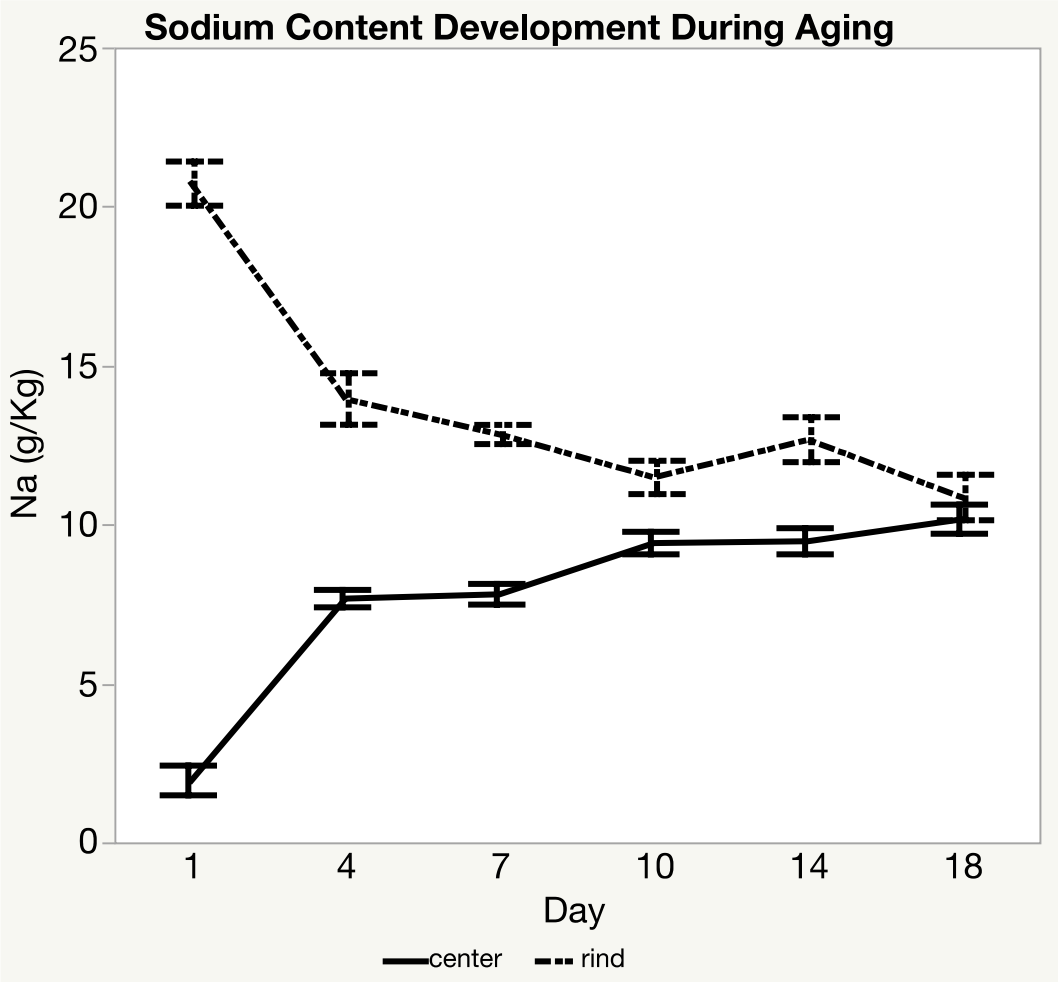

Tansman
Figure 6

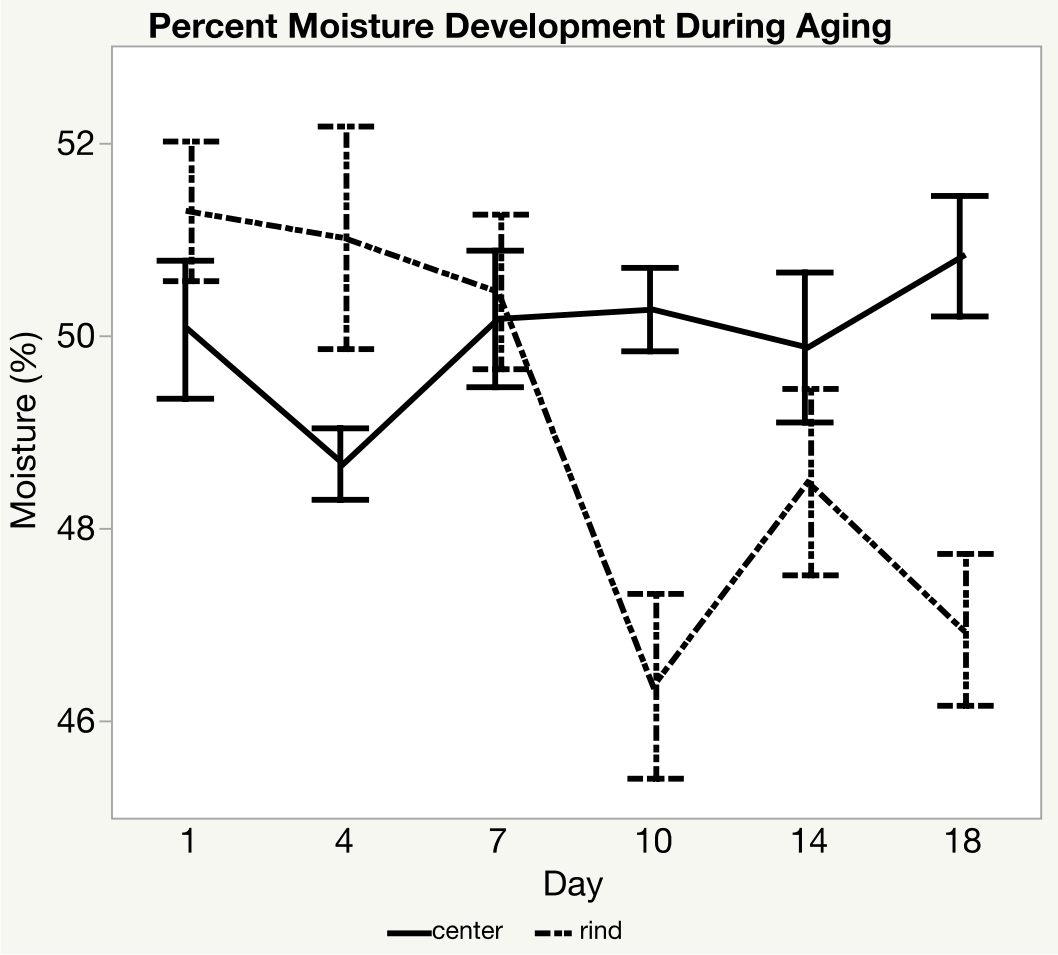

Tansman
Figure 7

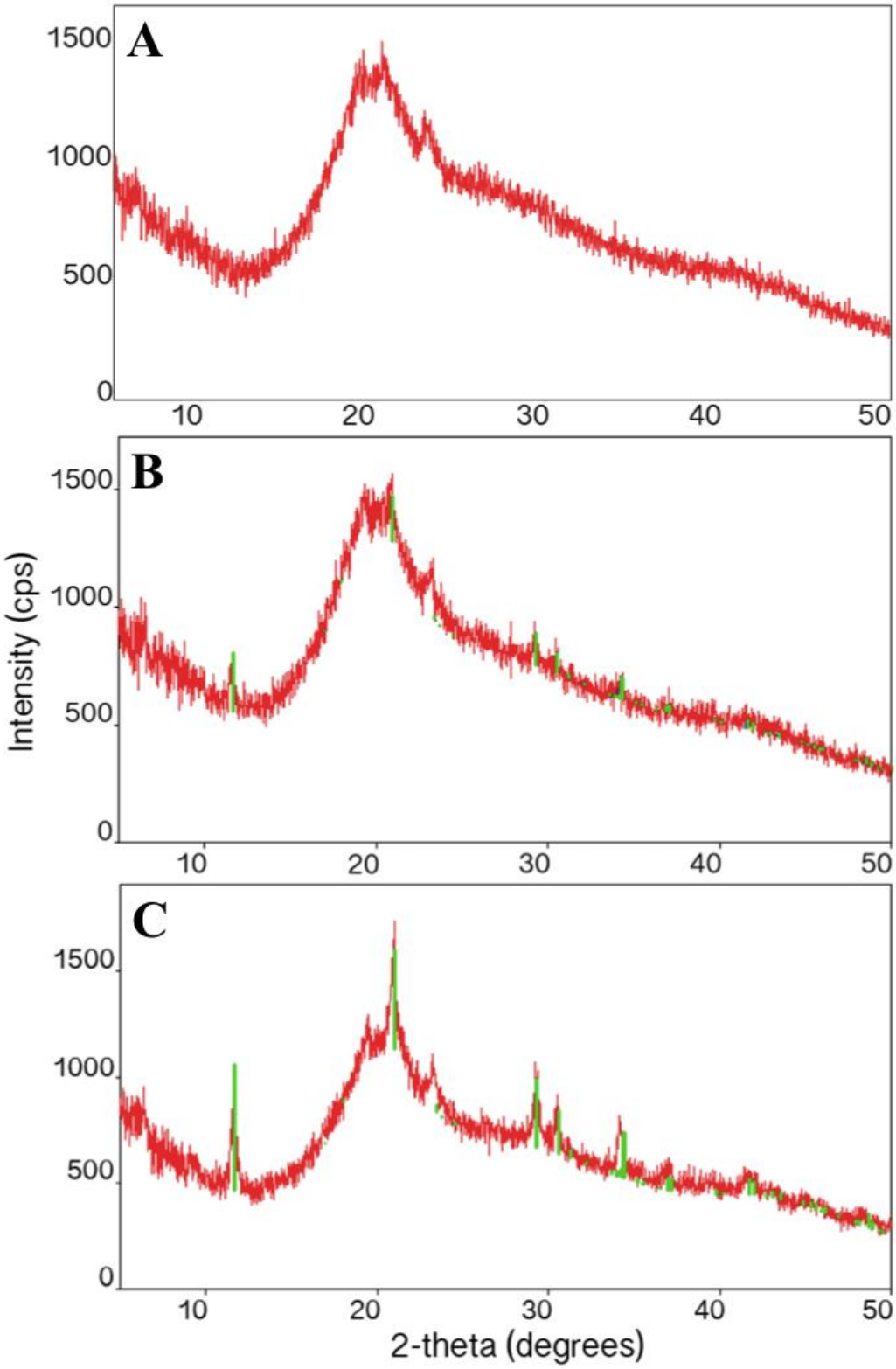

Tansman
Figure 8

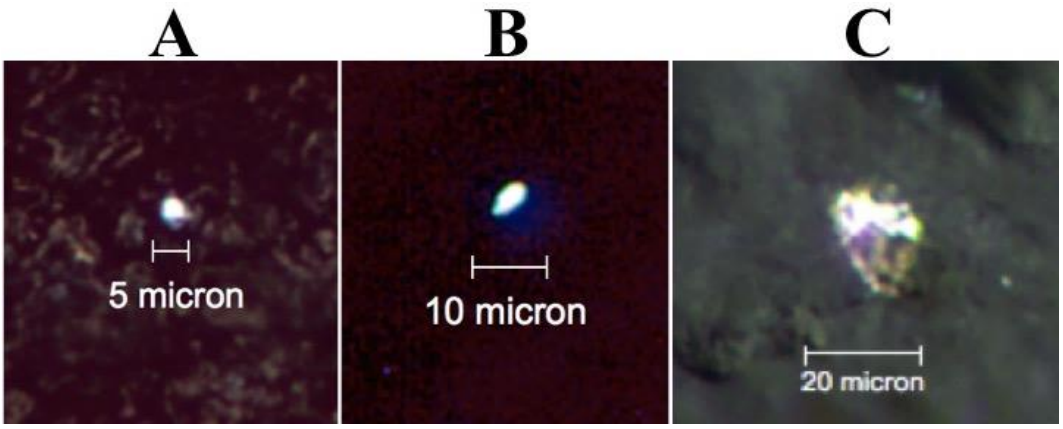

Tansman
Figure 9

CHAPTER 5: CRYSTALLIZATION AND DEMINERALIZATION PHENOMENA IN WASHED-RIND CHEESE

INTERPRETIVE SUMMARY

Most of the research that has been conducted on washed-rind (smear ripened) cheese has focused on identification of the bacteria, yeasts, and molds that compose the surface microflora and describing their metabolic processes. The present study explores a crystallization phenomenon that arises from the activity of the surface microflora. This report links this crystallization phenomenon to a mineral element diffusion phenomenon that has been previously reported in white mold cheese and represents an important homology between these two classes of cheese.

CRYSTALS IN WASHED-RIND CHEESE

Crystallization and demineralization phenomena in washed-rind cheese

Gil F. Tansman,* Paul S. Kindstedt,* and John M. Hughes†

*Department of Nutrition and Food Sciences and

†Department of Geology

University of Vermont,

Burlington, VT 05405, U.S.A.

Gil F. Tansman, Corresponding Author

234 Marsh Life Science, 109 Carrigan Dr.

e-mail: gtansman@uvm.edu

tel: 802-656-3374

fax: 802-656-0001

ABSTRACT

This report documents an observational study of a high moisture washed-rind cheese. Three batches of cheese were sampled on a weekly basis for six weeks and again at Week 10. Center, under-rind, rind, and smear samples were tested for pH, moisture, and selected mineral elements. Powder X-ray diffractometry and petrographic microscopy were applied to identify and image the crystal phases. The pH of the rind increased by over 2 pH units by Week 10. The pH of the under-rind increased but remained below the rind pH at all times, whereas the center pH decreased for most of aging and only began to rise after Week 5. Diffractograms of smear material revealed the presence of four crystal phases: brushite, calcite, ikaite and struvite. The phases nucleated in succession over the course of aging, with calcite and ikaite appearing around the same time. The data did not indicate whether the crystals were present exclusively in the smear or in the entire rind including the top 2 mm of cheese. A very small amount of brushite appeared sporadically in center and under-rind samples, but otherwise no other crystallization was observed beneath the rind. Micrographs revealed that crystals in the smear grew to 250 μm in length or more by Week 10 and at least two different crystal phases, probably ikaite and struvite, could be differentiated by their different optical properties. The surface crystallization was accompanied by a mineral diffusion

phenomenon that resulted, on average, in a 216.7%, 95.7%, and 149.0% increase in calcium, phosphorus, and magnesium, respectively, in the rind by Week 10. The diffusion phenomenon caused calcium, phosphorus, and magnesium to decrease, on average, by 55.0%, 21.5%, and 36.3%, respectively, in the center by Week 10. The present study represents the first observation of crystallization and demineralization phenomena in washed-rind cheese.

Key Words: crystal, ikaite, demineralization, washed-rind cheese

INTRODUCTION

Washed-rind cheese is a broad classification that includes cheeses of widely varying moisture content and aging time. The qualifying characteristic of these cheeses is the treatment of the rind with some kind of washing solution, which can be applied by hand or with an implement such as a brush. Cheeses treated in this manner tend to form a complex microbiota on the surface that may contribute to the appearance and flavor of the ripe cheese. The present observational study focuses on the development of a high moisture washed-rind cheese that is characterized by a thick bacterial smear.

There exists a striking homology between the ripening of washed-rind cheese and the ripening of white mold (bloomy rind) cheese in that both of these types of cheese possess a highly active surface biomass that is carefully cultivated by the cheesemaker. In white mold cheese, the surface flora's activity causes a local increase in pH at the surface which causes pH-sensitive calcium phosphate crystals to nucleate in the rind (Le Graet et al., 1983). The elevated pH reduces the solubility of calcium and phosphate in the rind

and causes calcium and phosphate ions to diffuse to the rind from the center along a concentration gradient. These ions are deposited in growing crystals, which results in calcium phosphate accumulation in the rind and concurrent diminishment in the center. Elevated rind pH during aging has been reported in washed-rind cheese (Gobbetti et al., 1997), but corresponding investigation of crystallization and demineralization in washed-rind cheese appears to be absent from the literature.

Rind alkalinization in washed-rind cheese is a function of the various microbial communities that colonize the cheese surface and metabolize cheese components. At the initial pH of washed-rind cheese (typically between 5.0 and 5.5) the bacterial species that characterize the mature smear of washed-rind cheese cannot grow (Gori et al., 2007) and instead, a succession of microbes colonizes the cheese surface as the collective microbial metabolism raises the pH (Mounier et al., 2006). The first species to appear are the yeasts, such as *Debaryomyces hansenii* (Riahi et al., 2007b), *Kluyveromyces lactis*, and *Saccharomyces cerevisiae* (Kagkli et al., 2006), that grow on account of their high acid and salt tolerance (Larpin et al., 2006). Yeast activities, including metabolism of lactic acid (Masoud and Jakobsen, 2005) and ammonia production (Gori et al., 2007), during early aging contribute to a significant increase in surface pH. The acid sensitivity of successive bacterial colonies varies, but in general the bacterial species begin to grow around pH 6 (Bockelmann and Hoppe-Seyler, 2001, Gori et al., 2007).

The main bacterial species that tend to appear on the cheese surface after the yeasts are Gram-positive bacteria including *Corynebacterium*, *Arthrobacter*, *Brevibacterium*, *Micrococcus*, and *Staphylococcus* (Feurer et al., 2004). The process of washing the surface of the cheese with a brine has the effect of spreading the bacterial

colonies over the rind and creating a uniform mass (Brennan et al., 2002). These bacteria form a sticky biofilm or microbial mat on the cheese surface (Leclercq-Perlat et al., 2004, Wolfe et al., 2014) that consists of the bacteria and excreted substances (Larpin et al., 2006), although an analysis of the extracellular components of the smear appears to be absent from the literature. The bacterial smear communities continue to metabolize the cheese substrate, with further release of ammonia (Leclercq-Perlat et al., 2000b) and consumption of lactate (Leclercq-Perlat et al., 2000a).

The isolation and identification of crystals from the smears of two washed-rind cheeses was reported by the authors of the present manuscript (Tansman et al., 2016). The crystals, which had never been observed in cheese, ranged in size up to 500 μm in length. One of the isolated crystals was identified as ikaite ($CaCO_3 \cdot 6H_2O$), which is a rare metastable crystal that is mostly associated with freezing marine and lacustrine environments. The other crystal was struvite ($NH_4MgPO_4 \cdot 6H_2O$), which is often associated with bacterial activity.

The primary goal of the present study was to observe the nucleation and growth of crystals in a washed-rind cheese during aging and to measure the changes in mineral element concentrations at different depths of the cheese. Novel crystallographic techniques were employed to observe the maximum size of crystals and to identify the crystal phases.

MATERIALS AND METHODS

CHEESE MANUFACTURE

Cheeses were obtained from The Cellars at Jasper Hill (Greensboro, VT; herein referred to as *The Cellars*). The cheese variety observed in the present study corresponded to *cheese A* in the work of Tansman et al. (2016). The general recipe for this variety is as follows: cheeses are manufactured from non-standardized raw cow's milk produced at Jasper Hill Farm during the winter months using a washed-rind procedure approximately similar to that described by Sozzi and Shepherd (1972). The milk is inoculated with cultures that are proprietary and therefore the specific cultures are not included in this description. The curds are dipped at pH 6.55 and drained in molds measuring 14 cm in diameter. The curds drain at room temperature until the pH reaches approximately 6.0, at which point they are transferred to a refrigerated chamber at approximately 2°C and drained overnight. The wheels are demolded at a pH of approximately 5.45 and dry salted to a target salt-in-moisture of approximately 2.6%. The outer diameter is wrapped with a strip of spruce bark fastened with a rubber band. Target cheese moisture content at demolding is approximately 55%, although considerable drainage continues during the first few days. The cheese is aged in a 13-14°C (94-95% humidity) room for the first week, after which it is transferred to a 10-11°C (96% humidity) aging vault. It is scrubbed with a medium-length-bristle brush dipped in brine three times in the first week and then twice per week until the fourth week. From demolding, the cheese is aged on wire racks for a total of six weeks and then wrapped in semi-permeable paper and stored at 4.5°C until shipment. At the time of wrapping, each wheel weighs approximately 570 grams. The cheese described by Sozzi and Shepherd

(1972) is considered ripe at 20 days, but due to the regulatory environment, the cheese in the present study is aged at a lower temperature and for a longer time before packaging and distribution.

Cheese Sampling

Cheeses were sampled at Weeks 1, 2, 3, 4, 5, 6, and 10, on the same day of the week. The Week 1 samples were delivered two days after demolding, which dictated the day of the week that the subsequent samples were collected. The cheeses were wrapped in cheese paper and delivered by overnight post to the Department of Nutrition and Food Sciences at the University of Vermont in insulated coolers with ice packs. Two wheels were collected from *The Cellars* at Weeks 1, 2, 3, 4, and 5. Four wheels were collected at Week 6, which was the last week of cave-aging and the first week of packaging and cold storage. Two of the wheels collected at Week 6 were used for analysis upon arrival and the two additional wheels were stored in an incubator at 4.5°C until Week 10, thereby simulating the storage conditions used in the manufacturing facility. The entire experiment was replicated three times using three different batches of cheese produced one week apart on the same day of the week.

Cheese Sectioning for Data Collection

An illustration of the sampling scheme is found in Figure 1 and is described as follows: The cheeses were precisely segmented with a wire cutter to remove an approximately 8.5 cm by 3 cm (L x W) section along the diameter of the cheese, which included a portion of the outer diameter (including a piece of the spruce bark) and the

approximate center of the cheese. Serial sections measuring roughly 1.5 cm were cut from the part of the excised portion that represented the approximate center of the wheel. Rind, under-rind, center, and smear samples were collected from the serial sections as follows: a 2 mm-thick sample that included the smear and underlying cheese for the *rind*; a 2 mm-thick sample underneath the rind sample for the *under-rind*; a 2 mm-thick sample from the center of the cheese for the *center*; a scraping of the surface biomass from the opposite face of the cheese from which the rind sample was taken for the *smear*. Smear samples were collected by gently scraping the cheese surface using a metal spatula. A harvestable smear biomass did not manifest until Week 3 in any of the batches; therefore, smear measurements were not available for any of the variables during the first two weeks.

Cheese samples were partitioned as described above for all analyses including powder X-ray diffractometry (**PXRD)**, pH, microscopy, elemental analysis, and moisture content analysis. Samples for PXRD, pH, and microscopy were partitioned from the cheeses on the same day that the cheeses arrived from *The Cellars,* or on the day that they were removed from incubator (at Week 10). The remnants of each cheese were carefully vacuum packaged and frozen at -20°C. Elemental analysis and moisture analysis were conducted on the previously-frozen samples at a later date using the same cheese sampling plan described above.

pH Measurements

The pH measurements were conducted using a flat pH electrode (Thermo Fisher Scientific, Waltham, MA). The rind measurements were collected from the exposed rind

surface, which became covered by the smear material by Week 3; the under-rind measurements were collected 2 mm below the surface, representing the upper portion of the under-rind; and the center measurements were collected approximately 13 mm below the under-rind measurement, which was the approximate center of the cheese. Readings were allowed to stabilize for one minute before recording. It should be noted that the pH sampling scheme involved only three measurement locations, in contrast to the other measurements, in which four different sampling locations were used.

Petrographic Microscopy

Small quantities of collected material from the various sampling locations were applied to glass microscope slides and gently pressed to translucent thinness using a glass coverslip. Micrographs were captured using a Nikon E200POL petrographic microscope with a rotating stage (Nikon Corporation, Tokyo, Japan) and a SPOT Idea 1.3 Mp color camera (SPOT Imaging Solutions, Sterling Heights, MI). When the polarizers were crossed, particles that were illuminated and displayed uniform extinction were identified as crystals.

PXRD

Aliquots of cheese from each sampling location were homogenized with a mortar and pestle and loaded onto glass diffraction slides. Data were collected on a MiniFlex II powder X-ray diffractometer (Rigaku, The Woodlands, TX). In order to minimize diffraction artifacts that tend to occur when smear samples dry during data collection, a small quantity of mineral oil was added to the surface smear samples to limit the sample

drying. Mineral oil was not applied to rind, under-rind, and center samples as these did not tend to dehydrate as quickly as the smear material. Diffractograms were generated at a speed of 2°2θ/minute between 5 and 50°2θ. Diffractograms were compared to existing diffraction reference cards archived in the ICDD database.

ELEMENTAL ANALYSIS

For elemental analysis, samples were digested following EPA Method SW846-3015, "Microwave Assisted Acid Dissolution of Waters and Wastewaters." Approximately 0.25 grams of homogenized sample from each sampling location were placed in a teflon reaction chamber and weighed to 0.001g, and 10mL concentrated nitric acid was added. The chambers were sealed and placed in the microwave system (CEM MARS-5, Matthews, NC, USA), which ramped the samples to 190°C over 15 minutes, and then held them at 190°C for 15 minutes. After cooling, the digested samples were transferred quantitatively to 50-mL volumetric flasks and brought to volume with 0.1N nitric acid.

The digests were analyzed for calcium, magnesium, and phosphorus by ICP-OES (Optima 3000DV, Perkin Elmer Corp, Norwalk, CT, USA) on a dual view instrument operating in Axial view with an RF power of 1,300 watts. Calibration standards were prepared according to instrument manufacturer's suggested guidelines, to cover the range of concentrations in the sample set. Two-point calibrations (plus a Calibration Blank) were used for ICP analysis. Continuing calibration verification samples, prepared from an independent source, were used to check the calibration

periodically. Concentrations of minerals were calculated on a cheese dry weight basis using the corresponding moisture data collected for each sample.

Moisture Analysis

The collected material from each sampling location was homogenized with a mortar and pestle. Approximately 1 gram of homogenized material from each sampling location was weighted into a pre-weighed aluminum drying dish and then placed in a draft oven at 100°C for 24 hours, which was found to dry the samples to a constant weight. These values were used to calculate moisture content and to convert corresponding elemental data to a dry weight basis.

Statistical Analysis

The experiment was conducted as a three-factor randomized block design with batches representing blocks and seven sampling points per batch. Two one-way analyses of variance were conducted using data for pH, selected mineral elements on a dry weight basis, and moisture content using the statistical package JMP Pro 12.0.0 (SAS Institute Inc., Cary, NC). The first ANOVA was conducted using data that started at Week 3 (5 time points) due to the absence of smear data for the first two weeks. The absence of smear data from the first two weeks made it impossible to calculate interactive effects for the first two weeks, and therefore introduced singularity errors into the statistical analysis. A second ANOVA was conducted, which omitted the smear treatment but included all time points. These two analyses were compared to determine if there were any differences between them in the significance of main or interaction affects in the

model. It should be noted that regardless of the ANOVA used, the pH variable had only 2 degrees of freedom because only three sampling locations (surface, under-rind, and center) were used in pH measurements.

RESULTS

MOISTURE, PH AND ELEMENTAL ANALYSES

Summary statistics for pH, selected mineral elements on a dry weight basis, and moisture content, are presented in Table 1; these summary statistics correspond to the initial ANOVA and omit data from the first two weeks of sampling due to unavoidable systematic absences in the smear data. The summary statistics in Table 1 indicate that all main and interactive effects for the mineral elements and pH were significant. Sampling Location and the interaction between Sampling Location and Week of Aging were significant for moisture content, but Week of Aging was not significant. It should be noted that in the ANOVA that contained all seven time points but omitted the smear treatment (data not shown), all main and interactive effects, including Week of Aging, were significant for all variables, which may reflect the significantly lower moisture readings for center samples in the first two weeks (Figure 2).

Graphical representation of pH over the aging timeframe (Figure 3) reveals that the average pH for all sampling locations was between 5.3 and 5.5 at Week 1 and dipped by 0.1 to 0.2 pH units by Week 2. Although the pH at the center continued to decline until Week 4 or Week 5, the rind pH and under-rind pH began to climb after Week 2, with the pH of the smear climbing much more precipitously. The pH of the rind increased nearly 1.5 pH units between Week 2 and Week 3, whereas the pH of the under-rind did

not increase to that extent until after Week 6. The pH of the rind continued to rise through Week 6, with little apparent change thereafter. After Week 6, the pH of the center, which had decreased by nearly 0.4 pH units during early aging, also climbed appreciably, although it remained lower than the under-rind throughout the experiment.

The increase in smear pH was accompanied by a large increase in the concentrations of calcium (Figure 4), phosphorus (Figure 5), and magnesium (Figure 6) in the rind. After exhibiting limited change during the first two weeks, the increases in the rind appeared almost linear between Week 2 and Week 6. The magnesium rind concentration continued to rise linearly through Week 10, while the calcium rind concentration increased at a slower rate, and the phosphorus rind concentration did not increase after week 6. Over the 10 weeks of aging, concentrations of the three elements in the under-rind and the center decreased almost linearly. The concentrations of calcium, phosphorus, and magnesium in the under-rind and the center were similar throughout aging. Concentrations of the three elements in the smear, which was sampled starting on Week 3, were consistently several times greater than corresponding element concentrations in the other sampling locations at any given time point.

Moisture content changed very little during aging (Figure 2). A slight increase was observed at center and under-rind locations between Week 1 and Week 6, while the moisture content of the rind decreased during the same time. Between Week 6 and Week 10, the moisture content of the rind recovered to Week 1 levels, while the moisture content of the center slightly decreased. The moisture content of the smear, which was consistently 10 to 15% higher than the other sampling locations, peaked at Week 6, and then returned to the Week 3 level by Week 10.

PXRD

Diffractograms collected from rind samples at Week 1 displayed a background pattern that was very similar to the diffraction pattern collected from day-old stabilized white mold cheese (Tansman et al., Under Review), and which was interpreted as the baseline pattern of the cheese matrix (data not shown). By Week 2, the rind showed evidence of small amounts of brushite ($CaHPO_4 \bullet 2H_2O$) crystallization, which increased in intensity at Week 3, indicating a relative increase in the mass fraction of brushite in those samples (data not shown). Week 3 and Week 4 rind samples, which both contained a small amount of smear material, were very similar, indicating that the increase in rind brushite between Week 3 and Week 4 was probably limited (data not shown). At several points during aging, diffractograms of sporadic under-rind and center samples also displayed evidence of brushite crystallization (data not shown), although the intensity of brushite peaks were never greater than those in the Week 2 rind samples, which indicated that the quantity of brushite in those samples was noteworthy but probably limited. The diffractograms of all other center and under-rind samples resembled the baseline pattern and were devoid of diffraction peaks (data not shown).

Diffractograms collected from smear samples displayed a different characteristic baseline pattern, although this baseline remained consistent for smear samples throughout the study (Figure 7). As a composite of the smear and the underlying cheese, rind diffractograms generally reflected the corresponding smear diffractograms, although tended to have more baseline noise and more preferred orientation, wherein diffraction peaks were distorted or missing altogether, which often made the diffractograms difficult

to interpret. Based on this study design, it is impossible to claim that crystals that were identified in smear samples, as detailed below, were not also present in the top 2 mm of underlying cheese, which along with the smear formed the rind samples. Nonetheless, the smear diffractograms, which were generally superior in quality to rind diffractograms, provided a superior record of crystal activity on the surface after Week 3. Detailed data from the smear samples are presented in Table 2 and Figure 7.

Table 2 tabulates the crystal phases that were identified in the smear of each cheese during aging. There was some variability among batches and between the replicate cheeses from the same vat. Some smear diffractograms exhibited preferred orientation, although this artifact was much less pronounced in Week 6 and Week 10 diffractograms. The absence or diminished intensity of some or all major diffraction peaks made conclusive identification of crystal phases in earlier samples difficult, which contributed to the variability in Table 2.

Brushite was conclusively identified in most smear diffractograms starting at Week 3 (Figure 7A,), which was the first time-point at which collectable smear material appeared on the cheese surface. At Week 4, the intensity of brushite peaks in smear diffractograms was greater (Figure 7B,), but by Week 5 brushite had disappeared from all smear diffractograms (Figure 7C). In contrast, brushite persisted in rind diffractograms for the duration of the experiment, indicating that after Week 5 brushite was present in the underlying cheese but not in the smear (data not shown).

Calcite ($CaCO_3$, ICDD card # 00-005-0586) was observed sporadically in Week 3 and Week 4 smear diffractograms (Table 2), and was observed in all smear diffractograms starting at Week 5. Calcite was somewhat difficult to conclusively

identify because the only large peak, which is at 29°2θ, coincides with a brushite peak at nearly the same angle. Therefore, conclusive identification of calcite was only possible if brushite was absent, if the calcite peak was much larger than the brushite peaks, or if the other, much smaller calcite peaks were visible, as in Figure 7C. Conclusive identification of calcite was possible in all smear diffractograms starting at Week 5 because none of the diffractograms at Week 5, 6 or 10 (Figure 7C, D and F, respectively) contained any brushite peaks.

Ikaite was identified or tentatively identified in most smear diffractograms by Week 5 (Table 2). Preferred orientation diffraction artifacts appeared to affect ikaite much more than other phases and appeared to be much more common in younger smear samples. These artifacts made conclusive identification of ikaite in Week 5 and in some Week 6 samples difficult, although conclusive identification of ikaite in all Week 10 diffractograms was straightforward. Figure 7C, which shows a smear diffractogram from Week 5, contains a single peak around 40°2θ that does not belong to the calcite pattern. This peak corresponded to a minor ikaite peak and was therefore tentatively attributed to a very small amount of ikaite in the sample with severe preferred orientation, and is an extreme example of the difficulty involved with identifying some crystal phases in younger samples. Ikaite in most Week 6 and all Week 10 diffractograms displayed some preferred orientation, although conclusive identification was much easier, as evident in Figure 7E (Week 6) and 7G (Week 10), in which all major peaks are present in the diffractogram, even though the intensities of some peaks are distorted compared to the green reference bars for ikaite.

Struvite was observed in an all smear diffractograms at Week 10 (Table 2). Although clearly present, the struvite peaks were small compared to the ikaite peaks (Figure 7H), possibly indicating that less struvite was present, although semi-quantitative comparison between different crystal phases is more complicated because crystal chemistry also affects the intensity of diffraction peaks.

PETROGRAPHIC MICROSCOPY

Figure 8 displays a series of petrographic micrographs that correspond to the diffractogram series in Figure 7, starting at Week 4. Small pinpoint crystals measuring up to 10 μm in diameter could be seen in all Week 4 smear samples (Figure 8A). These crystals corresponded to diffractograms containing brushite peaks. Crystals measuring up to approximately 200 μm appeared at Week 5 (Figure 8B) and tended to be larger and more abundant at Week 6 (Figure 8C). Week 5 and Week 6 diffractograms showed evidence of both calcite and ikaite crystals, which made it difficult to identify the larger crystals that formed at that time; however, the crystals displayed optical properties that were similar to crystals identified as ikaite in a previous study (Tansman et al., In Press).

By Week 10, in addition to the large and abundant crystals that were tentatively identified as ikaite, a second type of crystal, differentiable by its colorful hue, was observed in all smear samples (Figure 8D). In a previous study, crystals with high birefringence resembling these colorful crystals were identified as struvite (Tansman et al., 2016), and their manifestation in the present study coincided with the appearance of struvite in smear diffractograms. In order to conclusively determine if any of the large crystals at Week 10 were calcite, several Week 10 smears were allowed to dehydrate on

the glass microscope slide and were reexamined. All of the large crystals on the slide dehydrated and lost their optical properties, which is a behavior characteristic of ikaite and struvite, but not attributable to calcite. Thus, it appeared that calcite, although present in smears at Week 10 according to the diffractograms, did not grow as large as ikaite and struvite, and probably remained quite small.

DISCUSSION

MOISTURE DEVELOPMENT DURING AGING

Moisture loss is a complex process that is impacted by factors such as the humidity in the aging chamber, air flow, and the curd characteristics. The pattern of moisture development (Figure 2) was somewhat reminiscent of the moisture pattern observed by the authors of this manuscript in a recent study dealing with stabilized white mold cheese (Tansman et al., Under Review). Although the increased moisture content was a novel finding in the context of stabilized white mold cheese, there appears to be a greater precedent in washed-rind cheese. Other studies on washed-rind cheeses, aged under similar humidity and temperature, showed that the moisture content did not decrease during aging (O'Farrell et al., 2002, Riahi et al., 2007a). Notably, a study dealing with Vacherin (Sozzi and Shepherd, 1972), which is very similar to the cheese in the present study, appeared to show that the moisture content at the center of cheese from two different factories increased compared to the moisture content at the beginning of aging, while the rind moisture content decreased. The moisture data presented by Sozzi and Shepherd (1972) were in nearly perfect agreement with the moisture data in the

present study. Further investigation is needed to verify that this observation was not an artifact of the sampling scheme.

Accumulation of Mineral Elements in the Rind and Smear

By Week 10, the average calcium, phosphorus, and magnesium content of the rind increased by 216.7%, 95.7%, and 149.0%, respectively. The increase in mineral element content in the rind began after Week 2 (Figures 4, 5, and 6), and coincided with a large increase in surface pH (Figure 3). Evidence of brushite crystallization was apparent in diffractograms of Week 3 rind samples and thus appeared to be the most likely destination for calcium and phosphorus accumulating in the rind. The initial accumulation of mineral elements in the rind at Week 3 also coincided with the first harvestable surface biomass. The smear biomass that manifested at Week 3 was fairly limited but already contained three to four times the concentration of mineral elements (on a dry weight basis) as the composite rind (Figures 4, 5, and 6), suggesting that brushite crystallization was concentrated in the smear, although this cannot be conclusively determined from the data.

The graphical plots of calcium, phosphorus, and magnesium (Figures 4, 5, and 6) in the smear followed complex functions that sharply contrasted with the nearly linear increase in mineral elements in the rind as a whole, which may reflect the fact that as crystals were nucleating in the smear, additional smear material was also accumulating. The sampling method in the present study could not be used to quantify the accumulation of smear biomass, but it became progressively easier to collect large quantities of smear

as aging progressed, which suggested that the amount of biomass increased as aging progressed.

On a molar basis (data not shown), calcium and phosphorus in the smear increased at a similar rate between Week 3 and Week 4, which may reflect the growth of brushite in the smear (Figure 7A and B). From Week 4 to Week 5 phosphorus accumulation lagged behind calcium, which may reflect the disappearance of brushite and the growth of calcite and ikaite, both of which contain calcium but not phosphorus (Figure 7C, D and E). Although brushite tends to become increasingly insoluble as the pH is increased, its insolubility tapers around neutrality (Johnsson and Nancollas, 1992). In contrast, the solubility of carbonates, including calcite, continues to decrease by several degrees of magnitude as the pH shifts from slightly acid to slightly alkaline (Giannimaras and Koutsoukos, 1987). Although the brushite in the smear appeared to completely dissolve by Week 5, the concentration of phosphorus in the smear remained high compared to the rest of the cheese (Figure 5), even before struvite precipitation was evident. At Week 6, the concentration of phosphorus was still nearly double the concentration of phosphorus it the composite rind, suggesting that the diffusion of phosphorus into and out of the smear is a complex process.

The concentration of magnesium in the rind and smear was higher than in the center and under-rind by Week 3 (Figure 6) even though the magnesian phase struvite was not observed by PXRD before Week 10 (Table 2). Magnesium and calcium are both alkaline earth metals, and both brushite (Lee and Kumta, 2010) and calcite (Kunitake et al., 2012) can accommodate magnesium in calcium bonding sites. A small amount of atomic substitution in brushite and calcite could thus potentially explain the increased

level of magnesium in the rind and smear before the appearance of struvite. However, diffractograms of minimally substituted phases cannot be easily differentiated from pure phases using PXRD, and the crystallographic data in the present study cannot confirm this assumption. The greatest accumulation of magnesium, however, was almost certainly due to the formation of struvite by Week 10 (Figure 7H), which was accompanied by a large increase in the concentration of magnesium in the smear between Week 6 and Week 10 (Figure 6).

Extent of Demineralization

The initial mineral element content of the cheese in the present study (Figures 4, 5, and 6) was higher than the mineral element content of traditional white mold and stabilized white mold cheeses used in other studies (Le Graet et al., 1983, Tansman et al., Under Review), and this likely reflects the higher pH profile during the manufacture of the cheese in the present study. A comparison of mean mineral element contents at Week 1 and Week 10 revealed that over the experiment's duration mean calcium content decreased by 55.0%, mean phosphorus content decreased by 21.5%, and mean magnesium content decreased by 36.3%. The proportion of crystal phases in the smear could not be quantified in this study, but the greater decrease in calcium content could reflect the fact that ikaite and calcite nucleated several weeks before struvite and therefore could have resulted in more extensive diffusion of calcium from the center to the rind.

An under-rind sampling location was examined to determine if there was a difference in mineral element content between the center of the cheese and the under-

rind. Figures 4, 5, and 6 reveal that although there was a slightly lower concentration of each mineral element in the under-rind during Weeks 3 through 6 for calcium and phosphorus and at Week 6 for magnesium, the concentration of mineral elements in the center and under-rind converged by the end of the study.

Significance of Calcite, Ikaite, and Struvite

Carbon dioxide and ammonia concentrations were not measured in the present study but the manifestation of calcite, ikaite, and struvite indicates that sufficient carbon dioxide and ammonia accumulated in the cheese induce the precipitation of these minerals. These gases result from the metabolism of cheese components by cheese microorganisms (Riahi et al., 2007a). The observations in the present study suggest that surface crystallization is a result of rind alkalinization, which affects mineral solubility, as well carbonate and ammonia accumulation, which provides the ions necessary for calcite, ikaite, and struvite formation.

The observation that ikaite crystallized in the presence of calcite is interesting because both phases contain calcium and carbonate groups and would thus compete for the same ions. The coexistence of both of these phase in the smear by the end of aging is also interesting because previous research has shown that ikaite is metastable and tends to transform into calcite (Marland, 1975). The ability of both ikaite and calcite to persist is noteworthy and warrants additional investigation.

CONCLUSION

The processes of rind alkalinization, surface crystallization, and cheese demineralization that had been previously observed in white mold cheese were documented for the first time in washed-rind cheese. A progression of nucleation events that resulted in brushite crystallization and subsequent dissolution, as well as calcite, ikaite, and struvite precipitation was observed in the smear, and represents the first observation of these four crystal phases in the same cheese. These observations open new opportunities for exploring crystallization phenomena in cheese. Additional research is necessary to understand the impact that these crystals have on rind grittiness in washed-rind cheese.

ACKNOWLEDGEMENTS

This study was funded by United States Department of Agriculture Hatch Project VT- H02102. The National Science Foundation is gratefully acknowledged through support of grant EAR-0922961 for the purchase of the Powder X-ray diffractometer and through support of grant NSF-MRI 1039436 for the purchase of the Single Crystal X-ray diffractometer. *The Cellars at Jasper Hill* is also gratefully acknowledged for providing the cheeses used in this study.

REFERENCES

Bockelmann, W. and T. Hoppe-Seyler. 2001. The surface flora of bacterial smear-ripened cheeses from cow's and goat's milk. International Dairy Journal 11:307-314.

Brennan, N. M., A. C. Ward, T. P. Beresford, P. F. Fox, M. Goodfellow, and T. M. Cogan. 2002. Biodiversity of the bacterial flora on the surface of a smear cheese. Applied and Environmental Microbiology 68(2):820-830.
Feurer, C., T. Vallaeys, G. Corrieu, and F. Irlinger. 2004. Does smearing inoculum reflect the bacterial composition of the smear at the end of the ripening of a French soft, red-smear cheese? Journal of Dairy Science 87:3189-3197.
Giannimaras, E. K. and P. G. Koutsoukos. 1987. The crystallization of calcite in the presence of orthophosphate. Journal of Colloid and Interface Science 116(2):423-430.
Gobbetti, M., S. Lowney, E. Smacchi, B. Battistotti, P. Damiani, and P. F. Fox. 1997. Microbiology and biochemistry of Taleggio cheese during ripening. International Dairy Journal 7:509-517.
Gori, K., H. D. Mortensen, N. Arneborg, and L. Jespersen. 2007. Ammonia Production and its possible role as a mediator of communication for *Debaryomyces hansenii* and other cheese-relevant yeast species. Journal of Dairy Science 90:5032-5041.
Johnsson, M. S. A. and G. H. Nancollas. 1992. The role of brushite and octacalcium phosphate in apatite formation. Critical Reviews in Oral Biology and Medicine 3:61-82.
Kagkli, D., R. Tache, T. M. Cogan, C. Hill, S. Casaregola, and P. Bonnarme. 2006. *Kluyveromyces lactis* and *Saccharomyces cerevisiae*, two potent deacidifying and volatile-sulphur-aroma-producing microorganisms of the cheese ecosystem. Appl Microbiol Biotechnol 73:434-442.
Kunitake, M. E., S. P. Baker, and L. A. Estroff. 2012. The effect of magnesium sustitution on the hardness of synthetic and biogenic calcite. MRS Communications 2:113-116.
Larpin, S., C. Mondoloni, S. Goerges, J. Vernoux, M. Gueguen, and N. Desmasures. 2006. *Geotrichum candidum* dominates in yeast population dynamics in Livarot, a French red-smear cheese. FEMS Yeast Res 6:1243-1253.
Le Graet, Y., A. Lepienne, G. Brule, and P. Ducruet. 1983. Migration du calcium et des phosphates inorganiques dans les fromages à pâte molle de type Camembert au cours de l'affinage. Le Lait 63:317-332.
Leclercq-Perlat, M. N., G. Corrieu, and H. E. Spinnler. 2004. The color of *Brevibacterium linens* depends on the yeast used for cheese deacidification. Journal of Dairy Science 87(1536-1544).
Leclercq-Perlat, M. N., A. Oumer, J. L. Bergere, H. E. Spinnler, and G. Corrieu. 2000a. Behavior of *Brevibacterium linens* and *Debaryomyces hansenii* as ripening flora in controlled production of smear soft cheese from reconstituted milk: growth and substrate consumption. Journal of Dairy Science 83:1665-1673.
Leclercq-Perlat, M. N., A. Oumer, F. Buono, J. L. Bergere, H. E. Spinnler, and G. Corrieu. 2000b. Behavior of *Brevibacterium linens* and *Debaryomyces hansenii* as ripening flora in ccontrolled production of soft smear cheese from reconstituted milk: protein degradation. Journal of Dairy Science 83:1674-1683.
Lee, D. and P. N. Kumta. 2010. Chemical synthesis and stabilization of magnesium substituted brushite. Materials Science and Engineering C 30:934-943.
Marland, G. 1975. The stability of $CaCO_3$ $6H_2O$ (ikaite). Geochemica et Cosmochimica Acta 39:83-91.

Masoud, W. and M. Jakobsen. 2005. The combined effects of pH, NaCl, and temperature on growth of cheese ripening cultures of Debaryomyces hansenii and coryneform bacteria. International Dairy Journal 15:69-77.
Mounier, J., S. Goerges, R. Gelsomino, M. Vaacanneyt, K. Vandemeulebroecke, B. Hoste, N. M. Brennan, S. Scherer, J. Swings, G. F. Fitzgerald, and T. M. Cogan. 2006. Sources of the adventitious microflora of a smear-ripened cheese. Journal of Applied Microbiology 101:668-681.
O'Farrell, I. P., J. J. Sheehan, M. G. Wilkinson, D. Harrington, and A. L. Kelly. 2002. Influence of addition of plasmin or mastitic milk to cheesemilk on quality of smear-ripened cheese. Lait 82(82):305-316.
Riahi, H., I. C. Trelea, M. N. Leclercq-Perlat, D. Picque, and G. Corrieu. 2007a. Model for changes in weight and dry matter during the ripening of a smear soft cheese under controlled temperature and relative humidity. International Dairy Journal 17:946-953.
Riahi, M. H., I. C. Trelea, D. Picque, M. N. Leclercq-Perlat, A. Helias, and G. Corrieu. 2007b. A model describing Debaryomyces hansenii growth and substrate consumption during a smear soft cheese deacidification and ripening. Journal of Dairy Science 90:2525-2537.
Sozzi, T. and D. Shepherd. 1972. Evolution de la composition chimique et de la flore microbienne du fromage de Vacherin au cours de la maturation. Le Lait 52(513-514):203-219.
Tansman, G., P. S. Kindstedt, and J. M. Hughes. In Press. Minerals in food: crystal structures of ikaite and struvite from bacterial smears on washed-rind cheese. The Canadian Mineralogist.
Tansman, G., P. S. Kindstedt, and J. M. Hughes. Under Review. Crystallization and demineralization phenomena in stabilized paste white mold cheese. Journal of Dairy Science.
Wolfe, B. E., J. E. Button, M. Santarelli, and R. J. Dutton. 2014. Cheese rind communities provide tractable systems for in situ and in vitro studies of microbial diversity. Cell 158:422-433.

Table 1. Mean squares, probabilities (in parentheses), and degrees of freedom for pH, selected mineral elements on a dry weight basis, and moisture content starting on Week 3 (5 time points). Statistical significance (with $P < 0.05$) is denoted by an asterisk

Factors	df†	pH	Ca	P	Mg	Moisture Content
Batch (blocked)	2	0.140 (0.019*)	72.075 (0.166)	20.162 (0.044*)	0.305 (0.033*)	0.006 (<0.001*)
Week of Aging (Week)	4	4.714 (<0.001*)	394.890 (<0.001*)	46.369 (<0.001*)	3.673 (<0.001*)	0.0003 (0.243)
Sampling Location (SL)	3	32.244 (<0.001*)	55981.087 (<0.001*)	7154.049 (<0.001*)	72.062 (<0.001*)	0.101 (<0.001*)
Week x SL	12	0.855 (<0.001*)	315.298 (<0.001*)	86.462 (<0.001*)	3.158 (<0.001*)	0.0004 (0.027*)
Error	98	0.336	39.350	6.250	0.086	0.0002

*P < 0.05

†df for pH are 2 (blocked), 4 (Week), 2 (SL), 8 (Week x SL), and 73 (error)

Table 2. Crystal phases identified by PXRD in smear samples over 10 weeks of aging. Smear data were collected starting at Week 3. Italicized crystal names indicate tentative identification

Batch	Rep	3	4	5	6	10
1	1	Brushite	Brushite Calcite	Calcite *Ikaite*	Calcite Ikaite	Calcite Ikaite Struvite
1	2	Brushite	Calcite	Calcite *Ikaite*	Calcite Ikaite	Calcite Ikaite Struvite
2	1	Brushite	Brushite	Calcite *Ikaite*	Calcite *Ikaite*	Calcite Ikaite Struvite
2	2	Brushite	Brushite	Calcite	Calcite Ikaite	Calcite Ikaite Struvite
3	1	*Brushite* Calcite	Brushite	Calcite Ikaite	Calcite *Ikaite*	Calcite Ikaite Struvite
3	2	Brushite Calcite	Brushite	Calcite *Ikaite*	Calcite *Ikaite*	Calcite Ikaite Struvite

Figure Captions

Figure 1. Illustration of the sampling scheme used for sectioning cheese into smear, rind, under-rind, and center samples

Figure 2. Average present moisture of rind, under-rind, center, and smear sampling locations during aging. Error bars represent standard error from all three batches and duplicate cheeses at each time point

Figure 3. Average pH of rind, under-rind, and center sampling locations during aging. Error bars represent standard error from all three batches and duplicate cheeses at each time point

Figure 4. Average calcium concentrations of rind, under-rind, center, and smear sampling locations during aging on a dry weight basis (grams of calcium per kilogram of dry cheese or smear). Error bars represent standard error from all three batches and duplicate cheeses at each time point

Figure 5. Average phosphorus concentrations of rind, under-rind, center, and smear sampling locations during aging on a dry weight basis (grams of phosphorus per kilogram of dry cheese or smear). Error bars represent standard error from all three batches and duplicate cheeses at each time point

Figure 6. Average magnesium concentrations of rind, under-rind, center, and smear sampling locations during aging on a dry weight basis (grams of magnesium per kilogram of dry cheese or smear). Error bars represent standard error from all three batches and duplicate cheeses at each time point

Figure 7. Powder X-ray diffractogram series of batch 2 smears with reference bars for identified crystal phases including brushite (ICDD card # 01-072-1240), calcite (ICDD card # 00-005-0586), ikaite (ICDD card # 01-072-0670), and struvite (ICDD card # 00-015-0762) in the following order: Week 3 with brushite bars (A); Week 4 with brushite bars (B); Week 5 with calcite bars (C); Week 6 with calcite bars (D); Week 6 with ikaite bars (E); Week 10 with calcite bars (F); Week 10 with ikaite bars (G); Week 10 with struvite bars (H)

Figure 8. Petrographic micrograph series of batch 2 smear samples at Week 4 (A), Week 5 (B), Week 6 (C), and Week 10 (D) corresponding to diffractograms in of Weeks 4 through 10 in Figure 7

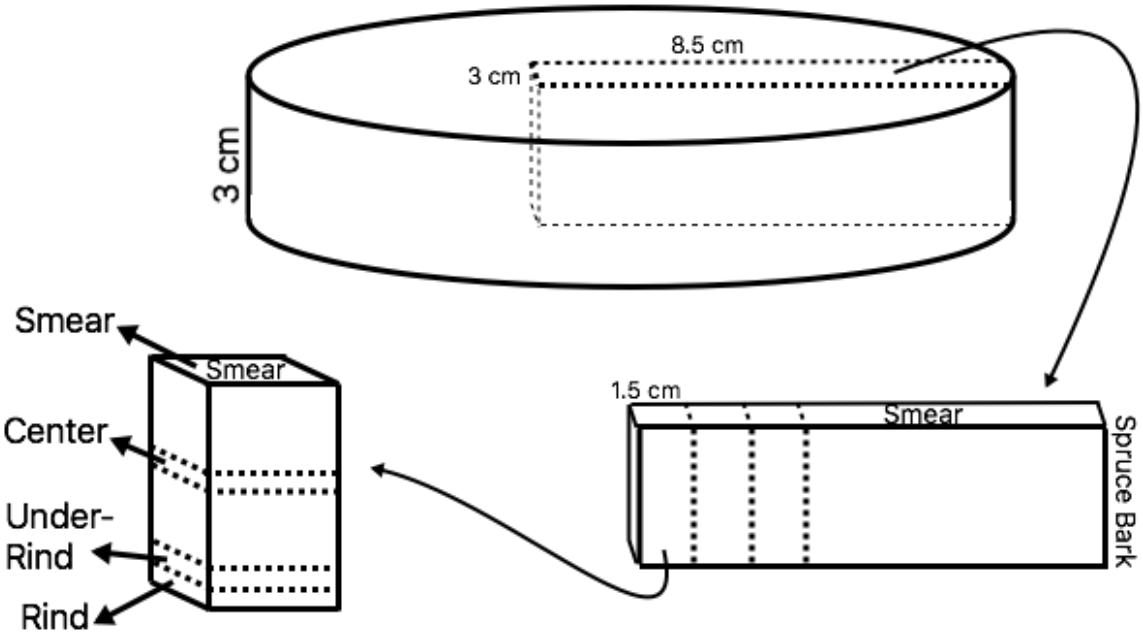

Tansman
Figure 1

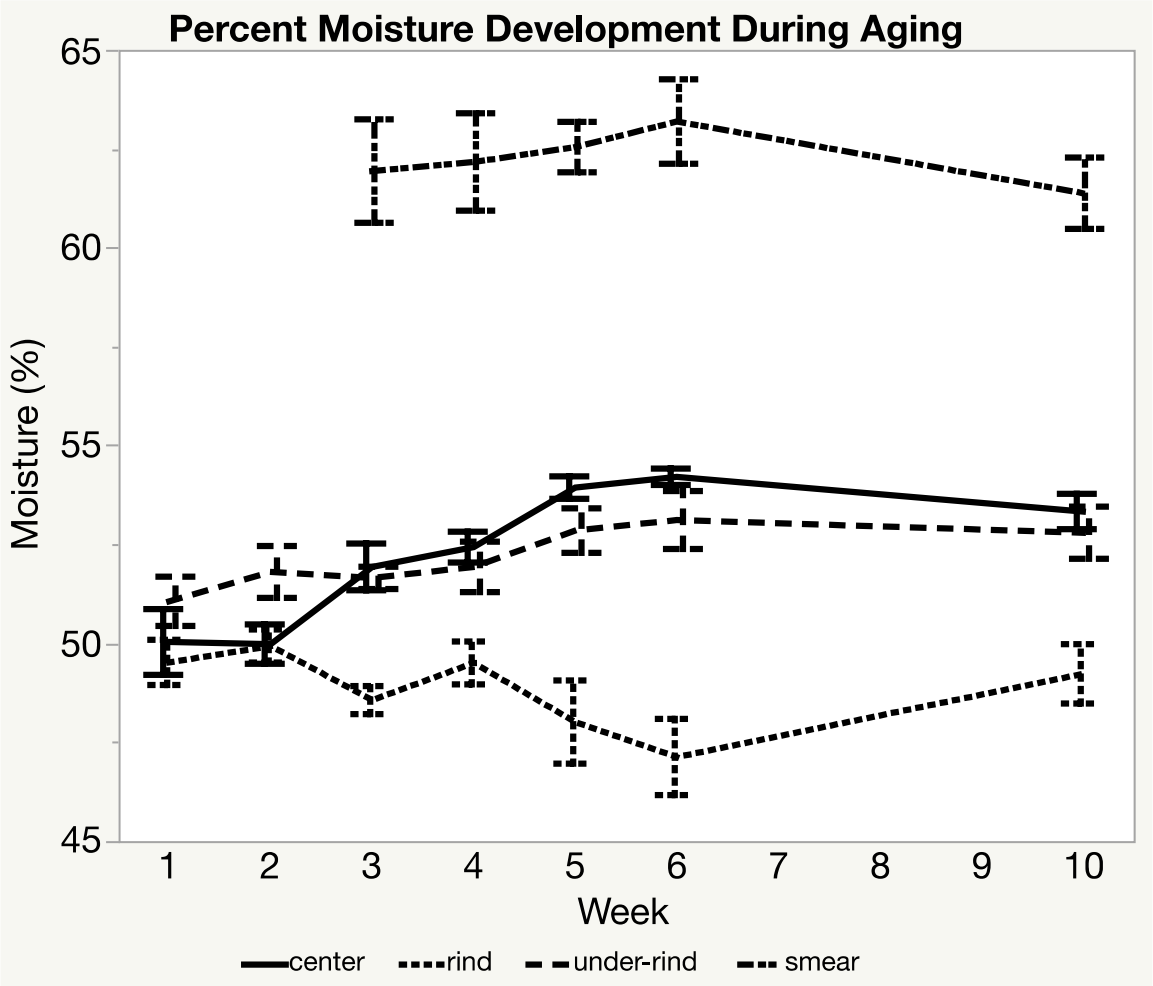

Tansman
Figure 2

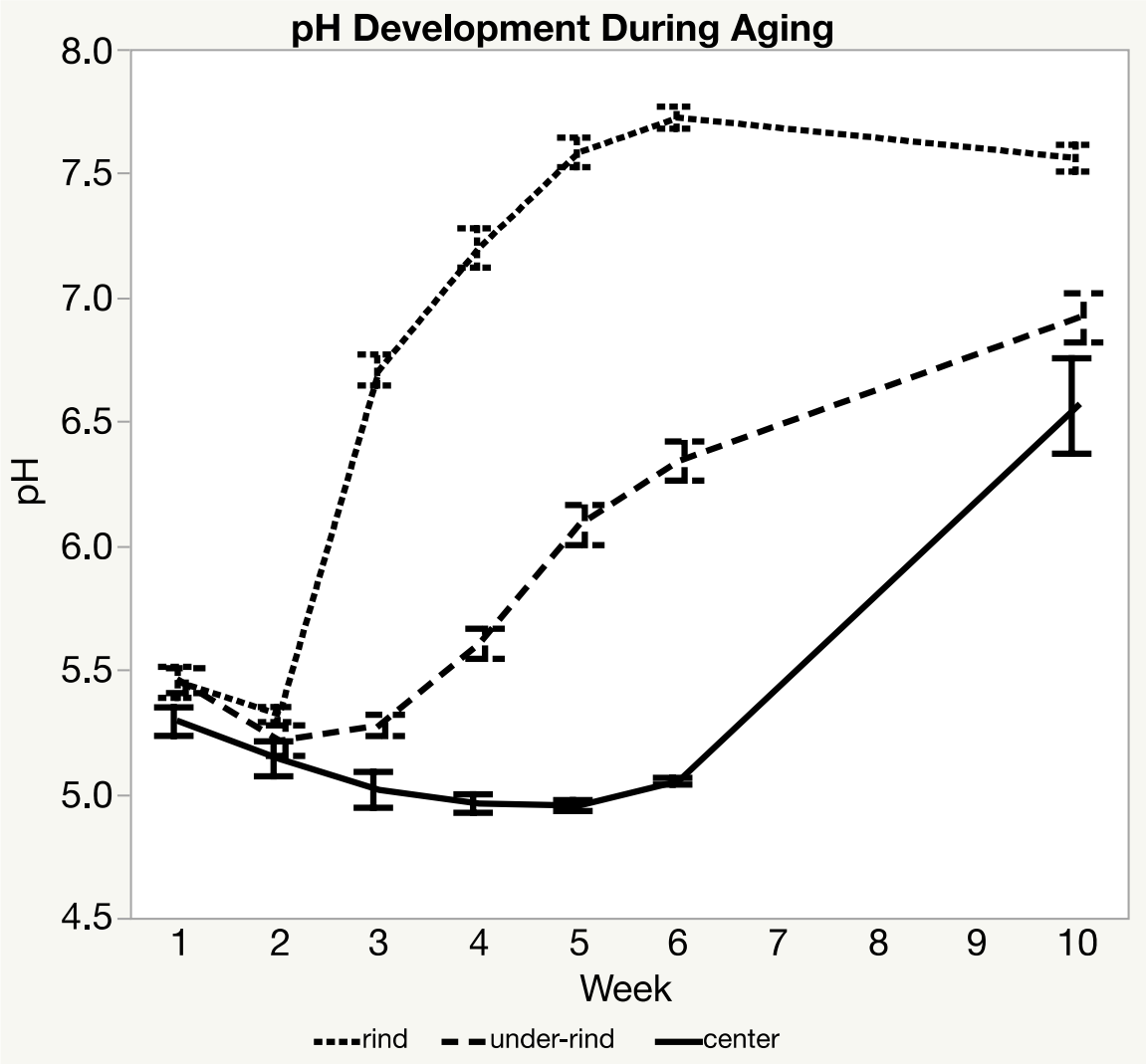

Tansman
Figure 3

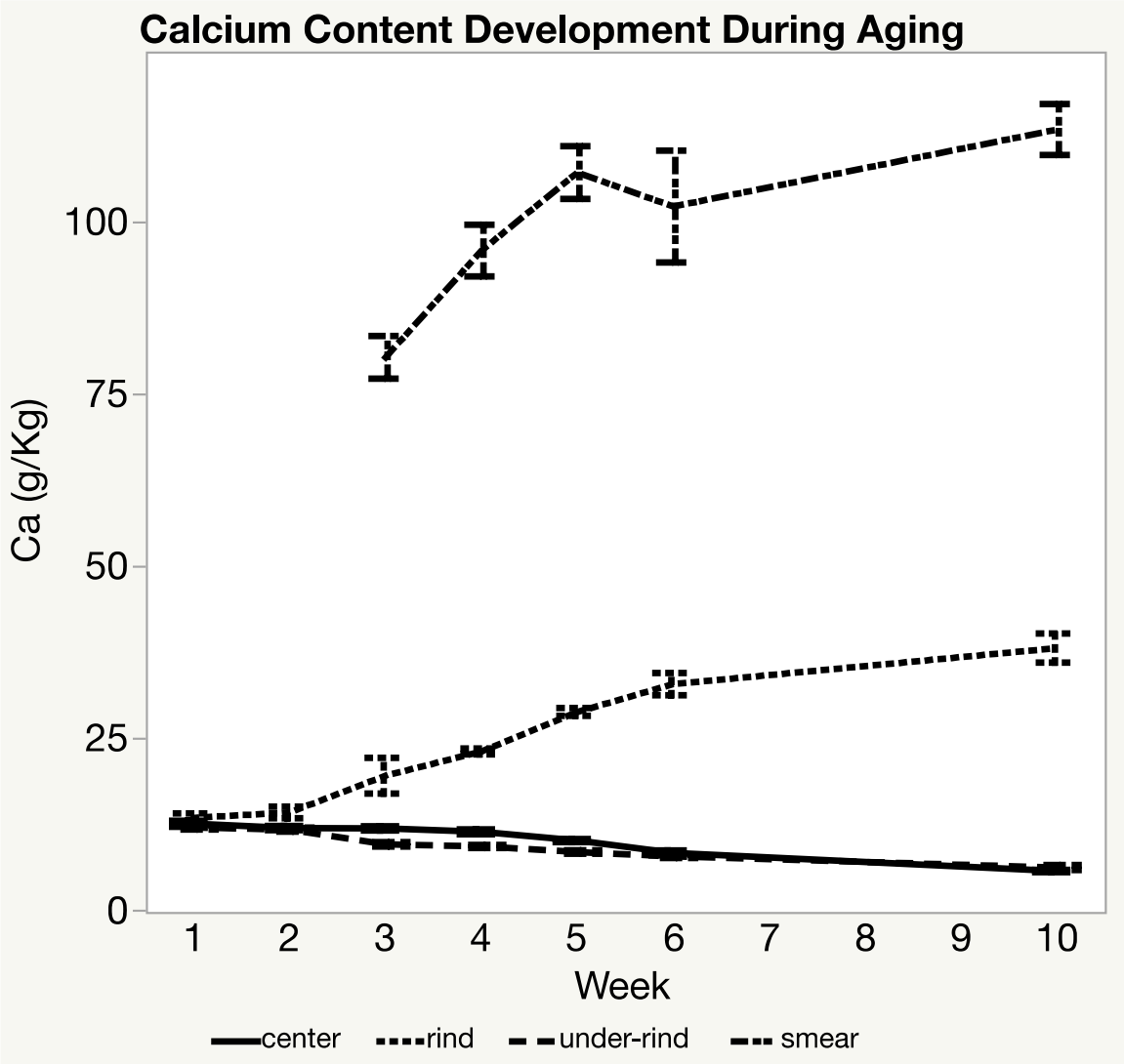

Tansman
Figure 4

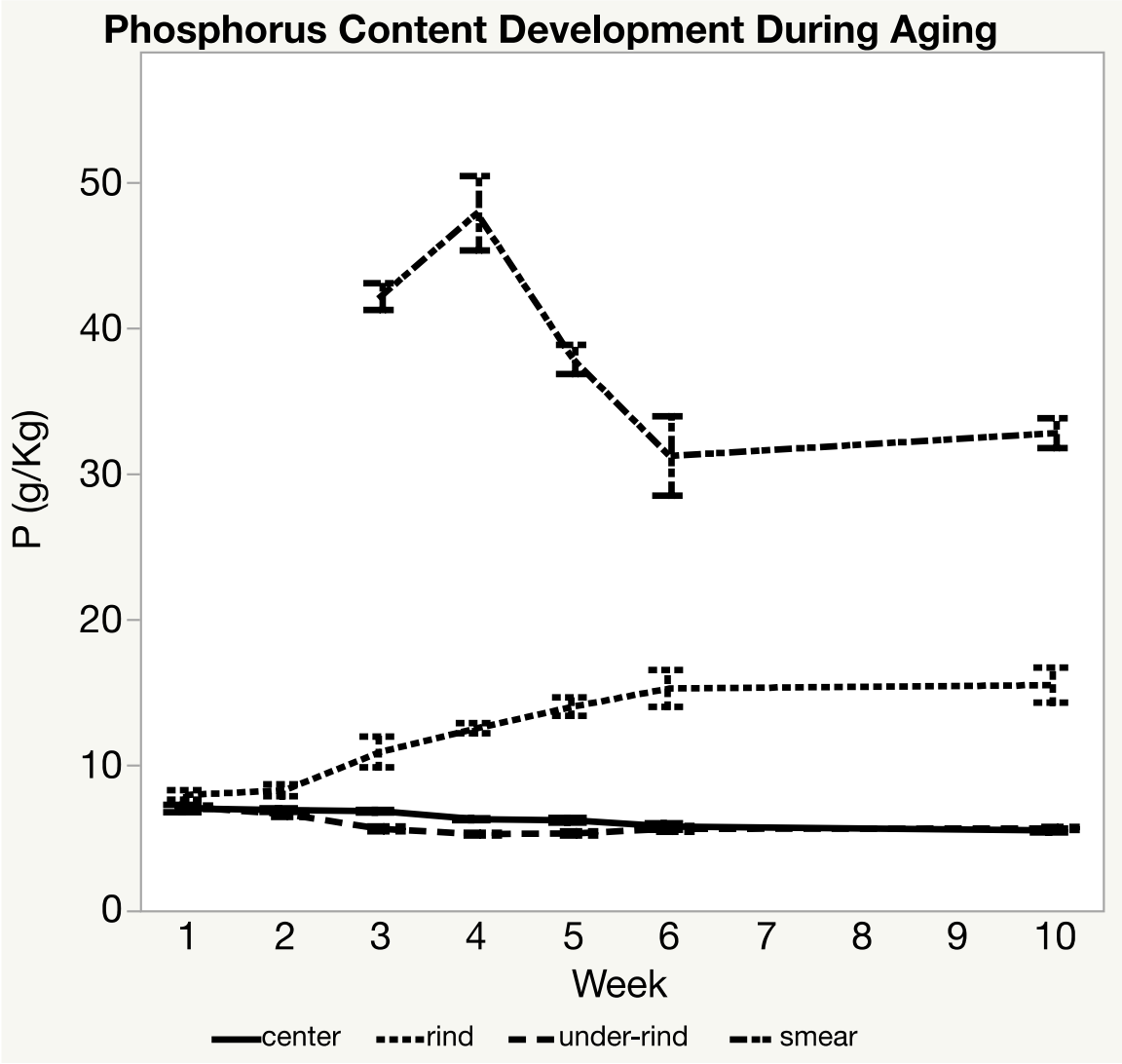

Tansman
Figure 5

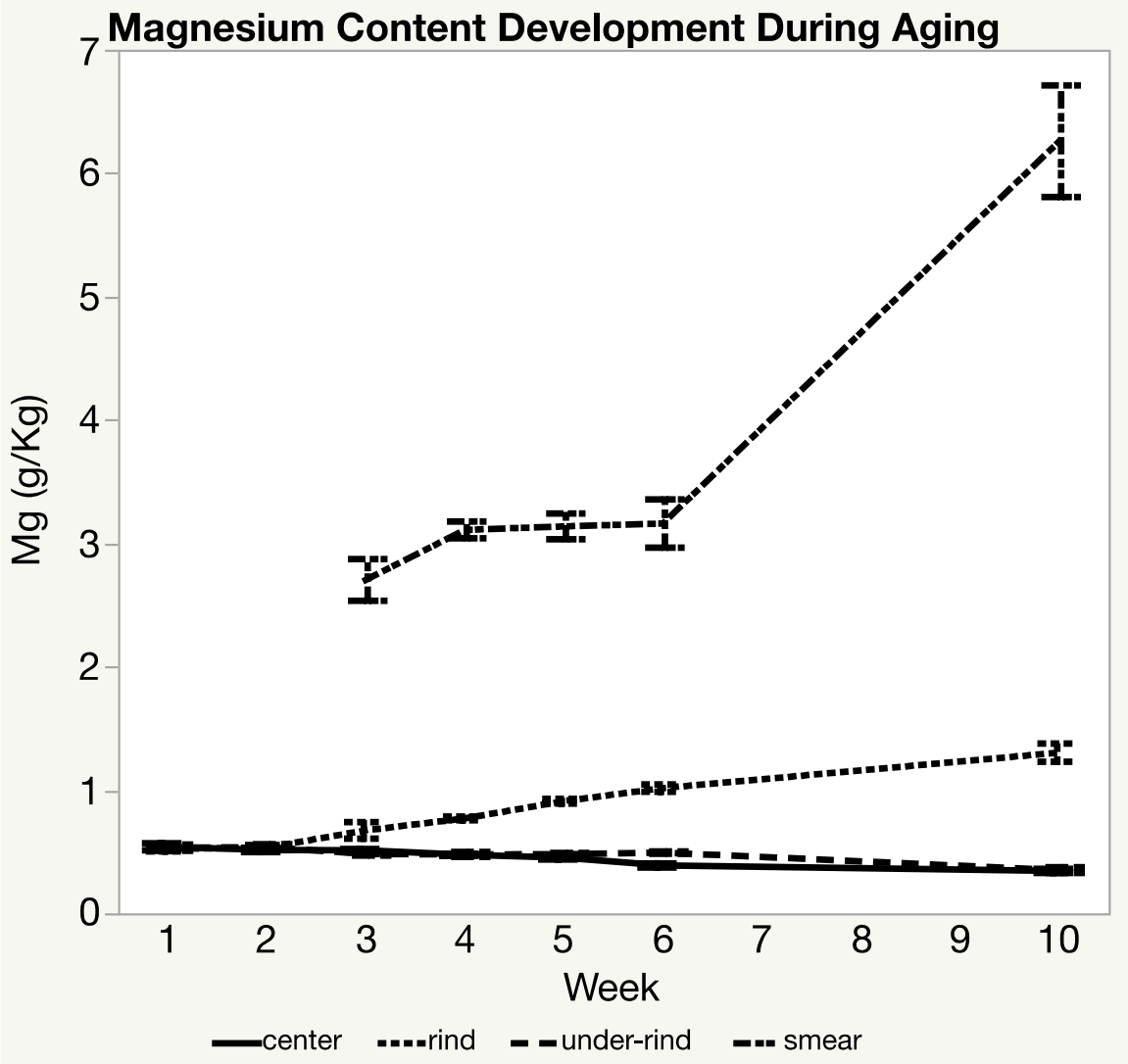

Tansman
Figure 6

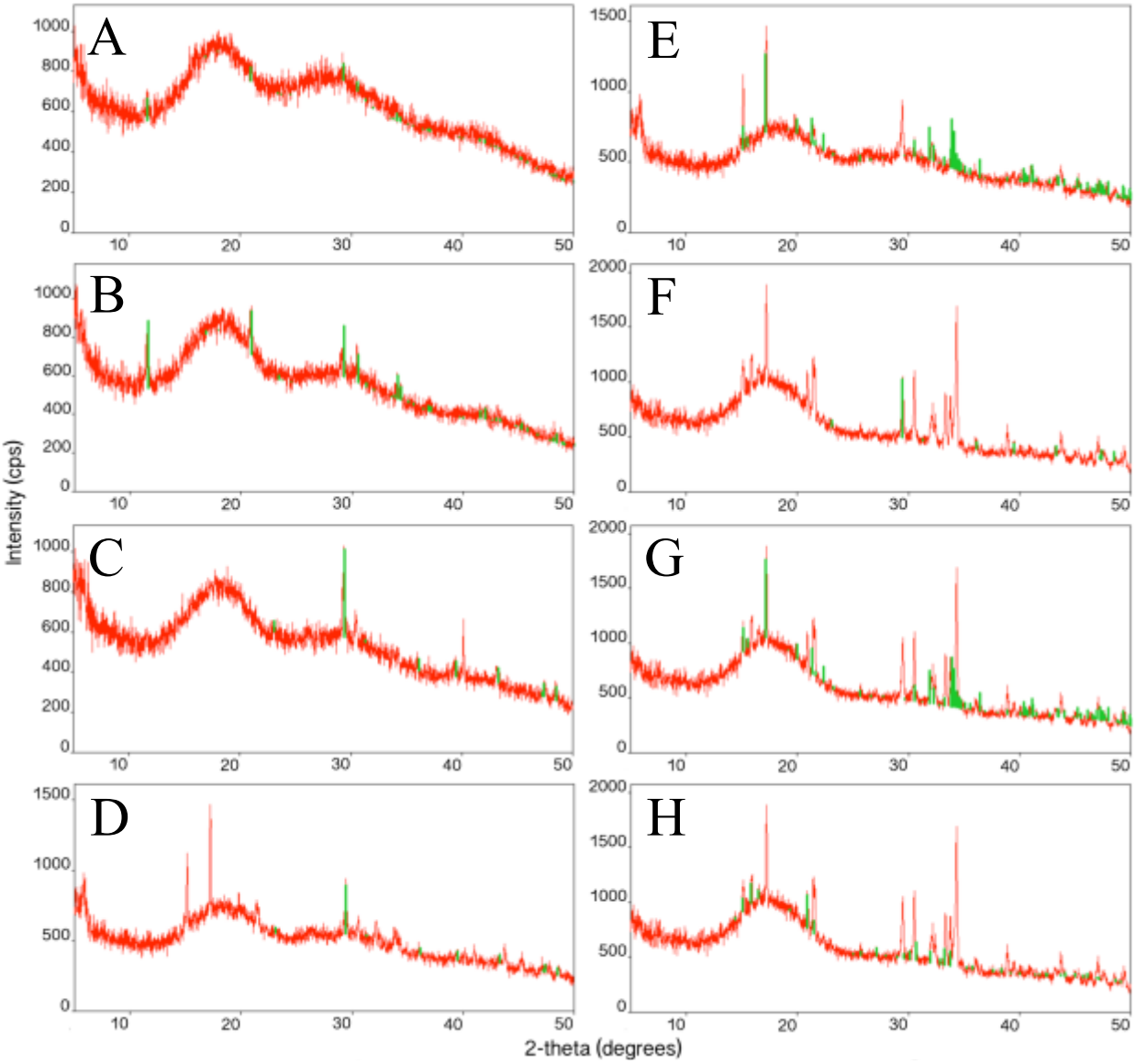

Tansman
Figure 7

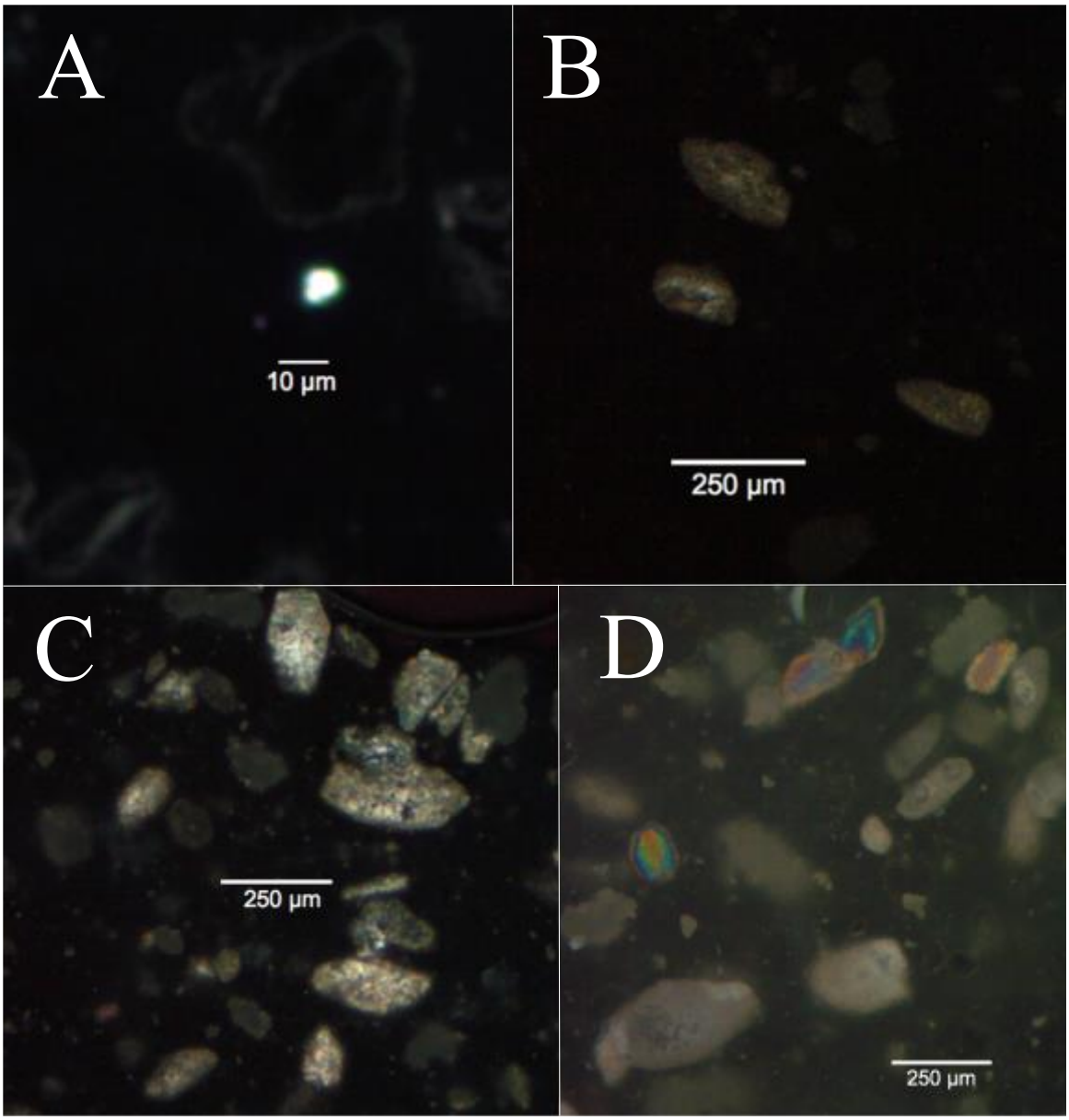

Tansman
Figure 8

CHAPTER 6: CONCLUSION AND FUTURE DIRECTIONS

Cheese ripening involves numerous biotic and abiotic processes, many of which are still not fully understood. An expanded understanding of these systems is desirable from the processing standpoint because it could provide cheesemakers with more control over the sensory characteristics of their finished product. The observations that were described in this dissertation highlight the tendency of soluble compounds in cheese, such as amino acids, mineral elements, and fermentation products, to form precipitates. These crystals can impart textural characteristics such as crunchiness and grittiness that are important for consumer acceptability. Chapter 2 presented a survey conducted with powder X-ray diffractometry (PXRD) that explored the diversity of crystals in hard cheeses such as Cheddar, Gouda, and Parmigiano-Reggiano and laid the groundwork for the cheese aging studies that followed. Conclusive identification of these precipitates provided insight into the diversity of ripening processes that induce these crystallization events.

The PXRD survey also made an initial foray to identify the crystals that form on the surface of soft washed-rind cheese. This endeavor provided preliminary data on the identity of the crystals but also demonstrated the need for additional optimization of the technique for use with cheese samples. Subsequent studies focused on crystallization phenomena in surface ripened cheeses and demonstrated the usefulness of additional crystallographic techniques including single crystal X-ray diffractometry (SCXRD) and petrographic microscopy. These techniques, along with measurements of pH and mineral element content, explored the complex and intriguing processes of mineral element diffusion and crystallization in white mold cheese and washed-rind cheese.

These phenomena have important implications including the direct impact that large crystals can have on cheese texture. These processes may also impact cheese softening through their indirect effect on protein-hydration; there are multiple schools of thought on this topic and further research is needed to determine how the mineral element concentrations of the soft surface ripened cheese affect cheese softening. This line of inquiry could define the role that is played by the mineral elements diffusion phenomena that were described in Chapters 4 and 5.

Collaboration with cheesemakers is the cornerstone of cheese-aging research and contributed to the real-world applicability of the findings in this dissertation. During my discussions with collaborators, I gleaned a trove of information on manufacturing practices, including practices that are aimed at differentiating cheeses in the market. One such innovation involves the use of popular beers in the wash-solution during the production of washed-rind cheese. This practice is an excellent means of crafting value in the marketplace, but cheesemakers are often curious how a practice like beer-washing affects aging processes. At a recent meeting in Somerset, England, where I presented research findings to a group of European cheesemakers, many attendees were curious about interactions between various washing solutions and the tendency of washed-rind cheeses to form gritty rinds. Research in this area would be tremendously beneficial to cheesemakers that are looking to modify their washing-solutions as a means of differentiating their products.

The use of high-end sea salts in cheese production is similar to the use of beer in that it may appeal to consumers, although it could potentially impact ripening processes in unexpected ways. For instance, compared to table salt, sea salt contains elevated levels

of certain ions that play a role in the crystallization phenomena described in Chapters 3, 4, and 5 of this dissertation. Elevated levels of magnesium, calcium, and phosphate could induce or inhibit the crystallization of various phases. The transfer of marine organisms from sea salt is another variable that could impact the ripening process at the rind, with possible implications for the type or abundance of crystals that form in the rind. These questions represent the cutting edge of our understanding of the washed-rind cheese system and extended research in this multi-disciplinary topic of study would likely yield intriguing discoveries.

Terroir, which I will modestly define here as the influence of geography on a cheese's properties, is a concept that has gained popularity in recent years. Product marketing frequently emphasizes the unique properties of products due to their places of origin. This concept may also have political and economic ramifications in negotiations of trade deals that involve protected origin claims. It is quite possible that the physical environment in which a washed-rind cheese is produced impacts the development of sensory properties, although research in this area is still in its infancy. For instance, the type of water that a cheesemaker uses to wash a cheese may differ in its concentration of dissolved ions, depending on the type of water that is available in the cheesemaker's region. These ions could potentially impact the formation of crystals by introducing the reactants necessary for crystallization or by introducing inhibitor ions with very low thresholds of inhibition. Research in this arena would be particularly interesting.

Crystallization in food is a fascinating topic that still has many unexplored areas of inquiry. This research could benefit producers, through the provision of valuable technical information, while also providing consumers with insight into the intricate

workings of the food system. It is my sincerest hope that research in this engaging area of study continues to produce intriguing observations, which may deepen our relationship with the familiar, yet mysterious, foods that we eat.

COMPREHENSIVE WORKS CITED

ABBONA, F., AND BOISTELLE, R. (1979) Growth morphology and crystal habit of struvite crystals ($MgNH_4PO_4$ $6H_2O$). *Journal of Crystal Growth* **46**, 339-354.

ABBONA, F., CHRISTENSSON, F., FRANCHINI ANGELA, M., AND LUNDAGER MADSEN, H.E. (1993) Crystal habit and growth conditions of brushite, $CaHPO_4 \cdot 2H_2O$. *Journal of Crystal Growth* **131**, 331-346.

ABRAHAM, S., CACHON, R., COLAS, B., FERON, G., AND DE CONINCK, J. (2007) Eh and pH gradients in Cemembert cheese during ripening: measurements using microelectrodes and correlations with texture. *International Dairy Journal* **17**, 954-960.

AFOAKWA, E.O., PATERSON, A., AND FOWLER, M. (2007) Factors influencing rheological and textural qualities in chocolate - a review. *Trends in Food Science & Technology* **18**, 290-298.

AGARWAL, S., SHARMA, K., SWANSON, B.G., YUKSEL, U., AND CLARK, S. (2006) Nonstarter lactic acid bacteria biofilms and calcium lactate crystals in Cheddar cheese. *Journal of Dairy Science* **89**, 1452-1466.

ALTUNKAYNAK, B.Z., ONGER, M.E., ALTUNKAYNAK, M.E., AYRANCI, E., AND CANAN, S. (2012) A brief introduction to stereology and sampling strategies: basic concepts of stereology. *NeuroQuantology* **10(1)**, 31-43.

AMRANE, A., PLIHON, F., AND PRIGENT, Y. (1999) Kinetics of growth and medium de-acidification for *Geotrichum candidum* and *Penicillium camemberti* cultivated on complex liquid media. *World Journal of Microbiology & Biotechnology* **15**, 489-491.

AMRANE, A., AND PRIGENT, Y. (2008) Diffusion of calcium and inorganic phosphate at the surface of a solid model medium in relation with growth of *Geotrichum candidum* and *Penecillium camembertii*. *Journal of Food Biochemistry* **32**, 813-825.

ARIFUZZAMAN, S.M., AND ROHANI, S. (204) Experimental study of brushit precipitation. *Journal of Crystal Growth* **267**, 624-634.

ARP, G., THIEL, V., REIMER, A., MICHAELIS, W., AND REITNER, J. (1999) Biofilm exopolymers control microbialite formation at thermal springs discharging in the alkaline Pyramid Lake, Nevada, USA. *Sedimentary Geology* **126**, 159-176.

ASKER, M.M.S., AND SHAWKY, B.T. (2010) Structural characterization and antioxidant activity of an extracellular polysaccharide isolated from *Brevibacterium otitidis* BTS 44. *Food Chemistry* **123**, 315-320.

BARAK, P., AND STAFFORT, A. (2006) Struvite: a recovered and recycled phosphorus fertilizer. *Proc. of the 2006 Wisconsin Fertilizer, Aglime & Pest Management Conference* **45**, 199-204.

BAUMGARTNER, L.K., REID, R.P., DUPRAZ, C., DECHO, A.W., BUCKLEY, D.H., SPEAR, J.R., PRZEKOP, K.M., AND VISSCHER, P.T. (2006) Sulfate reducing bacteria in microbial mats: changing paradigms, new discoveries. *Sedimentary Geology* **185**, 131-145.

BENZERARA, K., MIOT, J., MORIN, G., ONA-NGEUMA, G., SKOURI-PANET, F., AND FERARD, C. (2011) Significance, mechanisms and environmental implications of microbial biomineralization. *C. R. Geoscience* **343**, 160-167.

BIANCHI, A., BERRETTA, G., CASERIO, G., AND GIOLITTI, G. (1974) Amino acid composition of granules and spots in Grana Padano cheeses. *Journal of Dairy Science* **57(12)**, 1504-1508.

BISCHOFF, J.L., FITZPATRICK, J.A., AND ROSENBAUER, R.J. (1993a) The solubility and stabilization of ikaite ($CaCO_3$ $6H_2O$) from 0° to 25°C: environmental and paleoclimatic implications for thinolite tufa. *The Journal of Geology* **101**, 21-33.

BISCHOFF, J.L., STINE, S., ROSENBAUER, R.J., FITZPATRICK, J.A., AND STAFFORT, T.W. (1993b) Ikaite precipitation by mixing of shoreline springs and lake water, Mono Lake, California, USA. *Geochemica et Cosmochimica Acta* **57**, 3855-3865.

Bloss, F.D. (1961) An introduction to the methods of optical crystallography. Holt, Rinehart and Winston, New York.

Bloss, F.D. (2012) Crystallography and crystal chemistry. Hold, Rinehart, Winston, Inc., New York.

BOCH, R., DIETZEL, M., REICHL, P., LEIS, A., BALDERMANN, A., MITTERMAYR, F., AND POLT, P. (2015) Rapid ikaite ($CaCO_3$ $6H_2O$) crystallization in a man-made river bed: hydrogeochemical monitoring of a rarely documented mineral formation. *Applied Geochemistry* **63**, 366-379.

BOCKELMANN, W., AND HOPPE-SEYLER, T. (2001) The surface flora of bacterial smear-ripened cheeses from cow's and goat's milk. *International Dairy Journal* **11**, 307-314.

BOTTAZZI, V., BATTISTOTTI, B., AND BIANCHI, F. (1982) The microscopic crystalline inclusions in Grana cheese and their X-ray microanalysis. *Milchwissenschaft Milk Sci. Internat.* **37(10)**, 577-580.

BOTTAZZI, V., LUCCHINI, F., REBECCHI, A., AND SCOLARI, G.L. (1994) I cristalli del formaggio grana (Crystals present in Grana cheese). *Scienza e Technica Lattiero-Casearia* **45(1)**, 7-14.

BOUTROU, R., AZIZA, M., AND AMRANE, A. (2006) Enhanced proteolytic activities of *Geotrichum candidum* and *Penicillium camembertii* in mixed culture. *Enzyme and Microbial Technology* **39**, 325-331.

BOUTROU, R., FAMELART, M.H., GAUCHERON, F., LE GRAET, Y., GASSI, J.Y., PIOT, M., AND LEONIL, J. (2002) Structure development in a soft cheese curd model during manufacture in relation to its biochemical characteristics. *Journal of Dairy Research* **69**, 605-618.

BOUTROU, R., GAUCHERON, F., PIOT, M., MICHEL, F., MAUBOIS, J., AND LEONIL, J. (1999) Changes in the composition of juice expressed from Camembert cheese during ripening. *Le Lait* **79**, 503-513.

BRAISSANT, O., DECHO, A.W., DUPRAZ, C., GLUNK, C., PRZEKOP, K.M., AND VISSCHER, P.T. (2007) Exopolymeric substances of sulfate-reducing bacteria: interactions with calcium at alkaline pH and implications form for formation of carbonate minerals. *Geobiology* **5**, 401-411.

BRENNAN, N.M., WARD, A.C., BERESFORD, T.P., FOX, P.F., GOODFELLOW, M., AND COGAN, T.M. (2002) Biodiversity of the bacterial flora on the surface of a smear cheese. *Applied and Environmental Microbiology* **68(2)**, 820-830.

BRESE, N.E., AND O'KEEFFE, M. (1991) Bond-valence parameters for solids. *Acta Cryst* **B47**, 192-197.

BROOKER, B.E. (1987) The crystallization of calcium phosphate at the surface of mould-ripened cheeses. *Food Microstructure* **6**, 25-33.

BROOKER, B.E., HOBBS, D.G., AND TURVEY, A. (1975) Observations on the microscopic crystalline inclusions in Cheddar cheese. *Journal of Dairy Research* **42**, 341-348.

BROOKS, R., CLARK, L.M., AND THURSTON, E.F. (1950) Calcium carbonate and its hydrates. *Philosophical Transactions of the Royal Society of London* **243(861)**, 145-167.

BUCHARDT, B., ISRAELSON, C., SEAMAN, P., AND STOCKMANN, G. (2001) Ikaite tufa towers in Ikka Fjord, Southwest Greenland: their formation by mixing of seawater and alkaline spring water. *Journal of Sedimentary Research* **71(1)**, 176-189.

BUTTON, J.E., AND DUTTON, R.J. (2012) Cheese Microbes. *Current Biology* **22(15)**, R587-R589.

CHAUHAN, C.K., AND JOSHI, M.J. (2013) In vitro crystallization, characterization and growth-inhibition study of urinary type struvite crystals. *Journal of Crystal Growth* **362**, 330-337.

CHOU, Y.E., EDWARDS, C.G., LUEDECKE, L.O., BATES, M.P., AND CLARK, S. (2003) Nonstarter lactic acid bacteria and aging temperature affect calcium lactate crystallization in Cheddar cheese. *Journal of Dairy Science* **86**, 2516-2524.

CLAPHAM, L., MCLEAN, R.J.C., NICKEL, J.C., AND DOWNEY, J. (1990) The influence of bacteria on struvite crystal hand and its importance in urinary stone formation. *Journal of Crystal Growth* **104**, 475-484.

CLARKSON, J.R., PRICE, T.J., AND ADAMS, C.J. (1992) Role of metastable phases in the spontaneous precipitation of calcium carbonate. *J. Chem. Soc. Faraday Trans.* **88(2)**, 243-249.

CONOCHIE, J., CZULAK, J., LAWRENCE, A.J., AND COLE, W.F. (1960) Tyrosine and calcium lactate crystals on rindless cheese. *Australian Journal of Dairy Technology* **15(3)**, 120.

CONOCHIE, J., AND SUTHERLAND, B.J. (1965) The nature and cause of seaminess of Cheddar cheese. *Journal of Dairy Research* **32**, 35-44.

CORSETTI, A., ROSSI, J., AND GOBBETTI, M. (2001) Interactions between yeasts and bacteria in the smear of surface-ripened cheeses. *International Journal of Food Microbiology* **69**, 1-10.

CORTEZ, M.A.S., FURTADO, M.M., GIGANTE, M.L., AND KINDSTEDT, P.S. (2008) Effect of pH on characteristics of low-moisture mozzarella cheese during refrigerated storage. *Journal of Food Science* **73(9)**, 443-448.

COURIOL, C., AMRANE, A., AND PRIGENT, Y. (2001) A new model for the reconstruction of biomass history from carbon dioxide emmision during batch cultivation of *Geotrichum candidum*. *Journal of Bioscience and Bioengineering* **91(6)**, 570-575.

DECHO, A.W. (2010) Overview of biopolymer-induced mineralization: what goes on in biofilms? *Ecological Engineering* **36**, 137-144.

DHAMI, N., REDDY, M.S., AND MUKHERJEE, A. (2013) Biomineralization of calcium carbonates and the engineered applications: a review. *Frontiers in Microbiology* **4(314)**, 1-13.

DIECKMANN, G.S., NEHRKE, G., PAPADIMITRIOU, S., GOTTLICHER, J., STEININGER, R., KENNEDY, H., WOLF-GLADROW, D., AND THOMAS, D.N. (2008) Calcium carbonate as ikaite crystals in Antarctic sea ice. *Geophysical Research Letters* **35(8)**.

DIECKMANN, G.S., NEHRKE, G., UHLIG, C., GOTTLICHER, J., GERLAND, S., GRANSKOG, M.A., AND THOMAS, D.N. (2010) Brief communication: ikaite ($CaCO_3$ $6H_2O$) discovered in arctic sea ice. *The Cryosphere* **4**, 227-230.

DOVE, P.M., AND HOCHELLA, M.F. (1993) Calcite precipitation mechanisms and inhibitions by orthophosphate: in situ observations by scanning force microscopy. *Geochimica et Cosmochimica Acta.* **57**, 705-714.

DOX, A.W. (1911) The occurene of tyrosine crystals in Roquefort cheese. *J. Amer. Chem. Soc.* **33(423-425)**.

DRAKE, S.L., AND DRAKE, M.A. (2011) Comparison of salty taste and time intensity of sea and land salts from around the world. *Journal of Sensory Studies* **26**, 25-34.

DUGAT-BONY, E., GARNIER, L., DENONFOUX, J., FERREIRA, S., SARTHOU, A., BONNARME, P., AND IRLINGER, F. (2016) Highlighting the microbial diversity of 12 French cheese varieties. *International Journal of Food Microbiology* **238**, 265-273.

DUPRAZ, C., REID, R.P., BRAISSANT, O., DECHO, A.W., NORMAN, R.S., AND VISSCHER, P.T. (2009) Processes of carbonate precipitation in modern microbial mats. *Earth-Science Reviews* **96**, 141-162.

DUPRAZ, C., AND VISSCHER, P.T. (2005) Microbial lithification in marine stromatolites and hypersaline mats. *Trends in Microbiology* **13(9)**, 429-438.

Düsterhöft, E.M., Engels, W., and van den Berg, G. (2011) Dutch-Type Cheese. Encyclopedia of Dairy Sciences. Academic Press/Elsevier, London.

Dyar, M.D., Gunter, M.E., and Tasa, D. (2008) Mineralogy and Optical Mineralogy. Mineralogical Society of America, Chantilly, VA.

DYBING, S.T., WIEGAND, J.A., BRUDVIG, S.A., HUANG, E.A., AND CHANDAN, R.C. (1988) Effect of processing variables on the formation of calcium lactate crystals on Cheddar cheese. *Journal of Dairy Science* **71(7)**, 1701-1710.

FEENEY, E.P., GUINEE, T.P., AND FOX, P.F. (2002) Effect of pH and calcium concentration on proteolysis in Mozzarella cheese. *Journal of Dairy Science* **85**, 1646-1654.

FERREIRA, A., OLIVEIRA, C., AND ROCHA, F. (2003) The different phases in the precipitation of dicalcium phosphate dihydrate. *Journal of Crystal Growth* **252**, 599-611.

FEURER, C., VALLAEYS, T., CORRIEU, G., AND IRLINGER, F. (2004) Does smearing inoculum reflect the bacterial composition of the smear at the end of the ripening of a French soft, red-smear cheese? *Journal of Dairy Science* **87**, 3189-3197.

Fox, P.F., Guinee, T.P., Cogan, T.M., and McSweeney, P.L.H. (2000) Fundamentals of Cheese Science. Aspen Publishers Inc., Gaithersburg, Maryland.

FRANKS, J., AND STOLZ, J.F. (2009) Flat laminated microbial mat communities. *Earth-Science Reviews* **96**, 163-172.

GALEHOUSE, J.S. (1969) Counting grain mounts: number percentage vs. number frequency. *Journal of Sedimentary Research* **39(2)**, 812-815.

GARDI, J.E., NYENGAARD, J.R., AND GUNDERSEN, H.J.G. (2008) Automatic sampling for unbiased and efficient stereological estimation using the proportionator in biological studies. *Journal of Microscopy* **230(1)**, 108-120.

Garside, J. (1987) General principles of crystallization. In P. Lillford, and J.M.V. Blanshard, Eds. Food Structure and Behavior. Academic Press Ltd, UK.

GAUCHERON, F., LE GRAET, Y., MICHEL, F., BRIARD, V., AND PIOT, M. (1999) Evolution of various salt concentrations in the moisture and in the outer layer and centre of a model cheese during its brining and storage in an ammoniacal atmosphere. *Le Lait* **79**, 553-566.

GIANNIMARAS, E.K., AND KOUTSOUKOS, P.G. (1987) The crystallization of calcite in the presence of orthophosphate. *Journal of Colloid and Interface Science* **116(2)**, 423-430.

GOBBETTI, M., LOWNEY, S., SMACCHI, E., BATTISTOTTI, B., DAMIANI, P., AND FOX, P.F. (1997) Microbiology and biochemistry of Taleggio cheese during ripening. *International Dairy Journal* **7**, 509-517.

GONZALEZ-MUNOZ, M.T., LINARES, C., MARTINEZ-RUIZ, F., MORCILLO, F., MARTIN-RAMOS, D., AND ARIAS, J.M. (2008) Ca-Mg kutnahorite and struvite production by *Idiomarina* strains at modern seawater salinities. *Chemosphere* **72**, 465-472.

GORI, K., MORTENSEN, H.D., ARNEBORG, N., AND JESPERSEN, L. (2007) Ammonia Production and its possible role as a mediator of communication for *Debaryomyces hansenii* and other cheese-relevant yeast species. *Journal of Dairy Science* **90**, 5032-5041.

GRIFFITH, D.P. (1978) Struvite Stones. *Kidney International* **13**, 372-382.

Gripon, J.C. (1987) Mould-ripened cheeses. In P.F. Fox, Ed. Cheese: Chemistry, Physics, and Microbiology, 2. Elsevier Allpied Science Publishers LTD, Essex, England.

GULL, M., AND PASEK, M.A. (2013) Is struvite a prebiotic mineral? *Life* **3**, 321-330.

HAN, Z., ZHAO, Y., YAN, H., ZHAO, H., HAN, M., SUN, B., SUN, X., NOU, F., SUN, H., HAN, L., SUN, Y., WANG, J., LI, H., WANG, Y., AND DU, H. (2015) Struvite precipitation induced by novel sulfate-reducing bacterium *Acinetobacter calcoaceticu* SRB4 isolated from river sediment. *Geomicrobiology Journal* **32**, 868-877.

HARPER, W.J., SWANSON, A.M., AND SOMMER, H.H. (1953) Observations on the chemical composition of white particles in several lots of Cheddar cheese. *Journal of Dairy Science* **36(4)**, 368-372.

HELIAS, A., MIRADE, P.S., AND CORRIEU, G. (2007) Modeling of Camembert-Type cheese mass loss in a ripening chamber: main biological and physical phenomena. *Journal of Dairy Science* **90**, 5324-5333.

HIGLEY, M.C. (2015) A geochemical archive of climate variability in Kiritimati Island lake sediment. *Geological Society of America Abstracts with Programs* **47(7)**, 757.

Holt, C., Cox, A.J., Harries, J.E., and Hunkins, D.W.L. (1987) Application of ion chromatography to the characterization of biological calcium phosphates. Recent Developments in Ion Exchange, p. 22-28. Springer, Netherlands.

HOUGH, G., MARTINEZ, E., AND CONTARINI, A. (1990) Sensory and objective measurement of sandiness in Dulce de Leche, a typical Argentine dairy product. *Journal of Dairy Science* **73(3)**, 604-611.

HOUSE, W.A. (1987) Inhibition of calcite crystal growth by inorganic phosphate. *Journal of Colloid and Interface Science* **119(2)**, 505-511.

HOUSE, W.A., AND DONALDSON, L. (1986) Adsorption and coprecipitation of phosphate on calcite. *Journal of Colloid and Interface Science* **112(2)**, 309-324.

HU, Y.B., WOLF-GLADROW, D.A., DIECKMANN, G.S., VOLKER, C., AND NEHRKE, G. (2014) A laboratory study of ikaite ($CaCO_3$ $6H_2O$) precipitation as a function of pH, salinity, temperature and phosphate concentration. *Marine Chemistry* **162**, 10-18.

HUNTER, R.E. (1967) A rapid method for determining weight percentages of unsieved heavy minerals. *Journal of Sedimentary Petrology* **37(2)**, 521-529.

IMAI, E., HATAE, K., AND SHIMADA, A. (1995) Oral perception of grittiness: effect of particle size and concentration of the dispersed particles and the dispersion medium. *Journal of Texture Studies* **26**, 561-576.

IRLINGER, F., LAYEC, S., HENLINCK, S., AND DUGAT-BONY, E. (2015) Cheese rind microbial communities: diversity, composition and origin. *FEMS Microbiology Letters* **362**, 1-11.

IVORRA, J., ROSAS, J., AND PASCUAL, E. (1999) Most calcium pyrophosphate crystals appear as non-birefringent. *Ann Rheum Dis* **58**, 582-584.

JENSEN, H., BIGGS, C.A., AND KARUNAKARAN, E. (2016) The importance of sewer biofilms. *WIREs Water* **3**, 487-494.

JOHANSSON, E., MISKOVSKY, K., LOORENTS, K., AND LOFGREN, O. (2008) A method for estimation of free mica particles in aggregate fine fraction by image analysis of grain mounts. *Journal of Materials Engineering and Performance* **17(2)**, 250-253.

JOHNSON, M. (2014) Crystallization in Cheese. *Dairy Pipeline, Wiscosin Center for Dairy Research* **26(3)**, 1-5.

JOHNSSON, M.S.A., AND NANCOLLAS, G.H. (1992) The role of brushite and octacalcium phosphate in apatite formation. *Critical Reviews in Oral Biology and Medicine* **3**, 61-82.

JOHNSTON, J., MERWIN, H.E., AND WILLIAMSON, E.D. (1916) The Several Forms of Calcium Carbonate. *American Journal of Science* **246**, 473-512.

KAGKLI, D., TACHE, R., COGAN, T.M., HILL, C., CASAREGOLA, S., AND BONNARME, P. (2006) *Kluyveromyces lactis* and *Saccharomyces cerevisiae*, two potent deacidifying and volatile-sulphur-aroma-producing microorganisms of the cheese ecosystem. *Appl Microbiol Biotechnol* **73**, 434-442.

Kalab, M. (1995) Practial apsects of electron microscopy in cheese research. Plenum Press, New York.

KANEL, J., AND MORSE, J.W. (1978) The chemistry of orthophosphate uptake from seawater on to calcite and aragonite. *Geochimica et Cosmochimica Acta.* **42**, 1335-1340.

KARAHADIAN, C., AND LINDSAY, R.C. (1987) Integrated rales of lactate, ammonia, and calcium in texture development of mold surface-ripened cheese. *Journal of Dairy Science* **70(5)**, 909-918.

KILIC, N.K., AND DONMEZ, G. (2008) Environmental conditions affecting exopolysaccharide production by *Pseudomonas aeruginosa, Micrococcus* sp., and *Ochrobactrum* sp. *Journal of Hazardous Materials* **154**, 1019-1024.

Kosikowski, F.V., and Mistry, V.V. (1997) Cheese and Fermented Milk Foods. F.V. Kosikowski, Great Falls, VA.

KUNITAKE, M.E., BAKER, S.P., AND ESTROFF, L.A. (2012) The effect of magnesium sustitution on the hardness of synthetic and biogenic calcite. *MRS Communications* **2**, 113-116.

KUZ'MINA, M.A., ZHURAVLEV, S.V., AND O.V., F.-K. (2013) The effect of medium chemistry on the solubility and morphology of brushite crystals. *Geology of Ore Deposits* **55(8)**, 692-697.

LARPIN, S., MONDOLONI, C., GOERGES, S., VERNOUX, J., GUEGUEN, M., AND DESMASURES, N. (2006) *Geotrichum candidum* dominates in yeast population dynamics in Livarot, a French red-smear cheese. *FEMS Yeast Res* **6**, 1243-1253.

LARSEN, D. (1994) Origin and paleoenvironmental significance of calcite pseudomorphs after ikaite in the Oligocene Creede formation, Colorado. *Journal of Sedimentary Research* **A64(3)**, 593-603.

LAST, F.M., LAST, W.M., FAYEK, M., AND HALDEN, N.M. (2013) Occurrence and significance of a cold-water carbonate pseudomorph in microbialites from a saline lake. *J Paleolimnol* **50**, 505-517.

LAWRENCE, R.C., CREAMER, L.K., AND GILLES, J. (1987) Texture development during cheese ripening. *Journal of Dairy Science* **70**, 1748-1760.

LE CORRE, K.S., VALSAMI-JONES, E., HOBBS, P., AND PARSONS, S.A. (2005) Impact of calcium on struvite crystal size, shape and purity. *Journal of Crystal Growth* **283**, 514-522.

LE GRAET, Y., AND BRULE, G. (1988) Migration des macro et oligo-éléments dans un fromage à pâte molle de type Camembert. *Le Lait* **68(2)**, 219-234.

LE GRAET, Y., LEPIENNE, A., BRULE, G., AND DUCRUET, P. (1983) Migration du calcium et des phosphates inorganiques dans les fromages à pâte molle de type Camembert au cours de l'affinage. *Le Lait* **63**, 317-332.

LECLERCQ-PERLAT, M.N., BUONO, F., LAMBERT, D., LATRILLE, E., SPINNLER, H.E., AND CORRIEU, G. (2004a) Controlled production of Camembert-type cheeses. Part I: microbiological and physicochemical evolutions. *Journal of Dairy Research* **71**, 346-354.

LECLERCQ-PERLAT, M.N., CORRIEU, G., AND SPINNLER, H.E. (2004b) The color of *Brevibacterium linens* depends on the yeast used for cheese deacidification. *Journal of Dairy Science* **87(1536-1544)**.

LECLERCQ-PERLAT, M.N., HELIAS, A., AND CORRIEU, G. (2013a) Short communication: little change takes place in Camembert-style cheese water activities through ripening in terms of relative humidity and salt. *Journal of Dairy Science* **96**, 7521-7525.

LECLERCQ-PERLAT, M.N., OUMER, A., BERGERE, J.L., SPINNLER, H.E., AND CORRIEU, G. (2000a) Behavior of *Brevibacterium linens* and *Debaryomyces hansenii* as ripening flora in controlled production of smear soft cheese from reconstituted milk: growth and substrate consumption. *Journal of Dairy Science* **83**, 1665-1673.

LECLERCQ-PERLAT, M.N., OUMER, A., BUONO, F., BERGERE, J.L., SPINNLER, H.E., AND CORRIEU, G. (2000b) Behavior of *Brevibacterium linens* and *Debaryomyces hansenii* as ripening flora in controlled production of soft smear cheese from reconstituted milk: protein degradation. *Journal of Dairy Science* **83**, 1674-1683.

LECLERCQ-PERLAT, M.N., PICQUE, D., DEL CAMPO BARBA, S.T.M., AND MONNET, C. (2013b) Dynamics of *Penicillium camemberti* growth quantified by real-time PCR on Camembert-type cheeses under different conditions of temperature and relative humidity. *Journal of Dairy Science* **96**, 4031-4040.

LECLERCQ-PERLAT, M.N., PICQUE, D., RIAHI, H., AND CORRIEU, G. (2006) Microbiological and biochemical aspects of Camembert-type cheeses depend on atmospheric composition in the ripening chamber. *Journal of Dairy Science* **89(8)**, 3260-3273.

LECLERCQ-PERLAT, M.N., SICARD, M., PERROT, N., TRELEA, I.C., PICQUE, D., AND CORRIEU, G. (2015) Temperature and relative humidity influence the ripening descriptors of Camembert-type cheeses throughout ripening. *Journal of Dairy Science* **98**, 1325-1335.

LECLERCQ-PERLAT, M.N., SICARD, M., TRELEA, I.C., PICQUE, D., AND CORRIEU, G. (2012) Temperature and relative humidity influence the microbial and physicochemical characteristics of Camembert-type cheese ripening. *Journal of Dairy Science* **95**, 4666-4682.

LEE, D., AND KUMTA, P.N. (2010) Chemical synthesis and stabilization of magnesium substituted brushite. *Materials Science and Engineering C* **30**, 934-943.

LESSARD, M., BELANGER, G., ST-GELAIS, D., AND LABRIE, S. (2012) The composition of Camembert cheese-ripening cultures modulates both mycelial growth and appearance. *Applied and Environmental Microbiology* **78(6)**, 1813-1819.

LIN, Y.M., BASSIN, J.P., AND VAN LOOSDREHT, M.C.M. (2012) The contribution of exopolysaccharides induced struvites accumulation to ammonium adsorption in aerobic granular sludge. *Water Research* **46**, 986-992.

LIU, B., GIANNIS, A., ZHANG, J., V., C., AND WANG, J. (2013) Characterization of induced struvite formation from source-separated urine using seawater and brine as magnesium sources. *Chemosphere* **93**, 2738-2747.

LIU, Y., CUI, Y., MAO, H., AND GUO, R. (2012) Calcium carbonate crystallization in the presence of casein. *Cryst. Growth Des.* **12**, 4720-4726.

LUCEY, J.A., AND FOX, P.F. (1993) Importance of calcium and phosphate in cheese manufacture: a review. *Journal of Dairy Science* **76**, 1714-1724.

MARLAND, G. (1975) The stability of $CaCO_3$ $6H_2O$ (ikaite). *Geochemica et Cosmochimica Acta* **39**, 83-91.

MASOUD, W., AND JAKOBSEN, M. (2005) The combined effects of pH, NaCl, and temperature on growth of cheese ripening cultures of *Debaryomyces hansenii* and coryneform bacteria. *International Dairy Journal* **15**, 69-77.

MCCARTY, D.J., AND HOLLANDER, J.L. (1961) Identification of urate crystals in gouty synovial fluid. *Ann Intern Med* **54(3)**, 452-460.

MCLEAN, R.J.C., NICKEL, J.C., BEVERIDGE, T.J., AND COSTERTON, J.W. (1989) Observations of the ultrastructure of infected kidney stones. *J. Med. Microbiol.* **29**, 1-7.

METCHE, M., AND FANNI, J. (1978) Rôle de la flore fongique dans l'accumulation du calcium et du phosphore à la surface des fromages du type camembert. *Le Lait* **58(557)**, 336-354.

MIKKELSEN, A., ANDERSEN, A.B., ENGELSEN, S.B., HANSEN, H.C.B., LARSEN, O., AND SKIBSTED, L.H. (1999) Presence and dehydration of ikaite, calcium carbonate hexahydrate, in frozen shrimp shell. *J. Agric. Food Chem.* **47**, 911-917.

MILLER, M.A., KENDALL, M.R., JAIN, M.K., LARSON, P.R., MADDEN, A.S., AND TAS, A.C. (2012) Testing of brushite ($CaHPO_4 \cdot 2H_2O$) in synthetic biomineralization solutions and in situ crystallization of brushite micro-granules. *J. Am. Ceram. Soc.* **95(7)**, 2178-2188.

MILLERO, F., HUANG, F., ZHU, X., JLIU, X., AND ZANG, J. (2001) Adsorption and desorption of phosphate on calcite and aragonite in seawater. *Aquatic Geochemistry* **7**, 33-56.

MORALES, S.E., MOUSER, P.J., WARD, N., HUDMAN, S.P., GOTELLI, N.J., ROSS, D.S., AND LEWIS, T.A. (2006) Comparison of bacterial communities in New England sphagnum bogs using terminal restrictive fragment length polymorphism (T-RFLP). *Microbial Ecology* **52**, 34-44.

MORRIS, H.A., HOLD, C., BROOKER, J.B., AND MANSON, W. (1988) Inorganic constituents of cheese: analysis of juice from a one-month-old Cheddar cheese and the use of light and electron microscopy to characterize the crystalline phases. *Journal of Dairy Research* **55**, 255-268.

MOUNIER, J., GOERGES, S., GELSOMINO, R., VAACANNEYT, M., VANDEMEULEBROECKE, K., HOSTE, B., BRENNAN, N.M., SCHERER, S., SWINGS, J., FITZGERALD, G.F., AND COGAN, T.M. (2006) Sources of the adventitious microflora of a smear-ripened cheese. *Journal of Applied Microbiology* **101**, 668-681.

MUYNCK, W.D., DE BELIE, N., AND VERSTRAETE, W. (2010a) Microbial carbonate precipitation in construction materials: a review. *Ecological Engineering* **36**, 118-136.

MUYNCK, W.D., VERBEKEN, K., BELIE, N.D., AND VERSTRAETE, W. (2010b) Influence of urea and calcium dosage on the effectiveness of bacterially induced carbonate precipitation on limestone. *Ecological Engineering* **36**, 99-111.

NEILSON, M.J., AND BROCKMAN, G.F. (1977) The error associated with point counting. *American Mineralogist* **62**, 1238-1244.

NELSON, N.O., MIKKELSEN, R.L., AND HESTERBERG, D.L. (2003) Struvite precipitation in anaerobic swine lagoon liquid: effect of pH and Mg:P ratio and determination of rate constant. *Bioresource Technology* **89**, 229-236.

NOEL, Y., ZANNONI, M., AND HUNTER, E.A. (1996) Texture of Parmigiano Reggiano cheese: statistical relationships between rheological and sensory variates. *Lait* **76**, 243-254.

NOFFKE, N. (2009) The criteria for biogeneicity of microbially induced sedimentary structures (MISS) in Archean and younger, sandy deposits. *Earth-Science Reviews* **96**, 173-180.

NOOMEN, A. (1983) The role of the surface flora in the softening of cheeses with a low initial pH. *Neth. Milk Dairy Journal* **37**, 229-232.

O'FARRELL, I.P., SHEEHAN, J.J., WILKINSON, M.G., HARRINGTON, D., AND KELLY, A.L. (2002) Influence of addition of plasmin or mastitic milk to cheesemilk on quality of smear-ripened cheese. *Lait* **82(82)**, 305-316.

OMELON, C.R., POLLARD, W.H., AND MARION, G.M. (2001) Seasonal formation of ikaite ($CaCO_3$ $6H_2O$) in saline spring discharges at Expidition Fjord, Canadian High Arctic: assessing conditional constraints for natural crystal growth. *Geochemica et Cosmochimica Acta* **65(9)**, 1429-1437.

OREN, A., KUHL, M., AND KARSTEN, U. (1995) An endoevaporitic microbial mat within a gypsum crust: zonation of phototrophs, photopigments, and light penetration. *Marine Ecology Progress Series* **128**, 151-159.

PAK, C.Y., EANES, E.D., AND RUSKIN, B. (1971) Spontaneous precipitation of brushite in urine: evidence that brushite is the nidus of renal stones originating as calcium phosphate. *Proc. Nat. Acad. Sci.* **68(7)**, 1456-1460.

PARKER, M.L., GUNNING, P.A., MACEDO, A.C., MALCATA, F.X., AND BROCKLEHURST, T.F. (1998) The microstructure and distribution of micro-organisms within mature Serra cheese. *Journal of Applied Microbiology* **84**, 523-530.

Percival, S.L., Malic, S., Cruz, H., and Williams, D.W. (2011) Biofilms and Veterinary Medicine. Springer, Berlin.

PHOENIX, V.R., AND KONHAUSER, K.O. (2008) Benefits of bacterial biomineralization. *Geobiology* **6**, 303-308.

PICQUE, D., LECLERCQ-PERLAT, M.N., AND CORRIEU, G. (2006) Effect of atmospheric composition on respiratory behavior, weight loss, and appearance of Camembert-type cheeses during chamber ripening. *Journal of Dairy Science* **89**, 3250-3259.

PICQUE, D., LECLERCQ-PERLAT, M.N., GUILLEMIN, H., PERRET, B., CATTENOZ, T., PROVOST, J.J., AND CORRIEU, G. (2010) Camembert-type cheese ripening dynamics are changed by the properties of wrapping films. *Journal of Dairy Science* **93**, 5601-5612.

PURCELL, C.S., AND HICKEY, C.H. (1922) Note on the occurrence of struvite in canned shrimps. *Analyst* **47(550)**, 16-18.

REMOUDAKI, E., HATZIKIOSEYIAN, A., KOUSI, P., AND TSEZOS, M. (2003) The mechanism of metal precipitaiton by biologically generated alkalinity in biofilm reactors. *Water Research* **37**, 3843-3854.

RIAHI, H., TRELEA, I.C., LECLERCQ-PERLAT, M.N., PICQUE, D., AND CORRIEU, G. (2007a) Model for changes in weight and dry matter during the ripening of a smear soft cheese under controlled temperature and relative humidity. *International Dairy Journal* **17**, 946-953.

RIAHI, M.H., TRELEA, I.C., PICQUE, D., LECLERCQ-PERLAT, M.N., HELIAS, A., AND CORRIEU, G. (2007b) A model describing *Debaryomyces hansenii* growth and substrate consumption during a smear soft cheese deacidification and ripening. *Journal of Dairy Science* **90**, 2525-2537.

RIDING, R. (2000) Microbial carbonates: the geological record of calcified bacterial-algal mats and biofilms. *Sedimentology* **47(Suppl. 1)**, 179-214.

RIVADENEYRA, M.A., MARTIN-ALGARRA, A., SANCHEZ-NAVAS, A., AND MARTIN-RAMOS, D. (2006) Carbonate and phosphate precipitaion by *Chromohalobacter marismortui*. *Geomicrobiology Journal* **23**, 89-101.

RIZZO, A.A., SCOTT, D.B., AND BLADEN, H.A. (1963) Calcification of oral bacteria. *Ann NY Acad Sci* **109**, 14-22.

RODRIGUEZ-AGUILERA, R., OLIVEIRA, C., MONTANEZ, J., AND MAHAJAN, P.V. (2011) Effect of modified atmosphere packaging on quality factors and shelf-life of surface mould ripened cheese: part I constant temperature. *LWT - Food Science and Technology* **44**, 330-336.

RODRIGUEZ-RUIZ, I., VEESLER, S., GOMEZ-MORALES, J., DELGADO-LOPEZ, J.M., GRAUBY, O., HAMMADI, Z., CANDONI, N., AND GARCIA-RUIZ, J.M. (2014) Transient calcium carbonate hexahydrate (ikaite) nucleated and stabilized in confined nano- and picovolumes. *Crystal Growth and Design* **14**, 792-802.

ROGER, B., DESOBRY, S., AND HARDY, J. (1998) Respiration of *Penicillium camemberti* during ripening and cold storage of semi-soft cheese. *Lait* **78**, 241-250.

ROUSSEAU, M. (1984) Study of the surface flora of traditional Camembert cheese by scanning electron microscopy. *Milk Science International* **39(3)**, 129-135.

RYSGAARD, S., GLUD, R.N., LENNERT, K., COOPER, M., HALDEN, N., LEAKEY, R.J.G., HAWTHORNE, F.C., AND BARBER, D. (2012) Ikaite crystals in melting sea ice - inplications for pCO_2 and pH levels in Arctic surface waters. *The Cryosphere* **6**, 901-908.

SANCHEZ-MORAL, S., CANAVERAS, J.C., LAIZ, L., SAIZ-JIMENEZ, C., BEDOYA, J., AND LUQUE, L. (2003) Biomediated precipitation of calcium carbonate metastable phases in hypogean environments: a short review. *Geomicrobiology Journal* **20**, 491-500.

SANCHEZ-MORAL, S., LUQUE, L., CANAVERAS, J.C., LAIZ, L., JURADO, V., HERMOSIN, B., AND SAIZ-JIMENEZ, C. (2004) Bioinduced barium precipitation in St. Callixtus and Domitilla catacombs. *Annals of Microbiology* **54**, 1-12.

SCHLESSER, J.E., SCHMIDT, S.J., AND SPECKMAN, R. (1992) Characterization of chemical and physical changes in Camembert cheese during ripening. *Journal of Dairy Science* **75**, 1753-1760.

SCHMIDT, M., PRIEME, A., AND STOUGAARD, P. (2006) Bacterial diversity in permanently cold and alkaline ikaite columns from Greenland. *Extremophiles* **10**, 551-562.

SENCHENKOVA, S.N., KNIREL, Y.A., LIKHOSHERSTOV, L.M., SHASHKOV, A.S., SHIBAEV, V.N., STARUKHINA, L.A., AND DERYABIN, V.V. (1995) Structure of simusan, a new acidic exopolysaccharide from *Arthrobacter* sp. *Carbohydrate Research* **266**, 103-113.

SHAMS, M.A., AND JAYNES, H.O. (1983) Characterization of exopolysaccharide produced by *Corynebacterium* #98 in cheese whey substrate. *Journal of Food Science* **48**, 208-211.

SHELDRICK, G.M. (2008) A short history of SHELX. *Acta Crystallographica* **A64**, 112-122.

SHOCK, A.A., HARPER, W.J., SWANSON, A.M., AND SOMMER, H.H. (1948) What's in those "white specks" on cheddar. *Wis. Agr. Expt. Sta. Bull.* **474**, 31-32.

SINGH, R., D., P., AND JAIN, R.K. (2006) Biofilms: implications in bioremediation. *Trands in Microbiology* **14(9)**, 389-397.

SMITHSON, F. (1948) The application of phase-contrast microscopy to mineralogy and petrology. *Min Mag* **28**, 384-391.

SOETAN, K.O., OLAIYA, C.O., AND OYEWOLE, O.E. (2010) The importance of mineral elements for humans, domestic animals and plants: a review. *African Journal of Food Sciences* **4(5)**, 200-222.

SOMERS, E.B., JOHNSON, M.E., AND WONG, A.C.L. (2001) Biofilm formation and contamination of cheese by nonstarter lactic acid bacteria in the dairy environment. *Journal of Dairy Science* **84**, 1926-1936.

SOU, T., KAMINSKAS, L., NGUYEN, T., CARLBERG, R., MCINTOSH, M., AND MORTON, D. (2013) The effect of amino acid excipients on morphology and solid-state properties of multi-component spray dried formulations for pulmonary delivery of biomacromolecules. *European Journal of Pharmaceutics and Biopharmaceutics* **83**, 234-243.

SOZZI, T., AND SHEPHERD, D. (1972) Evolution de la composition chimique et de la flore microbienne du fromage de Vacherin au cours de la maturation. *Le Lait* **52(513-514)**, 203-219.

STICKLER, D.J. (1996) Bacterial biofilms and the encrustation of urethral catheters. *Biofouling* **9(4)**, 293-305.

Stoiber, R.E., and Morse, S.A. (1972) Microscopic identification of crystals. The Ronald Press Company, New York.

STRATFUL, I., SCRIMSHOW, M.D., AND LESTER, J.N. (2001) Conditions influencing the precipitation of magnesium ammonium phosphate. *Wat. Res.* **35(17)**, 4191-4199.

SUESS, E., BALZER, W., HESSE, K.F., MULLER, P.J., UNGERER, C.A., AND WEFER, G. (1982) Calcium carbonate hexahydrate from organic-rich sediments of the Antarctic Shelf: precursers of glendonites. *Science* **216(4)**, 1128-1130.

SURMAN, S.B., WALKER, J.T., GODDARD, D.T., MORTON, L.H.G., KEEVIL, C.W., WEAVER, W., SKINNER, A., HANSON, K., CALDWELL, D., AND KURTZ, J. (1996) Comparison of microscope techniques for the examination of biofilms. *Journal of Microbiological Methods* **25**, 57-70.

SWAINSON, I.P., AND HAMMOND, R.P. (2003) Hydrogen bonding in ikaite, $CaCO_3$ $6H_2O$. *Mineralogical Magazine* **67(3)**, 555-562.

TANSMAN, G., KINDSTEDT, P.S., AND HUGHES, J.M. (2014) Powder X-ray diffraction can differentiate between enantiomeric variants of calcium lactate pentahydrate crystal in cheese. *Journal of Dairy Science* **97(12)**, 7354-7362.

TANSMAN, G., KINDSTEDT, P.S., AND HUGHES, J.M. (2015a) Characterization of single crystals in the rinds of white mold and smear ripened cheeses with single crystal X-ray diffractometry. *Journal of Dairy Science* **98(Suppl. 2)**, 668-669.

TANSMAN, G., KINDSTEDT, P.S., AND HUGHES, J.M. (2015b) Identification of crystalline entities in the rinds of white mold ripened cheese and smear ripened cheese with powder X-ray diffractometry. *Journal of Dairy Science* **98(Suppl. 2)**, 668.

TANSMAN, G., KINDSTEDT, P.S., AND HUGHES, J.M. (2015c) Novel sample preparation for smear ripened cheese rinds evaluated by powder X-ray diffractometry. *Journal of Dairy Science* **98(E-Suppl. 2)**, 587-588.

TANSMAN, G., KINDSTEDT, P.S., AND HUGHES, J.M. (In Press) Minerals in food: crystal structures of ikaite and struvite from bacterial smears on washed-rind cheese. *The Canadian Mineralogist*.

TANSMAN, G., KINDSTEDT, P.S., AND HUGHES, J.M. (Under Review) Crystallization and demineralization phenomena in stabilized white mold cheese. *Journal of Dairy Science*.

TATENO, N., AND KYONO, A. (2014) Structural change induced by dehydration in ikaite ($CaCO_3$ $6H_2O$). *Journal of Mineralogical and Petrological Sciences* **109**, 157-168.

THOMAS, T.D., AND CROW, V.L. (1983) Mechanisms of D(-)-lactic acid formation in Cheddar cheese. *New Zealand Journal of Dairy Scienceand Technology* **18**, 131-141.

Thompson, S.W., and Hunt, R.D. (1966) Selected Histochemical and Histopathological Methods. Charles C Thomas, Springfield, Il.

TOSHIMA, T., HAMAI, R., TAFU, M., TAKEMURA, Y., FUJITA, S., CHOHJI, T., TANTA, S., LI, S., AND QIN, G.W. (2014) Morphology control of brushite prepared by aqueous solution synthesis. *Journal of Asian Ceramic Societies* **2**, 52-56.

TSIAMIS, G., KATSAVELI, K., NTOUGIAS, S., KYRPIDES, N., ANDERSEN, G., PICENO, Y., AND BOURTZIS, K. (2008) Prokaryotic community profiles at different operational stages of a Greek solar saltern. *Research in Microbiology* **159**, 609-627.

TUCKEY, S.L., AND RUEHE, H.A. (1938) An x-ray diffraction analysis of Cheddar cheese. *Journal of Dairy Science* **21(12)**, 777-789.

TUCKEY, S.L., RUEHE, H.A., AND CLARK, G.L. (1938) X-ray diffraction analysis of white specks in Cheddar cheese. *Journal of Dairy Science* **21**, 161.

VAN HULLEBUSCH, E.D., ZANDVOORT, M.H., AND LENS, P.N.L. (2004) Metal immobilisation by biofilms: mechanisms and analytical tools. *Re/Views in Environmental Science & Bio/Technology* **00**, 1-25.

VASSAL, L., MONNET, V., LE BARS, D., ROUX, C., AND GRIPON, J.C. (1986) Relation entre le pH, la composition chimique et la texture des fromages de type Camembert. *Le Lait* **66(4)**, 341-351.

VISSCHER, P.T., AND STOLZ, J.F. (2005) Microbial mats as bioreactors: populations, processes, and products. *Palaeogeography, Palaeoclimatology, Palaeoecology* **219**, 87-100.

VISSER, F.M.W. (1976) Method for the manufacture of rennet-free cheese. *Neth. Milk Dairy Journal* **30**, 41-54.

WANG, G., WANG, D., XU, X., AND YANG, F. (2013) Partial nitrifying granule stimulated by struvite carrier in treating pharmaceutical wastewater. *Appl Microbiol Biotechnol* **97**, 8757-8765.

WANG, X., AND MULLER, W.E.G. (2009) Marine biominerals: perspectives and challenges for polymetallic nodules and crusts. *Trends in Biotechnology* **27(6)**, 375-383.

WARE, C.I. (2003) A simple method to 'point count' silt using scanning electron microscopy aided by image analysis. *Journal of Microscopy* **212(2)**, 205-208.

Washam, C.J., Kerr, T.J., Hurst, V.J., and Rigsby, W.E. (1985) A scanning electron microscopy study of crystalline structures in commercial cheese. Developments in industrial microbiology, 26, p. 749-761.

WATSON, K.E., AND DEMER, L.L. (1996) The atherosclerosis-calcification link? *Curent Opinion in Lipidology* **7**, 101-104.

WHITICAR, M.J., AND SUESS, E. (1998) The cold carbonate connection between Mono Lake, California and the Bransfield Strait, Antarctica. *Aquatic Geochemistry* **4**, 429-454.

WOLFE, B.E., BUTTON, J.E., SANTARELLI, M., AND DUTTON, R.J. (2014) Cheese rind communities provide tractable systems for in situ and in vitro studies of microbial diversity. *Cell* **158**, 422-433.

WOLFE, B.E., AND DUTTON, R.J. (2012) Towards an ecosystem approach to cheese microbiology. *Microbiology Spectrum* **1(1)**, 1-9.

WOLFE, B.E., AND DUTTON, R.J. (2015) Fermented foods as experimentally tractable microbial ecosystems. *Cell* **161**, 49-55.

ZANNONI, M., L., B., AND A., H.E. (1994) Comparison of Parmigiano-Reggiano and American Parmesan cheeses by sensory analysis of texture. *Scienza E Technica Lattiero-Casearia* **45(6)**, 505-518.